INDIAN JOURNAL OF PHYSICS

VOL. XX

AND

PROCEEDINGS

OF THE

Indian Association for the Cultivation of Science, Vol. XXIX

(Published in Collaboration with the Indian Physical Society)

(With Eleven Plates)

PRINTED BY NISHITCHANDRA SEN, SUPERINTENDENT (OFFG.), CALCUTTA UNIVERSITY PRESS, 48, HAZRA ROAD, BALLYGUNGE, CALCUTTA, AND PUBLISHED BY THE SECRETARY, INDIAN ASSOCIATION FOR THE CULTIVATION OF SCIENCE

210, Bowbazar Street, Calcutta.

1946

Price Rs. 12 or £1-2-6

INDIAN JOURNAL OF PHYSICS

VOL. XX

1946

CONTENTS

PART I

PART II

PART III

PART IV

AUTHOR INDEX

EFFECT OF VARIATION OF THE MAGNITUDE AND PHASE ANGLE OF THE LOAD ON POWER OUTPUT IN COMMUNICATION CIRCUITS*

By V. V. L. RAO, D. APPA RAO AND M. KRISHNAMURTHI

ABSTRACT In communication circuits a great deal of stress is laid on the need for exact matching of the load to the source While this impedance matching principle is true as a general rule, under actual conditions, results indicate that over a wide range of values of impedance on either side of the source impedance, the loss due to mismatch is not appreciable The paper derives conditions for the maximum transfer of power to load when both the source and load are complex impedances, and treating the source as a fixed one Actually, it is found mathematically

(1) that when mismatch of impedance must exist, it is better to mismatch to a higher than a lower load impedance (in magnitude) ;

(2*a*) in the case of small phase angles of source, it is also derived that, where perfect matching is not possible, the load phase angle should be nearer zero, and

(2*b*) for higher phase angles of the source, matching becomes critical

INTRODUCTION

The subject of impedance matching in communication circuits has been dealt with in several text books and journals from a very general point of view, most often treating both the source and the load as pure resistances and thus ignoring the phase angle or power factor of both the source and the load. Also, often the source impedance is considered fixed and the load impedance variable. The object of this paper is to consider the effect on the power output when both the magnitude and phase angle of the load are treated as variable (one at a time), while the source itself is treated as a complex impedance. This paper also suggests choosing the magnitude of the impedance and phase angle of the load where perfect matching is not possible,

NOTATION

(1) Z_s = Impedance of the source
(2) Z_L = Impedance of the load
(3) ϕ_s = Phase angle of the source
(4) ϕ_l = Phase angle of the load
(5) E = E. M. F. of the source
(6) W_L = Power in the load

* Communicated by I. Ramakrishna Rao

CONDITIONS FOR MAXIMUM TRANSFER OF POWER

Any communication network can be reduced by Thevenin's theorem to a source, generating an E. M.F.,E, a complex impedance of the source Z_s in series with the generator and a complex load Z_L.

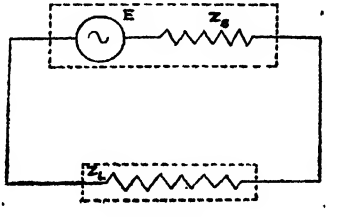

(FIG. 1)

Let us consider the conditions under which maximum power is transferred to the load.

With the above notation and Fig. 1, it is proposed to derive an expression for the power W_L in the load.

The power in the load is given by :

$$W_L = \tfrac{1}{2} |I|^2 \times |Z_L| \times \cos \phi_L \qquad \ldots (1)$$

But,
$$|I| = \frac{|E|}{|Z_s + Z_L|} \qquad \ldots (2)$$

Therefore,
$$W_L = \tfrac{1}{2} E^2 \times \frac{|Z_L| \cos \phi}{|Z_L + Z_s|^2} \qquad \ldots (3$$

(Signal Training Manual, 1936)

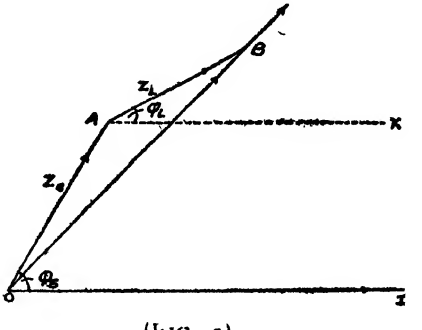

(FIG. 2)

From Fig. 2, $|Z_s + Z_L|^2 = |Z_s|^2 + |Z_L|^2 + 2|Z_L Z_s| \cos \phi_s$ ... (4)

Substituting this in equation (3) above, we have :

$$W_L = \tfrac{1}{2} |E|^2 \frac{|Z_L| \cos \phi_L}{|Z_s|^2 + |Z_L|^2 + 2|Z_L Z_s| \cos(\phi_s - \phi_L)} \qquad \ldots (5)$$

Equation (5) gives the general expression for the power in the load. It is often not possible to vary one or both of the factors, magnitude and phase of the source, while both the magnitude and/or the angle of the load can be varied for obtaining maximum transfer of power from the source to the load ; *i.e*, $|Z_s|$ and ϕ_s are often fixed and $|Z_L|$ and ϕ_L are usually variable.

(*a*) *Variation of* $|Z_L|$, *keeping* ϕ_L *constant*

Glasgow (1936) says that this condition actually obtains in practice in the speech coil of a dynamic loudspeaker. First let us keep ϕ_L constant and see the effect on W_L by varying $|Z_L|$ only.

By differentiating the expression (5) with respect to $|Z_L|$ and equating to zero,

we get $$|Z_L| = |Z_s| \qquad \ldots (6)$$

(Everitt, 1937)

(*b*) *Variation of* ϕ_L, *keeping* Z_L *constant and equal to* $|Z_s|$

After making $|Z_L| = |Z_s|$ let us vary ϕ_L to obtain maximum power in load.

Equation (5) becomes on substituting $|Z_s|$ for $|Z_L|$

$$W_L = \tfrac{1}{2} |E|^2 \frac{|Z|}{2|Z_s|^2 Z} \frac{\cos\phi_L}{(1+\cos(\phi_s - \phi_L))} \qquad \ldots (7)$$

On differentiating the above expression with respect to ϕ_L and equating to zero and solving, we get :

$$\sin\phi_L = -\sin\phi_s$$

$$\text{or } \phi_L = -\phi_s \text{ or } (n\pi + \phi_s) \text{ where n is old} \qquad \ldots (8)$$

Since the values of ϕ_L other than $(-\phi_s)$ result in an infinite value of W_L, the only possible solution is $\phi_L = -\phi_s$

Thus the two conditions for maximum power transfer to load are

$$\left.\begin{array}{ll} (1) & |Z_s| = |Z_L| \\ \text{and} \quad (2) & \phi_s = -\phi_L \end{array}\right\} \qquad \ldots (9)$$

(*c*) *Physical significance of the conditions for maximum transfer of power to the load*

The significance of equation (9) can be interpreted thus : If both the magnitude and angle of the load could be adjusted, then the load impedance should be conjugate of the generator or source impedance, *i.e.*, the resistive components should be equal, while their reactive components should also be equal in magnitude but opposite in sign—that is, if one is inductive, the other should be capacitative.

Symbolically, if $Z_s = R_1 + jx_1$;

then, Z_L should be ; $R_1 - jx_1$

Under these conditions, the impedances (Z_L and Z_s) are said to match and any deviation from these conditions is described as impedance mismatch.

EFFECT OF IMPEDANCE MISMATCH

In what follows, for convenience $|Z_L|$ and $|Z_s|$ are denoted merely by Z_L and Z_s.

From equation (9), values of Z_L and ϕ_L can be determined to obtain maximum power output in the load. It is often impossible to match the load to the source for all frequencies (e. g. speech coil of a loudspeaker to the plate of the output tube), since the load impedance is invariably a function of frequency in communication circuits.

It is therefore proposed to consider the effect of mismatch on the output (load) power.

(*a*) The effect of mismatch due to a difference between the load impedance Z_L and source impedance Z_s will be considered first, the phase angles being constant.

It has been derived that for maximum output Z_L should be equal to Z_s (*vide* equation 7). In this case, the power output is :

$$W_s = \tfrac{1}{2}|T|^2 \frac{\cos\phi_L}{2Z_s(1+\cos\phi_s-\phi_L)} \quad \ldots \quad (10)$$

When, however, $Z_L \neq Z_s$, we have the power output

$$W_s = \tfrac{1}{2}|E|^2 \frac{Z_L \cos\phi_L}{Z_L^2 + Z_s^2 + 2Z_L Z_s \cos(\phi_s - \phi_L)} \quad \ldots \quad (11)$$

Dividing (11) by (10) we have

$$\frac{W_L}{W_s} = \frac{2Z_L Z_s (1+\cos\phi_s-\phi_L)}{Z_L^2 + Z_s^2 + 2Z_L Z_s \cos\phi_s - \phi_L} = \frac{2(1+\cos\phi_s-\phi_L)}{\frac{Z_L}{Z_s} + \frac{Z_s}{Z_L} + 2\cos\phi_s - \phi_L} \quad \ldots \quad (12)$$

The power loss with reference to power output at matched condition is :

$$\frac{W_s - W_L}{W_s} = 1 - \frac{W_L}{W_s} = \frac{\frac{Z_L}{Z_s} + \frac{Z_s}{Z_L} - 2}{\frac{Z_L}{Z_s} + \frac{Z_s}{Z_L} + 2\cos\phi_s - \phi_L} \quad \ldots \quad (13)$$

From equation (13) the following conclusions can be drawn :—

(1) If ϕ_s and ϕ_L are constant, the percentage power loss due to an inequality between Z_L and Z_s is solely dependent on the ratio Z_L/Z_s and not on the individual values of Z_L and Z_s.

(2) As the expression contains only the difference between ϕ_L and ϕ_s and not their individual values the power loss percent will be the same for a given Z_s/Z_L although ϕ_s and ϕ_L may be given different sets of values, provided $(\phi_s - \phi_L)$ is constant.

(3) The power loss percent will be the same for a given Z_s/Z_L whether the sign of $(\phi_s - \phi_L)$ is positive or negative because, in either case, cos $(\phi_s - \phi_L)$ is the same.

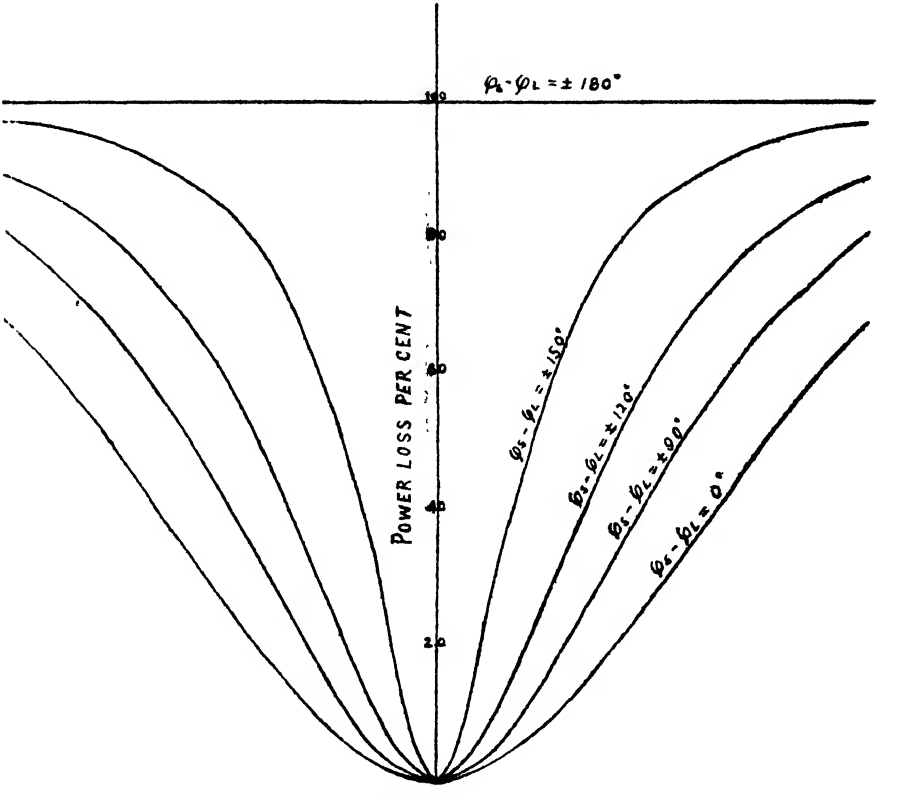

GRAPH 1
Z_s/Z_L Ratio

A graph (GRAPH 1) has been drawn showing the variation of power loss with the ratio Z_s/Z_L on a log-linear graph paper.

The conclusion (1) given above has been verified by calculating the power loss for various standard values of Z_s (*viz.*, 37, 50, 74, 200, 500, 550 and 600 ohms being the standard characteristic impedances for audio and radio-frequency transmission lines) and plotting the curve for Z_s/Z_L versus power loss percent. It found that all the curves coincide for a given value of $(\phi_L - \phi_s)$. For the curve for is which the value of $(\phi_L - \phi_s)$ is assumed to be 90°, the values of ϕ_s and ϕ_L are $-45°$ and $+45°$ respectively, making the difference of ϕ_L and ϕ_s equal to 90° in both cases. This curve also coincides with the previous one, thereby showing that the curve is universal for a particular value of $(\phi_L - \phi_s)$

(*a*) *Inferences from and applications of Graph No.* 1

(*i*) Maximum power is transferred to the load when $Z_L = Z_s$ $(\phi_s - \phi_L)$ being constant.

(*ii*) The output power is zero when $Z_L = 0$ *i. e.*, no power is delivered when the source is short-circuited.

(*iii*) The curve is symmetrical about $Z_s/Z_L = 1$ and an interesting property can be derived from this curve.

If Z_1 and Z_2 are two values of load impedance on either side of Z_s such that $Z_1 > Z_s > Z_2$ and also $Z_L = \sqrt{Z_1 Z_2}$, then, the power loss for Z_s/Z_1 = power loss for Z_s/Z_2, even though $(Z_1 - Z_s) > (Z_s - Z_2)$.

Alternatively, if Z_1 and Z_2 are two load impedances on either side of Z_s such that $(Z_1 - Z_s) = (Z_s - Z_2)$, then the loss of power due to the mismatch between Z_1 and Z_s will be less than that due to the mismatch Z_2 and Z_s so that an error of a few ohms on the higher side has less effect than the same numerical difference on the lower side of the source impedance.

(*iv*) Curves have been drawn for different values of $(\phi_s - \phi_L)$. in this set of curves that for $(\phi_s - \phi_L) = 0$ is the same as that given by Beitman (1943). It is found that the smaller the value of this difference the flatter will be the curve. This shows that for a given value of Z_s/Z_L, the power output will be greater the smaller the numerical value of $(\phi_s - \phi_L)$;

(*v*) when $(\phi_s - \phi_L)$ is equal to $\pm 180°$, no power is delivered to the load. The power loss is constant and equal to 100% for all values of Z_s/Z_L ; and

(*vi*) the curve for $(\phi_s - \phi_L)$ equal to zero, gives the minimum variation of percentage power loss for variation in the Z_s/Z_L ratio.

(*b*) The effect on power output due to mismatch of phase angles of the source and load will now be considered, the impedances of the source and load being as assumed to be matched $(Z_s = Z_L)$.

For maximum power output under the above conditions, $\phi_s = (-\phi_L)$.

Then the power output $(W_s) = \frac{1}{2} |E|^2 \frac{\cos(-\phi_s)}{2Z_s[1 + \cos(2\phi_s)]}$

$$= \tfrac{1}{2} |E|^2 \frac{1}{4Z_s \cos \phi_s} \qquad \ldots \quad (14)$$

When, however $\phi_s \neq -\phi_L$,

the power output $$(W_L) = \tfrac{1}{2} |E|^2 \frac{\cos \phi_L}{2Z_s (1 + \cos \phi_s - \phi_L)} \qquad \ldots \quad (15)$$

Dividing (15) by (14),

$$W_L/W_s = \frac{2 \cos \phi_L \cos \phi_s}{1 + \cos(\phi_s - \phi_L)}.$$

The power loss with reference to power output at matched condition is :

$$\frac{W_s - W_L}{W_s} = 1 - W_1/W_s = \frac{1-\cos(\phi_s+\phi_L)}{1+\cos(\phi_s-\phi_L)} \quad \ldots \quad (16)$$

The power loss values have been calculated for different values of ϕ_L ranging from -90° to $+90^\circ$ for five particular values of ϕ_s namely $+45^\circ$, -45°, $+80^\circ$, -80° and 0°. The results have been plotted in graph 2.

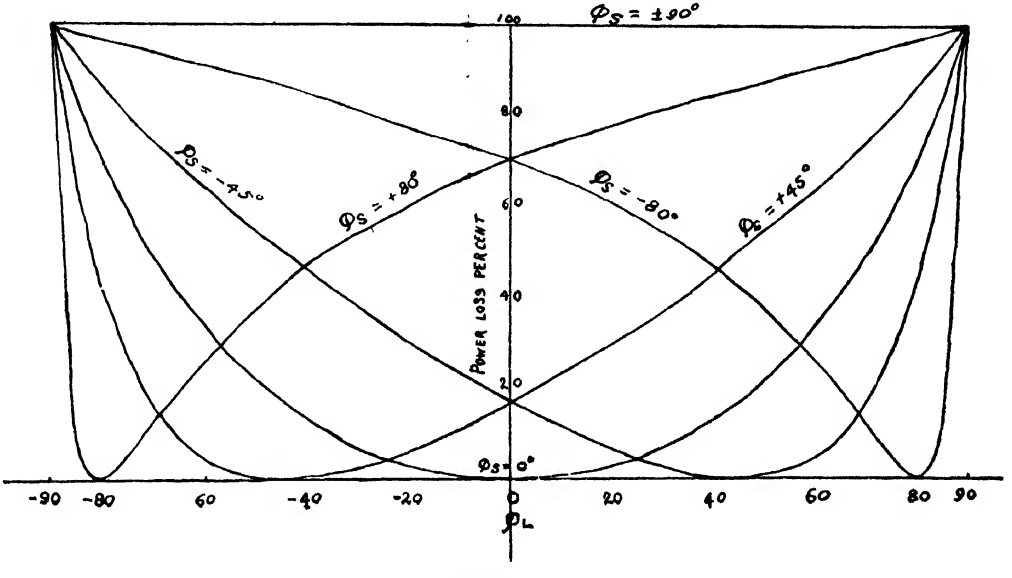

GRAPH 2

The following inferences can be drawn from the graph :

(1) Maximum power is delivered when $\phi_L = -\phi_s$.

(2) Output is zero both when $\phi_L = +90^\circ$ or -90°.

(3) At higher values of ϕ_s, the curves become steeper on either side of the matching point ($\phi_L = -\phi_s$). This means that the effect of mismatch increases as ϕ_s is increased and hence at the larger values of ϕ_s perfect matching becomes essential. It is therefore better to have ϕ_s as small as possible.

This same inference can be drawn from conclusion (*v*) para (*a*) above, where it is stated that for low power loss ($\phi_s - \phi_L$) should be as small as possible. The value of ($\phi_s - \phi_L$) when the angles are matched, is equal to $2\phi_s$ and if this is to be small, ϕ should be small. There can be most perfect matching with regard to impedances and phase angles in the case of pure resistances because, in that case, both the conditions, $\phi_s = -\phi_L$ and $\phi_s - \phi_L = 0$, are satisfied ($\because \phi_s = -\phi_L = 0$) ; and maximum output will be delivered to the load.

(4) For smaller values of ϕ_S (up to about 50°), if perfect matching is not possible, it is preferable to have ϕ_L some value between $(-\phi_S)$ and 0.

(5) When ϕ_S is $\pm 90°$, the output is zero for all values of ϕ_L.

RADIO LABORATORY,
PROVINCIAL BROADCASTING DEPARTMENT, GOVT OF MADRAS,
KILPAUK, MADRAS.

REFERENCES

Beitman, M. N., 1943, Practical Radio & Electronics Course for Home Study (Vol. I, p. 149) (Supreme Publications, Chicago).

Everitt, W. L., 1937, Communication Engineering, p. 51, 50 (McGraw Hill Book Co., New York).

Glasgow, R. S., 1936, Principles of Radio Engineering, p. 174 (McGraw Hill Book Coy., New York).

Signal Training Manual, 1936, Vol. 2, Part III (H.M.S. Office, London).

MAGNETIC STUDIES ON NICKEL IONS IN CRYSTALS

By A. MOOKHERJI

ABSTRACT. Measurements have been made of the anisotropies and the principal magnetic susceptibilities of a number of crystalline nickel salts. With the help of these measurements and the available X-ray data for these crystals, the contributions of the constituent paramagnetic units have been worked out. The constants of the crystalline electric field have been calculated on the basis of the theory of Van Vleck, Penney and Schlapp and the relative contributions of the different terms in the theoretical expressions derived according to their theory, to the effective magnetic moments in different directions of the paramagnetic units have been discussed. Finally the magnetic anisotropy has been discussed in relation to the Stark splitting due to the crystalline electric field.

INTRODUCTION

Penney and Schlapp (1932) have explained the observed deviations from the free-ion behaviour of the effective magnetic moments of the Ni^{++} ions in crystals attributing these deviations to the influence of strong and asymmetric crystalline fields in the neighbourhood of the paramagnetic ion. Their calculations are based on the assumption that the axes of the crystalline fields acting on the Ni^{++} ions in the crystals are coincident. Speaking in relations to the paramagnetic groups in the unit cell of the crystals, this is equivalent to assuming that all such paramagnetic groups in the unit cell of the crystal are oriented parallel to each other. Consequently the observed crystal anisotropy represents the anisotropy of the individual paramagnetic units in the unit cell. But X-ray studies on the fine structure of some of the nickel salts show that it is not true. The different paramagnetic groups in the unit cell of the crystal are oriented relative to one another in such a manner as to build up the symmetry of the unit cell from those of the individual units. Hence the crystal anisotropy is only the average effect of the different groups in the unit cell although the mean of the principal susceptibilities remains unaffected by it.

In this communication, the results of magnetic measurements on single crystal of some of the nickel salts, for which fine structure study is available, are correlated with the paramagnetic groups in the unit cell of the crystal and then discussed in the light of the theory of Penney and Schlapp.

EXPERIMENTAL

Cobalt-free nickel salts of reagent quality were used and crystals were grown out of aqueous solutions.

The magnetic anisotropy was measured by the rotational method of Krishnan and Banerjee (1934) and the absolute susceptibility along some convenient direction in the crystal was measured by the balancing method of the

TABLE I

Temperature = 30°C

Crystal	Crystallographic data	Made of Suspension	Orientation in the field	$\Delta\chi$	Magnetic Anisotropy
$NiSO_4.6H_2O$	Telragonal D_4^4; Z=4 a=b=9.6 Å c=18.3 Å	Tetrag. ax horiz.	Tetrag. ax. normal to the field	83	$\chi_1-\chi_{11}=83$
$NiSO_4.7H_2O$	Rhombic V_4; Z=4 a=11.8 Å b=12.0Å c=6.8 Å	'c' ax. vert. 'a' ,, ,, 'b' ,, ,,	'a' ax along field 'c' ,, ,, ,, 'a' ,, ,, ,,	163 124 33·5	$\chi_a-\chi_b=163$ $\chi_c-\chi_b=124$ Cal. $\Delta\chi=39$
$Ni(CH_3COO)_2.4H_2O$	Moncl. prism C_{2h}^5; Z= 2 a=8.49 Å b=11 77 ,, c=4.87 ,, $\beta=93°\ 25'$	'b' ax. vert. 'c' ,, ,, 'b' and 'c' axes horiz.	$\psi=136\ 7$ 'b' ax. normal field 'b' ,, ,, ,,	234 24 78	$\chi_1-\chi_2=234$ $\chi_1-\chi_3=167$ Cal. $\psi=38°.5$
$Co(CH_3COO)_2.4H_2O$	Moncl. prism a : b : c = .718 : 1 : 4028 $\beta=94°\ 23'$	'b' ax. vert. 'c' ,, ,, 'b' and 'c' axes horiz.	$\psi=-8\ 2$ 'b' ax. along field 'b' ,, ,, ,,	5,420 2,806 2,374	$\chi_1-\chi_2=5,420$ $\chi_1-\chi_3=2,494$ Cal. $\psi=-8°.5$

TABLE II

Crystal	Direction along which sus. was measured	Temperature °C	Density of the crystal	Vol. susceptibility	Corresponding gm. mol. susceptibility	Mean susceptibility at 30°C	Square of the effective moments μ_i^2 at 30°C
$NiSO_4.6H_2O$	Along χ_1 axis	30.0	2.080	32.17	4,068	4,040	$\mu_1^2 = 10.19$ $\mu_2^2 = 10.02$ $\overline{\mu^2 = 10\ 13}$
$NiSO_4.7H_2O$	Aiong 'a' axis	30.0	1.972	28.91	4,117	4,050	$\mu_a^2 = 11.53$ $\mu_b^2 = 9.997$ $\mu_c^2 = 10\ 30$ $\overline{\mu^2 = 10.61}$
$Ni(CH_3COO)_2.4H_2O$	Along χ_1 axis	28.8	1.749	31.7	4,510	4,350	$\mu_1^2 = 11.04$ $\mu_2^2 = 10\ 74$ $\mu_3^2 = 12.88$ $\overline{\mu^2 = 10\ 89}$
$Co(CH_3COO)_2\ 4H_2O$	Along 'b' axis	29.2	1.720	74 5	80,800	10,630	$\mu_1^2 = 28.37$ $\mu_2^2 = 15.11$ $\overline{\mu_3^2 = 22.26}$ $\mu^2 = 21.91$

same workers. These two measurements when combined give the three principal susceptibilities in the crystal.

RESULTS

The results of measurements are collected in Tables I and II and expressed in the usual units (10^{6} c.g.s. unit). $\chi_{\parallel}$ represents the gram molecular susceptibility along the axis of symmetry for tetragonal crystals and $\chi_{\perp}$ that along directions normal to it. χ_a, χ_b and χ_c represents the gram molecular susceptibilities along the three crystallographic axes of a rhombic crystal; for monoclinic crystals χ_3 represents the gram molecular susceptibility along 'b' axis while greater of the two in the (010) plane is represented by χ_1 and the smaller by χ_2; ψ is the angle which the 'c' crystallographic axis makes with χ_1-axis.

Effective magnetic moments of the crystals, μ_i, are calculated by the expression $\mu_i = 2.84\sqrt{\chi'_i T}$, where χ'_i are the susceptibilities corrected for diamagnetism (both for cation and anion) and $i = 1$, 2 and 3 or $\parallel$ and $\perp$. The diamagnetism for Ni^{++} and Co^{++} ions were calculated to be -17.3×10^{-6} and -18.3×10^{-6} respectively by the method of Slater as modified by Angus (1932). The following diamagnetic corrections were adopted for different groups as given by Stoner (1935):

SO_4^{--}	$CH_3(CHOO)_2$	H_2O
-33.6	-28.6	-13.0

MAGNETIC ANISOTROPIES OF CRYSTALS IN RELATION TO THE ANISOTROPIES OF THE CONSTITUENT PARAMAGNETIC UNITS

The results obtained in previous sections are discussed in this section in relation to X-ray data of the fine structure of the crystals.

$NiSO_4.6H_2O$.—This crystal has been analysed by X-ray methods by Beevers and Lipson (1932). It is assigned a space group D_4^4 with four molecules in the unit cell. They find that the six water molecules group round the metal ion and lie at the corners of an octahedron. Four of them form a square about Ni^{++} ion and the remaining two lie centrally above and below the square. There are four such groups in the unit cell. The distance (NiO_I) of oxygen atoms lying centrally above and below the square from the Ni^{++} ion is 2.02 Å. While the distance (NiO_{II}) of oxygen atoms in the plane from the Ni^{++} ion is 2.04 Å.

Let the gram molecular susceptibility along (NiO_I) be represented by K_1 and along (NiO_{II}) be represented by $K_{\parallel}$. Evidently K_1 is greater than $K_{\parallel}$. The inclination (γ) of $K_{\parallel}$-axis to 'c' crystallographic axis from X-ray data is 45.8.

Hence
$$K_1 - K_{\parallel} = \frac{\chi_1 - \chi_{\parallel}}{1 - \frac{3}{2}\sin^2 45.8}$$

using the values of $(\chi_1 - \chi_{\parallel})$ and $\bar{\chi}$ from Tables I and II, we obtain

$$\left.\begin{matrix} K_{\perp} - K_{\parallel} = & 311 \\ K = & 4,040 \end{matrix}\right\} \times 10^{-6} \text{ at } 30^{\circ}\text{C}.$$

Therefore the anisotropy of the paramagnetic unit $(\Delta K/K)$ is .077. The corresponding squares of the effective magnetic moments are

$$n_{\parallel}^2 = 9.68, \quad n_{\perp}^2 = 10.58, \quad \bar{n}^2 = 10.23.$$

$Ni(CH_3COO)_2.4H_2O$.—This crystal has been studied by X-ray methods by Hull (1934). Its space group is C_{2h}^5 with two molecules in the unit cell. If the distribution of oxygen atoms about the metal ion is taken to be the same as in $NiSO_4.6H_2O$, *i.e.*, four oxygens contributed by four water molecules forming a square about Ni^{++} ion and the other two contributed by two acetate groups lie centrally above and below the square, but at a smaller distance from the Ni^{++} ion than the other four oxygen atoms, one can calculate the anisotropy of the individual paramagnetic unit in the unit cell of the crystal in the following manner—

Let Z_1 and Z_2 represent the axes of the symmetry of the two units, (010) plane is the symmetry plane of the crystal, so the principal magnetic axes of one of the units is obtained from those of the other by reflection on the (010) plane. Since the paramagnetic unit possesses uniaxial magnetic symmetry, χ_1 will be the direction normal to the plane containing Z_1 and Z_2 axes and χ_2 will be the internal bisector of the angle (2ψ) between Z_1 and Z_2.

Therefore

$$\left.\begin{matrix} \chi_1 = K_{\parallel}, \quad \chi_2 = K_{\parallel}\cos^2\psi + K_{\perp}\sin^2\psi, \quad \chi_3 = K_{\parallel}\sin^2\psi + K_{\perp}\cos^2\psi, \\ \cos^2\psi = \dfrac{\chi_3 - \chi_2}{K_{\perp} - K_{\parallel}} \end{matrix}\right\} \quad \ldots \quad (1)$$

and $\frac{1}{3}(\chi_1 + \chi_2 + \chi_3) = \frac{1}{3}(K_{\parallel} + 2K_{\perp})$

Using the experimental values from Tables I and II we get

$$\left.\begin{matrix} K_{\perp} - K_{\parallel} = & 401 \\ K = & 4,350 \\ 2\psi = & 80.4 \end{matrix}\right\} \times 10^{-6} \text{ at } 30^{\circ}\text{C}.$$

Thus the anisotropy of the paramagnetic unit is .092. The corresponding squares of the effective moments are

$$n_{\parallel}^2 = 10.28, \quad n_{\perp}^2 = 11.27, \quad \bar{n}^2 = 10.94.$$

$NiSO_4\ 7H_2O$.—The fine structure study of this crystal by Beevers and Schwartz (1935) assigns it the space group V_4 with four molecules in the unit cell. The disposition of water molecules about Ni^{++} ion is the same as $NiSO_4.6H_2O$, *i.e.* six oxygens at the corners of an octahedron with Ni^{++} ion at the centre. The seventh water molecule does not come in contact with the metal ion. Four out of the six oxygen atoms form a square with Ni^{++} ion at the

centre, the other two are situated centrally above and below the square. The average distance ($Ni(O)_I$) of oxygen atoms in the plane from the Ni^{++} ion namely 2.01Å is smaller than the average distance ($Ni(O)_{II}$) namely 2.08Å of the other two oxygens from Ni^{++} ion. Hence $K_\parallel$, gram molecular susceptibility along the axis of symmetry of the group should be greater than $K_\perp$. gram molecular susceptibility for directions in the plane of the square.

If α, β and γ are the inclinations of $K_\parallel$ axis to the a, b and c crystallographic axes then we have

$$K_\parallel - K_\perp = \frac{\chi_b - \chi_a}{\cos^2\alpha - \cos^2\beta},$$

and also

$$K_\parallel - K_\perp = \frac{\chi_a - \chi_c}{\cos^2\alpha - \cos^2\gamma}.$$

The values of α, β and γ from X-ray data are 73.5°, 32.8° and 62.0° degrees respectively. These together with the data from Tables I and II give

$$\left.\begin{aligned} K_\perp - K_\parallel &= 258 \\ \bar{K} &= 4{,}050 \end{aligned}\right\} \times 10^{-6} \text{ at } 30°\text{C}.$$

Hence the anisotropy of the paramagnetic unit in $NiSO_4.7H_2O$ is .064.

The above value of ΔK shows that $K_\perp$ is greater than $K_\parallel$. Though it agrees well with that of $NiSO_4.6H_2O$ but disagrees with the suggestions from X-ray data of interatomic distances in $NiSO_4,7H_2O$. Since slight variations, of the coordinates of Ni^{++} ion and oxygens cause a great alteration in the nickel-oxygen distances, and since such variations are not improbable this disagreement of magnetic data with the proposed structure of the crystal by X-ray method is not a serious one.

The squares of the effective moments of the unit are

$$n_\parallel^2 = 9.67, \quad n_\perp^2 = 10.57, \quad \bar{n}^2 = 10.24.$$

Nickel Tutton Salts.—Krishnan and the present author (1937) made measurements on a large number of nickel tutton salts at room temperature. If the distribution of the oxygen atoms about the Ni^{++} ion is the same as in $NiSO_4.6H_2O$ and $NiSO_4.7H_2O$ which will be presumably so, then the anisotropy of the paramagnetic units of the crystal, and their relative orientations (2ψ) of the groups can be calculated by using equations (1) since the crystals are all monoclinic and contains two molecules in the unit cell (Hofmann, 1931). The following table gives the calculated values of $(K_\perp - K_\parallel)$ and 2ψ.

It is seen from Table (III) that $Ni(CH_3COO)_2.4H_2O$ has the highest percentage anisotropy ($\Delta K/K \times 100$), *i.e.*, 9.2% while the percentage anisotropy for single sulplates and the tutton salts vary from 7.3% to 5.1%.

TABLE III

Temperature 30°C

Crystal.	$K_1 - K_\parallel$	$\bar{K}$	2ψ	$\frac{\Delta K}{\bar{K}}$ = Anisotropy.
$NiRb_2(SO_4)_2.6H_2O$	281	4,080	88.5	.069
$NiCs_2(SO_4)_2.6H_2O$	261	4,080	88 5	.064
$NiTl_2(SO_4)_2.6H_2O$	222	4,040	88 4	.055
$Ni(NH_4)_2(SeO_4)_2\ 6H_2O$	212	4,120	84.8	.051
$NiK_2(SeO_4)_2.6H_2O$	292	4,160	90	.07
$NiRb_2(SeO_4)_2.6H_2O$	307	4,160	88.1	.073
$NiCs_2(SeO_4)_2.6H_2O$	299	4,150	84.4	.072
$NiTl_2(SeO_4)_2.6H_2O$	236	4,110	87 6	.057
$Ni(NH_4)_2(BF_4)_2.6H_2O$	213	4,060	87.6	.053
$NiSO_4\ 6H_2O$	311	4,040	—	.077
$NiSO_4\ 7H_2O$	258	4,050	—	064
$Ni(CH_3COO)_2\ 4HO$	401	4,350	80 4	092

CONSTANT OF THE CRYSTAL FIELD

The ground state of the Ni^{++} ion is $^3F_4$, the overall multiplet separation according to Laporte (1928) is 2347 cm^{-1}. Under the influence of a cubic field $^3F_4$ level splits up into a single and two tripiet levels. In case of Ni^{++} ion with positive D in equation (2) the single level lies lowest as is shown in figure (1). If now the spin and its coupling to the orbits is taken into account further splitting takes place. Penney and Schlapp (1932) have worked out the theoretical expressions for the principal magnetic moments of Ni^{++} ions in crystals assuming for simplicity that all the paramagnetic groups in the unit cell of the crystal are oriented parallel to one another. Consequently their expressions refer to magnetic moments in the three directions of the paramagnetic unit.

The Ni^{++} ion is considered to be subjected to an electric field which is predominantly cubic on which is superimposed a weak rhombic field. The axes of the cubic and rhombic fields are taken coincident. The potential of the field in the neighbourhood of the paramagnetic ion is given by

$$\phi = D(x^4 + y^4 + z^4) + Ax^2 + By^2 - (A + B)z^2 \qquad (2)$$

Since all the paramagnetic groups are taken as oriented parallel to one another, the squares of the effective magnetic moments, n_1^2, n_2^2 and n_3^2 of the paramagnetic unit along the z, y, and x-axes of the crystal field have the expressions—

$$\left.\begin{aligned} n_1^2 &= 8\left[\left\{1 + 8\lambda\alpha_1 + \frac{\theta_1}{kT} + \quad \cdots \right\} - 3kT\alpha_1\right] \\ n_2^2 &= 8\left[\left\{1 + 8\lambda\alpha_2 + \frac{\theta_2}{kT} + \quad \cdots \right\} - 3kT\alpha_2\right] \\ n_3^2 &= 8\left[\left\{1 + 8\lambda\alpha_3 + \frac{\theta_3}{kT} + \quad \cdots \right\} - 3kT\alpha_3\right] \end{aligned}\right\} \quad \cdots \quad (3)$$

where λ is the coefficient of spin-orbit coupling and is equal to 335 cm^{-1} for Ni^{++} ion.

$$\theta_1 = 2/3\lambda^2(\alpha_2+\alpha_3-2\alpha_1)$$
$$\theta_2 = 2/3\lambda^2(\alpha_1+\alpha_3-2\alpha_2)$$
$$\theta_3 = 2/3\lambda^2(\alpha_1+\alpha_2-2\alpha_3)$$

and α_1, α_2 and α_3 are constants of the crystal field. They are connected with D, coefficient of the rhombic field in the following manner—

$$\left.\begin{aligned}(18Dq_0-12\sigma)\left(10Dq_0+\frac{1}{\alpha_1}\right)&=60\delta^2\\ (18Dq_0-6\sigma-6\delta)\left(10Dq_0+\frac{1}{\alpha_2}\right)&=15(3\sigma+\delta)^2\\ (18Dq_0-6\sigma-6\delta)\left(10Dq_0+\frac{1}{\alpha_3}\right)&=15(3\sigma-\delta)^2\end{aligned}\right\} \quad \ldots \quad (4)$$

where $\sigma = a(A+B)/2$ and $\delta = a(A-B)/2$, q_0 and a are the ratio's of the matrix elements of actual system with eight electrons to those for one electron system for cubic and rhombic field respectively.

Hence it is possible to calculate Dq_0, aA and aB from a knowledge of α's, which are calculated from the magnetic measurements by the help of the following equations. These equations are obtained directly from (3)

$$\frac{\alpha_1-\alpha_2}{n_1^2-n_2^2}=\frac{\alpha_1-\alpha_3}{n_1^2-n_3^2}=\frac{1}{8}\left[\frac{1}{8\lambda-\frac{2\lambda^2}{kT}-3kT}\right]$$

and

$$\alpha_1+\alpha_2+\alpha_3=\frac{3}{8}\left[\frac{n^2-8}{8\lambda-3kT}\right].$$

Table IV gives the values of Dq_0, aA and aB for the three crystals $NiSO_4.6H_2O$, $NiSO_4.7H_2O$ and $Ni(CH_3COO)_2.4H_2O$ for which fine structure data are available. n_1^2, n_2^2 and n_3^2 are taken to correspond $n_\parallel$, $n_\perp$ and $n_\perp$ for the paramagnetic unit, which possesses an approximate axis of symmetry.

TABLE IV

Crystal	$n_\parallel^2$	$n_\perp^2$	$\bar{n}^2$	$\alpha_1 \times 10^{-5}$ cm^{-1}	$\alpha_2=\alpha_3$ $\times 10^{-5}$ cm^{-1}	Dq_0	aA	aB	$\frac{\Delta K}{K}\times 100$
$NiSO_4$ 6HO	9.68	10.51	10.23	−6.9	−9.2	1449	922	922	7.7
$NiSO_4.7H_2O$	9.67	10.52	10.24	−6.83	−9 25	1464	926	926	6 4
$Ni(CH_3COO)_2.4H_2O$	10.28	11.27	10 94	−9.24	−12.03	1087	670	670	9 2

$n_\parallel$ and $n_\perp$ represents the effective magnetic moments of the paramagnetic unit when the magneic field is applied along and perpendicular to the symmetry axis of the unit and $\bar{n}$ is the corresponding mean moment.

It is very satisfactory that Dq_0, aA and aB are very nearly equal in the two salts $NiSO_4.6H_2O$ and $NiSO_4.7H_2O$. Dq_0 which determines the size of the octahedron of water molecules about the Ni^{++} ion is almost of the same size in the above two salts but considerably greater in $Ni(CH_3COO)_2.4H_2O$.

RELATIVE CONTRIBUTIONS OF THE DIFFERENT TERMS TO THE EFFECTIVE MAGNETIC MOMENTS IN DIFFERENT DIRECTIONS OF THE PARAMAGNETIC UNIT

Equations (3) shows that in any direction the square of the effective magnetic moment consists of terms which are independent of temperature and terms which vary with temperature. For the three salts namely $NiSO_4.6H_2O$ and $NiSO_4.7H_2O$ and $Ni(CH_3OO)_2.4H_2O$ the contributions by the various terms are shown in Table V.

TABLE V

Crystal	Contribution to $n_{\parallel}^2$ by			Contribution to $n_{\perp}^2$ by		
	Temperature independent term.	Temperature dependent term.		Temperatnre independent term.	Temparature dependent term.	
	$8+64\lambda\alpha_1$	$24kT\alpha$	$8\theta_1/kT$	$8+64\lambda\alpha_3$	$24kT\alpha_2$	$8\theta_2/kT$
$NiSO_4.6H_2O$	8+1.479	.3488	−.1296	8+1.972	.4688	+.0647
$NiSO_4.7H_2O$	8+1.464	.3458	−.1373	8+1.983	4688	+.0686
$Ni(CH_3COO)_2\,4H_2O$	8+1.972	.4688	−.1592	2+8.577	.6112	+.0796

It willl be seen from the above table that the temperature-dependent term consists of two parts; one part varying directly with temperature while the other inversely as the temperature. At room temperature (*i.e.*, 30°C) the term varyirg inversely as temperature is alomost negligible. It does not contribute anything to the mean effective moment. The magnetic moment along the axis of symmetry of the paramagnetic unit is opposed by it, while it helps moments for directions normal to the axis of symmetry. The temperature-independent term greatly predominates over the contributions by other terms. The contribution of the term varying directly as the temperature is only 3 to 4% of the contribution of the term independent of temperature. The contribution of the spin-orbit interaction between the lowest and the upper components of the ground-term is only 16 to 20% of the spin-only value 8.

STARK SPLITTING AND MAGNETIC ANISOTROPY

If the crystalline field acting on the Ni^{++} ion is purely cubic, then Dq_0 which is proportional to the Stark-splitting by the cubic field is given by

$$Dq_0 = {}^4/_3\left[\frac{3kT-8\lambda}{n^2-8}\right]$$

For the three salts $NiSO_4.6H_2O$, $NiSO_4.7H_2O$ and $Ni(CH_3COO)_2.4H_2O$ these values are 1189, 1184 and 1044 cm^{-1} respectively. The presence of rhombic terms raises these values as shown in Table IV.

The cubic part of the field determines to a first approximation the mean square of the effective magnetic moment n^2, *i.e.* its deviations from the free ion value and that the rhombic part have very little effect on n^2 though the whole of the anisotropy is due to it. For Ni^{++} ions the cubic splitting also influences the percentage anisotropy to a certain degree. For according to Van Vleck (1932), the magnetic anisotropy of Stark level for Ni^{++} ion with positive D as shown in figure (1) exists only by virtue of the difference between the frequencies ν (ab), ν(ac) and ν(ad) or between ν(ac), ν(af) and ν(ag).

Since the rhombic separation is small in comparison with cubic separation the percentage anisotropy should be small. The following table gives the splitting by the two fields.

TABLE VI

Crystal	Overall Cubic splitting in cm^{-1}	Overall Rhombic splitting of Level 3 (approx.) in cm^{-1}	$\frac{\Delta K}{K} \times 100$
$NiSO_4.6H_2O$	26,100	7,250	7·4
$NiSO_4.7H_2O$	26,350	7,320	6.4
$Ni(CH_3COO)_2.4H_2O$	23,160	6,400	9.2

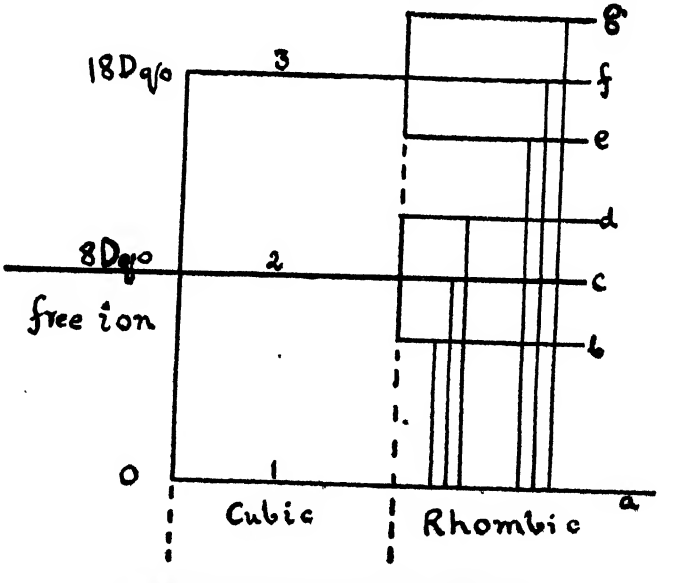

Stark patterns of Ni^{++} ion with positive D,

FIG. 1

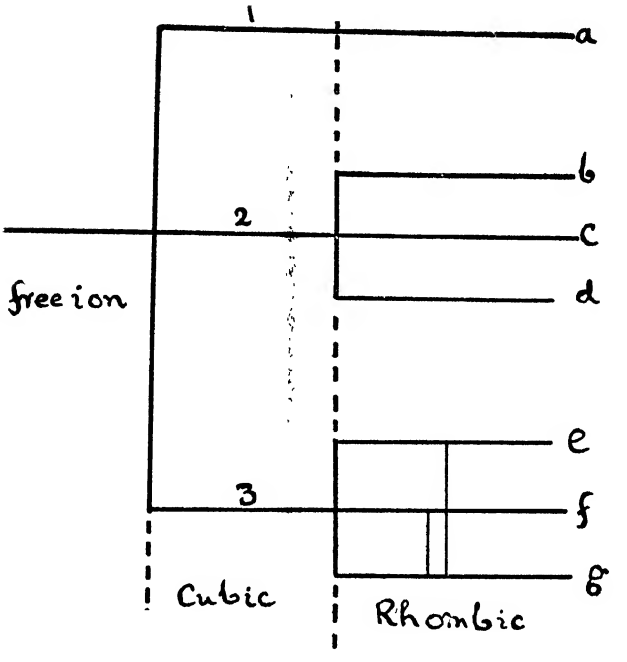

Stark pattern of Co^{++} ion with positive D.

FIG. 2

As will be seen from Table VI the paramagnetic unit in the salt $Ni(CH_3COO)_2\ 4H_2O$ has the least cubic and rhombic splitting but its anisotropy is the highest of the three, indeed it is the highest of all the nickel salts studied so far (Krishnan and Mookherji, 1937). If the rhombic splitting in the three crystals be the same, the less cubic splitting in $Ni(CH_3COO)_2.4H_2O$ makes the percentage difference between the frequencies ν(ab), ν(ac) and ν(ad) or between ν(ac), ν(af) and ν(ag) more and hence % anisotropy is also more. As a result of this the general impression is that the more the rhombic splitting the more will be the anisotropy of the paramagnetic unit will not be true for Ni^{++} ions, but will be true for Co^{++} ions. The Stark patterns of Co^{++} ion with positive D as shown in figure 2 is nothing but upside down of the Stark patterns for Ni^{++} ion with positive D. The anisotropy of 'g' in Fig. 2 exists by virtue of the difference between the frequencies ν(gf)-and ν(ge), 'g' being the ground state. The overall rhombic splitting in case of $Co(NH_4)_2(SO_4)_2.6H_2O$ as calculated by Penny and Schlapp (1932) with a field 20 (x^2-z^2) is 480 cm^{-1}, hence the percentage anisotropy in Co^{++} ion will be very high, which will be solely influenced by the rhombic splitting alone. In case of Co^{++} ions in crystals rhombic splitting will produce not only all the anisotropy but also will bring down n^2.

For comparison with $Ni(CH_3COO)_2.4H_2O$ we have studied a cobalt salt namely $Co(CH_3COO)_2.4H_2O$. In the paramagnetic unit of this salt whether

$K_{\parallel}$ is greater or smaller than $K_{\perp}$, the percentage anisotropy will not vary much from 76% which is the highest of all the cobalt salts studied so far (Krishnan and Mookherji *loc. cit.*). Rhombic splitting seem to be very high in this salt. Taking the same distributions of oxygen atoms about Co^{++} ion as in $Ni(CH_3COO)_2.4H_2O$ and taking $K_{\perp}$ greater than $K_{\parallel}$ one can calculate $(K_{\perp}-K_{\parallel})$ since the crystal is monoclinic and contains two molecules in the unit cell (Hull, 1934). The magnetic constants of the paramagnetic unit are

$$\left.\begin{aligned} K_{\perp}-K_{\parallel} &= 7890 \\ \bar{K} &= 10{,}630 \end{aligned}\right\} \times 10^{-6} \text{ at } 30^{\circ}\text{C}.$$

and the corresponding squares of the magnetic moments are

$$n_{\parallel}^2 = 13.4, \qquad n_{\perp}^2 = 32.8, \qquad n = 26.3,$$

which approximately fit with a rhombic field $200\,(x^2-z^2)$ giving a splitting of 2,400 cm^{-1}. Hence it would be very interesting to study this crystal at low temperatures and see whether the experimental results agree with those calculated by Penny and Schlapp with $Dq_0 = 12.00\ cm^{-1}$ and a rhombic field $200(x^2-z^2)$.

In conclusion the author wishes to express his thanks to the Committee of Management of the Indian Association for the Cultivation of Science for the facilities of the Laboratory, where the experimental works were carried out and also to Professor K. Banerjee, D.Sc., F.N.I. for his interest in the work. Thanks are also due to Mr. R. K. Sen, M.Sc., for his valuable discussions.

BIRLA COLLEGE, PILANI,
JAIPUR STATE.

REFERENCES

Angus, W. R. (1932), *Proc. Roy. Soc.*, **A.**, **136**, 569.
Beevers, C A. and Lipson, H. (1932), *Z. Kristallo.*, **83**, 123.
Beevers, C. A. and Schwartz (1935), ,, ,, **91**, 157.
Hoffmann (1931), *Z. Kristallo*, **78A**, 279.
Hull (1934), *Phys. Rev.*, **46**, 329.
Krishnan, K. S. and Banerji, S. (1934), *Philos. Trans*, **234A**, 265.
Krishnan, K S. and Mookherji, A. (1937), *Philos. Trans.*, **237A**, 135.
Laporte, O. (1928), *Zeit fur Physik.*, **47**, 761,
Penney, W. G. and Schlapp, R. (1934). *Phys, Rev.*, **42**, 666.
Stoner, E. C. (1935), Magnetism and Matter, 470 (1937).
Van Vleck, J. H. (1932), *Phys. Rev.*, **41**, 208.

TEMPERATURE VARIATION OF INTENSITY OF LUMINESCENCE UNDER X-RAY EXCITATION

By H. N. BOSE

ABSTRACT. The variation of the intensity of X-ray luminescence with temperature ranging from 30°C to 150°C for sodium chloride, sodium chloride with copper, potassium chloride, potassium chloride with copper, potassium bromide, potassium bromide with copper, uranyl nitrate, naphthalene and anthracene has been obtained, the measuring instrument being a photocell with amplifying device. The variation curve is found to be of distinctly two types. The intensity of luminescence for sodium chloride, sodium chloride with copper, potassium chloride and the same with copper varies with temperature, at first slowly, then quickly, finally reaching almost a steady value in the temperature range under investigation. For potassium bromide and potassium bromide with copper, possibly only the later portion of the curve is obtained. For others the intensity of luminescence is almost temperature independent till the melting point is reached when intensity falls to zero. The inclusion of copper ions does not seem to make any qualitative difference in the behaviour of the phosphors.

It has been known for a long time that temperature is an important factor in determining the intensity of luminescence of a phosphor. Substances are known which fluoresce only at low temperature. An excited electron can release its energy and come back to its lowest state in two ways, either with emission of radiation or by dissipation of energy as heat. The variation of the relative probabilities of the two processes will obviously depend on the behaviour of the normal and excited states of the crystal with change of temperature. Various mechanisms have been suggested by Seitz (1939), Mott (1938) etc., to account for increase of probability of transference of excitation energy into heat with the rise of temperature.

At the present time the difficulties of directly determining the energy zones of even a simple crystal with sufficient accuracy are extremely great ; inspite of the great deal of work done up to date, the mechanism of the production of luminescence with all its varied phenomena is as yet obscure. It is not unreasonable to expect that the investigations into the variation of intensity of luminescence with temperature may throw some light on the mechanism of luminescence, on the nature of the radiative centres etc. The temperature variation of the intensity of luminescence has, as yet, received very little attention from the experimental workers; the only work done is that of Randall (1937). He measured the intensity of luminescence at different temperatures (90°K – 600°K) for a number of sulphide phosphors. He has observed in general a drop in the intensity of luminescence with the rise of temperature. In certain phosphors, the intensity drops also at low temperatures; the cause of this drop is rather uncertain. Mott and Gurney (1940) have, however, tried to explain

it on the assumption that the incident light is of a wavelength which produces only excitations in the lattice. His results are shown in Fig. 1.

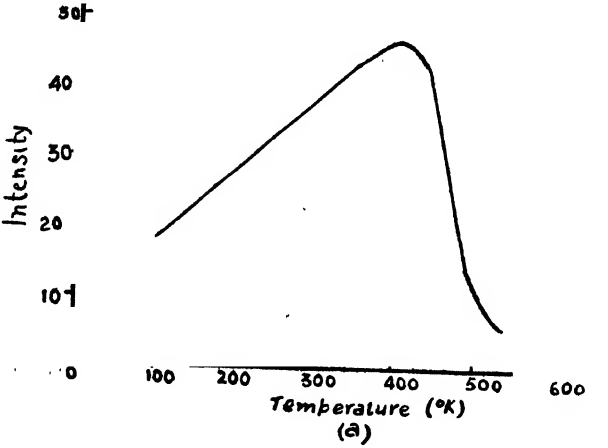

FIG. 1

Temperature variation of the intensity of fluorescent radiation in zinc sulphide phosphor.
(*a*) Impurities Mn, Mg, Ba, Si

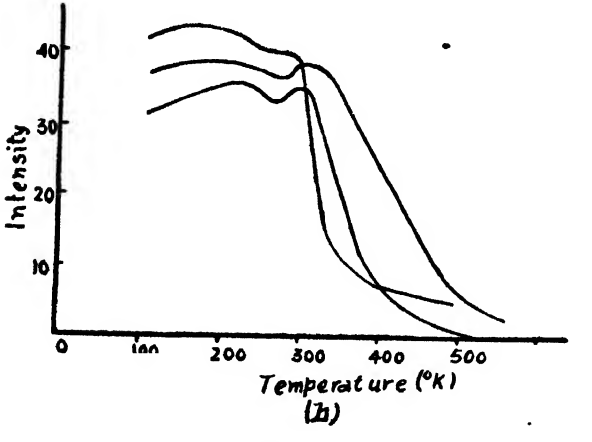

FIG. 1

(*b*) Various specimens activated by Ag, Cu, Mg

The present work differs from that of Randall in that the intensity of luminescence of different types of phosphors under X-ray excitation has been measured here while Randall measured the intensity of luminescence of phosphors like ZnS, ZnS + CdS etc., under ultraviolet excitation. As has been pointed out by Randall in ultraviolet excitation, the constancy of the absorption

coefficient over wide range of temperature has to be assumed. This still awaits experimental confirmation. The absorption coefficient of X-rays does not change with temperature and so the number of free electrons produced inside the crystals can be taken to be the same irrespective of temperature for all practical purposes.

EXPERIMENTAL ARRANGEMENT

X-ray from a Hadding tube, run at 30 K.V.—5 mA was the exciting radiation. The intensity of X-rays could be kept almost steady during the small period of time required for a single experiment. This could be verified by observing the intensity of luminescence at small intervals at the room temperature. Experimental substances were taken in the form of pressed powder blocks which were placed inclined at nearly 45° to the incident X-rays and the luminescence light focussed by a lens on the photocell. The current in the milliammeter was first observed without the luminescent substance and indicator adjusted to zero. Subsequent measurements covered the range from 30°C to 150°C and the substance was placed inside a nichrome wire heater. The

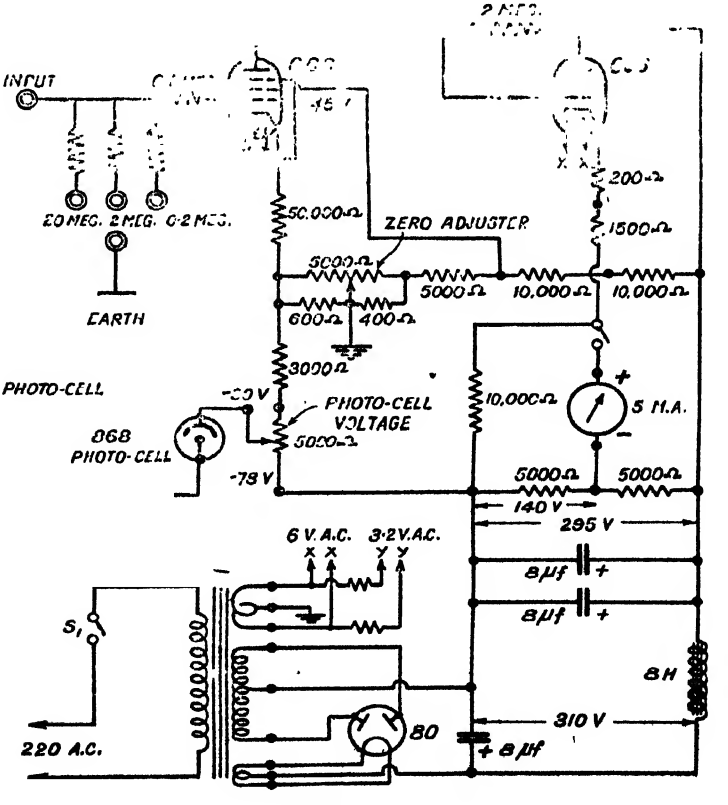

FIG. 2

temperature of the sample was measured with a calibrated thermo-couple placed in contact with the back side of the sample.

The measuring instruments *consisted of a photocell (type 868 R.C.A.) followed by a D. C. amplifier operating a milliammeter. The voltage applied to the photocell is adjustable and may be varied between 30 to 78 volts. The D. C. amplifier has been specially designed to have linear characteristics which did not sensibly change with use. The photocell possesses a dark current of about 1/100 of a micro ampere. Imput resistances of 0.2 megohms, 2 megohms and 20 megohms are provided inside the meter to change the range of sensitiveness. A circuit diagram is shown in Fig. 2.

The measurements were also repeated with another photovoltaic cell connected directly to the galvanometer. As only relative values are required for the present purpose, readings of the meters have been plotted against temperature.

RESULTS AND DISCUSSIONS

Luminescence of sodium chloride and sodium chloride with copper impurity:

Temperature intensity curves are shown in figure 3. Samples of pure * chloride and copper activated sodium chloride were the same for which the lumi-

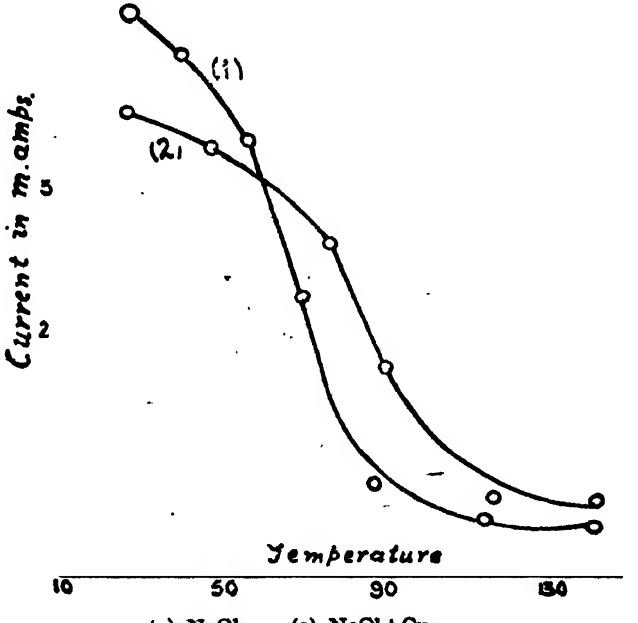

(1) NaCl. (2) NaCl+Cu.

FIG. 3

* Foot candle meter was constructed and calibrated in the Wireless Laboratory of Physics, Calcutt University.

nescence spectra have been photographed. A fall in the intensity with the rise of temperature is observed in both cases. The rate of decrease, at first small, quickly rises to a maximum and then falls again to almost zero value. The temperature at which the sharp decrease in intensity occurs is however different for the two samples. From the spectra of luminescence we find that the spectral region of emission does not appreciably change with the introduction of copper. However the intensity of luminescence decreases with the inclusion of copper ions as impurity. The temperature at which the steep fall in intensity occurs is also raised; the ratio of the limiting intensity of luminescence at high temperature to its intensity at 80°C is however greater for the impure sample.

Luminescence of potassium chloride and potassium chloride with copper impurity :

In this case also all experimental samples were prepared from the same material. The general nature of the results is the same as that found for sodium chloride. The inclusion of copper ions affects the total intensity of the phosphors, the temperature of maximum rate of change of intensity, and the residual intensity in the same way (Fig 4).

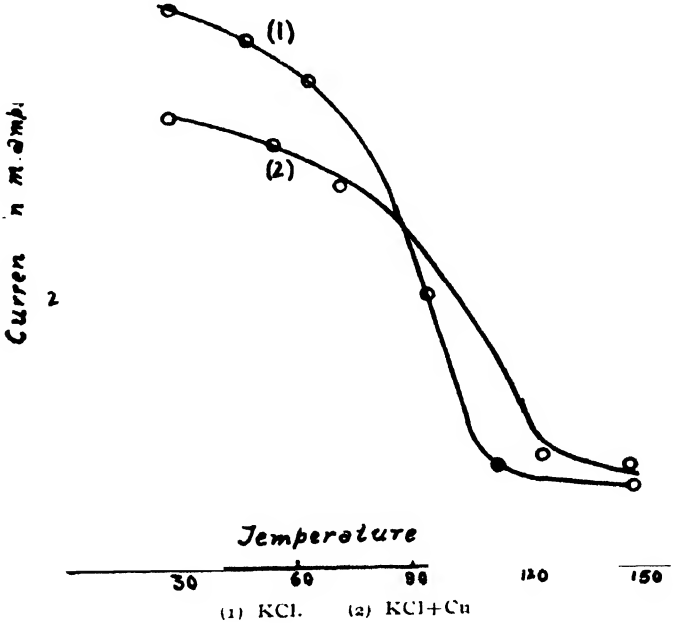

(1) KCl. (2) KCl+Cu

FIG. 4.

Luminescence of potassium bromide and potassium bromide with copper impurity :

In case of potassium bromide the intensity decreases gradually and no sudden decrease in intensity at a particular temperature is perceptible as in the

preceding two cases. The inclusion of copper ions does not also seem to produce any great change in the behaviour of the intensity of luminescence of the phosphors with change of temperature (Fig. 5).

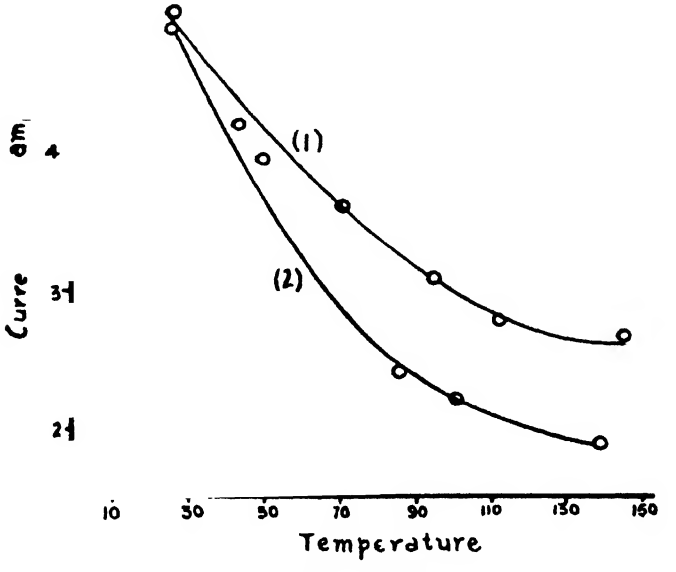

(1) KBr+Cu (2) KBr

FIG. 5

Luminescence of uranyl nitrate :

The change of intensity of luminescence of uranyl nitrate with rise of temperature is shown in Fig. 6. The intensity of luminescence remains constant within experimental accuracy and suddenly falls to zero value at about 59°C. Uranyl nitrate used here was the hydrated variety containing six molecules of water of crystallisation. This hydrated uranyl nitrate melts, i.e., dissolves in its water of crystallisation, at about 59°C. The abrupt cessation of luminescence is therefore due to the breaking up of the lattice of the solid state.

Luminescence of naphthalene :

The temperature-intensity curve of naphthalene is shown in Fig. 7. The intensity of luminescence remains approximately constant up to about 80°C where naphthalene melts and ceases to show any perceptible luminescence.

Luminescence of anthracene :

Anthracence melts at about 216°C. The results of measurements above 150°C are not very accurate. The general nature of results appears to be the

same as that in the case of naphthalene or uranyl nitrate. The intensity of luminescence does not vary appreciably with temperature till the melting point is reached when the intensity suddenly drops to zero (Fig. 8).

All substances have been purified by repeated crystallisation before use; however it is quite possible that they nevertheless retained traces of unknown

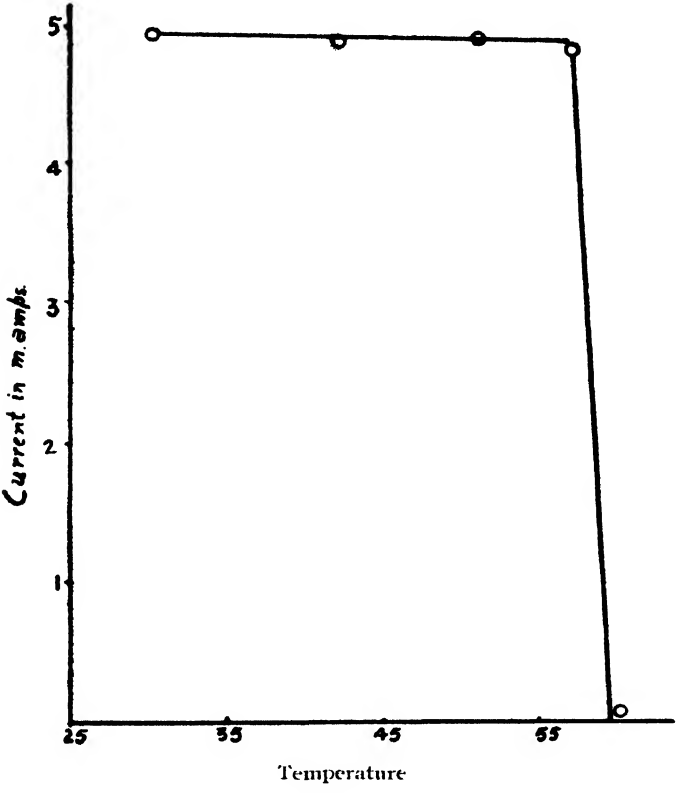

FIG. 6

impurities. Levy and West (1939) measured, by the spectroscopic method, the intensity of fluorescence and phosphorescence of zinc sulphide and found that it is greatly affected by minute traces of impurity. It is therefore difficult from the present measurement alone to come to a definite conclusion about the intensity of luminescence of the pure phosphors and the effect of inclusion of a particular impurity. Inspite of this limitation it is however reasonable to think that the present investigation yields certain general results which are at least qualitatively correct.

The temperature variation of intensity of luminescence is found to be distinctly of two kinds. Crystals like naphthalene, anthracene and uranyl nitrate retain much of their molecular character in the solid state. The aromatic molecules like those of naphthalene and anthracene possess electrons which are

free to move round the molecule; possibly these are the electrons which are also responsible for the optical behaviour of crystals. In the case of uranyl nitrate the optical electrons of UO_2 group are responsible for the luminescence spectra; for, under ultraviolet excitation uranyl salts are found to fluoresce in the crystalline state as well as in solution; the fluorescence spectra in the two states are also identical except that the bands emitted in solution are more diffuse.

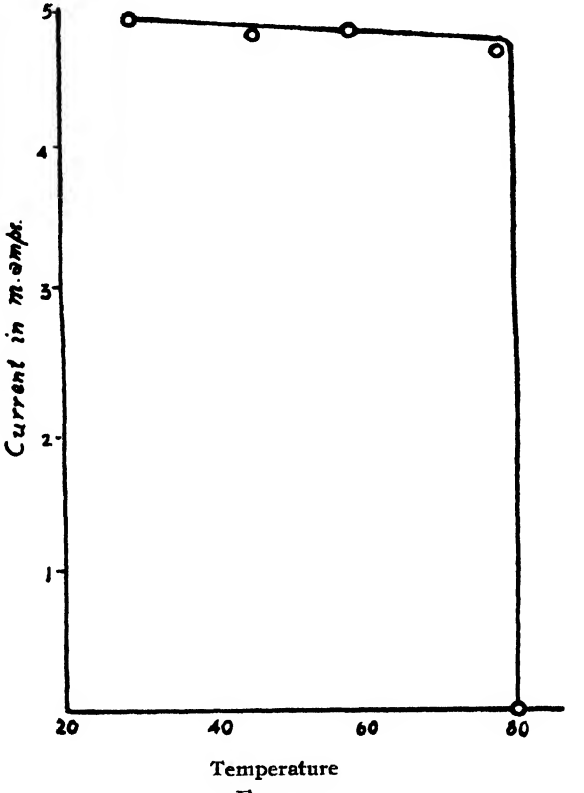

FIG. 7

In naphthalene, anthracene and uranyl nitrate, the optical electrons, though excited, do not leave the molecules or atomic groups to which they belong. In such crystals the intensity of luminescence is almost independent of temperature. There is thus an apparent connection between the rapid extinction and photo-ionisation of molecules.

Since the mass absorption coefficient of X-rays is independent of temperature, the number of photoelectrons produced per second within the crystal by the incident X-rays may be assumed to be constant. These electrons moving inside the lattice in all directions suffer collisions with the electrons and nuclei of the crystal and excite some of the optical electrons. The results of the present investigations show that the number of inelastic collisions suffered by the

photoelectrons with the molecules of a crystal is not much influenced by rise of temperature at least within the range of temperature under consideration.

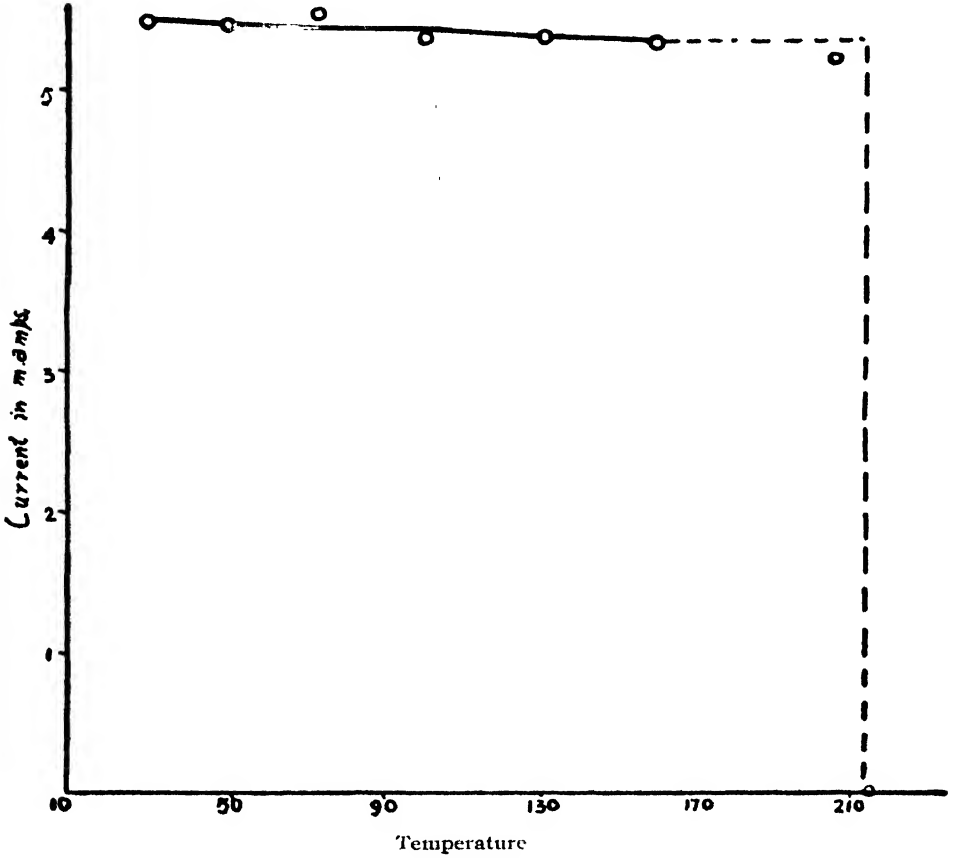

FIG. 8

The mechanism of luminescence of sodium chloride and potassium chloride crystals will be discussed in a separate paper (Luminescence of solids under X-rays). Without making any assumption as to the nature of the radiative centres we can assume that the number of centres where the electron can release its energy as radiation is not very large ; in general the released electron comes back to the valence band without emission, releasing its energy as heat ; otherwise the efficiency of luminescence would have been much larger. Even at those centres there is a probability that the non-radiative transitions should occur ; Peierls (1932) has considered the possibility of such transition. Though it is not yet possible to give quantitative data, he finds that the probability of non-radiative processes increases rapidly as the temerature is raised. In order to be able to interpret the cruve in detail we need further knowledge about the radiative centres. If the centres be such as have been created by X-ray itself

(stoichiometric excess of sodium) then the rate of decrease of intensity of luminescence will be determined by the rate of production of such centres. Such centres created probably by the trapping of electrons will be brought back to their normal state by their release of thermal energy. In that case the sudden fall in intensity will occur at a temperature at which the trapped electron finds it most convenient to be rescued from the trap. The residual intensity may be due to the presence of a temperature independent mechanism for radiative transition even in these crystals. This is further justified by the presence of two bands in the spectra, one of them being rather sharp.

The behaviour of potassium bromide seems to be just intermediate between the two kinds of phosphors considered. It therefore appears that in potassium bromide two types of centres—one like that of uranyl nitrate and another similar to those in NaCl or KCl—are present; possibly only the later portion of the curve is obtained there.

The effect of inclusion of copper ions on the intensity of luminescence leads us to the conclusion that, unlike the thalium activated sodium chloride under ultraviolet excitation, in X-ray luminescence the impurity ions (at least the copper ions) are not directly responsible for the luminescence. The impurity influences the luminescence indirectly in this case; the intensity is decreased slightly, which is analogous to the quenching effect found in certain cases of ultraviolet excitation. In those cases the effect is explained as collision of second kind with the quencher whereby the energy is transferred without emission. In solids the mechanism cannot be the same; but it is possible that some of the excited electrons release their energy near the impurity centre without radiating.

My thanks are due to Prof. S. N. Bose, Khaira Professor of Physics, Calcutta University, for facilities of work in his laboratory and for his kind interest during the progress of the work.

I am also indebted to Prof. S. K. Mitra, Ghose Professor of Physics for having lent the Foot candle meter.

KHAIRA LABORATORY OF PHYSICS,
CALCUTTA UNIVERSITY.

REFERENCES

Levy, L. & West, D. W., 1939, *Trans Farad. Soc.*, **35**, 128
Mott, N.F. and Gurney, R.W., 1940, Electronic processes in ionic crystals (Oxford), p 223
Mott, N. F., 1938, *Proc. Roy. Soc.*, **167**, 384
Peierls, R., 1932, *Ann. d Physik*, **13**, 1905
Randall, J. T., 1937, *Proc. Phys. Soc.*, **49** (extra part), 46.
Seitz, F., 1939, *Trans. Farad. Soc.*, **35**, 79.

ON THE X-RAY DIFFRACTION PATTERNS OF BLEACHED JUTE FIBRE

By S. C. SIRKAR* and S. K. CHOWDHURY

PLATES IA & IB

ABSTRACT. The half widths of the (002), (020) and (120) reflections from jute fibre of five trade qualities in the bleached condition have been compared with those observed in the case of these fibres before bleaching. It is observed that the width of both (002) and (120) reflections becomes smaller and that of (020) reflection becomes larger with the bleaching of the fibre in the case of high quality white, Tossa and White top jute, but no marked change in the half widths of the reflections is observed with the bleaching of the fibre in the case of low quality White and Chinsura green jute fibre. It is pointed out that in the case of the former three qualities some of the linkages between the glucose residues are damaged on bleaching the fibre and thereby the length of the chain is diminished. Side bonds, however, are formed even in absence of the lignin molecules and the width of the micelles is thereby increased in these cases on bleaching the fibre. Itlis also pointed out that of all the qualities studied Tossa (high quality) has the largest chain length.

INTRODUCTION

In the preliminary investigations on the structure of bleached jute fibre Sirkar, Saha and Rudra (1944) observed that a faint broad ring passing through the (002) reflection in the pattern due to the untreated jute fibre disappears on bleaching the fibre. Later Sirkar and Saha (1946) pointed out that the results obtained by them in the case of high quality Bogi jute fibre indicated a diminution of the length of the micelles with the bleaching of the fibre. As these results have some bearing on the methods which may be employed for restoring the strength of the bleached jute fibre, the width of the (020), (002) and (120) reflections has been studied in the case of high quality White and Tossa, White top, low quality White and Chinsura green jute fibre in the bleached condition and these results have been compared with those observed in the case of these fibres before treatment. The results have been discussed in the present paper.

EXPERIMENTAL

Small bundles of samples, each about one foot in length, were collected to represent the five qualities of jute fibre mentioned above from the large bundles kindly supplied by the Director, Technological Reseach Laboratories, Indian Central Jute Committee. A small portion of each of these samples was dried in the sun and weighed. It was then bleached in aqueous solution of ClO_2 for two days, washed and dried in the sun and was again weighed. A loss of about 10% in the weight was observed in each case after the fibre had

* Fellow of the Indian Physical Society.

been bleached. The X-ray diffraction patterns due to these bleached fibres were obtained with a technique similar to that used by Sirkar and Saha (1946). In each case the pattern due to the original untreated sample was also obtained under identical experimental arrangements. The slit system was narrow enough to allow the (020) reflection to be recorded clearly in the photograph of the diffraction pattern. Microphotometric records of the (002), (020) and (120) reflections were obtained with a Moll type self recording microphotometer. Care was taken to allow the spot of light focussed on the film to move through the middle of each of these reflections across its width.

RESULTS & DISCUSSION

The photographs of the patterns due to four of the five qualities studied are reproduced in Plate IA. Those due to low quality white have not been reproduced. It is observed that in the case of all the five qualities the faint ring passing through the (002) reflection disappears completely with the bleaching of the fibre. This indicates that lignin in cellulose is amorphous and has a diffuse spacing of about 4.0 A.U. This is in agreement with the results obtained by Wedekind and Katz (1929) in the case of lignin extracted from cellulose, who also observed only one diffuse ring corresponding to a spacing of 4.0 A.U. The intensity of this ring observed in the case of jute fibre, however, is two small to account for the presence of 10% of lignin in the fibre. This fact shows that lignin is present only in very thin layers and the number of grating elements in the total thickness is too small to produce any diffraction pattern of large intensities. If the lignin molecule be quite large and the thickness of the layer of lignin within the fibre be such as can accommodate only one molecule, the x-ray pattern will hardly resemble the diffraction pattern due to a liquid or an amorphous substance, but on the contrary, it will resemble the pattern due to gaseous scattering which is diffuse and of small intensity. This feebleness of the ring due to lignin observed in the case of jute fibre probably indicates that the major portion of lignin present in the fibre forms a layer only about a molecule thick. A similar phenomenon has been observed by Katz and Mark (1925) in the case of absorption of water by cellulose fibre. Up to a certain percentage of water absorbed by the fibre they observed only a diffuse scattering which increased in intensity with the increase in the percentage of water absorbed and the ring due to water appeared only when the fibre was macroscopically wet.

Some of the microphotometric records obtained for measuring the widths of the (020), (120) and (002) reflections are reproduced in Plate IB which shows that although the (002) reflections produce large densities (020) reflections are rather feeble. Attempt has, however, been made to calculate the values of m_2 and m_3 which denote the number of times the unit cell is repeated along the *b*-and *c*-axis respectively by Laue's method employed previously by Sirkar and Saha (1946). The results are given in Table I. It can also be seen from Plate II

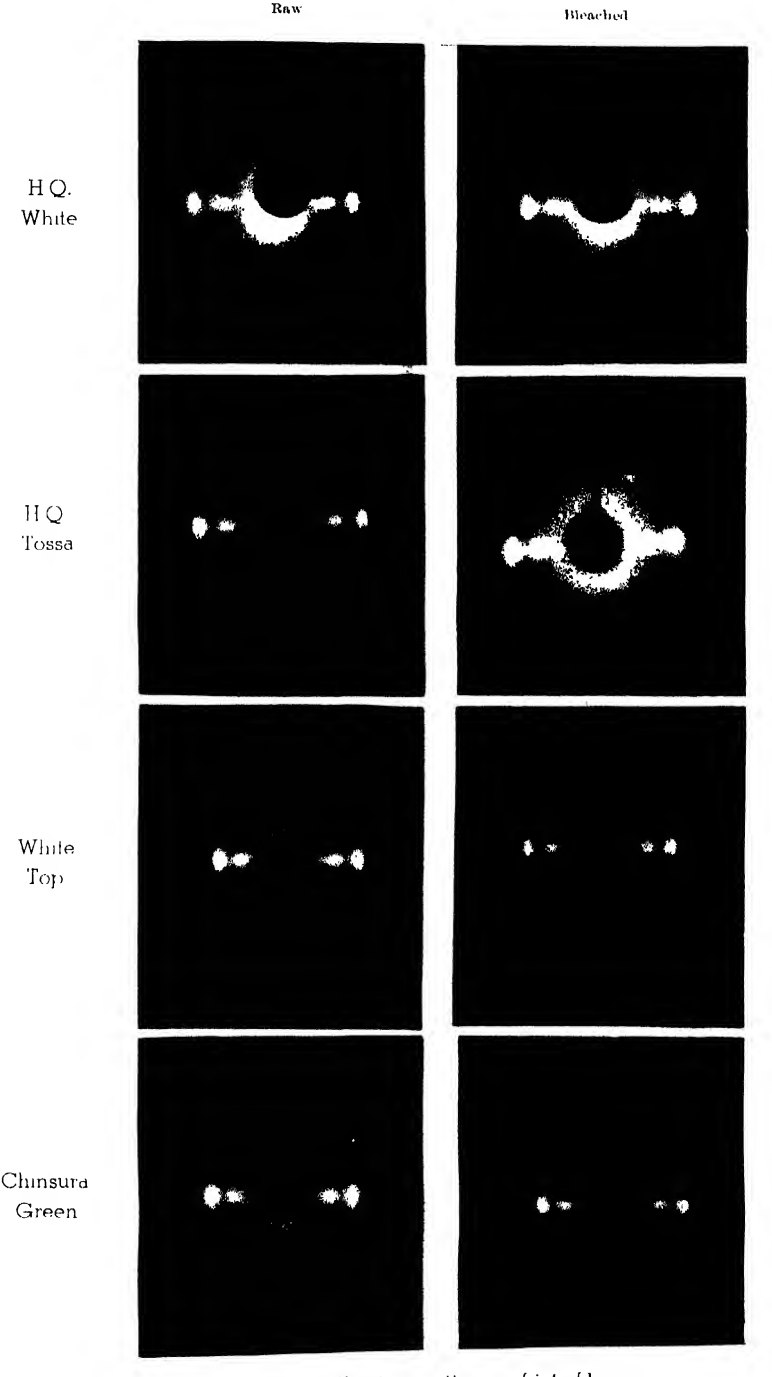

X-ray diffraction patterns of jute-fibres.

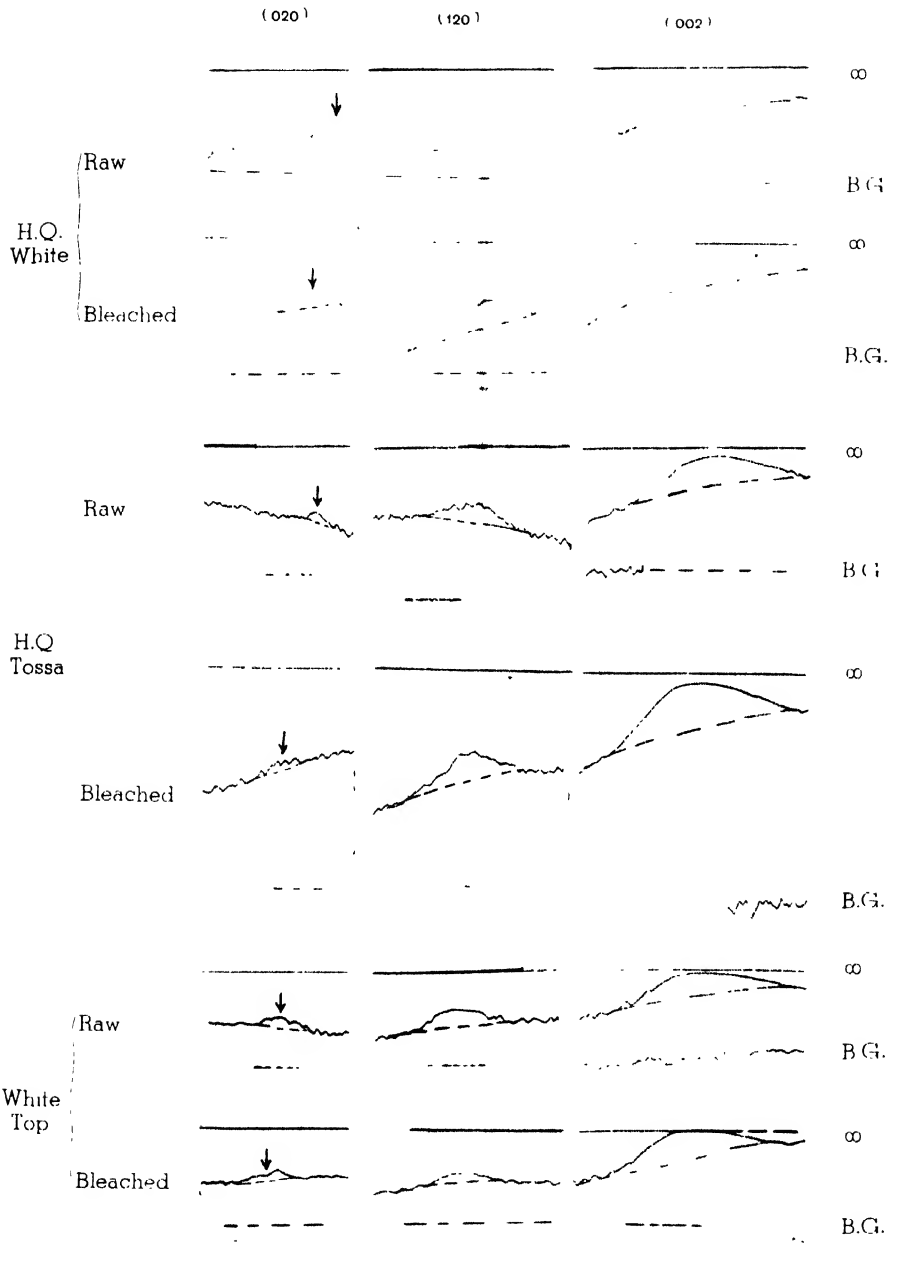

Microphotometric Records.

B.G. — Back-ground. ∞ - Infinite density.

that the half width of (120) reflection diminishes slightly on bleaching the fibre in the case of high quality White and Tossa jute and White top jute.

TABLE I

Quality of jute	Half width in radian		m_2	m_3
	(020)	(002)		
High White	.012	.022	11	8
,, ,, bleached	.015	.018	9	10
High Tossa	.009	.022	15	8
,, ,, bleached	.011	.018	12	10
White top	.011	.023	12	8
,, ,, bleached	0.014	.019	10	9

The results given in Table I show that in the case of each of the three qualities mentioned the chain length diminishes on bleaching the fibre while the value of m_3 increases. No such changes were observed in the case of low quality White and Chinsura green. In the case of bleached White top jute m_3 was calculated from the microphotometric record of a second photograph obtained with smaller exposure because the (002) reflection has infinite density in the record reproduced. The results given in Table I show that some of the oxygen bridges between glucose residues are broken up when lignin is removed by ClO_2, but the side bonds attach more such units together to increase the thickness of the micelle in absence of lignin. Hence it appears that although lignin molecules do not enter into the lattice of cellulose the micelles are held together by these molecules probably through some form of secondary bonds.

The values of m_2 are calculated in the present investigation direct from the width of (020) reflection and are therefore more accurate than those calculated by Sirkar and Saha (1946) from widths of other reflections. It is significant that high quality Tossa which has a strength larger than that of all the fibres studied has also the longest chain length ($m_2=15$). This fact corroborates the conclusion drawn by Sirkar and Saha (1946)from the results obtained by them that besides the presence of lignin, the length of the micelle is also partly responsible for the strength of the fibre. It is now quite evident from the above discussions that lignin does not act as a mere cement but some secondary chemical bonds are probably involved in making the jute fibre quite strong inspite of the fact that the length of its micelles are about one-tenth that of the micelles in ramie. The OH group of water absorbed by bleached jute fibre probably further weakens the oxygen bridges already damaged during removal of lignin and the chain length is still more diminished, so that in the wet condition bleached jute fibre possesses practically negligible tensile strength. Any attempt at restoring the

strength of the bleached fibre should therefore be directed at finding some reagent which may help in the formation of bridges between neighbouring glucose residues, increasing thereby the length of the chain.

ACKNOWLEDGMENT

The work was done under a scheme drawn up by Prof. M. N. Saha, F.R.S., and financed by the Indian Central Jute Committee. The authors are indebted to Prof. Saha for his kind interest in the work and for providing all facilities for the work in the Palit Laboratory, and to the Indian Central Jute Committee for the financial help.

PALIT LABORATORY
PHYSICS DEPARTMENT,
UNIVERSITY COLLEGE OF SCIENCE,
CALCUTTA.

REFERENCES

Katz, J. R. and Mark, H. (1925), Sorption of water by cellulose, *Z. Physik. Chem* **115**, 385.

Sirkar, S. C., and Saha, N. N. (1946), The orientation and size of micelles in jute fibre. *Proc. Nat. Inst. Sc. India*, **12**, 151.

Sirkar S. C., Saha N. N. and Rudra, R. M. (1944), X-ray analysis of jute fibre of different qualities under various conditions. *Proc. Nat. Inst. Sc. India*, **10**, 325.

Wedekind, E. and Katz, J. R. (1929), Structure of lignin. *Ber.*, **62B**, 1172.

ON THE RAMAN SPECTRA OF A FEW ALIPHATIC KETONES AT LOW TEMPERATURES

By S C. SIRKAR* and B. M. BISHUI

(Plate II)

ABSTRACT. The Raman spectra of acetone, diethyl, methyl-ethyl-and di-*n*-propyl ketone have been studied in the solid state at about −170°C and in the liquid state at the room temperature. The polarisation of the Raman lines in the liquid state has also been studied. It is observed that some of the prominent Raman lines undergo changes in position and intensity with the solidification of the substances at the low temperature. The line 1705 cm.$^{-1}$ due to the oscillation of the C=O group seems to be diminished in intensity in the solid state in the case of acetone, diethyl ketone and di-*n*-propyl ketone. A new line is observed in the low frequency region in each of the spectra of solid methyl, ethyl and diethyl ketone. These results have been discussed.

INTRODUCTION

The Raman spectra of a few aliphatic sulphides were studied previously in the solid state at low temperatures by the present authors (Sirkar & Bishui, 1943) and it was observed that some of the Raman lines undergo changes in frequency and intensity with the solidification of the substances at low temperatures. These changes indicate distortion of the molecules and in some cases probably formation of secondary association bonds between them, giving new lines in the low frequency region. The alternative explanation regarding the origin of the new lines in the low frequency region is that they are due to some types of lattice oscillations in which only electrostatic intermolecular field is involved. If this second explanation be correct it is expected that molecules having similar structure would give similar lines in the low frequency region in the solid state. In order to elucidate this point the investigations have been extended to four aliphatic ketones, the molecules of two of which are similar to those of two of the sulphides studied earlier, with the only difference that the sulphur atom of the sulphides is replaced by the C=O group. These results are discussed in the present paper.

EXPERIMENTAL

The technique used in the present investigation for studying the Raman spectra of the substances at the low temperatures is the same as employed in the previous investigation (Sirkar & Bishui, 1943). The substances studied are acetone, diethyl, methyl ethyl and di-*n*-propyl ketone. All these liquids were obtained from Kahlbaum's original bottles and redistilled in vacuum. The

* Fellow of the Indian Physical Society.

polarisation of the Raman lines due to the liquids have been studied by photographing the horizontal and vertical components simultaneously with the help of a double-image prism. The Fuess spectrograph used in the investigation gave a coma extending upto about 38 cm^{-1} on the Stokes side of 4046 A. U., and therefore the presence of any new Raman line with a lower frequency shift could not be detected. Inspite of the special care taken to solidify the substances slowly in order to obtain a homogeneous transparent mass, the spectrum of the scattered light showed the presence of strong continuous background due to extraneous light, and therefore it has not been possible to record all the faint Raman lines in the solid state. The spectrogram due to solid acetone, however was found to be quite satisfactory. For these reasons no special care has been taken to record all the faint Raman lines in the liquid state of these substances.

RESULTS AND DISCUSSION

The results are given in Table I-IV. The polarisation of the lines is indicated by the letter P and total depolarisation by D. The approximate intensities are given in parentheses. The lines in the low frequency region ($\Delta \nu < 120$ cm^{-1}) and those with higher frequencies are discussed separately in the following paragraphs.

TABLE I

Acetone

Liquid at about 30°C		Solid at about −170°C Present authors
Previous authors	Present authors	
392 (2) D	392 (1) e ; D	95 (ob) k ?
487 (½) ?	487 (0) e ?	
527 (2) P	528 (3) e, k ; D	
789 (5) P	790 (8) e, k ; P	800 (3) e, k
903 (0) ?	903 (0) e, k ; P	
1065 (1) P	1065 (1) e, k ; P	1062 (0) e, k
	1222 (2) k ; D	
1221 (1) D	1358 (0) k ; P	
1358 (0) P	1423 (4b) e, k ; D	1430 (1) e, k
1423 (3b) D	1705 (5) e ; P	1702 (1) e
1705 (5) P		
2689 (0) ?	2690 (0) e, k ; P	
2857 (ob) ?	2857 (2b) e, k ; P	
2923 (10) P	2923 (10) e, k ; P	2925 (5) e, k
2964 (4) —	2964 (3) e, k ; D	2976 (3) e, [k]
3006 (4) —	3006 (3) e, k ; D	3008 (3) e, k

TABLE II

Diethyl Ketone

Liquid at about 30°C		Solid at about −170°C
Kohlrausch and Köppl	Present authors	Present authors
228 (0) e		
342 (½) e, c		95 (3b) k ?
408 (3b) k, e, c	406 (3b) e, k , P	417 (1b) e
589 (1) k, f, e		
728 (1)	746 (2b) e, k , P	786 (1b) e, k
1092 (2b k, e	786 (2b) e, k ; P	
	950 (1b) e, k ; P	950 (1b) e, k
1155 (0) e	1010 (1b) e, k ; P	
1230 (0) e	1093 (4) e, k ; P	1005 (0b) e, k
	1238 (2) k ; P	1095 (1) e, k
1418 (4b) k, e	1271 (0) k ?	
1457 (4b) k, e	1418 (2b) e, k $\rho>0.5$	1418 (1b)
	1460 (3b) e, k $<6/7$	1460 (1) e, k
1710±8 (4b) f, e	1706 (5b) e ; P	1702 (1) e
2670 (0) k		
2800 (5b) k		2890 (0b) k
2882 (7b) k, i, e	2893 (10b) e, k, q ; P	2920 (2) e, k
2916 (8) k, i, e	2940 (10) e, k, q ; P	2948 (4) e, k
2936 (10b) p, k, i, e	2988 (6) e, k q, $\rho>.5<6/7$	2982 (3) e, k, q
2979 (5b) q, p, k, e		

TABLE III

Methyl Ethyl Ketone

Liquid at 30°C		Solid at about −170°C
Kohlrausch and Köppl	Present authors	Present authors
258 (1) e, k	260 (1) e ; D ?	90 (2) k ?
408 (3) c, e, k	401 (3) e, $\rho<6/7$	
	510 (0) e ?	
592 (3) c, e, f, k	590 (4) e, k ; P	590 (1b) e, k
763 (7) c, e. f, k	760 (8) e, k ; P	770 (2) e, k
812 (0) e		
947 (1b) e, k	950 (1b) e [k] ; P	
1001 (1b) e, k	1002 1b) e, k ; P	
1088 (3) e, k	1090 (4) e, k ; P	1090 (0) e, k
1165 (½) e, k	1170 (3 k ; P	
1247 (½) e, k	1252 (1) k ?	
1412 (3b) e, k	1350 (1) e, k ?	
1450 (3b) e, k	1419 (5) e, k ; D	1416 (1) e, k
	1460 (4) e. k ; D	1460 (0) e
1711±10 (3b) e, f	1705 (6) e ; P	1702 (0b) e
2917 (10b) e, i, k, q	2890 (5) e, k ; P	2896 (1) k
2900 (6b) e, k, p, q	2932 (10b) e, k ; P	2932 (5b) e, k
	2986 (5) e, k ; D	2986 (3) e, k
	3004 (2b) e, k ; D	3000 (1) k

TABLE IV

Di *n*-propyl Ketone

Liquid at about 32°C		Solid at about −170°C
Kohlrausch and Köppl	Present authors	Present authors
305 (5) e, f, k	308 (2) e ; ?	90 (ob) k ?
424 (1b) e		230 (o) e
527 (½) e	520 (ob) e ; ?	308 (o) e
529 (½) e		
626 (½) e		
716 (2) e, k	720 (ob) e, k ; ?	
814 (1) e, k		
866 (2) e, k	870 (ob) e, k ; ?	
914 (4) e, k	914 (1) e, k ; ?	
1037 (3b) e, k	1038 (4d) e, k ; P	1038 (1d)
1114 (3b) e, k	1118 (2) e, k ; P	
1201 (1) e, k	1206 (ob) k ; ?	
1269 (1) e, k	1270 (o) k ; ?	
1288 (1) e, k	1290 (o) k ; ?	
1410 (4b) e, k	1415 (2) e, k ; D	
1443 (7sb) e. k	1458 (5) e, k ; D	1440 (1)
1707±8 (4b) e, f	1705 (5) e ; P	1700 (1)
2735 (2) k	2740 (3) k ; ?	
2875 (12b) e, i, k	2880 (10) e, k ; P	
2913 (10) e, i, k, q	2918 (4d) e, k ; P	2886 (3)
2938 (10) e, i, k, q	2942 (10) e, k ; P	2925 (3)
2966 (9) e, k, q	2974 (5) e, k ; D	2966 (3)

LINES IN THE LOW FREQUENCY REGION

In all these cases a new line at about 95 cm^{-1} on the Stokes side of 4046 A.U. has been observed in the spectrograms due to the solid state. A weak broad band is, however, present exactly in this place in the spectrum of the incident light also. Hence it is difficult to say whether this line is a genuine new Raman line appearing in all these cases. Excitation by 4358 A.U. does not help to solve this question, because there is a strong mercury band at this

distance on the Stokes side of that line also. Careful examination of the spectrogram shows that in the case of diethyl and methyl ethyl ketone there is actually a new line at about 95 cm^{-1} and 90 cm^{-1} respectively superposed on the band observed in the incident spectrum. Hence it can be concluded that there are no new lines of frequencies larger than 38 cm^{-1} in the Raman spectrum of solid acetone, although two lines at 70 and 80 cm^{-1} are observed in the case of solid methyl sulphide. These results are therefore not explained satisfactorily by the hypothesis that these new lines are due to lattice oscillations in which only electrostatic fields take part. Similarly in the case of di-*n*-propyl ketone the band at 95 cm^{-1} is very weak and may be the same band observed in the incident spectrum, but in the spectrogram due to solid ethyl sulphide there is an intense band of frequency 96 cm.$^{-1}$ These results rather indicate that the nature of the new lines in the solid state is somehow dependent upon the presence of some particular atoms in the molecule, *e g*, the sulphur atom in the case of alkyl sulphides and oxygen in the case of ketones. More data, however, are required before such a hypothesis can be substantiated.

CHANGES OBSERVED IN THE LINES DUE TO INTRAMOLECULAR OSCILLATIONS

Acetone.—Before discussing the results obtained in the case of solid acetone we shall first discuss those due to the liquid state in order to find out the symmetry of the molecule in this state. If the two CH_3 groups were rotating freely about the C-C bond the molecule would not possess any symmetry element and all the Raman lines would be polarised. Since some of the lines are found to be totally depolarised the molecule has some elements of symmetry. The number of Raman lines expected in the case of a symmetry C_{2v} is indicated in Table V. It can be seen that eight polarised and sixteen totally depolarised

TABLE V

Acetone $CH_3.CO.CH_3$

C_{2v}	E	C_2	σ_v	σ'_v	n_i	T & R	n'_i	Raman effect.
Γ_1	1	1	1	1	9	1	8	P
Γ_2	1	1	−1	−1	5	1	4	D
Γ_3	1	−1	1	−1	9	2	7	D
Γ_4	1	−1	−1	1	7	2	5	D
U_i	10	2	6	2				
$h_i\chi'_i$	30	−2	6	2				
$h_i\psi_i'$	24	0	6	2				

Raman lines are expected in this case. The polarisation was studied previously by Simons (1932) and has been studied by the present authors also. The number

of polarised lines actually observed suggests that the molecule possesses the symmetry C_{2v} in the liquid state and there is no free rotation about the C-C bond.

In the solid state the line 1705 cm^{-1} shifts to 1702 cm^{-1} and is weakened considerably. The line 790 cm^{-1} and the C-H lines 1423 cm^{-1} and 2964 cm^{-1} shift respectively to 800 cm^{-1}, 1430 cm^{-1} and 2976 cm^{-1}. These changes suggest that the molecule is distorted in the solid state. The presence of continuous background due to extraneous light made it difficult to find out whether some of the fainter lines are actually present in the spectrogram due to the solid state or not.

Diethyl ketone.—The results given in Table II show that in the case of diethyl ketone in the liquid state none of the lines is totally depolarised. This shows that the molecule does not possess either any plane of symmetry or a twofold axis of rotation. Although the values of factor of depolarisation of the lines 1418 cm^{-1}, 1460 cm^{-1} and 2988 cm^{-1} are all greater than 0.5 yet they are found to be less than 6/7. In this case also the line 1706 cm^{-1} due to C=O group shifts to 1702 cm^{-1} and diminishes in intensity at the low temperature. The line 2893 cm^{-1} which according to Kohlrausch and Köppl (1934) consists of two lines at 2882 cm^{-1} and 2916 cm^{-1} was not clearly resolved into two components in the spectrogram obtained with the Fuess spectrograph used in the present investigation, but at the low temperature in the solid state this line is split up into two sharp lines 2890 cm^{-1} and 2920 cm^{-1}. As can be seen from Table II the lines 2940 cm^{-1} and 2988 cm^{-1} due to C−H valence oscillations shift to 2948 cm^{-1} and 2982 cm^{-1} respectively in the solid state. In this case all the prominent Raman lines appear in the spectrogram due to the solid state.

Methyl ethyl ketone.—In the case of methyl ethyl ketone although two different groups are attached to the C=O group the molecule possesses a plane of symmetry, because all the lines 1419 cm^{-1}, 1460 cm^{-1}, 2986 cm^{-1} and 3004 cm^{-1} are found to be totally depolarised, in the present investigation. The polarisation of the Raman lines of this substance was also studied previously by Simons (1932) and the line 406 cm^{-1} and these lines except 3004 cm^{-1} which was not resolved in his spectrogram were reported to be totally depolarised. The line 406 cm^{-1}, however, is not observed in the present investigation to be totally depolarised. In this case also the line 1705 cm^{-1} diminishes in intensity in the solid state. Besides this line, the line 1170 cm^{-1} was not clearly visible in the spectrogram due to the solid state owing to the presence of strong continuous background. The hydrogen lines do not undergo much changes in intensity with the solidification of the substance but two of them, *e.g.*, 2890 cm^{-1} and 3004 cm^{-1} shift to 2896 cm^{-1} and 3000 cm^{-1} respectively. Kohlrausch and Köppl (1934) reported only two hydrogen lines 2917 cm^{-1} and 2980 cm^{-1}, probably because these were not resolved into their components by the spectrograph used by them. The changes mentioned above may be due to distortion of the molecules in which the hydrogen atoms are involed.

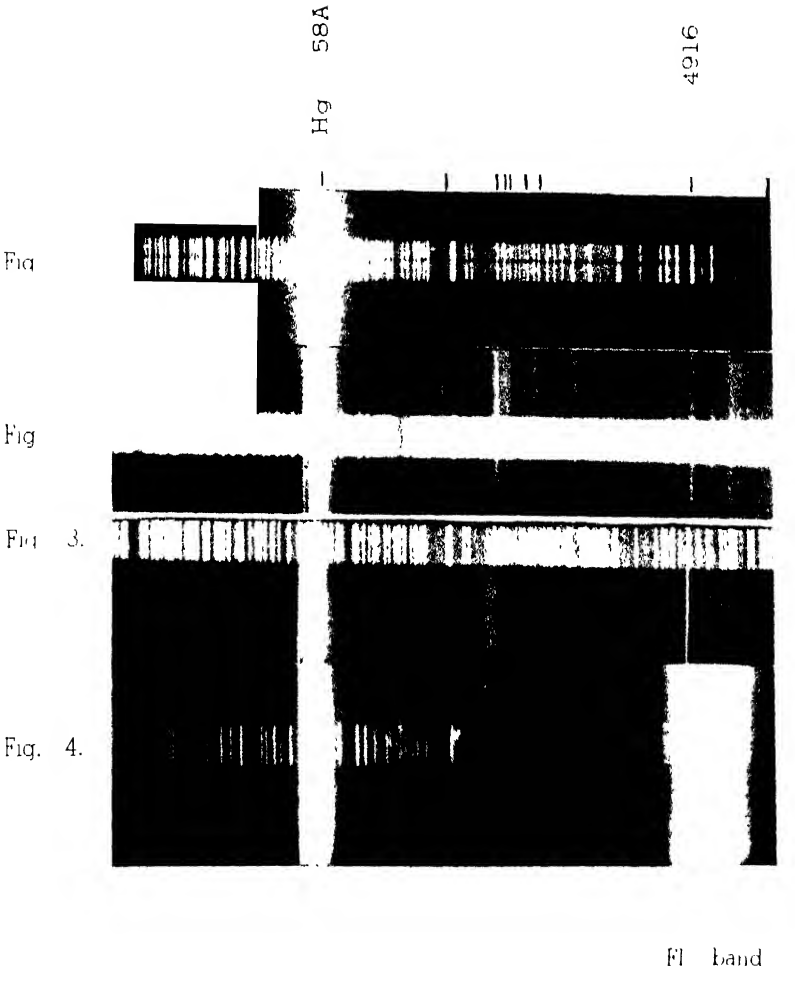

Raman Spectra.

Fig 1. : Acetone at about −170°C
„ 2. : „ „ „ − 30°C
„ 3. : Di-*n* propylketone − 30°C
„ 4. : „ −170 C

Di-n-propyl ketone.—Most of the Raman lines due to this substance in the liquid state are found to be polarised. As in the case of methyl ethyl ketone some of the hydrogen lines are totally depolarised. Hence the molecule seem to possess a plane of symmetry or twofold axis of rotation. All the Raman lines due to this substance excepting those due to the C-H valence and bending oscillations are very weak. Hence the Raman spectrum due to the solid state obtained in the present investigation is incomplete. The hydrogen lines 2880 cm^{-1}, 2918 cm^{-1}, 2942 cm^{-1} and 2974 cm^{-1} are observed to change to three lines 2886 cm^{-1} 2925 cm^{-1}, and 2966 cm^{-1} in the solid state. The line 1705 cm^{-1} is weakened in the solid state in this case also These suggest changes in the intermolecular field and probably some distortion of the molecule also in the solid state.

The spectrogram due to the solid di-*n*-propyl ketone at $-170°C$ shows a very intense broad fluorescence band in the region of 4920 A.U No trace of such fluorescence is observed in the liquid state, as can be seen from Plate II. It has been found that this fluorescence does not appear immediately with the solidification of the substance at about $-32°C$, but it appears only when the solidified mass is further cooled down. At first the fluorescent spectrum consists of a continuous broad band starting from about 4920 A.U. extending upto about 5300 A.U., but when the temperature reaches about $-170°C$ the band becomes stronger and narrower and the maximum occurs at about 4920 cm^{-1}. Another faint band at about 5200 A.U. was visually observed, but it was not recorded in the spectrogram due to insensitivity of the plate in this region. These results were reported briefly in a previous communication (Sirkar and Bishui, 1945). The enhancement of the intensity of feeble fluorescence bands due to impurities at low temperatures is well known, but the results obtained in the present investigation are different from such well known phenomenon in this respect that the spectrogram due to liquid di-*n*-propyl ketone is absolutely free from fluorescence and it is only the strain produced by contraction of the solid at low temperature which gives rise to such a strong fluorescence. The intensity of the fluorescent radiation observed in this case seems to be larger than that of the total scattering, because although extraneous light was present in the scattered light and the spectrum was photographed with a narrow slit of the spectrograph the band is found to be more intense than any of the undisplaced lines.

ACKNOWLEDGEMENTS

The work was partly carried out at the Indian Association for the Cultivation of Science and partly in the Palit Laboratory, Physics Department, University College of Science, Calcutta. The authors are indebted to Prof. M. N. Saha, F.R.S., and to the authorities of the Indian Association for the

Cultivation of Science for kindly providing facilities for these investigations and for the award of a scholarship to one of the authors (B. M. B.)

PHYSICS DEPARTMENT,
92, UPPER CIRCULAR ROAD,
CALCUTTA.

REFERENCES

Kohlrausch, R. W. F. and Köppl, F. (1934), Studies in Raman effect. *Zeit f. Phys. Chem. B*, **24**, 370.

Simons, L. (1932), Polarisation of Raman Lines. *Fenn. Comm. Phys. Math.*, **6**, Nr·13.

Sirkar S. C. and Bishui, B. M. (1943), On the Raman Spectra of a few alkyl sulphides in the solid state. *Proc. Nat. Inst. Sc. India*, **9**, 287 ; (1945), Fluorescence of dipropyl ketone at low temperatures *Nature*, **186**, 333

The following special publications of the Indian Association for the Cultivation of Science, 210, Bowbazar Street, Calcutta, are available at the prices shown against each of them :—

No.	Subject	Author	Price Rs. A. P.
III	Methods in Scientific Research	Sir E. J. Russell	0 6 0
IV	The Origin of the Planets	Sir James H. Jeans	0 6 0
V	Separation of Isotopes	Sir Lewis L. Fermor	0 6 0
VI	Garnets and their Role in Nature.	Sir Lewis L. Fermor	2 8 0
VII (1)	The Royal Botanic Gardens, Kew.	Sir Arthur Hill	1 8 0
(2)	Studies in the Germination of Seeds.		
VIII	Interatomic Forces	Prof. J. E. Lennard-Jones	1 8 0
IX	The Educational Aims and Practices of the California Institute of Technology	R. A. Millikan	0 6 0
X	Active Nitrogen A New Theory	Prof. S. K. Mitra	2 8 0

A discount of 25% is allowed to Booksellers and Agents.

RATES OF ADVERTISEMENTS

Third page of cover	Rs. 25, full page
do. do.	,, 15, half page
do. do.	,, 8, quarter page
Other pages	,, 19, full page
do.	,, 11, half page
do.	,, 6/8, quarter page

Suitable reductions are allowed for six or more consecutive insertions.

Building a Watershed

Preliminaries are complete and surveys are now being made for the construction of the eight dams and a barrage across the Damodar River. Indicating a capital expenditure of fifty-five crores of rupees, the Damodar Project would be "an example in the multi-purpose development of a watershed for India." Steel will be used for this gigantic project.

DAMODAR VALLEY PROJECT

7,60,000 ACRES OF IRRIGATION

A series of reservoirs providing flood control, supply of water for irrigation and a system of hydro-electric and thermal power stations inter-connected by transmission lines—these are the main features of the multi-purpose project planned for Bengal and Bihar.

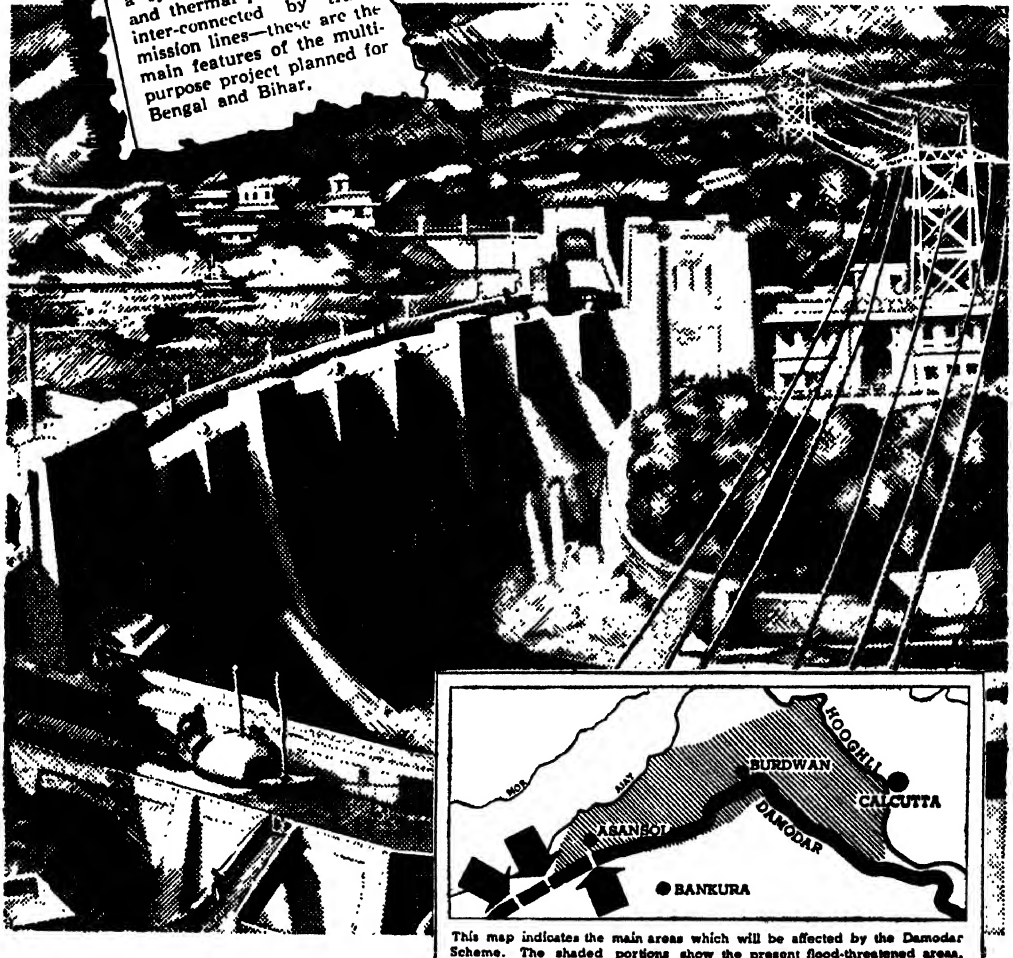

This map indicates the main areas which will be affected by the Damodar Scheme. The shaded portions show the present flood-threatened areas, while the arrows point to three possible barrage locations on the river course.

A CALCULATION OF THE DIAMAGNETIC SUSCEPTIBILITY OF LI^+, NA^+ AND K^+ FROM THOMAS-FERMI CHARGE DISTRIBUTION

By OM PARKASH SHARMA

ABSTRACT. After giving a brief outline of the present theories of diamagnetism, the importance of the "electron subtraction" method for calculating the finite ion-radius is pointed out. The ionic radii of Li^+, Na^+ and K^+ are calculated by this method graphically from Thomas-Fermi statistical charge distribution. Using the value of ρ_{ion} the values of χ_M for Li^+, Na^+ and K^+ are then calculated. As compared with other theoretical values the results obtained by the author agree better with the experimental values. A useful and very simple curve tracer is also described.

INTRODUCTION

According to the classical theories of diamagnetism, the effect of a magnetic field (H), on a system composed of electrons in motion about a fixed nucleus, is equivalent (to a first approximation) to the imposition on the system, of a uniform rotation about the field direction (Larmor precession) with an angular velocity $2\pi\omega_0 = \frac{eH}{2mc}$ where ω_0 is the precessional frequency, other constants having the usual significance. This rotation of electorns produces a magnetic moment opposed to the field. The atomic diamagnetic susceptibility is given by the expression (Pauling (1927).

$$\chi_A = -\frac{e^2}{4mc^2}\sum_k r_k^2 \sin^2\theta_k \qquad \ldots (i)$$

where $r_k \sin\theta_k$ is the projection of r_k, the distance of the kth electron from the nucleus, normal to the field direction and $r_k^2\sin^2\theta_k$ is the time average of $r_k^2 \sin^2\theta_k$. If the system under consideration has got an initial magnetic moment, both diamagnetic and paramagnetic effects are present, the magnitude of the latter being much greater. If the system, however, has initially zero magnetic moment, which is true for spherically symmetrical charge distribution of the closed-core type, there is no paramagnetic effect.

For systems with spherically symmetrical charge distribution, the quantum theory gives

$$r_k^2 \sin^2\theta_k = 2/3 r_k^2$$

thus

$$\chi_A = -\frac{e^2}{6mc^2}\sum_k \bar{r}_k^2$$

or $$\chi_M = -\frac{Le^2}{6mc^2}\sum_k r_k^2 = -2.83\times 10^{10}\sum_k r_k^2 \quad \ldots (ii)$$

where L is the Avogadro's number.

Van Vleck (1932) and Pauling (*loc. cit.*) have calculated the expression for r_k^2 from the new quantum mechanics. From the charge distribution conception of atoms, Pauling has calculated the diamagnetic susceptibility for inert-gas like configurations The calculated values, however do not agree with the experimental values, probably due to some error in the determination of the screening constants.

A very useful method of computing the charge distribution in spherically symmetrical systems has been developed by Hartree (1928). The method, though very laborious and approximte, has been applied to a number of problems. Stoner (1934) has calculated the diamagnetic susceptibilities of a number of ions in the following manner.

If dN/dr denotes the radial charge density in electrons per unit radial distance

then $$\bar{r}^2 = \int_0^\infty r^2 \frac{dN}{dr}\, dr \Big/ \int_0^\infty \frac{dN}{dr}\, dr$$

as $\int_0^\infty \frac{dN}{dr}\, dr$ gives the total charge in the ion, the diamagnetic susceptibility from (*ii*) is

$$\chi_M = -2.83\times 10^{10}\int_0^\infty r^2 \frac{dN}{dr}\, dr \quad \ldots (iii)$$

Expressing the radial distance (r) in atomic units ($.528\times 10^{-8}$ cm.)

$$\chi_M = -2.83\times 10^{10}(.528\times 10^{-8})^2 \int_0^\infty \rho^2 \frac{dN}{d\rho}\, d\rho$$

where $\rho = \frac{r}{a_0}$ and $a_0 = .528\times 10^{-8}$ cm.;

hence $$\chi_M = -.790\times 10^{-6}\int_0^\infty \rho^2 \frac{dN}{d\rho}\, d\rho \quad \ldots (iv)$$

Determination of the ionic radii and the calculation of χ

The values of χ (Table II) as determined experimentally from solutions or solid alkali halides, differ from those theoretically calculated from relation (*iv*) or those given by Slater, Pauling, etc. The difference is genuine, and may be accounted for on the following lines.

Goldschmidt (1940) has suggested that in alkali halide crystals the electronic charge of the ion is not extended to infinity but may be supposed to be present in a definite region. This 'rigid-sphere' concept, though not very sound, may be nearer to the actual state of affairs. In the present work the ionic radius ρ_{ion} (or the radius of the rigid sphere in Goldschmidt's words) has been determined by the "electron subtraction" method, used by J. N. Nanda (1945). This method has been preferred, on account of the fact that it takes into account the effect of the presence of the valence electron on the

charge in the ion. The effect of the neighbouring ions, however, has not been taken into account. The above idea, combined with the effect of the neighbouring ions, will be useful for the exact theoretical calculations of χ of the ions in crystals and also in solutions.

The ρ_{ion} is determined from the atomic field given by Thomas and Fermi (1928) using the electron subtraction method. Thomas-Fermi field has been used as it is easier and less laborious than other methods. From the statistical calculations, Fermi has shown that the number of electrons in an atom (At. No. $= Z$) is given by

$$\int_0^{\infty} \left(\frac{2mc^2}{\rho a_0}\chi'\right)^{\frac{3}{2}} \frac{8\pi}{3h^3} 4\pi\rho^2 a_0^3 d\rho$$

where ρ is in atomic units and χ is some function of ρ. Substituting the values of the constants the integral becomes

$$1.195 \int^{\infty} (\chi Z)^{\frac{3}{2}} \rho^{\frac{1}{2}} d\rho.$$

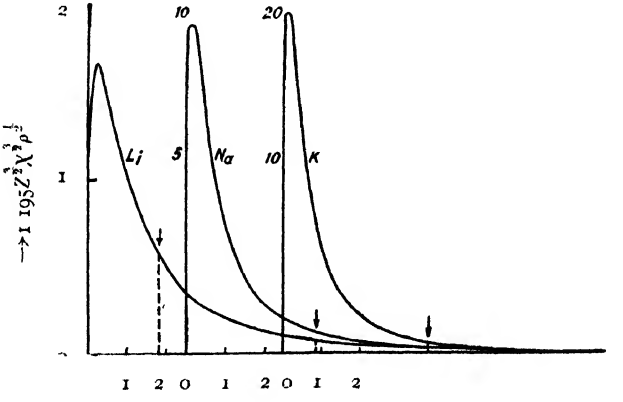

Thomas-Fermi charge distribution for Li, Na and K and their ionic radii (↑) on electron subtraction method

Fig. 1

The integral is evaluated graphically by plotting between ρ and $1.195\chi Z^{\frac{3}{2}}\rho^{\frac{1}{2}}$ and, the region of the valence electron being determined from

$$.195 \int_{\rho=}^{\rho=\infty} (\chi Z)^{\frac{3}{2}} \rho^{\frac{1}{2}} d\rho = 1$$

and ρ_{ion} determined from the graphs (Fig. 1). The ordinate scales for the three are different.

[While plotting these graphs on a big graph paper (56cm × 43cm) it is found that it is very difficult to draw a smooth curve of such a length The 'Frenchcurves' obtainable in the market are not of much use. Out of necessity a very simple curve tracer named (C.V.) was designed. A thin silicon steel strip about 40 cms. long 1.7 cms. wide and .034 cm thick, cut from a transformer stamping is taken. A piece of lead sheet of the same length, 1.5 cms wide and about .15 cm. thick is bent and fixed along the length of the strip, covering nearly .8 cm. of its width. A thin layer of lacquer polish is applied on lead (as otherwise the lead stains the graph paper and the hands) and the lower corners of the strip rounded. This, in simple, is the curve tracer. When a curve is to be drawn, the (C.V.) is bent to the proper shape of the curve and the curve traced. After use it is placed over a plane surface and straightened by simultaneously pressing and rubbing it with the hand. This has saved much of my time and unnecessary trouble of rubbing].

The values of ρ_{ion} for Li^+ Na^+ and K^+ as determined by electron subtraction method are compared with those found by Goldschmidt (1940) and Huggins and Meyer by different methods (Table I).

TABLE I

Ionic Radii

No.	Ion	Ion		
		Goldschmidt	Huggins and Meyer	Electron* subtraction method
1	Li^+	.78 Å	.475 Å	.985Å
2	Na^+	.98 Å	.875 Å	1.759 Å
3	K^+	1.35 Å	1 185 Å	1.996 Å

Now for the determination of χ_M Stoner has suggested that for ions in crystals and in solutions a limit will be imposed to the diamagnetically effective 'spread' of the charge distribution and we further suppose that the valence electron of the alkali atom, which is bound to the halide atom due to its electron—affinity, thus forming it a negative ion, is still equally effective on the remaining charge in the alkali ion, as it is in a free alkali atom. Hence therefore we shall consider the susceptibility integral for the total atom and restrict the integration to finite ρ_{ion}, thus in place of (*iv*) we have

$$\chi_M = .790 \times 10^{-6} \times 1.195 \int^{\rho_{ion}} (\chi Z)^{\frac{3}{2}} \rho^{\frac{5}{2}} d\rho.$$

The integral is evaluated graphically (Fig. 2). The ordinate scales are different and zero has been shifted. The values of χ_M as determined for Li^+ Na^+ and K^+

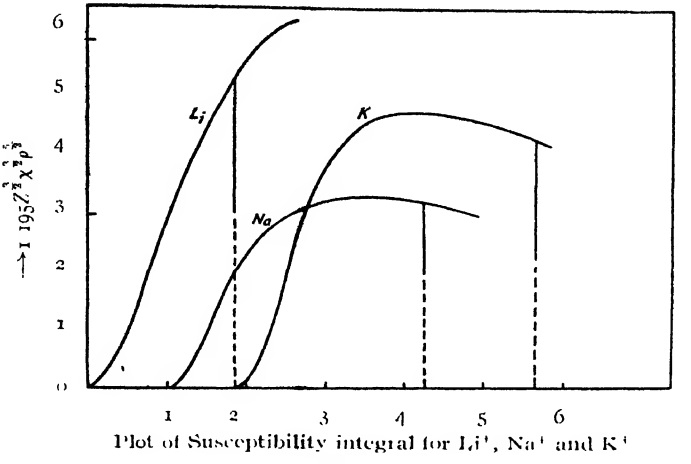

Plot of Susceptibility integral for Li^+, Na^+ and K^+

Fig. 2

by the author are compared with the theoretical and experimental values obtained by others. (Table II, taken from Bhatnagar and Mathur (1935) to which the year of the previous work and the values calculated by the present author have been added.)

TABLE II

Gram-ionic Susceptibilities

Ion	Theoretical values				Experimental values			
	Pauling 1927	Stoner (Hartree) 1929	Slater (Brindly) 1931	Sharma 1945	Hocart 1929	Pascal	Kido 1932	Ikenmeyer 1929
Li^+	0.63	.70	.67	1 29	...	...	1.6	...
Na^+	4.2	5.47	4.2	10 89	8.2 ± .9	7 6	7.6	10.4
K^+	16.7	17.64	14 4	19 06	16.5 ± 9	16.0	13.6	16.9

The values obtained by the author agree better, especially for Li^+ and Na^+ with the recent experimental values.

ACKNOWLEDGMENTS

In the end I wish to thank Dr. H. R. Sarna of the Govt. College, Lahore, for his valuable suggestion and Mr. J. N. Nanda and Dr. A. M. Mian, whose

inspiration made me do these calculations. I must also thank Prof. J. B. Seth under whose patronage the work was completed.

I must thank Mr. J. N. Nanda for lending me the manuscript of his paper and constant help that he gave me at every step.

* These are ionic radii for free ions, only the field of the valence electron being taken into account.

PHYSICS LABORATORY,
GOVERNMENT COLLEGE,
LAHORE.

REFERENCES

Bhatnagar and Mathur, 1935, Physical Principles and Applications of Magneto-Chemistry, p. 142.

Fermi, 1928, *Zeit. f. Phy.*, **48**, 73.

" " " " " **49**, 550.

Hartree, 1928, *Proc. Camb. Phil. Soc.*, **24**, III.

Ikenmeyer, 1929, *Ann. Der Phys.*, **1**, 169.

Nanda, 1945, *Ind. Jour. Phys*, **18**, 19.

Pauling, 1927, *Proc. Roy. Soc.*, **114**, 181.

Stoner, 1934, Magnetism and Matter, pp. 257, 259.

Thomasafld Goldschmidt, 1940, Theory of Solids, pp. 92-93.

Van-Vleck, 1932, The Theory of Electric and Magnetic Susceptibilities, Chap. VIII.

ULTRA VIOLET BANDS OF ZINC IODIDE—PART I

By P. TIRUVENGANNA RAO and K. R. RAO*

(Plate III)

ABSTRACT. A brief system (designated as D) consisting of about ten diffuse bands, is detected among the bands of the zinc iodide molecule, in the region λ 3277—3193 and found to have the same final state as the system (here designated as C) previously established by Wieland. The view is advanced that the two systems are components of an electronic transition $^2\Pi - {}^2\Sigma$ with the $^2\Pi$ interval 370 cms^{-1}, agreeing closely with the value 386 cms^{-1}, predicted by Howell for the zinc halide bands. The occurrence of a third system E is also reported.

INTRODUCTION

In a recent paper, Howell (1943) photogrphed the emission spectrum of HgF in a high frequency discharge and analysed the ultra violet bands into two systems which he considered as components of a single doublet system arising from the electronic transition $^2\Pi - {}^2\Sigma$. The seperation of $^2\Pi$ level was 3940 cm^{-1} which agrees very closely with the atomic coupling constant 4205 cm^{-1} for the mercury atom corresponding to the $6s\,6p\,{}^3P$ state. Further as Cornell (1938) has pointed out in the case of HgCl, the two systems in HgF occur near the mercury resonance line λ2537. From these two features, Howell concluded that the electronic transition involved in the emission spectrum of HgF should essentially be between non-bonding or atomic orbitals. If this view is correct, the same feature must present itself in the band systems of all the halides of mercury, cadmium and zinc, as pointed out by Howell.

Extending the study of the emission bands of the HgCl molecule, Rao and Ramachandra Rao (1944) confirmed the existence of a similar $^2\Pi - {}^2\Sigma$ transition band system with the $^2\Pi$ separation equal to 3890 cm^{-1}. A doublet separation of the same order (3538 cm^{-1}) was round by Rao, Sastry and Krishnamurty, (1944) also in the Hg I molecule between the C and D systems.

Howell, applying this argument to the known band systems of CdF, CdCl ZnF and ZnCl, found in each case the occurrence band systems ascribable to $^2\Pi - {}^2\Sigma$ electronic transition with $^2\Pi$ interval agreeing with the corresponding atomic interval. A systematisation from this point of view is not clear with respect to the band systems of ZnBr and ZnI. Even the origin of the absorption bands ascribed by Walter and Barratt to the zinc bromide molecule, was considered doubtful by Howell when he compared them with the known band systems of zinc iodide. In view of this, an investigation of the band systems of the zinc halides has been undertaken by the authors. The results obtained for the zinc iodide molecule are presented in this paper (a brief report of which was published in Curr. Sci., 15, p. 122, 1946).

* Fellow of the Indian Physical Society.

EXPERIMENTAL

The usual H type discharge tube containing zinc iodide, excited by an one-fourth kilowatt transformer, is employed for producing the emission bands. In a second series of experiments the zinc iodide is contained in a quartz tube with an end-on sealed in window of quartz. The tube is excited by a high frequency oscillator of low power, with external electrodes and continuously evacuated by a Cenco High-Vac pump. Photogrphs of the emission spectrum are taken when the discharge takes place predominantly through the zinc iodide vapour. Constant heating by an etna burner is found necessary to maintain this discharge. Hilger quartz spetiographs of medium and E_1 types are employed.

RESULTS

Only one system has till now been definitely established for the ZnI molecule. Wieland (1929) has given the analysis identifying the head at λ 3318 as the (o, o) band, and has just mentioned the occurrence of a weak group of three bands at λ 3236.

The experimental work described above, carried out with a pure specimen of ZnI (supplied by B.D.H.) in the discharge tube, has led the authors to establiish definitely the existence of the three following different systems in the ultra violet, which, on the analogy of the HgI bands, are designated as the C. D and E systems respectively.

TABLE I

System	Region	Electronic transition
C*	λ 3393-3257	$^2\Pi—^2\Sigma$
D	λ 3278-3193	
E	λ 2392-2300	Probably $a^2\Sigma—^2\Sigma$

* Due to Wieland.

In the system C, analysed by Wieland no more sequences could be obtained than were reported by Wieland. But under the higher dispersion used in this work, the (o, o) band is distinctly seen to be accompanied by a subsidiary head on the longer wavelength side, which, from its intensity and separation from the main head, cannot be regarded as due to an isotope of zinc. The two components, 3317.9 and 3317.6 may be the P and Q heads of the (o, o) band. No such well separated components are seen in the case of the (1,o) and (2,o) bands but they appear to be broadened out slightly.

A close examination of the violet end of this C system has revealed the existence of a brief and new system (D). The first evidence of this is the observation of three or perhaps four well marked and prominent doublets (Plate III) which are diffuse, slightly broad and headless. Attempts to include

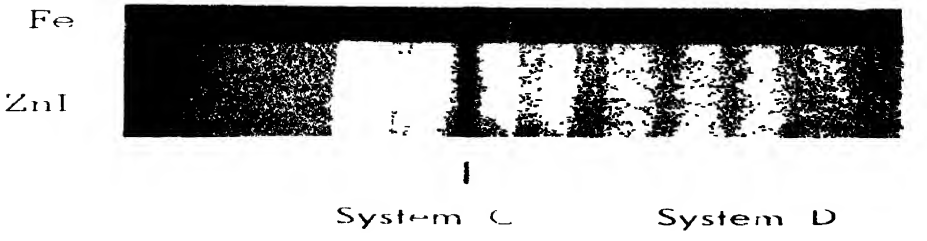

Zinc Iodide Bands (Fig. A)

hem as higher members of the C (Wieland) system, seemed to be unjustified from a consideration of the much higher intensity of these pairs as compared to the fading intensity of the system at this end. A further clue to regard these pairs as forming another system is afforded by a measurement of the wave-lengths. An interval of about 220 cm^{-1} is found to repeat itself in some of these members, this interval being of the order of magnitude of the vibrational constant ω'' of the C system. The wave-lengths, wave numbers and intensity data of the bands of this system are given in Table II. Two of the bands λ 3265.7 and λ 3262.5 which are included in this table consist perhaps of overlapping faint band heads belonging to both the systems. Their classification is hence not shown. The vibrational analysis of the bands is given in a diagonal array in Table III. The line ν 30715 occurs at two places. The (0, 0) band is suggested at ν 30499.

Exact vibrational constants cannot justifiably be determined. From the order of the $\Delta G'(v)$ values, the vibrational constants of the final state are regarded as identical with those of the C system. On this basis, the vibrational constants of the upper state for this C system have been calculated as.

$$\omega' = 2117 \text{ cms}^{-1}$$
$$x'\omega' = 2.5 \text{ ,,}$$
$$\nu = 30506.3 \text{ ,,}$$

TABLE II

ZnI Bands (system D)

Wavelength	Wave number	Intensity	Classification
3277.7	30499	0	(0,0)
3265.7	30612	2	( )
3262.5	30642	3	( )
3257.2	30692	2	(3,2)
3254.8	30715	2	(1,0)
3235.7	30896	4	(3,1)
3232.5	30927	3	(2,0)
3215.0	31095	3	(4,1)
3212.5	31119	3	(3,0)
3196.5	31275	2	(5,1)
3193.5	31305	3	(4,0)

TABLE III

Vibrational analysis of system D

	0		1		2	
0	30499(0)					
	216					
1	30715(2)*					
	212					
2	30927(3)	212	30715(2)*			
	192		181			
3	31119(3)	223	30896(4)	204	30692(2)†	
	186		199			
4	31305(2)	210	31095(3)			
			180			
5			31275(2)			

* Occurs at two places.

† Too diffuse to be measured accurately.

The correctness of the identification of system D for ZnI is further strengthened when it is seen that the difference between the (o, o) bands (ν30129.5) of system C and (ν30499.4) of system D is equal to 370 cms.$^{-1}$, which is in excellent agreement with the predicted value 386 cms.$^{-1}$ for zinc halides. The systems C and D may therefore be regarded as the two components of a $^2\Pi - {}^2\Sigma$ transition analogous to those found previously in zinc fluoride and zinc chloride.

System E

In addition to systems C and D, a third system (designated as E, *cf.* Table I) is also obtained in the region λ2392 to λ2300. The bands of this system are not so diffuse as those of the D system but they are faint even when photographed, after long exposures of about five hours, with a medium Hilger quartz spectrograph. They are degraded probably to the red but the direction could not be definitely seen. A preliminary examination of the wave numbers of the band heads indicated a recurring interval of the order of 216, equal approximately to the vibrational constant $\omega'' = 223$, of the common ground state of systems C and D. It is considered that the system may correspond to the transition $a^2\Sigma - {}^2\Sigma$. Further work on this system as well as on the absorption bands of zinc halides is still in progress and a complete account will be presented in a subsequent communication.

ACKNOWLEDGMENTS

Our thanks are due to Mr. C. Rama Sastry for his help in the experimental work and the use of the high frequency oscillator set. One of the authors (P.T.R.) is indebted to the Andhra University for the award of a Research Fellowship.

ANDHRA UNIVERSITY,
WALTAIR.

References

Howell, 1943, *P.R.S.*, **182**, 95.
Cornell, 1938, *Phy. Rev.*, **54**, 341.
Rao and Ramachandra Rao, 1944, *Curr. Sci.*, **13**, 279.
Rao, Sastry and Krishna Murty, 1944, *Ind. Jour. Phy.*, **18**, 323.
Wieland, 1929, *Helv. Phy. Acta.*, **2**, 46 and 77.

THE LATTICE STRUCTURE OF CLAY MINERALS

By S. N. BAGCHI

ABSTRACT. A review of the work done so far on the crystal structure of 8 clay minerals has been given.

INTRODUCTION

Clay, or, the clay fraction of soil and natural deposits such as bentonite and kaolin comprises all inorganic ingredients included in the mechanically separated fraction of these systems having particle-size smaller than 2 microns in diameter (Atterberg, 1912). It is mainly colloidal in nature. Most of the physical and chemical properties of soils and other clayey deposits which are of importance in practical agriculture, in ceramics and in constructional engineering are now known to be determined to a large extent by the nature and amount of their colloidal constituents, and the importance of detailed investigations of these constituents by physical and chemical methods is now increasingly felt for purposes of soil systematics, soil classification, and standardisation of clay material for use in the industries.

CRYSTALLINE CHARACTER OF CLAYS
THE PRINCIPAL GROUPS OF CLAY MINERALS

Following Van Bemmelen (1888), the finest fraction of soil has often been regarded as a loose 'absorption compound' or a mixed gel of silica, alumina, iron oxide and water (Wiegner, 1924) present in indefinite proportions so as to constitute some sort of an 'absorption complex'. From studies of synthetic precipitates formed under different conditions from solutions comparable to those which might be expected to give rise to the 'absorption complex' of soil, (Mattson, 1930) postulated that this complex arises from a mutual precipitation of electropositive and electronegative sols. such as colloidal alumina, ferric oxide and silica under isoelectric conditions.

The 'mixed gel' hypothesis for a long time kept in the background the crystalline character of soil colloids now fully established through x-ray studies (Hendricks *et al.*, 1930 ; Kelley *et al.*, 1931 ; Hofmann *et al.*, 1934 ; Nagelchmidt, 1934) and optical (Ross *et al.*, 1930, 1934 ; Marshall, 1930, 1935 ; Correns and Mehmel, 1936). These investigations have shown that the clay fraction is made up of a number of secondary silicate minerals with occasional admixtures of small quantities of rock-forming minerals , silica and oxides as well as hydroxides of iron and aluminium ; and in some cases, of certain amorphous inorganic substances.

Secondary silicate minerals which occur only in the clay fraction are usually known as *clay minerals*. Four groups of these clay minerals have been distingtished. These are—

(*a*) the *kaolin group* (Ross, *loc.cit*), comprising (*i*) the four polymorphic forms kaolinite, dickite, nacrite and halloysite, having the same chemical composition $Al_2O_3 . 2SiO_2.2H_2O$, (*ii*) anauxite often considered as a variety of kaolinite but having a $SiO_2 : Al_2O_3$ ratio greater than 2.0, and (*iii*) hydrated halloysite (Hofmann, *loc. cit*) which has the chemical composition $Al_2O_3.2SiO_2.4H_2O$ and which on drying in air loses two molecules of water giving halloysite.

(*b*) the *montmorillonite group* consisting of the minerals montmorillonite, beidellite, saponite, nontronite, etc., having the general formula $(R^{++}_{2-n}\ R^{+}_{n})\ (Al^{+++}_{m}\ Si^{++++}_{4-m})O_{10}\ (OH)_2,\ xH_2O$ (Ross and Hendricks, 1941; Hendricks, 1942) derived from the ideal formula $(Al_2)\ (Si_4)\ O_{10}\ (OH)_2$ of pyrophyllite ;

(*c*) the *illite group* or the hydrous micas having the general formula (Grim *et al.*, 1937) $2K_2O.3R^{++}O.8R_2^{+++}O_3.24SiO_2,\ 12H_2O$ and distinguished from muscovite mica, $K(Al_2)\ (AlSi_3)O_{10}(OH)_2$, by their relatively small content of potassium and large percentage of water ; and

(*d*) the *attapulgite group*, whose only known member is the fibrous clay mineral, attapulgite, having the composition $(OH_2)4(OH)_2Mg_5Si_8O_{20}.4H_2O$ (Bradley, 1940).

THE ATOMIC STRUCTURE OF CLAY MINERALS

As the clay minerals are the dominant constituents of most clays, the physical and chemical properties of the latter will be largely determined by their nature and relative proportions in the clay. Characteristic differences between the properties of the individual clay minerals have been observed. These have often been traced to differences in their crystalline structure.

The elucidation of the general scheme of structure of the clay minerals and certain other minerals, *e.g.*, micas, chlorites, talc and pyrophyllite, related to them, is due to Pauling, (1930). From dimensional considerations of the unit in the basal plane of the two forms of silica, β-tridymite and β-cristobalite, as well as of the pseudo-hexagonal (monoclinic) crystals of hydrargillite and muscovite, Pauling was led to postulate two structural units for clay and other related minerals. One is the octahedral hydrargillite or gibbsite unit composed of two sheets of closely packed hydroxyl groups built around Al^{+++} ions occupying the interstices of the hydroxyl groups In accordance with the electrostatic valence rule of Pauling (1929), each octahedron shares three edges and only two-thirds of the possible aluminium positions are occupied. In the octahedral brucite unit, having a similar structure, all the available positions are filled up by magnesium ions. The second unit of structure consists of hexagonal layers of linked SiO_4-tetrahedra, each tetrahedron containing a Si^{+++} ion at the centre and four oxygen ions at the corners. Unlike β-tridymite and β-cristobalite where alternate vertices of the tetrahedra point in opposite

directions, these hexagonal layers of linked tetrahedra have all their vertices pointing in the same direction. Oxygen ions forming the bases of the

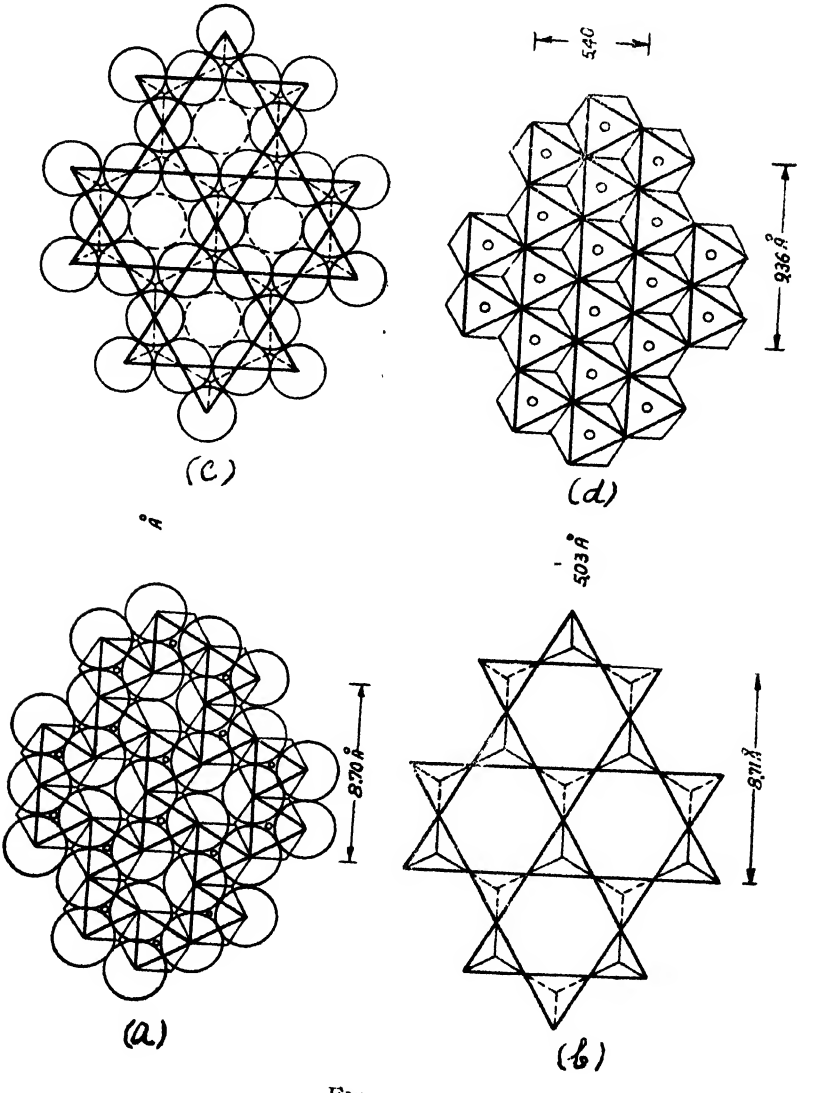

FIG. 1
(After Pauling)

(*a* A hydrargillite layer of octahedra
(*b*) A tetrahedral layer from β-cristobalite or β-tridymite. A silicon ion is located at centre of each tetrahedron and an oxygen ion at each corner.
(*c*) A tetrahedral layer in which all the tetrahedra point in the same direction.
(*d*) A complete layer of octahedra (Brucite layer).

tetrahedra have their valencies satisfied, each $O^{=}$ ion being common to two SiO_4 tetrahedra. But the oxygen ions at the unshared tetrahedral corners have only half of their valencies satisfied and it is necessary that they be held by further bonds. This is achieved by the superposition of the silica layer on the hydrargillite layer such that the tetrahedral vertices coincide with two thirds of the shared octahedral corners. This superposition is really a fusion of the two layers such that the vertical oxygens replace the OH groups at the shared octahedral corners and act as connecting links between the two layers. The unsymmetrical packet thus formed is found in clay minerals of the kaolin group. Symmetrical packets also occur as in montmorillonites and micas, and are formed by attaching a second tetrahedral layer to the other side of the hydrargillite layer. The various clay mineral and minerals related to them are distinguished by the manner of stacking of these packets (further discussed on pp. 5-6). Minerals like chlorite (Pauling, *loc. cit*) and vermiculite (Gruner, 1934; Hendricks 1938) are formed by the superposition of such packets interleaved respectively with units of brucite and neutral water molecules.

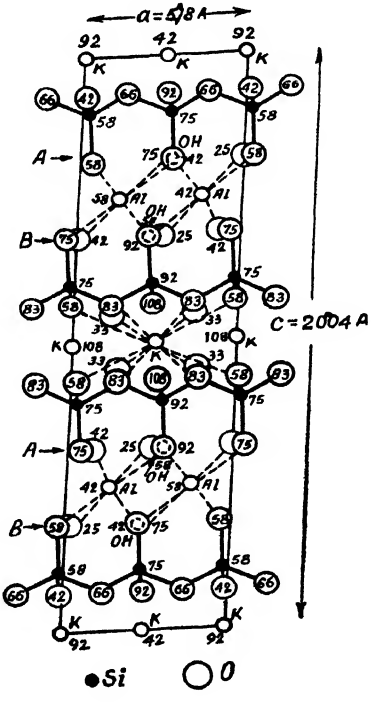

FIG. 2

The structure of Mascovite projected on (010)

(After Jackson and West)

The heights of the atoms above the face of the unit cells, as measured along the axis of projection, are indicated by the numbers. An atom on the lower face of the unit cell is indicated by 0, on the top face by 100, and intermediate heights are given accordingly

A crystal consisting of symmetrical packets of fused silica and hydrargillite layers has the composition $Si_4Al_2O_{10}(OH)_2$ and represents the mineral pyrophyllite. When octahedral layers of brucite replace those of hydrargillite we get talc having the composition $Si_4Mg_3O_{10}(OH)_2$. Gruner (*loc. cit.*) and Hendricks (1938) have verified these structures for talc and pyrophyllite. From single crystal measurements Hendricks concluded that the structures are fixed in the *a*- and *c*-directions but the individual $(OH)_2Al_2Si_4O_{10}$ or $(OH)_2Mg_3Si_4O_{10}$ packets are randomly shifted along the *b*-axis. He preferred the space group C_s^4 to the space group C_{2h}^6 proposed by Gruner.

When silicon ions in pyrophyllite are replaced by aluminium ions of coordination number 4, negatively charged layers are developed. Electroneutrality is maintained by the incorporation of further positive ions into the structure. There is room for these ions between the layers in pockets formed by two opposite hexagonal rings of the basal oxygen ions belonging to contiguous tetrahedral silica layers. In muscovite mica having the composition $K(Si_3Al)Al_2O_{10}(OH)_2$ every fourth Si^{++++} ion is replaced by an Al^{+++} ion and the pockets are filled up by K^+ ions (FIG. 2)

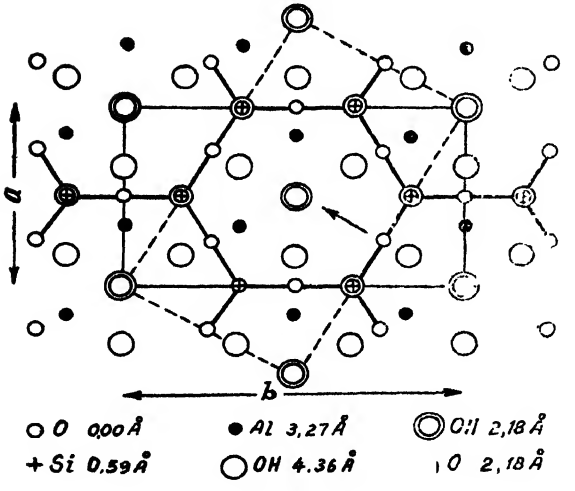

FIG. 3
(After Gruner)

Sheet of $2[(OH)_4Al_2Si_2O_5]$ proposed by Pauling. Height of atomic positions may vary slightly.

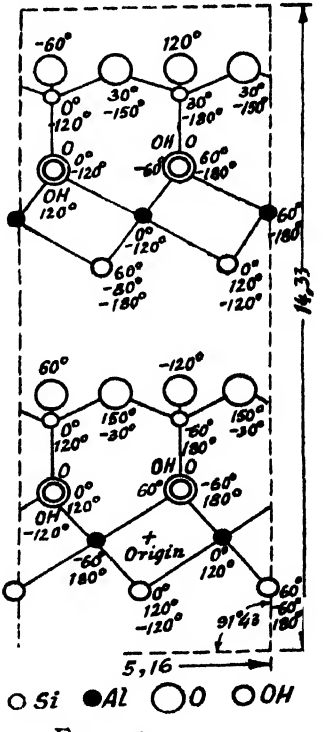

FIG. 4
(After Gruner)

One half of the unit cell of nacrite. The plane of the paper is the principal glide plane containing the origin.

A similar replacement in talc gives rise to biotite having the formula $K(Si_3Al)Mg_3O_{10}(OH)_2$.

In chlorites the negative charge of the substituted pyrophyllite layers is balanced by brucite layers which have acquired a positive charge through the replacement of a part of Mg^{++}ions by Al^{+++}ions.

(*i*) *Minerals of the kaolin group.*—Ross and Kerr (1931) made an extensive study of the mineralogy and chemical composition of the kaolin group of minerals including the amorphous substance allophane. Almost a complete lack of isomorphous replacement is one of the distinctive features of these minerals. This has been traced to the unsymmetrical structure of kaolins which cannot bear the strain arising from the incorporation of cations other than Si^{++++} and Al^{+++} or of layers (*e.g.*, brucite) having lattice dimensions different from those of gibbsite or silica (Pauling, *loc. cit.*). Gruner (1932, *a*, *b* ; 1933) worked out the detailed crystal structures of the three polymorphic varieties, kaolinite, dickite and nacrite. All the three give monoclinic crystals and are formed by the stacking of unsymmetrical packets of fused silica and hydrargillite layers ; the packet of kaolinite is shown in Fig. 3, but each shows a characteristic manner of stacking which is different from that of the others and gives rise to different monoclinic angles (β) as will appear from Fig. 4(*a-c*). Gruner's crystallographic data are given below :—

Kaolinite	Dickite	Nacrite
$a=5.138$Å	$a=5.14$Å	$a=5.16$Å
$b=8.900$Å	$b=8.94$Å	$b=8.93$Å
$c=14.506$Å	$c=14.42$Å	$c=18.66$Å
$\beta=100°.12'$	$\beta=96°.50'$	$\beta=91°.43'$
$Z=4$	$Z=4$	$Z=8$
$C_s^4=Cc$.	$C_s^4=Cc$	$C_s^5=Cc$.

Z—denotes the number of molecules of the formula $Al_2Si_2O_5(OH)_4$; $C_s^4=Cc$ represents the notation of the space group.

A displacement of the packets relative to one another is possible along both the a and b-axes. The monoclinic angle β is determined by the shift of one packet over the other in the direction of the a-axis. The shifts are respectively $\pi/2$, $\pi/3$ and $\pi/12$ for kaolinite, dickite and nacrite ($a=2\pi$). As the (010) plane constitutes a glide plane of symmetry any amount of shift parallel to the b-axis is theoretically possible consistent with a fixed monoclinic angle. Certain observed reflections in the case of kaolinite limit the shifts to intervals of $\pi/3$, $2\pi/3$, and $4\pi/3$ ($b=2\pi$). But Gruner found that only the two positions A and B (Fig. 5a) in which the shifts along the b-axis are respectively o and $4\pi/3$ are in equally good agreement with the calculated intensities and a choice between

the two is difficult. For a particular sample of Brooklyn kaolinite he preferred the B-position. For dickite, the A-position (Fig. 5b) in which the shift along the b-axis is $\pi/3$ is accepted. In nacrite the shift is $2\pi/3$ (Fig. 5d).

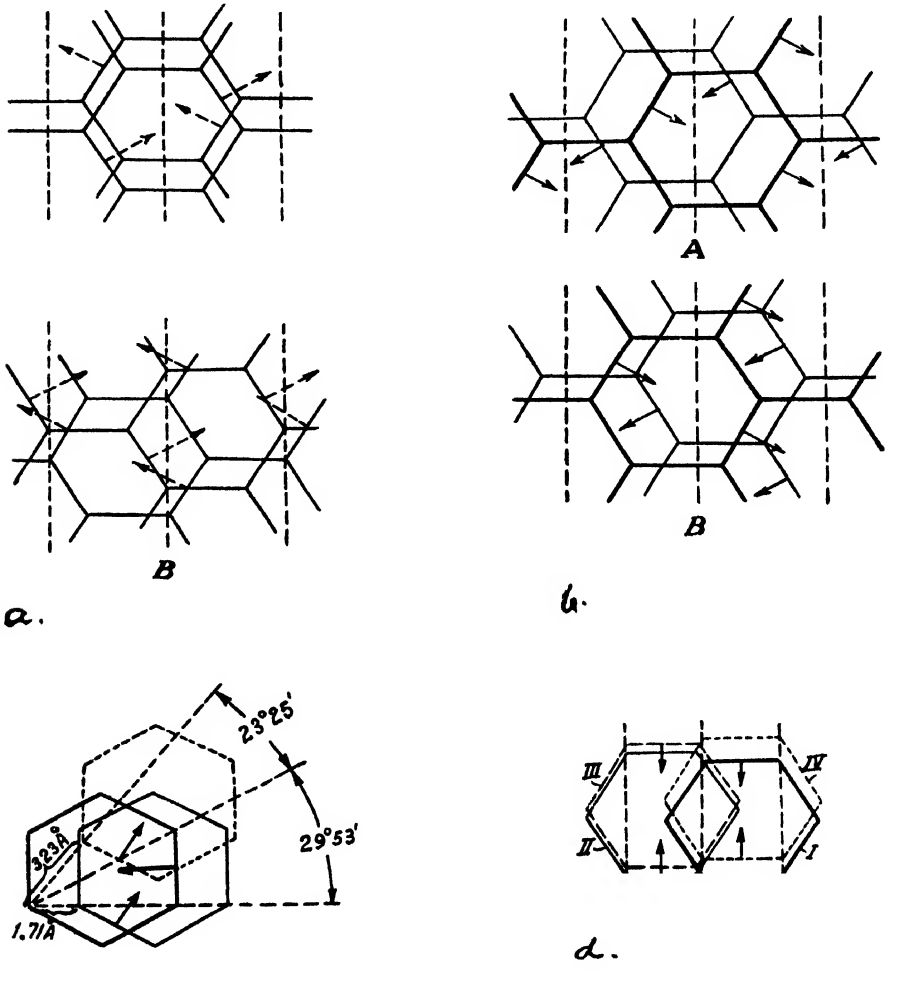

FIG. 5
(After Gruner)

(*a*) The two possible shifts of sheets in the kaolin structure. Dotted lines are glide plane of C's. Arrows indicate planes of synemery in individual sheets.

(*b*) The two possible shifts of sheets in the dickite structure. Dotted lines are glide planes of C's. Arrows indicate planes of symmetry in individual sheets. Heavy lines represent lower layers.

(*c*) The shift in dickite as compared with that of kaolinite. Heavy-lined hexagon represents stationary SiO_4 sheet for both dickite and kaolinite. Light-lined hexagon represents upper adjoinjng sheet of kaolinite.

(*d*) The shifts of the four layers in nacrite when seen in a direction normal to the base (001). The dotted lins are glide planes of symmetry of C's.

The space group which is identical for the three minerals contains only a glide plane of symmetry which lies in the plane of the a- and c-axes. All packets face in the same direction giving rise to the polar hemihedral space group C_s^4.*

The unit cell of kaolinite and dickite consists of two unsymmetrical packets while that of nacrite is made up of four such packets (Fig. 5, a-d). The ordinary planes of symmetry of contiguous sheets make angles of 120° in kaolinite and dickite ; but in nacrite each sheet is rotated through 180° in its own plane with respect to its nearest neighbour and the sheets 2 and 3 are each shifted through $2\pi/3 \times b$ relative to packets 1 and 4 respectively.

From measurements on single crystals Hendricks (1938) later on gave the following crystallographic data for nacrite.

$$a = 8.94\text{Å}$$
$$b = 5.14\text{Å}$$
$$c = 43.00\text{Å}$$
$$\beta = 90°.20'$$
$$Z = 6[(OH)_8Al_4Si_4O_{10}]$$
$$C_s^v = Cc.$$

This structure is different from the one due to Gruner in that the former postulates 6 kaolinitic layers in the unit cell instead of 4 and the directions of the a and b axes have been reversed.

In order to explain the high silica-alumina ratio of anauxite Gruner assumed a replacement of octahenral Al^{+++} by Si^{++++}. Bragg (1937) and Hendricks (1936), doubted this hypothesis. The latter suggested a defect of $Al(OH)_3$ giving rise to holes in the structure. Gruner (1937), showed that this structure does not agree with the observed densities. Gruner's alternative suggestion that whole units of tetrahedral SiO_4 occupy positions of octahedral units of $AlO_2(OH)_4$ is not structurally convincing according to Hendricks. The latter finally suggested a structure of anauxite formed by the incorporation of excess of silica in the kaolinite lattice as neutral silica layers following the kaolinite layers in irregular sequence.

There is some confusion regarding the nomenclature of halloysite, $Al_2O_3 2SiO_2 2H_2O$, and the hydrated mineral, $Al_2O_3 2SiO_2 4H_2O$. Hofmann, Endell and Wilm (1934) described the latter as halloysite. On heating at 50°C it gave a product which they identified as kaolinite. Mehmel (1935) showed that this product is not kaolinite but a new mineral which he designated as metahalloysite. The following nomenclature due to Hendricks (1939) will be adhered to in the sequel.†

* The space group C_{2h}^6 suggested by Ksanda and Barth (1936) has been eliminated (Hendricks, 1938) as single crystals show strong pyroelectric effect by the Martin method.

† Recently Hendricks (1943) suggested the name 'endellite' for the more hydrated mineral.

Halloysite, $Al_2O_3 2SiO_2 2H_2O$ (metahalloysite of Mehmel).

Hydrated halloysite, $Al_2O_3 2SiO_2 4H_2O$ (halloysite of Hofmann, *et al*, Mehmel and others).

According to Mehmel, hydrated halloysite (Mehmel's halloysite) is built up in the direction of the c-axis from alternating layers of $H_2Si_2O_5$ and $Al(OH)_3$. They are not linked up by principal valencies and do not form a fused packet. In halloysite (Mehmel's metahalloysite), on the other hand, the two layers are condensed with the elimination of $2H_2O$ giving rise to a fused packet having the composition $(OH)_4.Si_2Al_2O_5$ of kaolinite. Mehmel gave the following crystallographic data for the two minerals :—

Hydrated halloysite.	Halloysite.
$a = 5.20$Å	$a = 5.15$Å
$b = 8.92$Å	$b = 8.00$Å
$c = 10.25$Å	$c = 7.57$Å
$\beta \sim 100°$	$\beta \sim 100°$
$Z = 2$	$Z = 1$
$C_s^3 = Cm$.	$C_s^1 = Cm$.

The structures indicated in Fig. 6(b,c) differ from that of kaolinite Fig. (6a). The space group C_s^3 contains an ordinary plane of symmetry parallel to (010) while the space group C_s^1 to which kaolinite belongs has a glide plane of symmetry parallel to (010). This difference in the space groups is reflected in the dimensions of the unit cells. That of halloysite consists of only one packet while two packets go to form the unit cell of kaolinite.

Hendricks objected to the above structures on the ground that the interaction of the hydroxyl groups of the layers of $Si_2O_3(OH)_2$ and $Al(OH)_3$ as a result of which water is considered to be eliminated (see above) would require a large activation energy and consequently would not be expected to take place readily at such low temperatures as 50°C. He further pointed out that the intensity data do not agree with the proposed structures. He suggested an alternative structure for hydrated halloysite in which neutral kaolinitic layers $[(OH)_4Si_2Al_2O_5]_n$, are interleaved with single layers of water molecules. According to Hendricks there is no reason for considering halloysite to possess a structure different from kaolinite, dickite and nacrite. In his opinion, the slight difference between the powder diagrams of halloysite and other kaolinitic minerals may be considered to arise from differences in the degree of organisation of the crystallities, (*cf.* also Nagelschmidt, 1939).

Edelman and Favejee (1940) suggested a structure of hydrated halloysite in which every alternate SiO_4-tetrahedron is inverted and the vertical oxygens are replaced by hydroxyl groups to balance the charges. This layer together with one of $Al_2(OH)_6$ would give the composition $[Al_2(OH)_5OSi_2O_3(OH)]_n$ or $[Al_2O_3 2SiO_2 3H_2O.]_n$ Additional water molecules required for the formula, $Al_2O_3 2SiO_2\ 4H_2O$, of hydrated halloysite are supposed to exist in

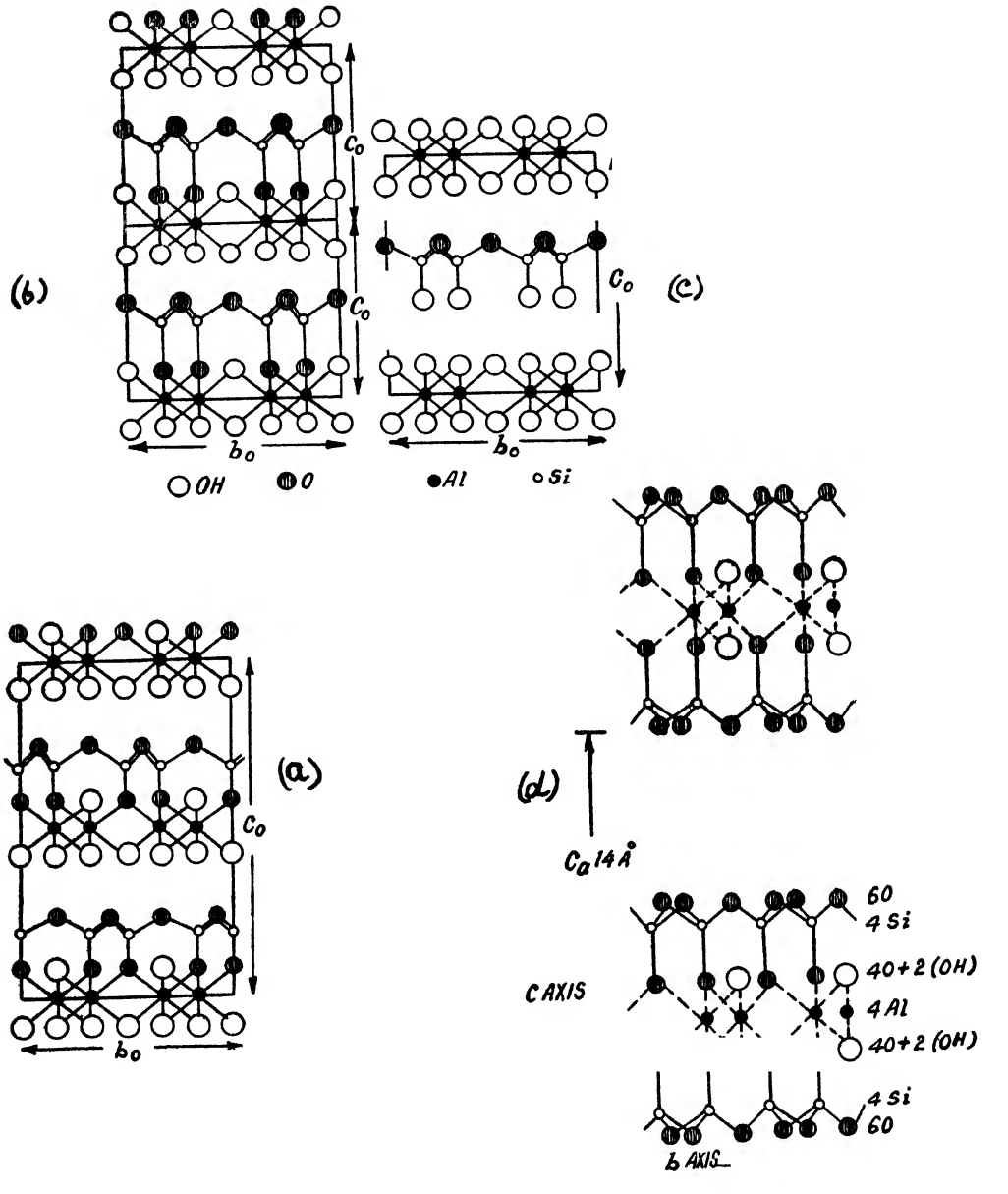

FIG. 6

(*a*—*c* after Mehmel)

(*a*) Schematic diagram of the projection on the plane (100) of (*a*) kaolinite.

(*b*) Schematic diagram of the projection on the plane (100) of (*b*) halloysite.

(*c*) Hydrated halloysite.

(*d*) Schematic diagram of the crystal structure montmorillonite. (After Hofmann).

between the sheets. The change to halloysite takes place by the loss of one such water molecule, the other molecule being obtained from the interaction of an (OH) group of the hydrated silica sheet with an (OH) group af the adjacent sheet of $Al_2(OH)_6$. The two sheets are thus linked through the residual oxygen atom (see Fig. 7). This structure is also open to Hendricks' criticism stated above.

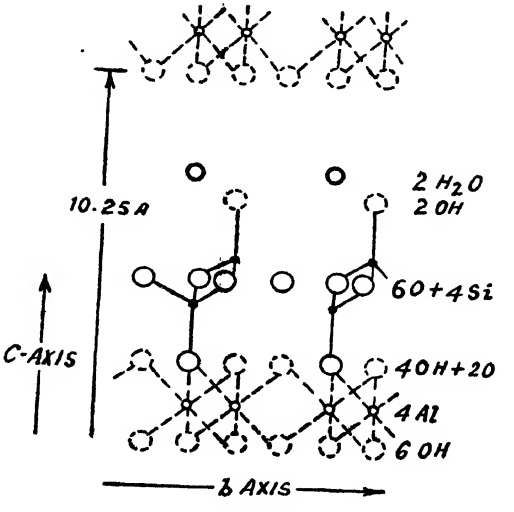

FIG. 7
(After Edelman and Favejee)
Schematic presentation of the crystal structure of hadrated halloysite

A monoclinic holohedral structure (C_{2h}) of halloysite has been suggested by Stout (1939) from a study of the x-ray diagrams of halloysite before and after fixation phosphates by this mineral. The unit cell in this structure would consist of two kaolinitic packets having their OH-layers facing each other.

(*ii*) *Minerals of the montmorillonite group.*—Hofmann, Endell and Wilm (1933), proposed a symmetrical pyrophyllite-like structure of montmorillonitic minerals (Fig. 6d). These minerals, however, seldom have the ideal composition $Al_2O_3 4SiO_2 H_2O$, of pyrophyllite. Wide variations in composition are encountered. Isomorphous replacements within the lattice are responsible for them. In the mineral montmorillonite, $[Al_{1.67}Mg_{.33}(Si_4)O_{10}(OH)_2]Na_{.33}$, having a SiO_2/Al_2O_3 ratio of about 4.0, isomorphous replacements, *e.g.*, of octahedral Al^{+++} by Mg^{++} or Fe^{+++} and of Si^{++++} by tetrahedral Al^{+++} are limited. Extensive replacements give rise to a number of end members.

Beidellite having the SiO_2/Al_2O_3 ratio 3:1, is the end member obtained by the replacement of a part of the Si by tetrahedral Al*. The negative charge developed in the silica layer as a result of this replacement is balanced by the

* Grim (1942) believes beidellite to be a mixture of montmorillonite and limonite.

incorporation of mono-, or, bi-valent cations as in micas and/or by the replacement of octahedral Al^{+++} by Mg^{++}. A small quantity of the octahedral Al^{+++} may also be replaced by Fe^{+++} and Fe^{++}. Complete replacement of octahedral Al^{+++} by Mg^{++} would give rise to saponite. Nontronite is the end member obtained by the replacement of the octahedral Al^{+++} by Fe^{+++} and Fe^{++}. A differentiation of these end members on the basis of the powder diagrams alone is not possible excepting perhaps nontronite whose Fe has a much higher scattering power than Al or Mg.

Hofmann, Endell, and Wilm assume an orthorhombic cell for montmorillonite with dimensions $a=5.095$ Å, $b=8.83$ Å and $c=15.2$ Å. Gruner (1935) however, believes that minerals of the montmorillonite group belong to the monoclinic system. According to Hofmann and Maegdefrau (1937), the individual packets lie parallel to and equidistant from one another but are not similarly oriented in the a- and b-directions. Because of this random orientation there is, strictly speaking, no space lattice but each packet forms some sort of a surface lattice. This 'cross-grating effect' follows from the complete absence of (hkl) interferences. Only (hko) and (001) interferences referred to the space lattice are observed.

Some orientation of the packets in the a-and b-directions has been suggested by Hendricks and Ross (1939).

A characteristic feature of the montmorillonite lattice, one which differentiates it from pyrophyllite having a similar structure, is the variable *c*-axis of the former depending on the content of water. This unique property of unidimensional inner-crystalline swelling is shown by only two other known substances, graphitic acid (Hofmann and Frenzel, 1932) and violet basic cobalt sulphate (Feitknechet and Fischer, 1935), The water molecules are loosely held between the packets and are readily given up on heating. Hofmann observed a reversible dehydration up to a temperature of 550°C. The lattice is preserved even at 800°C but breaks down at about 1000°C. Maegdefrau and Hofmann found a continuous variation of the swelling with the humidity. Nagelschmidt (1936), however, observed a stepwise variation; the (001) spacing increased from 10.5 Å to 15.2 Å and from 15.2 Å to 15.6 Å as the number of water molecules per 'ignited' unit cell, *i.e.*, per $Al_4Si_8O_{22}$, increased respectively from 2 to 10 and from 10 to 21. For a number of water molecules varying from 10 to 21 no significant variation in the spacing was observed but in the range 20-40 H_2O the spacing increased rapidly to 18.4 Å. From studies of x-ray diagrams of oriented samples of montmorillonite Bradley, Grim and Clark (1937) showed that the stepwise increase in swelling is to be attributed to the formation of definite hydrates containing 2, 8, 14, 20 and 26 molecules of water corresponding to (001) spacings respectively equal to 9.6 Å, 12.4 Å, 15.4 Å, 18.4 Å, and 21.4 Å.

No entirely satisfactory and generally accepted explanation has been offered regarding the manner in which the water molecules are held between the packets. Hofmann (1937), Nagelschmidt and others believe that the water molecules form

closely packed sheets between the basal planes. According to Hendricks and Jefferson (1938), however, the water molecules are not densely packed but form a hexagonal net by secondary bonds between O and H atoms of adjacent water molecules in a given net as shown in Fig. 8(*a-b*). One-fourth of the hydrogen

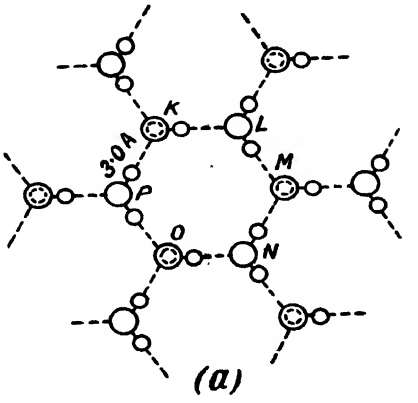

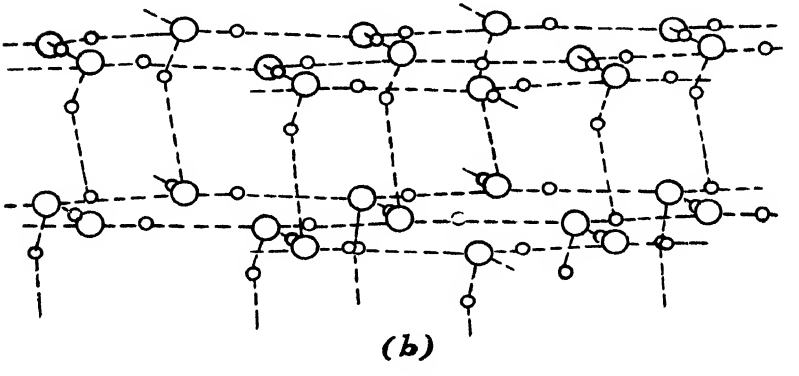

FIG. 8
(After Hendricks and Jefferson)

(*a*) Hexagonal net of water molecules. Large spheres represent oxygen atoms and small spheres hydrogen atoms, dotted lines indicate bonding through hydrogen.
(*b*) Probable structure of multiple water layers.

atoms in the net, or in other words, one hydrogen atom in every two water molecules remains 'free', *i.e.*, not bonded in this manner. The net itself is tied up to the neighbouring silica layer or other hexagonal layers by the attraction between such 'free' H atoms and oxygen atoms of the adjacent layers*. The

* When the surface of the clay mineral contains hydroxyl groups (*e.g.*, kaolinite) some of these hydroxyl groups are free so as to bind their hydrogen atoms to oxygen atoms of the water layer.

oxygen atoms in a given water layer lie in one plane. In this configuration each layer contributes 4 molecules of water to the structural unit as against 6 molecules in the close packed arrangement. The observed variation in the (001) spacing arises from a variation in the spacing between the cleavage planes. Cleavages along (001) planes give rise to crystallites containing different numbers of water layers corresponding to the different hydrates $2H_2O$, $6H_2O$, $10H_2O$, etc. The observed (001) spacing at a fixed humidity is only an average of the spacings of the various hydrates. It is this average spacing which varies continuously with the humidity. The stepwise variation observed by Nagelschmidt is difficult to explain in the light of this hypothesis. It is also difficult to understand why other clay minerals and even pyrophyllite which has the same structure as montmorillonite do not swell.

Hofmann and Bilke (1937) showed that at a fixed humidity the swelling of montmorillonite depends on the nature of the exchangeable cations as well as on the p_H. No satisfactory explanation of this 'cation effect' has also been forthcoming. A mere hydration of the cations (Wiegner, 1931; Bär and Tenderloo, 1936) would explain neither the magnitude of the swelling nor the differences in the relative effects of the various cations. From a study of the low temperature endothermic effect shown by 'thermal curves', Hendricks, Alexander and Nelson (1940) concluded that only a very small fraction of the water can be attributed to a hydration of the cations in the case of Mg-, Ca- and Ba-montmorillonites, the greater part of the water beings tacked between the packets as hexagonal nets. No water of hydration could be detected in the case of Na-, K-, and Cs-montmorillonites.

The characteristic swelling of montmorillonite is probably to be attributed to the polarising properties of the cations (W. Russel, 1934) lying on the surface of the packets. Montmorillonite contains a much larger quantity of such cations than any other clay mineral. In view of extensive and different types of isomorphous replacements in montmorillonite considerable strains are brought to bear on the lattice which hamper the growth of the crystals to large dimensions and only minute crystallites are formed (*cf.* Hendricks, 1942). This gives rise to an extensive outer surface and a large number of exposed cations. The latter have their coordination valencies only partially satisfied and this further reinforces the tendeney of the cations to polarise water molecules and draw them to the surface. A layer of water molecules thus condensed on the surface may be covered by other layers in accordance with the mechanism suggested by Hendricks and Jefferson.

Clay minerals other than montmorillonite and also pyrophyllite do not contain any appreciable quantity of cations on the surface and consequently do not swell. The micas which also do not swell no doubt contain some cations in between the packets. However, unlike montmorillonite, a comparatively small percentage of these cations is exposed. This is due to the formation of larger crystals favoured by absence of strains arising from different types of isomorphous replacements.

There is yet another reason for the nonexpanding lattice of the micas (Grim *loc. cit*). Unlike montmorillonite where isomorphous replacements mainly take place in the octahedral layer, they are almost entirely restricted to the silicate layer in the micas. The centre of the negative charge within the packets lies nearer to their surfaces in micas than in montmorillonite and consequently the cations in the former are strongly bonded to the surface and, through them, the packets themselves are firmly held and do not admit of any expansion in the c-direction. On account of a greater separation of the charges in montmorillonite, the packets are tied together comparatively loosely through the cations interposed between them and thus help the water molecules to force the packets apart.

Several investigators (Holzner, 1936 ; Bragg, 1938 ; De Lapparent, 1938) have taken exception to the pyrophlyllite structure of montmorillonite on the ground that it does not satisfactorily explain the characteristic swelling (and high base exchange capacity) of this mineral. Edelman and Favejee (1940) proposed an alternative structure (Fig. 9) in which the silica layer on either side of the hydrargillite layer has the configuration of β-cristobalite (Fig. 1, b) hydrated as in halloysite and has the formula $O_2Si_4O_6(OH)_2$. The mineral

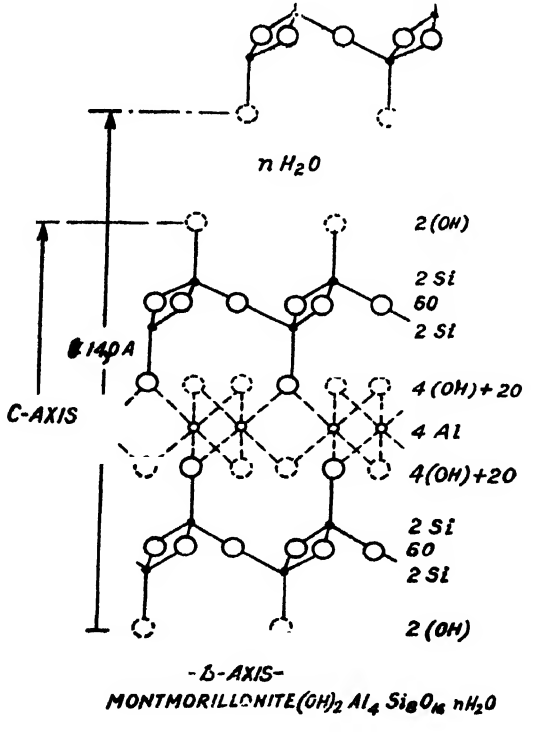

FIG. 9
(After Edelman and Favejee)
Schematic presentation of the structure of Montmorillonite.

itself has the composition $(OH)_{12}Al_4Si_8O_{16}.nH_2O$. Grim prefers this structure as in his opinion it offers a better explanation of the swelling. He considers that the projecting OH ions in this structure favour the formation of water layers as suggested by Hendricks and Jefferson.

Other structures have been suggested but have not met with general approval as they have no particularly strong points in their favour. The pyrophyllite structure suggested by Hofmann is usually accepted as it provides the best all round explanation of the behaviour of montmorillonites if isomorphous replacements as well as individual properties of cations are also taken into consideration.

Minerals of the illite group or hydrous micas.—Until recently there has been some confusion regarding the existence of micas as a distinct group of clay minerals. Hendricks and Fry (1930) recognised certain minerals in soil colloids which they designated as ordovician bentonite', a term used by Ross and Shannon (1926). Ross and Kerr (1931) described similar minerals as potassium bearing clay minerals. Hofmann and his coworkers (1937) first definitely distinguished mica-like minerals as essentlal constitutents of clays and named them 'glimmerton'. Almost simultaneously, Grim, Bray and Bradley detected mica-like clay minerals in a variety of soils, clays and shales from Illinois and placed them in a distinct group under the name "illite". The group-name "hydrous micas" proposed by Hendricks for all such micaceous clay minerals is more suggestive as it brings out their chemical and structural relationships to muscovite mica ; the hydrous micas, though structurally similar to muscovite, contain more water and less K than the latter.

The general formula, $2K_2O$, $3R^{++}O$ $8R_2^{+++}O_3$ $24SiO_2.2H_2O$ of hydrous micas is derived from the ideal formula $K(Al_2)(AlSi_3)O_{10}(OH)_2$ of muscovite mica by the replacement of some K by H_2O. Balancing of the charges is effected by the replacement of Si^{++++} by tetrahedral Al^{+++} or of O^{--} by OH^- (Hendricks, 1937). Only 15% of the Si, and not 25% as in muscovite mica, is replaced by Al giving a relatively smaller amount of K. Possible replacements of Mg^{++} for octahedral Al^{+++} balanced by the substitution of $(OH)^-$ for O^{--} may partly account for a higher percentage of water in the hydrous micas than in muscovite (Hofmann and Maegdefrau 1937). Both ferrous and ferric iron may also replace some octahedral Al. Isomorphous replacements, however, are not so extensive in the hydrous micas as in montmorillonites.

Gruner (1935) and others have postulated a monoclinic cell for hydrous micas similar to that of muscovite ; the cell dimensions, however, have not been recorded*. Hofmann and Maegdefrau, on the other hand, believe that their diffraction data can be explained by assuming an orthorhombic cell having the dimensions a = 5.18 Å, b = 8.97 Å, c = 19.84 Å.

(*iv*) *Minerals of the attapulgite group.*—J. Delapparent (1935) gave the name attapulgite to a clay mineral found in fuller's earth from Attapulgus,

* Presumably they have accepted the cell dimensions of muscovite ;

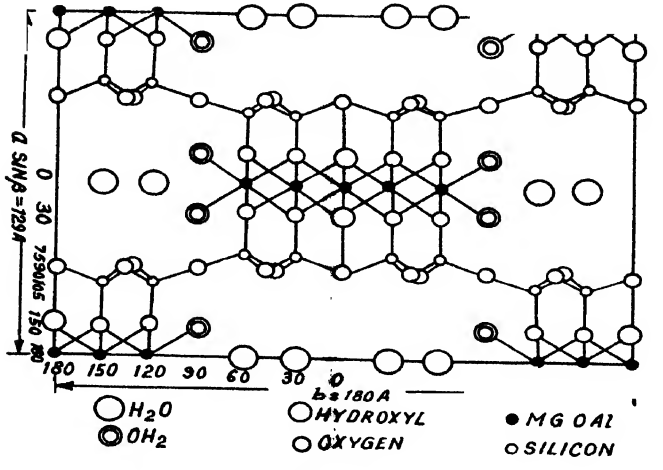

FIG. 10
(After Bradley)

Idealized proposed structure for attapulgite projected on to (001).

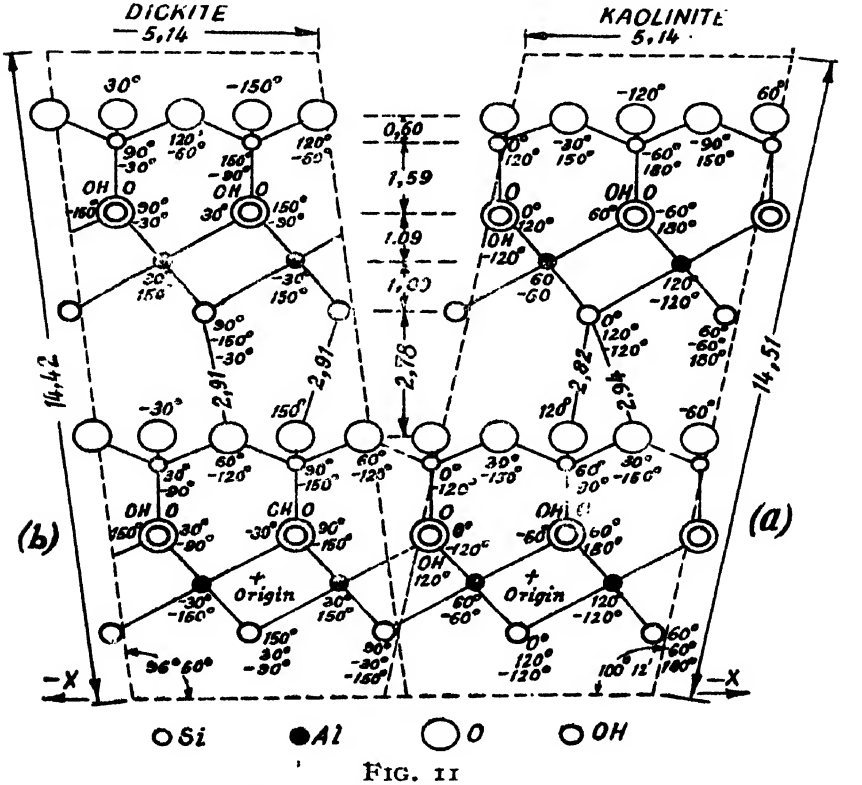

FIG. 11

Comparison of the dickite and kaolinite unit cells. The plane of the paper is the principal glide plane of symmetry containing the origin. Y-co-ordinates are given in degrees.

Georgia and Mormoiron in France. Formerly (Kerr, 1937) it was considered to belong to the montmorillonitic group of minerals. X-ray studies by Bradley (1940) however, showed "fibre diagrams".

The structure proposed by Bradley (Fig. 10) consists of a brucite layer fused between two silica layers. The brucite layer is, however, not continuous and the structure extends only in one direction instead of two as in the case of other clay minerals. Consequently, instead of sheets, fibres or rods with the c-axis parallel to the length of the fibres are obtained. The silicon-oxygen chains running parallel to the c-axis along (ooZ) and ($\frac{1}{2}\frac{1}{2}$Z) are similar to amphibole chains (Warren, 1929) so that the silicate layer as viewed from above is continuous. Chains of water molecules wich also run parallel to the c-axis fill the interstices between the ribbons and this water is lost below 100°C without materially altering the diffraction patterns. An equal amount of water is co-ordinated about Mg. It is less easily removed. Finally, the water which is expelled above 500-600°C comes from the OH groups of the lattice, the unit cell containing four of them.

The periodicity along the c-axis is 5.29 Å. Bradley gives the following dimensions of the cell:

$$a \sin\beta = 12.9 \text{ Å}, \quad b = 18{,}0 \text{ Å}, \quad c = 5.20 \text{ Å}$$

The cell has the ideal composition $(OH_2)_4(OH)_2\ Mg_5\ Si_8\ O_{20}\ 4H_2O$. There are two such molecules in the unit cell and the space group is probably $C_{2h}^3 - C^{2/m}$.

(*v*) *Mixed Structures.*—Mixed structures formed by the interstratification of more than one mineral have been encountered in minerals like vermiculites (22,23), cronstedite and faratsihite (Hendricks, 1939). The possibility of occurrence of such mixed structures in clays was pointed out by Hendricks. He Hendricks, and Teller, 1942) has given a theoretical treatment of diffraction of x-rays by such mixed structures. Another type of mixed structures has been visualised by Nagelschmidt (1944). It might result, say, "from weathering of illite particles in which the centre would have illite, the outer layers montmorillonite, composition. If the weathering had not gone very far such particles would give mica bulk effects (for instance, x-ray diffraction, chemical analysis) but montmorillonite surface effects (for instance, mixed base equilibria)" Definite evidence for such mixed structures in clays is however still lacking.

IDENTIFICATION OF CLAY MINERALS IN SOIL COLLOIDS

The importance of identification of clay minerals and assessment of their relative proportions in clay fractions for purposes of soil systematics and from the point of view of theoretical as well as applied soil science is now generally recognised. Both physical and chemical methods have been requisitioned for

this purpose. In view of isomorphous replacements and the possibility of occurrence of more than one clay mineral in the same clay fraction and owing, further to the association of silica, sesquioxides and other necessary materials, identification of the mineral constituents of the clay fraction on the basis of total analysis alone is not possible though a fairly satisfactory correlation has often been obtained between the mass chemical composition of the clay fraction expressed as its SiO_2/R_2O_3 ratio and various physical and chemical properties of clays, *e.g.*, swelling, viscosity, dispersibility, heat of wetting and base exchange capacity. While this ratio as a 'single value' soil constant is apparently of some importance, it is of little value for the identification of the mineral constituents of the clay fraction. Marshall (1935) tried to identify clay minerals in some clays by properly fitting their analytical data in the known lattice structures of the clay minerals. For this purpose, he assumed the following major replacements within the lattice (*a*) tetrahedral $Al^{'''}$ for $Si^{''''+}$, the resultant negative charge being balanced by one equivalent of cation per atom of Al; (*b*) $Fe^{++'}$ for $Al^{'''}$ in the octahedral layer; (*c*) either one $Mg^{+'}$ for one octahedral $Al^{'''}$ with incorporation of cations to balance the negative charge, or, 3 $Mg^{''}$ for 2 $Al,^{'''}$ which gives a neutral layer. The following minor replacements were also considered: (*a*) octahedral $Al^{'''}$ by $Ti^{''''}$, the positive charge developed when the latter is tetravalent being balanced within the lattice by the replacement of $Al^{'''}$ by Mg^{++} (*b*) $Si^{''''+}$ by $P^{'''''+}$, the resulting positive charge being balanced by the simultaneous replacement of $Si^{''''++}$ by tetrahedral Al^{+++}. However, even when such replacements are taken into account, a correct fitting of the analytical data in the lattice structures will hardly be possible when more than one clay mineral are present in the clay fraction and their relative proportions are not known.

Methods using adsorption of dyes (Hardy, 1931; Huttig, 1931) and preferential adsorption of certain cations (Schatchtschabel, 1940; Hendricks and Alexander, 1940) are not sufficiently developed for purposes of unequivocal identification or differentiation of the various clay minerals. Physical methods have been found to be more suitable for this purpose. These are based on a comparative study of clays and standard specimens of clay minerals by x-ray, thermal and optical methods. On being heated, these clay minerals lose water (present both as H_2O molecules and as OH groups of the lattice) each in a characteristic manner and methods have been proposed for identifying them based on this effect of heat. One of them, the so-called 'differential thermal' method which is originally due to Le Chatelier (1887), consists in following the temperature of the specimen relative to an inert material, *e.g.*, calcined alumina, when the two are heated continuously at the same rate. An endothermic change is indicated by a lag in the temperature of the specimen and an exothermic change by a sudden elevation of the temperature relative to the inert material. The number and character of such breaks, and the temperatures at which they occur serve as the criteria for identifying the clay minerals. Nagelschmidt considers that endothermic effects in clay minerals are to be attributed to the release of adsorbed

water and to a breakdown of the lattice, exothermic effects probably arising from oxidation of divalent Fe^{++} ion, or the formation of new silicates at higher temperatures. The 'thermal method' was first applied to clays by Orcel (1926) and to soils by Agafonoff (1935). Norton (1939) and more recently, Grim and Rowland (1942) have introduced improvements in the technique for differential thermal analysis.

In the so-called vapour pressure method used by Puri (1925) Orcel (1927), Thomas (1928) and Alexander (1936), the temperature of the material kept in vacuum is gradually raised and changes in the vapour pressure measured. The curve obtained by plotting the vapour pressure against temperature is considered characteristic of the mineral.

In the 'dehydration methods,' the loss in weight of the sample when heated to constant weights at various temperatures is measured and identification carried out from an analysis of such features of the temperature-dehydration curves as relative propertions of 'adsorbed' and crystal lattice' water and the critical temperature at which the lattice water is expelled, it being assumed that the loss of weight is due entirely to loss of water and no volatile matter or substance which gives up volatile matter on heating is present. Three different techniques are followed in regard to the manner of heating the specimen giving what are called methods, of (*a*) continuous heating, (*b*) single heating, and (*c*) intermittent heating. In (*a*) heating is done at a constant rate over the range 20°C to 1000°C andthe specimen weighed in *situ* (Longchambon, 1936). In (*b*) several lots of the same specimen are heated each to a different temperature, cooled, and then weighed (Dunstall, 1938). In (*c*), which is the most common in use, the same sample is heated and weighed at suitable intervals of temperature (Kelley and others, 1939)

In the so-called 'rehydration-dehydration' method suggested by Berkelhamer (1943), the amount of water taken up by clay minerals previously heated to 300°C and that lost between 300°C and 600°C is used as criterion for their differentiation and identification.

Examination under the microscope and determinations of refractive indices are the optical methods usually employed for the identification of minerals. Owing to the fine grain-size of clay minerals a direct microscopic examination of individual crystals is not possible.* However, in view of the platy nature of the crystallites they may be deposited from a suspension as fairly oriented optical units of microcrystalline aggregates which are more suitable for optical studies. These units show double refaction but in the majority of cases, the extinction is neither perfect nor sharp. Sometimes, when the particles are not deeply coloured, they show pleochroism. On account of the imperfectly crystallised state of the aggregates and in view of the presence of materials other than clay minerals in the clay fractions, Hendricks (1930) measured only the mean refractive index (r.i.) of the aggre-

* Ross and Kerr (1930), found a few comparatively large single crystals of kaolinite, dickite and nacrite.

gates. Kelley (1939) and others (Grimetal, 1937) however, determined the refractive indices in three directions. All of them used the immersion method.

Several limitations of the optical method for purposes of identifying clay minerals in clays, however, exist. The r.i. of any clay mineral varies within wide limits owing to isomorphous replacements with a consequent overlapping of the refractive index of different clay minerals. The r.i. of some clay mineral also varies with their water content and the immersion liquid (Correns and Mehmel 1936, Barner 1936). In the case of soil colloids further difficulties arise from coatings of oxides and hydroxides of iron on the aggregates. On account of these complications identification of clay minerals is seldom possible by the optical method alone.

X-ray analysis offers the most powerful method for identifying the mineral constituents of clays. It is also the only method with the help of which in addition to the dominant clay minerals in the clay fraction, accessory minerals as also clay minerals occurring in much smaller quantities can be detected. It was first used by Hendricks and Fry (1930) and subsequently by Kelley (1931), Hofmann (1934), Negelschmidt (1934), Edelman (1939), Grim (1935), Clark (1937) and others (Mehmel) 1938). The identification is carried out in a strictly empirical manner by comparing the powder diagram of the clay fraction with those of known minerals. Since all the clay minerals have essentially the same general scheme of structure, their diffraction patterns are extremely similar. The most characteristic differences are provided by their basal spacings (001) which permit an unequivocal identification and differentiation of the clay minerals even in mixtures; other lines are practically of no value for this purpose.

In addition to the peculiar and specific difficulties confronting each of the above physical methods of identification, they are all subject to the common limitation that they normally do not go beyond indicating the general group to which a clay mineral found in a given clay fraction belongs. Distinction between closely related individual members of the same group, *e.g.*, kaolinite and halloysite, or, montmorillonite and beidellite, is often not possible. The occurrence of mixed structure would further enhance the difficulties. However, a judicious combination of these physical methods supplemented by exhaustive chemical analysis is likely to give an insight into the detailed mineralogical make-up of the clay fraction.

A powerful tool for the differentiation of clay minerals has been recently provided by the electron microscope. The various clay minerals give characteristic and sufficiently distinctive electron micrographs (Ardenne 1940, Eitel 1939-40, Shaw 1941, Humbert 1941, Shaw 1942). The montmorillonites (except nontronite) and illite "show structures ranging from a fluffy, amorphous-appearing material to well defined, extremely thin plates. Nontronite is characterised by flat, frayed fibres. Kaolinite and dickite both have

hexagonal plate-shaped crystals. Dickite crystals are much thicker than most kaolinite crystals. Halloysite is characterised by long split rods."*

BASE EXCHANGE AND CRYSTAL STRUCTURE

Differences in the lattice structures of clay minerals are strongly reflected in their base exchange properties. Since Way (1860), a part of the mono and bi-valent cations of clay has been known to be readily exchanged for the cations of added salts. These are the so-called exchangeable cations or bases of the clay. The work of Kelley (1936), Marshall (1930-1935) and Nagleschmidt (1938) has definitely shown that the exchangeable cations are integral constituents of the lattice. The relation between base exchange and crystal structure has been discussed by Hofmann (1934-1937), Van der Meulen (1935), Edelman (1935) Schofield (1934) and others. Two factors mainly determine cation exchange, *viz.*, the physical accessibility of the cation and the nature and strength of the force with which it is held within the lattice. Grinding facilitates physical accessibility, as by this process the cations in the interior of the lattice are brought to the surface. Kelley and his co-workers have shown that grinding increases the base exchange capacity (b.e.c.) of a wide variety of minerals. The b.e.c. of the felspars which are considered to give some of the clay minerals on weathering increases markedly on grinding, *e.g.*, from 5.0 to 91 5 milliequivalents per 100 gms. in the case of orthoclase. Felspars are composed of linked Si- and Al-tetrahedra, one equivalent of cations, *e.g.*, K, Na, or Ca being required for each Al atom to balance the charge. These balancing cations are exposed on grinding and are readily exchanged.

Zeolites have a high base exchange capacity. They are also built up by linked Si and Al tetrahedra but unlike the felspars they have a honeycombed structure and the bases required to balance the negative charges of the Al-tetrahedra are accessible being located inside intercommunicating channels which permit the free passage of added cations through the interior of the crystals. Hence, as also pointed out by Kelley and Jenny, the size of the crystals need not be reduced by grinding in order to replace the balancing cations.† The b.e.c. of permutite is not affected by grinding which is consistent with the amorphous nature of this substance.

Grinding tends to reduce the sheets of mica to extreme thinness, thus exposing a large number of K^+ ions originally lying inaccessible in between the packets. The b.e.c. of muscovite increases from 10.5 to 76.0 m.e./100 gm. Both K and Mg are 'extracted' from biotite by a neutral solution of NH_4Ac and the quantity of each especially that of Mg, increases on grinding. The solid

* Electronmicroscopy appears to be the only method for differentiating raolintie from halloysite.

† The data recorded in their paper, however, indicate an increase in the b.e.c. of the zeolite, natrolite, from 74.5 to 108.5 m.e. per 100 gm. on grinding. No reference to this increase has been made by the authors nor have they tried to explain it.

always adsorbs a quantity of NH_4 equivalent only to that of K found in the extract. Apparently the exposed Mg^{++} ions of the broken octahedra are replaced by NH_4^+ but NH_4 silicate being unstable the solid readily parts with this NH_4.

Talc shows no base exchange capacity even after extensive grinding as indicated by the fact that particularly no NH_4 is adsorbed by the solid. As in the case of biotite, however, Mg is extracted by the NH_4Ac solution and its amount considerably increases on grinding ; "at the same time, the substance appears to undergo decomposition".

Pyrophyllite and kaolinite which usually do not contain any appreciable quantity of mono-and bi-valent cations and have a small base exchange capacity show increases in b.e.c. ranging from 4 to 158.5 m.e./100 gm. and 8 to 100.5 gm respectively on being ground to extreme fineness.* Kelley and his co-workers believe that the cation exchange power of these minerals is traceable to the H^+ ions of the OH groups of the crystal lattice. Kaolinite possesses two types of OH planes, one immediately on the exposed surface of a lattice package and the other, a subsurface OH plane covered by a network of O ions. The latter OH groups are also accessible through the hexagonal gaps in the superimposed O-network Only the subsurface OH planes are present in pyrophyllite. Grinding in a ball mill may split the crystals parallel to the basal planes or perpendicular to them. In the first case, new planes containing H^+ions would be exposed. In the second, the octahedral and tetrahedral layers would be broken. Hofmann, Endell and Wilm (1934) suggested that the cations are held by the free valency of the broken tetrahedra on the edges of the Si-O planes. Kelley and Jenny criticised this hypothesis as it, according to their opinion, violates the law of electroneutrality. They, however, lose sight of the fact that when a crystal is broken, simultaneously with the negative part of the bond there exists the corresponding positive part which would remove from the solution equivalent amount of the anion. The large increase in b.e.c. of kaolinite and pyrophyllite as a result of extensive grinding is, according to Kelley and Jenny, "due in large part, octahedral layers". The broken bonds may also polarise and adsorb water molecules which dissociate on the clay surface into OH and H^+ ions.

Hofmann, Endell and Wilm (1934) suggest that the high b.e.c. of extremely fine-grained kaolinite is due to lattice distortion. They have, however, not discussed the nature of such distortion and the part it is expected to play in fixing cations. Lattice distortion may produce an electrical field in the neighbourhood but it is not likely to explain the high b.e.c. of finely ground kaolinite.

Shaw (1942) studied the effect of 'dry' as well as 'wet' grindings on the b.e.c. and 'electronmicrography' of kaolinite. The b.e.c. increased to a greater extent on dry grinding. Wet grinding gave thinner flakes by cleavages along (001) planes having the hexagonal shape characteristic of unground kaolinite. The increase

* Schachtschabel (1940) could not find any increase in the b.e.c. of kaolinite on grinding.

in b.e.c. on wet grinding should be attributed in the light of Kelley's hypothesis to the greater number of planar OH groups thus exposed. Here again, some doubt as to the acid character of these OH groups and their possible contribution to the b.e.c. is cast by the fact that talc which also contains similar OH groups, shows practically no b.e.c. even on extensive grinding. It is, however, possible that the acidic properties of the OH groups is not shown up in view of the stronger basic character of Mg compared with Al.

The electronmicrographs reveal thicker but smaller particles as a result of dry grinding but their hexagonal character has almost disappeared. The smaller particle-size indicates a large number of broken bonds to which the high b.e.c observed on dry grinding is attributed.

Shaw and also Grim consider that a large portion of the b.e.c. of the hydrous micas is also due to broken bonds.

Montmorillonite is differentiated from other clay minerals by its high b e.c. The b.e.c. is attributable in a large measure to the mono-- and bi-valent cations which are incorporated into the lattice for balancing the negative charges developed as a result of isomorphous replacements. A quantitative agreement between the observed b.e.c. and that calculated on the basis of isomorphous replacement has been claimed by Nagelschmidt (1940) (see also Marshall 1935). Gieseking (1939) as also Hendricks and co-workers 1943) showed that these balancing cations can be exchanged for large organic cations. Different organic cations give different values of the basal spacing (001) which definitely show that the exchangeable cations are held in between the packets. Hendricks, Nelson and Alexander (1940) consider that about 80 of the exchange positions of montmorillonite are located on the basal planes and the remainder on the edges of the flakes. Kelley and Jenny (1936) report a considerable increase in the b.e.c. of bentonite on grinding. One palausible explanation of this increase is that the grinding exposes fresh layers of the blancing cations and also subsurface OH planes of the lattice. Electronmicrographs show that while very fine fractions of montmorillonite consist of particles having the thickness of a unit cell, coarser fraction contain thicker particles which on "wet washing" give particles unit cell thick. From studies of adsorption of gases Hendricks and Nelson (1943) concluded that air-dried montmorillonite usually gives aggregates having the thickness of about 50 unit cells. Hence it is probable that montmorillonite also contains aggregates having thickness of several cells and grinding like 'wet washing' reduces their thickness.

The increase in b.e.c. on grinding may also be brought about by the appreance of a large number of broken bonds.

Grinding obviously reduces the average particle-size of the clay crystals. However, no quantitative information regarding the variation of the average particle-size on grinding as also the effect of such variations on the b.e.c. is available. The clay fraction, even in the unground state, is a heterodisperse system. Subfractions having particle-sizes [more correctly, equivalent spherical diameters, (e.s.d.)] ranging between specified limits have been isolated by the

controlled centrifugalisation of the entire clay fraction and their b.e.c.'s determined. In the case of kaolinite and kaolinitic clays the b.e.c. increases with diminishing particle size (Harman 1940, Spiel, 1940, Mukherjee, *et al.*, 1942). An inspection of the electronmicrograph (Shaw 1942) shows that a decrease in the average e.s.d. is accompanied by a decrease in both the cross-sectional area and the thickness of the particles. Consequently, the broken bonds as well as the exposed basal OH groups of the lattice increase in number thus giving rise to a larger b.e.c. There is some confusion regarding the part played by the e.s.d. on the b.e.c. of montmorillonite. Hauser and co.workers (Hauser, 1941; Hauser *et al.*, 1937) claim to have shown that the b e.c. does not depend on the e s.d. According to them, this is due to the peculiar lattice structure of montmorillonite which admits of ionic exchange in between the packets. A definite increase in the b.e.c. with diminishing e.s.d. has, however, been observed in the case of bentonites as well as montmorillonitic hydrogen clays by Marshall (1935) and also Mitra *et al* (1942, 1943). Electronmicrographs (Shaw 1942) show that coarser particles of bentonites are not only thicker than the finer ones but have definitely larger cross-sectional areas. The smaller this area the greater will be the number of broken bonds, which would account for the higher b.e.c. of the finer fractions even if a complete exchange of the cations in between the packets took place. The finer fractions, amongst themselves, do not appear to show any great difference in regard to the cross-sectional area and the thickness. It is just possible that the very fine fractions studied by Hauser and coworkers consisted of particles having practically the same cross-sectional area but slightly different thickness. In that case, the number of broken bonds remaining practically constant no alteration in the b.e.c. of such fractions would be expected if all the interplanar cations were exchangeable.

Of the two factors, physical accessibility and the nature and strength of the force with which the cations are held by the lattice, the latter mainly determines the differences in the relative effects of various cations in regard to their capacity to replace the cations of the clay lattice. The lyotrope series Ba>Ca>Sr>Mg>Cs>K>Na>Li has often been observed in these exchange reactions. Considerations of ionic size, valency, mobility and hydration have been brought forward to account for this series. The H^+ ion often occupies an anomalous position in the series, and usually has a much greater exchanging power than the monovalent cations (Wiegner, 1925; Jenny, 1932, 1936).

Most of the earlier work on cation exchange in clays was done on systems whose mineralogical compositions were not unequivocally known. The pure clay minerals have been used only recently for these investigations. Page (1939), Bär and Tenderloo (1934) and Schachtschabel (1940) have observed certain specificities in the exchange behaviour of the various clay minerals which have been traced to their characteristic lattice configurations. Page brought forward evidence to show that ions of a size permiting them to fit closely into the cavities formed by the hexagonal net of oxygens are least replaceable. Schachtschabel (1940) found that for NH_4-montmorillonite, H^+ and K^+ have nearly the same

exchanging power; all the divalent cations have nearly the same effect which is definitely smaller than that of the univalent cations. NH_4-kaolinite gives the same sequence of the relative effects of cations as NH_4-montmorillonite. H^+, K^+ and in particular NH^+_4, are more tightly held by muscovite than the divalent cations. The relative ease of replacement of NH_4^+ from the three minerals follows the order montmorillonite > kaolinite > muscovite. When a mixture of montmorillonit and muscovite is treated with a solution containing Ca-and NH_4-acetates, the mica takes up more of the NH_4 and the montmorillonite more of the Ca^{++}. Hendricks and Alexander (1940) found a preferential adsorption of H^+ by mica and of Ce^{+++} by montmorillonite from a solution containing the two cations.

The work of Schachtschabel and Hendricks illustrates the modern trend of base exchange studies in clays which points to an increasingly wider acceptance of the clay mineral concept for a clearer understanding of base exchange phenomena. Further, base exchange criteria such as those suggested by Schachtschabel and Hendricks are sufficiently promising to warrant more systematic studies for their acceptance as a method for an unequivocal differentiation of the clay minerals and their identification in soil colloids.

University College of Science and Technology,
Calcutta.

References

Agafonoff. V., 1935, *Trans. Third. Int. Cong. Soil Sci.*, **3**, 74.
Alexander, L. T. and Haring, M. M., 1936, *J. Phys. Chem.*, **40**, 195.
Ardenne, M., Endell, K. and Hofmann, U., 1940, *Ber. deut Keram. Gesell.*, **21**, 209.
Atterberg, A., 1912, *Int. Mit. fur Bodenk.*, **2**, 312.
Bär, A. L. S.-and Tenderloo, H. J. C. 1936, *Koll. Beih*, **47**, 97.
Baren, F. A. Van, 1936, *Z. Krist.*, **95**, 266.
Berkelhamer, L. H., 1943, *J. Amer. Ceram. Soc.*, **26**, 120.
Bradley, W. F., 1940, *Am. Min.*, **25**, 405.
Bradley, W. F., Grim, R. E. and Clark, G. L., 1937, *Z. Krist.*, **97**, 216
Bragg, W. H., 1938, *Proc. Roy. Inst. Gt. Britain*, **30**, 39.
Bragg, W. L., 1937, Atomic Structure of Minerals, p. 225 (Oxford University Press).
Clark, G. E., Grim, R. E. and Bradley, W. F., 1937, *Z. Krist.*, **96**, 322.
Correns, C. W. and Mehmel, M., 1936, *Z. Krist.*, **95**, 337.
De Lapparent, J., 1935, *Compt. rend.*, **201**, 481.
De Lapparent, J., 1938, *Z. Krist.*, **98**, 233.
Dunstall, W. J., 1938, Science Diploma Paper, Imperial College of Science, London.
Eitel, W., *et al.*, 1939, 1940, *Ber. deut. Keram. Gesell.*, **20**, 165 ; *Naturwissens chaften*, **28**, 300, 367, 397.
Edelman, C. H., 1935, *Trans. Third. Intl. Cong. Soil Sci.*, 397.
Edelmann, C. H., Baren, F. A. Van and Favejee, J, CH. L., 1934, *Med. Land. Wageningen*, **434**, 1.
Edelman, C. H. and Favejee, J. CH. L., 1940, *Z. Krist.*, **102**, 417.
Feitknecht, W. and Fischer, G., 1935, *Helv. Chim. Acta.*, **18**, 40.

Gieseking, J E., 1939, *Soil Sci* , **47**, 1.
Grim, R. E., 1942, *J. Geol.*, **50**, 225.
Grim. R. E., Bray, R. H. and Bradley, W. F , 1937, *Am. Min.*, **22**, 813.
Grim, R. E , Kerr, P. F. and Bray, R H , 1935, *Bull. Geol. Soc. Amer* , **46**, 1960
Grim, R. E , and Rowland, R. A , 1942, *Am. Min.* **27**, 746, 801,
Gruner, J. W , 1932, a, *Z. Krist.*, **83**, 75; *Z. Krist.*, **83**, 394,
Gruner, J. W . 1933, *Z, Krist.*, **85**, 345.
Gruner, J. W., 1934, *Am. Min.*, **19**, 557; *Z., Krist.*, **88**, 412.
Gruner J. W , 1937, *Am. Min.*, **22**, 855.
Gruner, J W., 1935, *Am Min* , **20** 475; *Am. Min.*, **20**, 699.
Hardy, F., 1931, *J Agric, Sci.*, **21**, 150.
Harman, C. G and Fraulini, F , 1940, *J. Amer. Ceram. Soc.* **23**, 252.
Hauser, E. A. and LeBau, D. S., 1941, *J. Phys. Chem.*, **45**, 54.
Hauser, E. A. and Reed, C. E., 1937, *J. Phys. Chem* , **41**, 911.
Hendricks, S. B. and Fry, W H., 1930, *Soil Sci.*, **29**, 457.
Hendricks, S. B., 1942, *J. Geol* , **50**, 276.
Hendricks, S. B and Jefferson, M. E., 1938, *Am. Min.*, **23**, 851.
Hendricks, S. B,. 1938, *Z. Krist.*, **99**, 264; *Am. Min*,, **23**, 295; *Z. Krist.*, **100**, 509.
Hendricks, S. B., 1936. *Z. Krist* , **95**, 247
Hendricks, S. B., and Alexander, L. T , 1939, *Soil Sci.*, **48**. 257.
Hendricks, S. B, 1943, *Am. Min.* **28**, 1.
Hendricks, S. B. and Ross, C. S., 1939, *Z. Krist.*, **100**, 251.
Hendricks, S. B. and Jefferson, M. E., 1938, *Am. Min.*, **23**, 863.
Hendricks, S. B., Alexander, L. T. and Nelson, R. A., 1940, *J. A. C. S.*, **62**, 1457.
Hendricks, S. B. 1939, *Am. Min* **24** 529.
Hendricks, S. B. and Teller, E., 1942. *J. Chem Phys.*, **10**, 147
Hendricks, S. B. and Alexander, L. T., 1940, *Proc. Soil. Sci, Soc. Amer .*, **5**, 95.
Hendricks, S B., 1940, *J. Phys. Chem.*, **45**, 65.
Hendricks, S. B. and Nelson, R. A., 1943, *Soil Sci.*, **56**, 285
Hofmann, U. and Frenzel, A., 1932, *Koll Z.*, **61**, 297.
Hofmann, U., Endell, K and Wilm, D , 1934, *Z. angew. Chem* , **47**, 359.
Hofmann, U , Endell, K. and Wilm, D , 1933, *Z. Krist.*, **86**, 340.
Hofmann, U. and Bilke, W., 1937, *Koll. Z.* **77**, 238.
Hofman, W. and Maegdefrau, E., 1937. *Z. Krist* , **98**, 31.
Holzner, J., 1936, *Chem. der. Erde*, **9**, 464.
Humbert, R. P. and Shaw, B T., 1941, *Soil Sci.*, **52**, 481.
Hüttig, G. E. and Peter, A., 1931, *Koll Z.*, **54**, 140.
Jackson, W. W. and West, J., 1931, *Z. Krist.*, **76**, 211.
Jenny, H., 1932, *J. Phys, Chem.*, **36**, 2217 (1932) 1936, **40**, 501.
Ksanda, C. J. ano Barth, T. F. W , 1936, *Am, Min.*. **20**, 631.
Kelley, W. P., Dore, W. H. and Brown, S. M., 1931, *Soil, Sci.*, **31**, 25.
Kelley, W. P., Jenny, H. and Brown S. M , 1936, *Soil Sci.*, **41**, 259.
Kelley, W. P., Woodford, A. O., Dore, W. H. and Brown S. M., 1939, *Soil, Sci.*, **47**, 178.
Kelley, W. P. Dore, W. H. and Woodford, A. C. and Brown, S. M , 1939, *Soil, Sci.*, **48**, 201.
Kelley, W. P. and Jenny, H., 1936, *Soil Sci.*, **41**, 367.
Kerr, P. F., 1937, *Am. Min.*, **22**, 534
Longchambou, H , 1936,, *Bul. Soci. franc. Min.*, **59**, 145.
LeChatelier, H., 1887, *Z. Physic. Chem.*, **1**, 396.
Maegdefrau, E and Hofmann, U., 1937, *Z., Krist.*, **98**, 299.
Marshall, C. E., 1930, *Truns., Farad. Soc.*, **26**, 173.
Marshall, C. E., 1935, *Z. Krist.*, **90**, 8.

Marshall, C. E. 1935, *Z. Krist.*, **91**, 431.
Mattson. S. 1930, *Soil Sci.*, **30**. 459. 1931, **31**, 57, 1937, **43**, 421.
McMurchy, R. C , 1934, *Z. Krist* , **88** ,420
Mehmel, M , 1935, *Z. Krist.* **90**. 35 .
Mehmel, M., 1938. *Ber deut. Keram , Gesell.* ,**19**, 295
Mitra, R. P., Bagchi, S. N. and Roy, S. P and Mukherjee, S , 1943, *Ind Jour Agric Sci.*, **13**, 18.
Mitra, R. P., Sinha, R K. Roy, S P., Mukherjee, S , 1942, *Ind. Jour. Agric Sci.*, **12**, 638
Mukherjee, J. N., Mitra. R. P. and Chakravarty. S. K , 1942, *Ind. Jour. Agric. Sci.*, **12**, 291.
Nagelschmidt, G., 1934, *Z. Krist.*, **87**, 120.
Nagelschmidt, G.. 1939, *J. Agric Sci.*, **29**, 477.
Nagelschmidt, G , 1936. *Z. Krist* , **93**, 481.
Nagelschmidt, J. B., 1935., *Min Mag.*, **25**, 140
Nagelschmidt, G , 1944, *Imp. Bur. Soil Sci. Tech. Comm.*, **42**.
Norton, F. H., 1939, *J. Amer. Ceram. Soc.*, **22**, 54.
Orcel, J., 1926, *Compt. Rend* , **183**, 565.
Orcel, J., 1927, *Bull. Soc. Franc. Min.*, **50**, 75.
Pauling, L , 1930, *Proc. Nat. Acad. Sci , U. S. A.*, **16**, 123.
Pauling, L., 1930, *Proc. Nat. Acad. Sci., U. S. A.*, **16**, 578.
Pauling, L.. 1921, *J. A. C. S.*. **51**, 1010.
Puri, A. N., Crowther, E M. and Keen, B. A., 1925, *J. Agric. Sci.*, **15**, 68.
Ross, C. S. and Kerr, P. F., 1930, *U. S Geol. Survey, Prof. Paper* , **165E**, 151.
Ross, C. S. and Kerr, P. F., 1934, *U. S Geol. Survey, Prof Paper.*, **185G**, 135.
Ross, C S. and Hendricks, S. B., 1941, *Proc. Soil Sci. Soc. Amer.*, **6**, 58.
Ross, C. S. and Shannon, J. 1926, *J. Amer. Ceram. Soc.*. **9**, 77,
Ross, C. S. and Kerr, P., F. 1931, *J. Sed. Pet* , **1**, 59
Russell, E. S. 1934, *Phil. Trans. Roy. Soc.* (*Lond*)., **233A**, 361.
Schofield, R. K. 1939. *Soil S and Fertilizers.*, **2**, 1.
Schachtschabel, P. 1940, *Koll. Beih.*, **51**, 199.
Stout, R., 1939. *Proc. Soil Sci. Soc. Amer.*, **4**, 177.
Shaw, B. T. and Humbert, R. P., 1941, *Proc. Soil Sci. Soc. Amer.*, **6**, 146.
Shaw, B. T. 1942, *J. Phys. Chem* , **46**, 1032.
Spiel, S., 1940, *J. Amer. Ceram. Soc* , **23**, 33.
Thomas, M. D., 1928, *Soil Sci* , **25**, 409.
Van Bemmelen, J. M.. 1888, *Landw. vers. stat.*, **35**, 67.
Vandar Meulen. J. B., *Rec Trave hein Pays Bas*, **54**, 107
Warren, B. E. 1929, *Z. Krist.*, **72**, 42.
Way, J. T.. 1860, *Jour. Roy. Agric. Sci.*, **11**, 313.
Wiegner, G., 1924, Boden and Bodenbuildung, T. Steinkopff. Leipzig.
Wiegner, G., 1925, *Koll. Z. Erg. Bd.*, **36**, 344.
Wiegner, G., 1931, *J. Soc. Chem. Ind.*, **50**, 65, 103.

INTER-ELECTRODE CAPACITANCES OF TRIODE VALVES AND THEIR DEPENDENCE ON THE OPERATING CONDITION

By S. C. MITRA and S. R. KHASTGIR*

ABSTRACT. A double-beat method was adopted for the measurement of inter-electrode capacitances and their variations under the usual operating conditions. The theory of the method and the procedure are fully described and the experimental results obtained with eight different triodes are given in the paper. No grid-bias was employed and the effect of varying the filament current and the anode current for three different anode voltages on the inter-electrode capacitances was studied. The filament and anode-voltage applied were suited to the individual valves employed in the investigation. The main features of the experimental results are discussed and their interpretations given.

INTRODUCTION

It is now common knowledge that the effects of inter-electrode capacitances are of considerable importance, especially in the region of very high radio frequencies. In modern valves these capacitances are made as small as possible and in cases where these capacitances are not negligible methods are adopted to neutralise the effects of these inter-electrode capacitances as far as practicable. In view of the importance of the effect of inter-electrode capacitances, their actual measurements for various thermionic valves are also of considerable practical value. Since there are large and perceptible variations of the inter-electrode capacitance with the changes in the space-charge between the electrodes or with the alterations in density of the moving electrons under various operating conditions, an exact and accurate knowledge of such variations is of practical importance.

In a triode the capacitances between the three electrodes may be represented by C_{gf}, C_{ag}, and C_{af}. These are respectively the grid-filament the anode 1-grid and the anode-filament capacitances. It is obvious that when considering any one of these inter-electrode capacitances, the effect of the other two in series, joined with it in parallel can not be neglected. It is possible, however, to obtain the individual values of the inter-electrode capacitances with much difficulty, when there is no filament current and no grid or plate voltage. Many practical difficulties, however, arise when the filament carries a current and there is an anode current with a voltage on the plate or the grid. It was therefore thought desirable to develop a method of measuring the inter-electrode capacitances of a triode valve over a certain range of working conditions.

Following a double-beat resonance method measurements of the individual values of the grid-filament, anode-grid and anode-filament capacita-

* Fellow of the Indian Physical Society.

nces were made at a frequency of 1 Mc/s with different anode and filament currents for specified anode voltages. Measurements were also made with the filament cold and an estimate was made of the capacitances between the active portions of the electrodes as distinct from the total capacitance which includes the effect of wirings, leads etc. In the actual circuit, the following eight triode valves of different types were studied :—

(1) Philips E 406 (N)

(2) Philips B 406

(3) Philips B 405

(4) Cossor 41 MP

(5) Mazda PP 3/250

(6) Hivac PX 230

(7) American 2A3

(8) Philips TC 03/51

In all cases no grid-bias was applied to the grid. The maximum range of anode current corresponding to any triode could not, however, be utilised, as in most cases the anode current was found to diminish considerably as soon as the R.F. electrical oscillations were induced into the inter-electrode capacitances which were connected across the tuning condenser of the resonance system. The method and the details of the experimental procedure are set forth in a subsequent section.

PREVIOUS WORK ON INTER-ELECTRODE CAPACITANCES OF A THERMIONIC VALVE

The inter-electrode capacitances of a valve are usually measured by a bridge method using A.C. of 400 or 1,000 cycles/sec., with telephone as a balance indicator. Jones (1937) in a recent work employed a high frequency bridge and carried out some systematic measurements of the individul values of the inter-electrode capacitances of several triode valves with different anode voltages, and with varying filament and anode currents within working ranges of the valves. Measurements at 1 Mc/s. revealed the following main features :—

(1) The grid-filament capacitance increased with anode current up to the point at which the grid current began to flow.

(2) The increment of grid filament capacitance corresponding to a given anode current diminished with the increase of anode voltage.

(3) The increase of grid-filament capacitance did not depend merely on mutual conductance, anode circuit conductance or anode current. It increased with filament temperature and was therefore probably affected by the initial velocity of the electrons.

(4) The grid-anode capacitance was found to diminish with the increase of the anode current and the reduction was found to be much smaller proportionately than the increase of grid-filament capacitance.

(5) Every type of valve examined showed effect of the same kind. Even the small "acorn" triodes and pentodes showed increase of grid-filament capacitance amounting to 50% of the 'cold' value.

Much work on the inter-electrode capacitances was, however, made both theoretically and experimentally, in connection with what is known as the Miller effect. The theoretical treatment of the effect of inter-electrode capacitances in a triode network was developed by many, of whom Nichols (1919), Miller (1919), Hartshorn (1927) and Colebrook (1929) are most outstanding. The effect was theoretically shown to be equivalent to an input impedance across the grid and the filament The conclusions about the input impedance which again could be resolved into input capacitance and input resistance of the triode network and also about voltage amplification were in some measure verified by the measurements of the inter-electrode capacitances and of the voltage amplification.

THEORETICAL CONSIDERATIONS— EQUIVALENT NET WORK OF A TRIODE

A triode is represented in FIG. 1, where Z_a and Z_g are the external

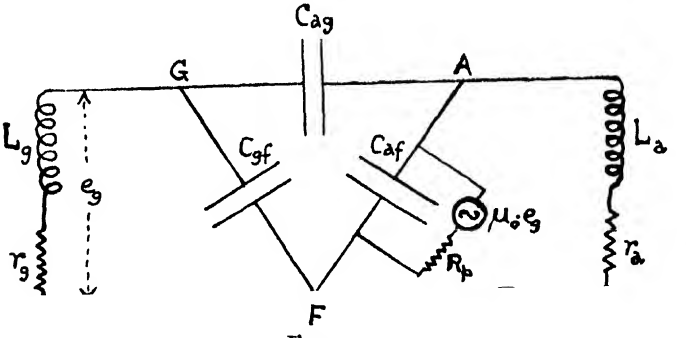

FIG. 1
Triode Net work

impedances of the anode-filament and the grid-filament circuits respectively. Let C_{gf}, C_{ag} and C_{af} be the grid filament, the anode-grid and the anode-filament capacitances respectively. Representing the resistance to the convection current between the filament and the anode by R_p, which is in shunt with the capacitance C_{af}, and remembering that a potential e_g impressed on the grid introduces an E.M.F. equal to $\mu_0 \cdot e_g$ in the anode circuit, the input impedance can be obtained by including in the anode circuit a fictious generator giving a voltage $\mu_0 . e_g$ and solving the Kirchoff equations for the network. (here μ_0 is the amplification factor of the valve).

Unless the frequency is very high and is o er 10^6 cycles per sec. the anode-filament capacitance C_{af} can be neglected, as it is shunted by R_p which is low compared with the impedance due to C_{af}. For low frequencies ($\omega < 10^6$) neglecting C_{af}, the effective input impedance is given by

$$Z_g = \frac{1}{jC_{gf}\omega} \cdot \frac{1 + j\omega C_{ag} r}{1 + j\omega C_{ag} r + \frac{C_{ag}}{C_{af}}(1 + \mu_0 r'/R_p)} \quad \ldots (1)$$

where $$r = \frac{R_p Z_a}{R_p + Z_a}$$ and $\omega = 2\pi \times$ frequency.

Writing the general form for Z_a, *viz.*, $Z_a = r_a + jx_a$

it can be shown that $$Z_g = -\frac{ac + bd}{c^2 + d^2} + j\frac{ad - bc}{c^2 + d^2} \quad \ldots (2)$$

$$= -r_g + jx_g$$

where the coefficients have the values

$$a = R_p + r_a - \omega R_p r_a C_{ag}$$
$$b = \omega R_p r_a C_{ag} + x_a$$
$$c = \omega^2 R_p r_a C_{gf} C_{ag} + \omega x_a (C_{gf} + C_{ag} + \mu_0 C_{ag})$$
$$d = \omega^2 R_p x_a C_{gf} C_{ag} - \omega R_p (C_{gf} + C_{ag}) - \omega r_a (C_{gf} + C_{ag} + \mu_0 C_{ag})$$

Assuming again the output inpedance to be *inductive*, *i e.*, putting $x_a = \omega L_a$ and denoting the amplification factor of the valve by μ_0, the input resistance r_g and input capacity C_g are given by

$$r_g = \frac{R_p C_{ag}(R_p r_a C_{ag} + r_a^2 \mu_0 C_{ag} + r_a^2 C_{ag} - \mu_0 L_a)}{[R_p(C_{gf} + C_{ag}) + r_a(C_{gf} + C_{ag} + \mu_0 C_{ag})]^2} \quad \ldots (3)$$

and $$C_g = C_{gf} + C_{ag}\left(1 + \frac{\mu_0 r_a}{R_p + r_a}\right) \quad \ldots (4)$$

When $r_a = 0$ the input capacity is reduced to

$$C_g = C_{gf} + C_{ag} \quad \ldots (5)$$

For high frequencies ($\omega > 10^6$) where the anode-filament-capacitance C_{af} cannot be neglected, the effective input impedance will be given by

$$Z_g = \frac{ac + bd}{c^2 + d^2} + j\frac{bc - ad}{c^2 + d^2}$$

where the coefficients have the values

$$a = \omega R_p r_a (C_{af} + C_{ag}) + x_a$$
$$b = \omega R_p x_a (C_{af} + C_{ag}) - R_p - R_a$$
$$c = \omega r_a (C_{gf} + C_{ag} + \mu_0 C_{ag}) + \omega R_p (C_{gf} + C_{ag}) - \omega^2 R_p r_a (C_{gf} C_{ag} + C_{gf} C_{af} + C_{ag} C_{af})$$
$$d = \omega x_a (C_{gf} + C_{af} + \mu_0 C_{af}) + \omega^2 R_p r_a (C_{gf} C_{ag} + C_{gf} C_{af} + C_{ag} C_{af})$$

Since ω is large, we can neglect the ω terms of the lower order in comparison with those of the succeeding and higher orders.

Now putting $\lambda_a = \omega L_a$ or $\frac{1}{\omega C_0}$, we get approximately

$$r_a = 0$$

$$C_g = \frac{C_{gf}C_{af} + C_{gf}C_{ag} + C_{ag}C_{af}}{C_{ag} + C_{af}}$$

$$= C_{gf} + \frac{C_{ag}C_{af}}{C_{ag} + C_{af}} \qquad \ldots \quad (6)$$

Thus at very high frequencies the input capacity of a triode network is practically independent of the constants of the external output circuit It can be looked upon as a 'grouped' capacitance with the grid-filament capacitance placed in parallel with series combination of the anode-grid and the anode-filament capacitances. The input capacity can therefore vary only when the individual capacitances change with the change of the working conditions.

METHOD OF DETERMINING THE INDIVIDUAL VALUES OF INTER-ELECTRODE CAPACTIANCES

(a) *Individual values of capacitances with no filament current and no anode voltage*

The method adopted consists in taking three separate observations of grouped capactiances :

(i) With grid and filament connected together, the capacitance across the anode and grid (or filament) is determined.

Denoting this by C_1, we have

$$C_1 = C_{ag} + C_{af} \quad \text{(grid and filament shorted)} \ldots \quad (7)$$

(ii) With anode and filament connected together, the capacitance across the grid and anode (or filament) is next determined.

Denoting this by C_2, we have

$$C_2 = C_{ag} + C_{gf} \quad \text{(anode and filament shorted)} \ldots \quad (8)$$

(iii) With anode and grid connected together, the capacitance across the filament and grid (or anode) is then found.

If this is C_3, we have

$$C_3 = C_{gf} + C_{af} \qquad \text{(anode and grid shorted)} \ldots \quad (9)$$

From (7), (8) and (9) it is evident

$$\left.\begin{aligned} \tfrac{1}{2}(C_1 + C_2 - C_3) &= C_{ag} \\ \tfrac{1}{2}(C_1 + C_3 - C_2) &= C_{af} \\ \tfrac{1}{2}(C_2 + C_3 - C_1) &= C_{gf} \end{aligned}\right\} \qquad \ldots \quad (10)$$

By measuring C_1, C_2 and C_3 the individual values of C_{ag}, C_{gf} and C_{af} are then obtained from (10).

(b) Individual values of inter-electrode capacitances of the triode under working conditions with filament and anode voltages

From the theoretical considerations it is evident that in the triode network with an output circuit employed under the working conditions, the input capacity of the triode at very high radio frequencies is approximately given by (6), viz.,

$$C_g = C_{gf} + \frac{C_{ag}C_{af}}{C_{ag} + C_{af}}$$

Thus, (i) if a comparatively large capacity ($C \gg C_{af}$) is placed across the anode-filament capacitance, the input capacity as given by (6) will be reduced to

$$C_1 = C_{gf} + C_{ag} \qquad (11)$$

Again, (ii) if a comparatively large capacity ($C \gg C_{ag}$) is inserted across the anode-grid capacitance, the input capacity as given by (6) under such condition will be given by

$$C_2 = C_{gf} + C_{af} \qquad \ldots \quad (12)$$

Next, (iii) when a relatively large capacity ($C \gg C_{gf}$) is placed in parallel with the grid-filament capacitance, the effective capacity between the anode and the grid will be given by

$$C_3 = C_{ag} + \frac{C_{gf}C_{af}}{C_{gf} + C_{af}} = C_{ag} + C_{af} \qquad \ldots \quad (13)$$

from (11), (12) and (13), the individual values of the inter-electrode capacitances of the triode come out as follows :

$$\left.\begin{aligned} C_{gf} &= \frac{C_1 + C_2 - C_3}{2} \\ C_{af} &= \frac{C_2 + C_3 - C_1}{2} \\ C_{ag} &= \frac{C_3 + C_1 - C_2}{2} \end{aligned}\right\} \qquad \ldots \quad (14)$$

For measuring the variations of the individual capacitances for various values of filament current and anode current and under specified values of the anode voltage, the values of the 'grouped' capacitances C_1, C_2 and C_3 are measured for different values of filament current and anode current under the desired conditions. Curves are then drawn showing the variations of C_1, C_2 and C_3. From these curves, the variations of the individual inter-electrode capacitances for varying values of filament current and anode current under desired conditions are obtained with the help of (14).

METHOD OF MEASURING THE 'GROUPED' CAPACITANCES AND EXPERIMENTAL PROCEDURE

The experimental arrangement is shown in Fig. 2 and the procedure is described below :

The particular 'grouped' capacitance C_1, C_2 or C_3 was connected by extremely short leads in parallel with the tuning condenser of capacity C of

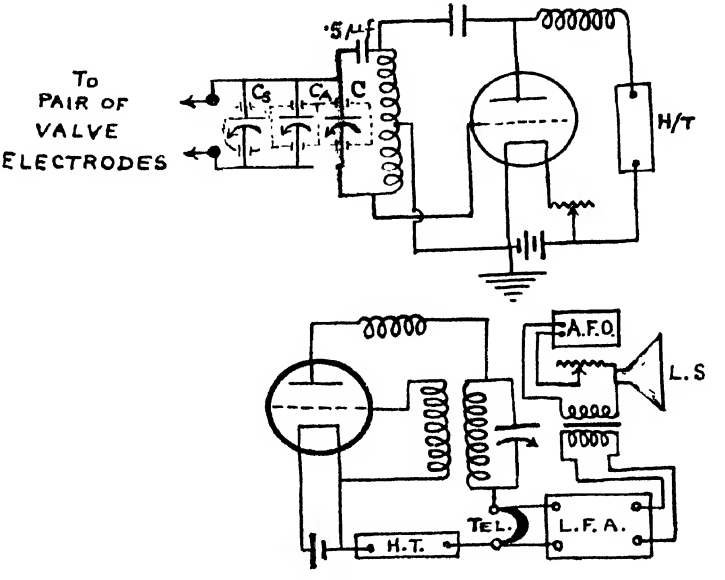

FIG. 2

Experimental arrangement

A. F. O—Audio frequency oscillator
L. F. A.—Low frequency amplifier
L. S.—Loud speaker
Tel.—Telephone

the oscillatory circuit of a suitable Hartley oscillator. The change in the value of this 'grouped' capacitance, when the inter-electrode space was filled with electrons, was balanced by changing the capacity of a small calibrated variable air condenser C_A in parallel with C and the desired 'grouped' capacitance so that the total capacity $(C_{1,2,3}+C+C_A)$ remained constant. High frequency oscillations from the oscillator were received by an oscillator-detector valve-circuit. When the detector circuit was nearly in tune with the oscillator, the familiar heterodyne whistle was heard in the telephone placed in the anode-circuit of the receiver. The audio-frequency voltage developed across the telephone was amplified by a three-valve amplifier of the conventional type and fed into a loudspeaker which gave a loud musical note. On introducing into the same loudspeaker an audio-frequency current from an audio-oscillator capable of producing an intense note of fixed

frequency, beats were heard by suitably adjusting the heterodyne frequency. The latter adjustement was made by varying the small variable condenser C_A. In parallel with C_a was also used a specially constructed variable vernier condenser C_s constructed from a spherometer. With this condenser very small variations of capacity could be effected. A variable resistance was placed in the secondary of the transformer used with the loudspeaker to match the intesity of the heterodyne whistle with that of the audio-frequency note. Adjustments of the small variable condenser C_A or the spherometer condenser C_s in the oscillator to produce no beats were then successively made with filament ' cold ' and with different values of the filament current and anode current which were noted. The variation in the value of any particular ' grouped ' capacitance with the change in the filament current (or the anode current) was thus accurately determined over a certain range of filament current or anode current suited to the value under examination.

A suitable D.C. meter with a coil of H.F. impedance was inserted in the anode circuit for measuring the anode current and a suitable ammeter in the filament curcuit for measuring the filament current of the experimental valve.

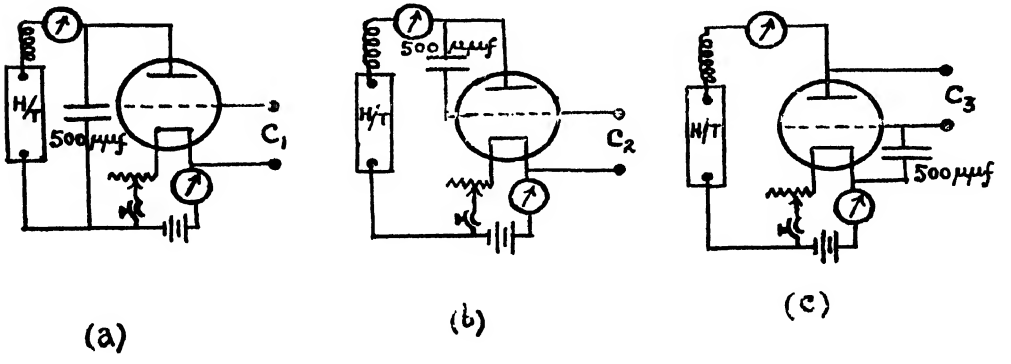

FIG. 3

Experimental valve connection

In Fig. 3 are shown the electrical connections and the insertion of a condenser of relatively large capacity in the circuit of the experimental valve for obtaining the ' grouped ' capacitances C_1, C_2 and C_3.

In the spherometer condenser a circular disc formed the fixed plate of this air-condenser and a similar circular disc, placed vertically above and parallel to the former, could be pushed by the central leg (which was cut short) when the graduated spherometer disc was given a right-handed turn. On giving a left-handed turn to the spherometer disc, the central leg would move up and the upper circular disc of the vernier condenser could be pulled up by a steel spring suitably fixed. Earthed guard-rings made up of thin brass foils, were inserted round the two parallel discs. The spherometer disc had a graduated

scale with 50 big divisions, each of which was further divided into 5 small divisions so that a turn through one small division would mean a very small change of capacity of the order of $10^{-3}\mu\mu f$.

It can be seen from the circuit diagram of the oscillator system that one plate of each of the condensers which were in parallel was also earthed. It was so arranged that the rotating plates of the condensers each of which was enclosed inside a shielded box were at the earthed end. Each of the smaller condensers was varied by turning a long glass rod fixed to the condenser knob. The effect of hand capacity was thus reduced to a minimum.

EXPERIMENTAL RESULTS

(i) *Measurements of inter-electrode capacitances without filament current and without anode voltage.*

Following the method outlined in Sec. 4(a) the inter-electrode capacitances with no electrons in the inter-electrode space were then determined. The results are given in Table 1. The amplification factor as obtained by C_{gf}/C_{af} is also entered in the table.

TABLE I

Capacitances in $\mu\mu F$

Valves	C_{gf}	C_{ag}	C_{af}	
1. Philips E 406 (N)	9.0	8.3	3 1	3.0
2. ,, B 406	5.6	4.8	3.8	1.4
3. ,, B 405	5.8	4.7	4.65	1.3
4. Cossor 41 MP	9.35	8.15	4.75	1.9
5. Mazda PP3/250	11.9	12 2	5.2	2.3
6. Hivac PX 230	5.7	7.9	2 75	2.7
7. American 2A3	7 4	14 4	6 8	1.1
8. Philips TC 03/5,	3 9	3.5	—	—

(ii) *Measurement of inter-electrode capacitances with varying anode current for three different anode voltages* :

The method outlined in sections 4(*b*) and (5) was followed :

First a capacity $500\mu\mu f$ was placed across the anode-filament electrodes. With such a relatively large capacity, the effective capacity between the grid and filament electrodes was measured. This measurement gave the value of the 'grouped' capacitance C_1,

where $$C_1 = C_{gf} + C_{ag} \quad \ldots \quad (15)$$

Secondly, with a capacity 500$\mu\mu f$ across the anode-grid electrodes, the effective capacity between the grid and the filament electrodes was measured. This gave the value of the 'grouped' capacitance C_2, where

$$C_2 = C_{gf} + C_{af} \quad \ldots \quad (16)$$

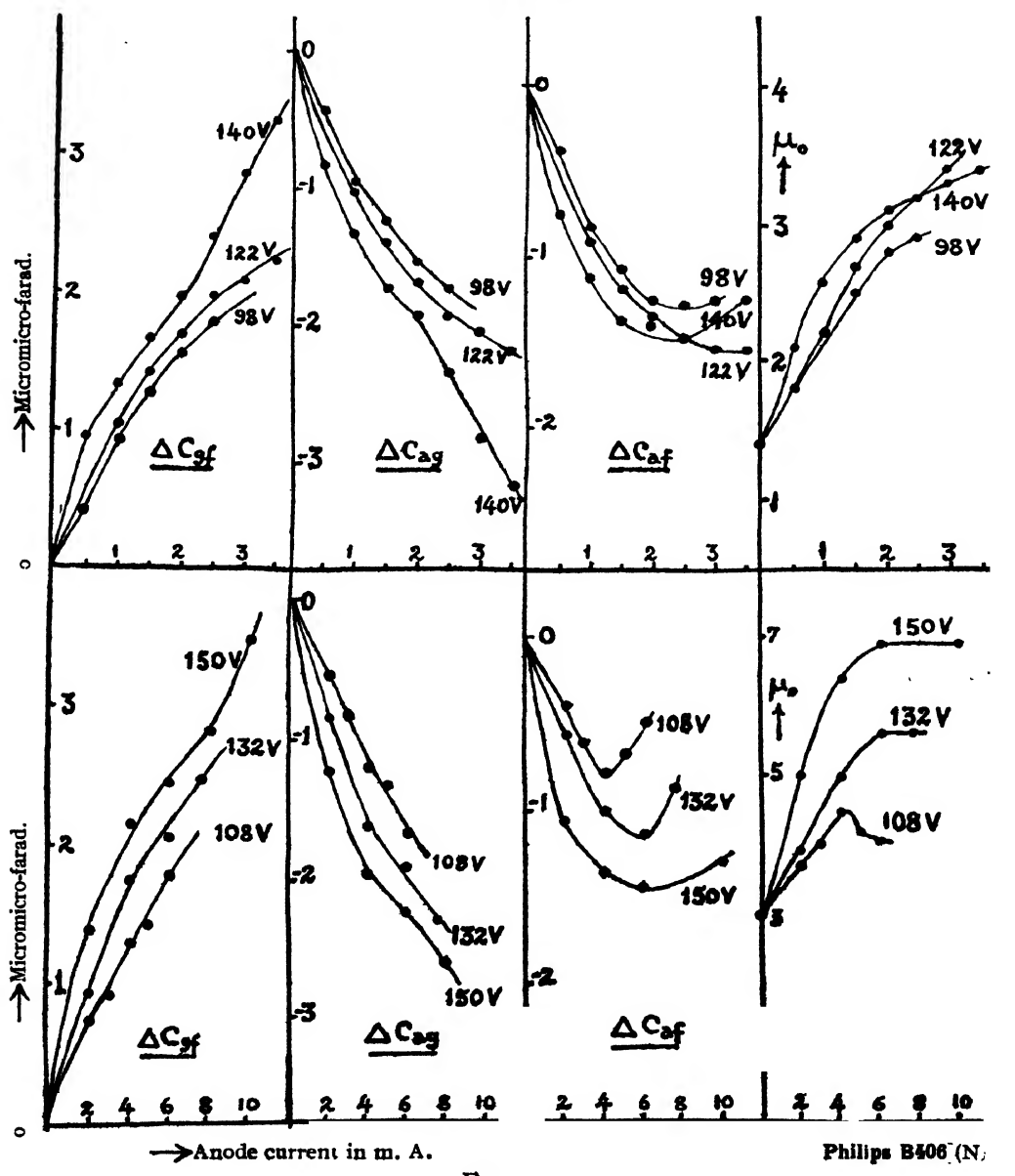

FIG. 4

Thirdly, with a capacity 500$\mu\mu f$ placed in parallel with the grid-filament capacitance, the effective capacity between the anode and the grid electrodes was measured. This yielded the value of the 'grouped' capacitance C_3,

where $$C_3 = C_{ag} + C_{af} \quad \ldots \quad (17)$$

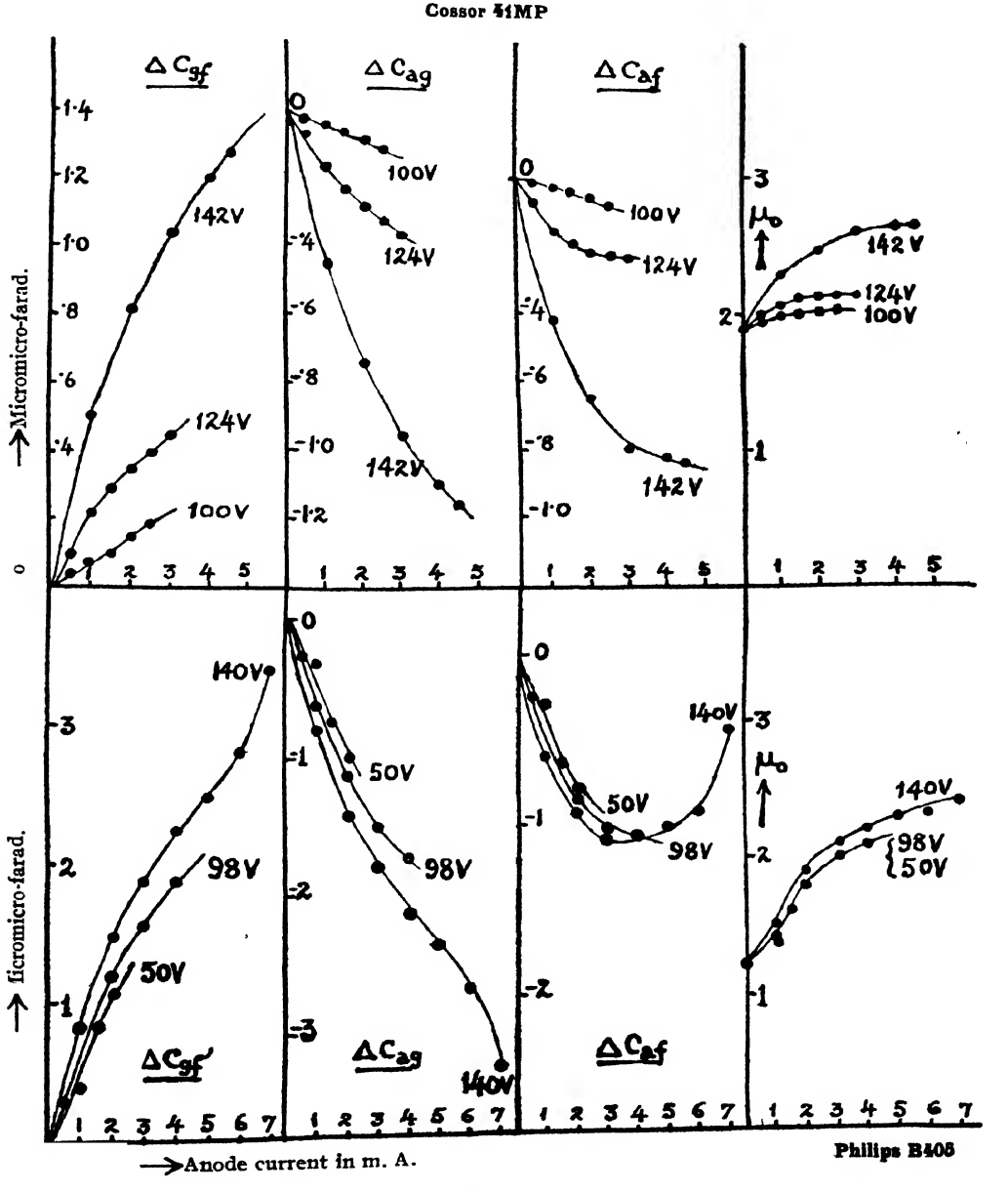

FIG. 5

The values of C_1, C_2 and C_3 were measured for no filament current (*i.e.*, for no anode current). With increasing values of filament current and anode current for a fixed anode voltage, the changes of C_1, C_2 and C_3 were then obtained and curves were drawn showing ΔC_1, ΔC_2 and ΔC_3 against

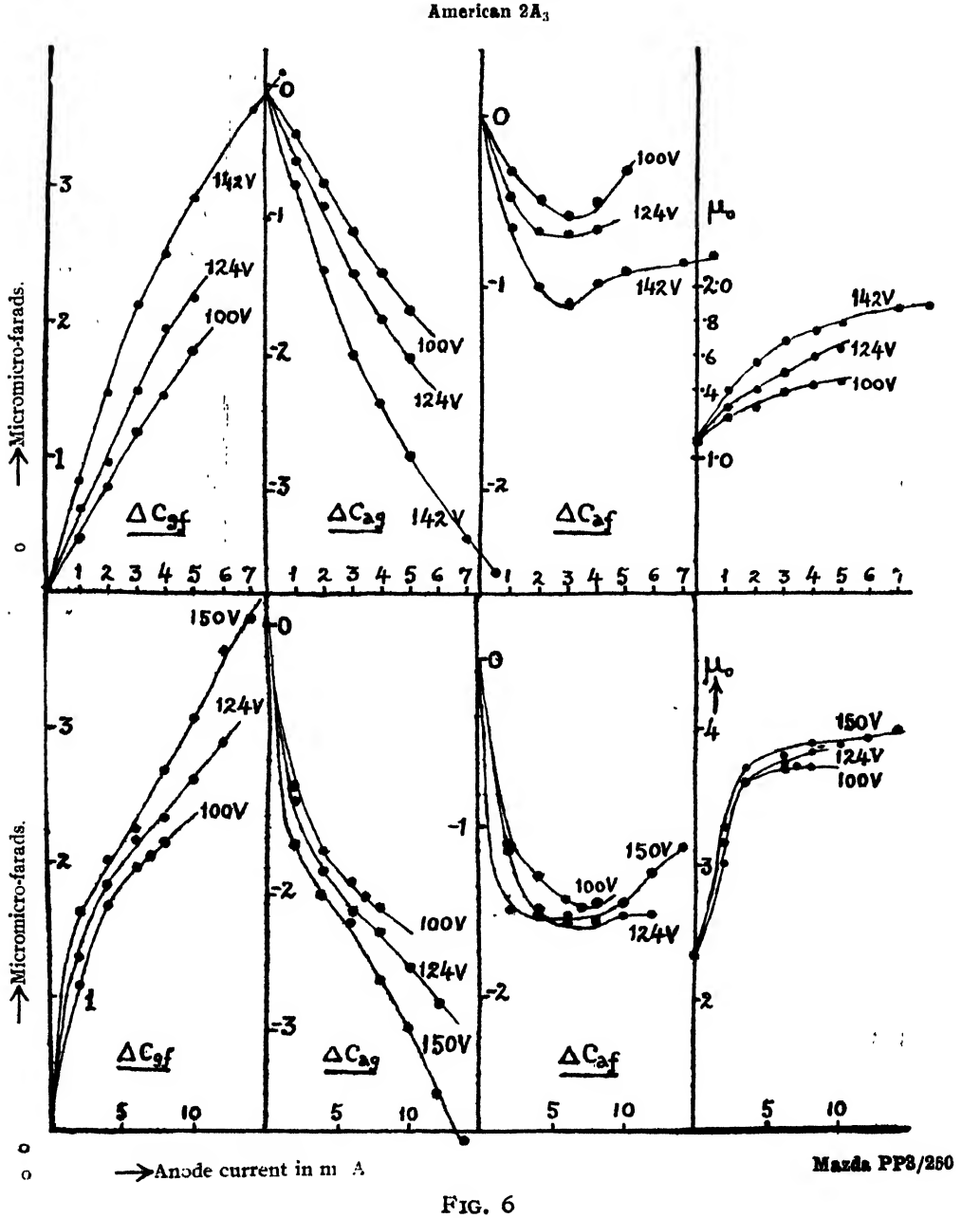

FIG. 6

anode current for three different anode voltages. From these curves the changes in the individual inter-electrode capacitances *viz.*

ΔC_{gf}, ΔC_{ag} and ΔC_{af} were determined from (14) for different values of the anode current and for the three fixed anode voltages. Since the inter-electrode capacitances for no filament current were originally measured the acutal values of C_{gf}, C_{ag} and C_{af} could be easily found for different anode-currents for the three fixed anode voltages.

The changes in the individual capacitances *i.e.* ΔC_{gf}, ΔC_{ag} and ΔC_{af} for the Philips E406 (N) and B406 valves are shown Fig. 4. In Figs. 5 and 6 are given the variations of the inter-electrode capacitances for the Philips B405, Cossor 41MP, Mazda PP3/250 and American 2A3 valves. Similar variations for the Hivac PX230 and the Philips TC 03/51 are illustrated in Fig. 7, the values of μ_o as obtained from C_{gf}/C_{af} are also shown in Figs. 4, 5 and 6. Variations of the inter-electorode capacitances with anode current for three fixed anode voltages were studied.

SUMMARY OF EXPERIMENTAL RESULTS

Summing up all the experimental results with triodes having no grid-bias, the main features which were observed, except in the case of the Philips TC 03/51 valve, are the following :—

I. (*a*) There was a steady increase of the grid-filament capacitance with the incrase of anode current within the experimental range.

(*b*) For the same anode current the observed of the grid-filament capacitance was larger for a larger anode voltage, except in the case of Hivac PX 230 valve, where the increase was smaller for a larger anode voltage.

II. (*a*) There was a comparatively slow but steady decrease of the anode-grid capacitance with the gradual increase of anode current.

(*b*) For the same anode current, the observed decrease of the anode-grid capacitance was large for a larger anode voltage, except in the case of Hivac PX 230 valve, where the decrease was smaller for a larger anode voltage.

III. There was a gradual decrease of anode-filament capacitance with the anode current with an occasional increase with further increase of anode current.

IV. There was a rapid rise in the amplification factor as obtained from the ratio of C_{gf}/C_{af} with anode current assuming or tending to assume a saturation value for higher values of the anode current.

The ultra-short wave transmitting valve (Philips TC 03/51) showed the following distinctive features :—

(*a*) The grid-filament capacitance was found in general to decrease steadily with the increase of the anode current up to a point beyond which there was a rise again with further increase of anode current. The turning point appeared at a higher value of the anode current for the higher anode voltage ; *e.g.*, the value of ΔC_{gf} was found to increase at 10 m.A., 5 m.A. and

2 m.A. respectively for 150 volts, 120 volts and 90 volts on the anode (see FIG. 7).

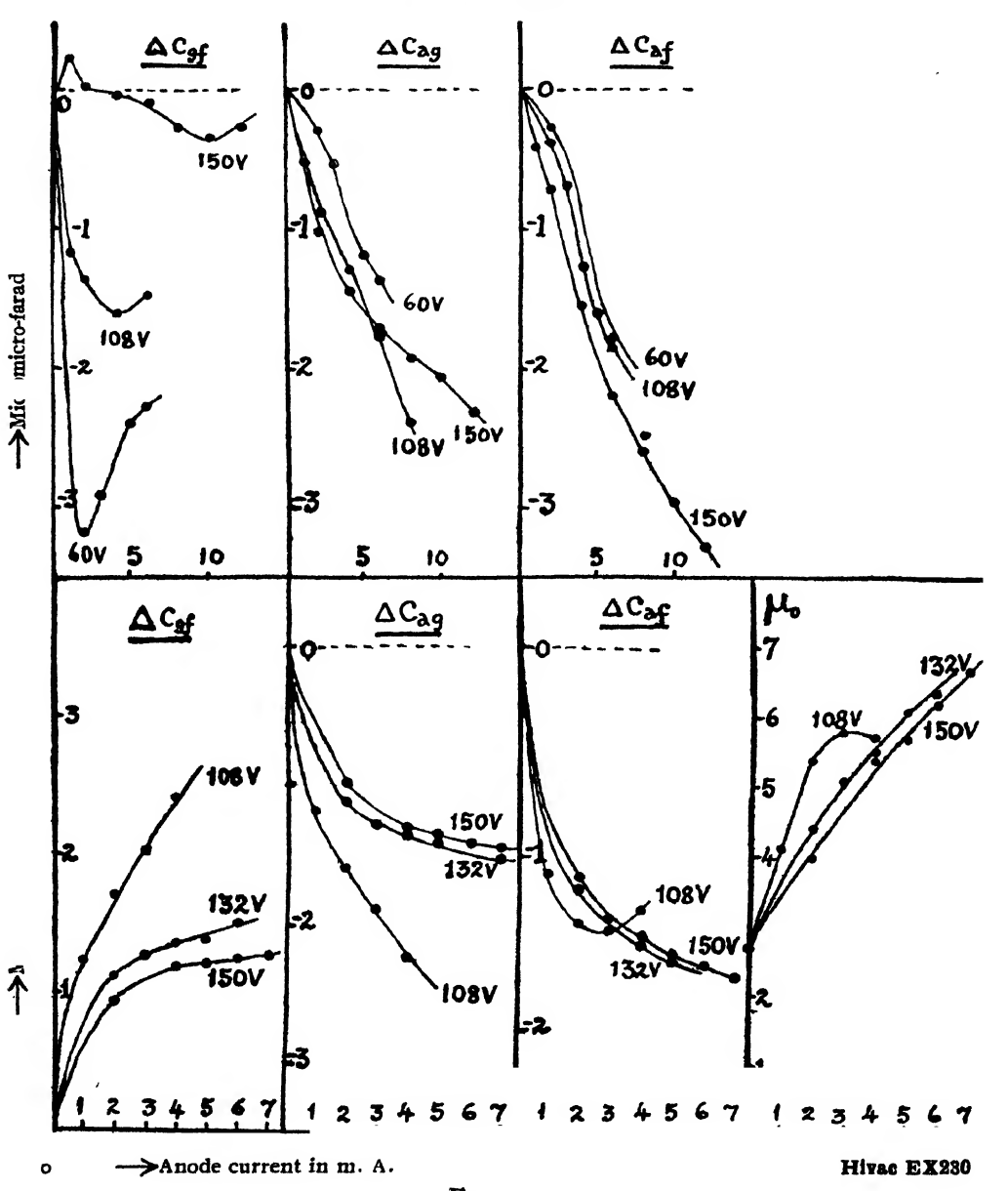

FIG. 7

(*b*) For 150 volts on the anode there was an initial increase of the grid-filament capacitance, a feature which was not observed for the lower anode voltages.

(*c*) The anode-grid and the anode-filament capacitances were found to decrease steadily with the increase of the anode voltages for all the three anode voltages employed.

The observed variations of the grid-filament capacitance and of the anode-grid capacitance for the *maximum* change of anode current for different anode voltages are shown in TABLE II for all the thermionic valves :—

TABLE II

Valves	V_a Volts	Δi_a (m.A.)	ΔC_{gf} ($\mu\mu$F)	ΔC_{ag} ($\mu\mu$F)
(1) Philips E406 (N)	150	0-10	+3.46	−3 19
C_{gf}=9.0$\mu\mu$F	132	0-7.5	+2.48	−2.30
C_{ag}=8.3 ,,	108	0-6	+1.77	−1.66
(2) Philips B 406	140	0-3.5	+3.25	−3.16
C_{gf}=5.6$\mu\mu$F	122	0-3.5	+2.23	−2.17
C_{ag}=4.8 ,,	98	0-2.5	+1 78	−1.27
(3) Philips B 405	140	0-7	+3.40	−3.25
C_{gf}=5.8$\mu\mu$F	98	0-4	+1.86	−1.74
C_{ag}=4.7 ,,	50	0-2	+1 06	−0.96
(4) Cossor 41MP	142	0−4.5	+1.27	−1.16
C_{gf}=9.35$\mu\mu$F	124	0−3	+0.44	−0.37
C_{ag}=8.15 ,,	100	0−2.5	+0.19	−0.12
(5) Mazda PP 3/250	150	0−14	+3.80	−3.83
C_{gf}=11.9 $\mu\mu$F	132	0−12	+2.89	−2.80
C_{ag}=12 2 ,,	108	0−8	+2 15	−2.1
(6) Hivac PX 230	150	0−7	+1.27	−1.44
C_{gf}=5.7$\mu\mu$F	132	0−6	+1.51	−1.53
C_{ag}=7.9 ,,	108	0−4	+2 41	−2.25
(7) American 2A3	142	0−8	+3.82	−3.61
C_{gf}=7.4$\mu\mu$F	124	0−5	+2.16	−2.03
C_{ag}=14.4 ,,	100	0−5	+1.78	−1.68
(8) Philips TC/03/51	150	0−12	−0.26	−2.32
C_{gf}=3.9$\mu\mu$F	108	0−8	−1.56	−2.39
C_{ag}=3.5 ,,	60	0−6	−2.28	−1.36

INTERPRETATION OF EXPERIMENTAL RESULTS

We shall now explain the experimental results regarding the variations of the grid-filament and the anode-grid capacitances with the variations of the anode current. The nature of the variations of the anode-filament capacitance (or of the ratio C_{gf}/C_{af}) would, however, depend on the rates of change of the grid-filament and the anode-grid capacitances with anode current for the individual valves.

Any inter-electrode capacitance of a triode should naturally depend on the presence of electrons coming from the hot filament towards the anode. The electrons usually bring about two effects: (1) a reduction in the dielectric constant of the inter-electrode medium and (2) a conductivity effect across the

electrodes. The first would cause a steady reduction of the inter-electrode capacitance with the increase of the electronic current through it. The second would involve a slight and apparent increase of the inter-electrode capacitance, since the conductivity acquired by the medium introduces a damping (a series resistance) in the resonance circuit, thus increasing the apparent capacitance between the two electrodes in the conducting medium, the other factors, namely the inductance and resistance of the LCR-circuit remaining the same for a given frequency of the alternating field. Thus with a larger anode current, when there would be a greater conductivity effect, the apparent increase of the inter-electrode capacitance would also be greater. In the experiments of Khastgir and Chowdhury (1940), on dielectric constants of electronic medium, this apparent increase of the inter-electrode capacitance was found to be negligibly small for lower radio frequencies (less than 400 Kc/s) and for about 1 Mc/s, this was found to be about half the decrease of the same capacitance due to the reduction of the effective dielectric constant of the electronic medium The conductivity effect due to high frequency oscillations in the electronic medium during observation is, however, extremely small in the high-vacuum thermionic valves. On the whole, therefore, the inter-electrode capacitance would drecease with the increase of electron concentration, *i.e.*, with the increase of anode current (for a given anode voltage). This normal feature is usually observed in the case of the *anode-grid capacitance.*

In the case of the *grid-filament capacitance* also a similar decrease of the capacitance value with the increase of anode current would be observed, *provided there is no space-charge.* In the neighbourhood of the filament, for low anode voltage and large filament current, there is always some space-charge. The effect of the space-charge is significant. Referring to Fig. 8, where some poten-

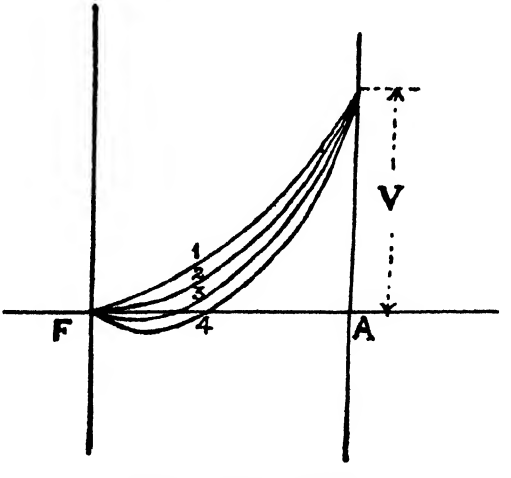

Effect of space charge.

FIG. 8

tial distribution curves between the anode and the filament for different amounts of space-charge are shown, it is clear that the effect of space-charge is to produce a curvature of the potential distribution curve. When the space-charge is sufficient, the potential curve shows a negative gradient in the neighbourhood of the filament and the curve passes through the zero potential (with respect to the filament) at some distance x from the filament (curves 3 and 4). At distances less than x, the potential shows a negative value. With increasing anode potential, the space-charge becomes small and the distance x shortens. For sufficiently high anode potential, when the space-charge is considerably reduced, the potential gradient becomes always positive (curves 1 and 2). In short it can be said that owing to the space charge and the influence of initial velocities of the electrons, the surface of zero potential shifts shightly towards the anode and the effective distance between the grid and the filament is slightly reduced as the space-charge is increased. With a large space-charge, therefore, there will be an increase in the effective capacity between the electrodes. In the grid-filament space this space-charge effect usually overcomes the normal effect (when there is no space-charge), *viz.*, a decrease in the effective capacity of the grid-filament space due to the reduction of the effective dielectric constant of the electronic medium. An increase in the effective value of the grid-filament capacitance with an increase in the anode current is thus expected from this point of view. Further, according to this view the increase of the grid-filament capacitance for a given anode current would be less for a higher value of the anode voltage.

While the former conclusion, *viz.*, an increase of the grid-filament capacitance with an increase of anode current, is substantiated in our experiments within the range under investigation, the latter conclusion, regarding the relative increase of the grid-filament capacitance with the magnitude of the anode voltage for a given anode current, is, however, found to hold only in the case of one valve (Hivac PX 230). With the remaining valves the sequence was found to be reversed. This indicates that there must be some other factor or factors affecting the variation of the inter-electrode capacitances. The main factor appears to be the emission of secondary electrons at the grid and the anode for the higher anode voltages. When such secondary emission takes place at the grid surface, the latter acquires a positive potential. With a perceptible positive potential on the grid, the following effects will have to be considered.

(*i*) In *the grid-fitament space*, the electrons flowing from the filament to the grid would move faster with a positive than with a neutral grid. Hence for a given thermionic current given by $n.e.v.$ (where n=electron density, v=electron velocity and e=electronic charge), the average electron density would be less, as the velocity of the electrons would be larger, so that the decrease of the grid-filament capacitance due to change of the dielectric constant of the electronic medium would be smaller for the higher anode voltages for which there is secondary emission. Thus for higher anode voltages, the increase of the grid-filament capacitance due to space-charge would indeed appear larger. The experimental result that in all valves excepting the one already mentioned, the

increase of grid-filament capacitance, for the same anode current, was greater for the higher anode voltages can thus be explained as due to the effect of secondary emission at the grid surface. In the Hivac PX 230 valve, the anode-current vs. filament-current for the higher anode voltage clearly showed that the secondary emission was indeed small, so that the exceptional result with this valve are to be expected.

The increased conductivity due to the emission of secondary electrons for higher anode voltages would, again, cause an apparent increase in the inter-electrode capacitances. This would also affect the relative increase of the grid-filament capacitance for different anode voltages in a way similar to what has been actually observed with most of the valves. (*ii*) The effect of the secondary emission will also explain the sequence observed in the decrease of the *anode-grid capacitance* of most of the valves with different amounts of anode voltages. Positive potential on the grid would retard the electrons going from the grid to the anode. As a consequence with a high anode voltage producing secondary emission, for the same anode current, the number of electrons per c.c. would be larger than when there is little or no secondary emission for the lower anode voltages. This would result in a larger decrease of the anode-grid capacitance for the higher anode voltages. The observed result that for a given anode current the decrease of anode-grid capacitance for most of the triodes under examination was larger for the higher anode voltages can thus be explained. With little or no secondary emission at the grid as in the case of Hivac PX 230 triode, the decrease of the anode-grid capacitance would evidently be smaller with higher anode voltages, as with a higher value of anode voltage the electron velocity v would be much larger, and the electron density n would be necessarily smaller for the same value of the anode current given by $n.e.v$.

It is possible that other factors may also affect the variation of the inter-electrode capacitances. The works of Schottky (1914), Epstein (1919), Fry (1920) and others on the increase of grid-filament capacity due to the space-charge effect clearly showed the dependence of grid-filament capacitance on the inter-electrode distances and the potential applied to the anode. The relative positions of the electrodes in different valves would thus, to some extent, determine the effective value of the inter-electrode capacitances.

In the case of the Philips TC $03/5_1$ valve, the variation of the inter-electrode capacitance between the grid and the filament with the changes of anode current was found to be somewhat different from what is generally observed with the other valves (Fig. 7). The relative positions of the electrodes of the transmitting valve must have been such that the space-charge effect on the grid-filament capacitance did not immediately come into operation. With a high voltage the effect made its appearance for a relatively large value of the anode current. With a lower anode voltage the effect showed itself at a smaller value of the anode current. Beyond this value of anode current, therefore, an increase in the grid-filament capacitance was observed with further increase of the anode current. For anode currents less than this value, there was a decrease in the value of the

grid-filament capacitance as expected. An initial increase in the grid-filament capacitance for the highest anode voltage employed ($V_a = 150$ volts) was, however, an unusual observation. But this can perhaps be explained as due to the copious emission of secondary electrons at the anode and the grid for such high anode voltage. The increase in the conductivity of the inter-electrode space due to the emission of secondary electrons at a high anode voltage would effect a perceptible apparent increase in the value of the inter-electrode capacitance. For smaller anode currents therefore this increase in the inter-electrode capatitance will make itself felt in the final result. For smaller anode voltages, for which there is no secondary emission, this initial increase is not expected. This is exactly what was observed.

PHYSICS DEPARTMENT
DACCA UNIVERSITY.

REFERENCES

Colebrook, (1929), Experimental wireless and wireless engineer, Vol. 6, p 486
Epstein, (1919), *Deutch. Phys. Gesell. Verh.* **21**, 85-99.
Fry, (1920), *vide* Van der Bijts Thermionic vacuum Tube, p. 63.
Hartshorn, (1927), *Proc. Phys. Soc.* (London), **39**, 188.
Jones, (1937), *Jour. Inst. Elec. Eng.* **81**, 158.
Khastgir and Chowdhury, (1940), *Ind. Jour. Phys.* **14**, 111.
Miller, (1919), *Scientific papers of Bureau of Standards*. 351 (Nov ').
Nichols, (1919), *Phys. Rev.*, **13**, 6, 404.
Schottky, (1914), *Phys. Zeitscher*, **15**.

ULTRAVIOLET BANDS OF CADMIUM IODIDE

By C. RAMASASTRY and K. R. RAO*

(Plate IV)

ABSTRACT. The emission bands of cadmium iodide as excited in a transformer and n a high frequency oscillatory discharge, are photographed with a Hilger quartz Litrow spectrograph. A doublet system due to the electronic transition $^2\Pi - {}^2\Sigma$, analogous to the halide bands of related molecules is established. The far ultraviolet system, partially recorded by Wieland is extended and the vibrational formula

$$\gamma = 41912.4 + [108.5(v'+\tfrac{1}{2}) - 1.0(v'+\tfrac{1}{2})^2] - [179.1(v''+\tfrac{1}{2}) - 0.8(v''+\tfrac{1}{2})^2]$$

is calculated. The common final $^2\Sigma$ state is probably the ground state of the molecule.

INTRODUCTION

The first extensive work on the band spectrum of cadmium iodide was done by Wieland (1929) who recorded the following characteristic systems and divided them into three classes. The last column in the Table I is the new designation suggested by us in conformity with that of the iodide bands of zinc and mercury.

TABLE I

Region	Class	New Designation
λ 6600 – λ3600	III	B
A group of three bands at about λ3560	--	C
λ 3500 – 3250	I	D
λ 2550 – λ 2350	II	E

The wave-lengths of the group of three violet degraded bands of system C are 3586.3(0), 3563.2(3), 3541.1(4). The method of excitation was a high frequency discharge through the vapour of cadimium iodide and the largest dispersion used was about 10 A per millimeter at λ 2500. A complete vibrational analysis was given only of one of these system (Class I) and regularities were shown among the bands of the Class II system. The visible system (Class III) was at first ascribed to the triatomic molecule CdI_2 but later work by the same author indicated that this system too was due to the diatomic molecule CdI.

* Fellow of the Indian Physical Society.

In recent work on the structure of the band spectra of the halides of Group II-b elements of the Periodical Table by Howell (1943) and by Rao and others (1944a, 1944b, 1946) the view was established that these molecules give rise to band systems corresponding to the electronic transition $^2\Pi—^2\Sigma$, in which the electronic width of the $^2\Pi$ term is related to the corresponding atomic interval of the metal atom and that the transition is between the non-banding or atomic orbitals.

Examining the cadmium iodide bands in the light of this view, Howell suggested that the system analysed by Wieland between λ 3500-λ3250 is one of the components of the predicted $^2\Pi-^2\Sigma$ systems, the other missing component is to be sought among the fragmentary group in the vicinity of λ3550 mentioned by Wieland. The system, further to the ultraviolet lying, at λ2400, is interpreted as probably due to the transition $^2\Sigma-^2\Sigma$ the lower $^2\Sigma$ state being the ground state of the molecule. The present work is carried out in order to establish, if possible, the missing component of $^2\Pi-\Sigma^2$ system and to study the vibrational analysis of the far ultraviolet system (system E).

EXPERIMENTAL

As in the previous work on the bands of the iodides of zinc and mercury, two different sources of excitation have been employed for the excitation of cadmium iodied bands—a transformer discharge and a high frequency valve oscillatory discharge through the vapour. The h. f. oscillator set was specially constructed by one of the authors for the purpose. A much higher temperature of the vapour was found necessary with cadmium iodide than with either zinc or mercury iodides. A discharge tube of quartz or of special ignition pyrex had to be employed and heating was done continuously by a set of etna burners along the length of the tube.

RESULTS

About 90 bands were measured between λ3516.8 to 3288.2 in system D by Wieland comprising of the sequences from (0.8), to (4.0). In addition to these bands, the authors obtained on their plates a number of new bands towards the violet end of the system as seen in the reproduction (Plate IV A). The wave-length data of these additional bands is given in Table II.

Two possibilities of assignment of these bands are considered, one being to regard them as the extension of the system D, the bands forming higher members of the sequence (3,0) and (4,0) obtained by Wieland. But a somewhat abrupt increase in the intensity of the bands is observed at γ 30434.8 and 30257.1, leading to the possibility of regarding these bands as forming a different system altogether. The vibrational scheme given in Table III was then examined giving $\Delta G(v'')$ values agreeing with those of the final $^2\Sigma$ state. If this were correct, it would seem that this may be the missing component system with the interval between the (0,0) bands equal to $30434.8-29532.9=901.9$ cm. This is much too different from the

predicted separation of 1140 cm. Further, the missing system more probably lies towards the longer wave-length side of the main component, as observed by Howell. On this aocount, the new bands are believed to form part of system D itself. A search further to the violet did not reveal any bands ascribable to CdI molecule.

TABLE II

Wavelength	Wave number	Int.
3340.06	30257.1	2
3300 41	30290 6	1
3297.23	30319.8	1
3293.97	30349.8	0
3291 17	30375.6	0
3287.83	30406.5	0
3284 87	30434 8	4
3282.08	30459 7	1
3279 17	30487.8	2
3276.06	50515 7	2
3273.26	30541.8	0

TABLE III

	0	(177.7)	1	(169.1)	2	(167.9)	3	(165.8)	4	(166 2)	5	6
0	30434.8		30257.1									
1			30459.7		30290.6							
2					30487.8		30319.9					
3							30615.7		30349.9			
4									30541.8		80376.6	
5												30406.5

The three bands, (designated by us as system C) mentioned by Wieland, are distinctly observed on our plates (Plate IV A) and their wave lengths obtained from a quartz Littrow plate are given in Table IV.

TABLE IV

λ	ν (int)	δν	(v', v'')
3541.04	28232.9 (6)		(0,0)
3563.52	28054.5 (4)	178 4	(0,1)
3585.84	27880.2 (2)	174.3	(0,2)

If, on the analogy of the remaining halide bands, both the components of the doublet system, $^2\Pi—^2\Sigma$ are observable on the spectrogram, one of the components being feebly developed, then these three bands are the only bands which must be regarded as constituting the missing system.

TABLE V

CdI—Ultraviolet System. λ 2550—2350

Wieland		Authors		Classification
ν cm.$^{-1}$	Int.	ν cm.$^{-1}$	Int.	(v′, v″)
		39349 7	0	(0,15)
		477.8	1	(1,15)
		526 6	1	(0,14)
		673 7	0	(0,13)
		726.8	1	(2,14)
		82 .1	0	(3,14)
		891.7	1	(2,13)
		954-0	1	(1,12)
		980.1	0	(3,13)
		40053.7	1	(2,12)
		113.5	1	(1,11)
		156.1	0	(3,12)
		177 5	0	(0,10)
		226 5	2	
		270 2	4	(1,1)
40435.0	2	440 7	3	(1,9)
443.5	1			
		483 4	1	(3,10)
		510,4	0	(0,8)
		553 1	1	(2,9)
600.0	2	608 3	4	(1,8)
607.5	1			
648 0	0	646.4	1	(3 9)
		679.6	1	(0,7)
		717 4	1	(2,8)
768 0	2	775.8	4	(1,7)
775 5	1			
812 5	0	810.4	1	(3,8)
		40839.5	0	(0,6)
4087 5	2	878.2	3	(2,7
939 5	3	934 1	2	(1 6)
943 5	1			
		999.3	1	(0,5)
41046 0		41050.1	4	(2,6)
112.3	1	112.9	3	(1,5)
		163.5	0	(0,4)
211 0	3	220.7	3	(2,5)
217.0	3			
		243.2	0	(4,6)
281 5	1	279.9	1	(1,4)
315 0	1	325 9	3	(3,5)
385.0	3	389 9	4	(2,4)
		456 2	0	(1,3)
488.0	2	489-1	3	(3,4)
		525,0	0	(5,5)
562.5	2	561.6	3	(2,3)
		585 7	0	(4,4)
		626.4	0	(1,2)
661 0	3	664 0	3	(3,3)
732 0	1	737 3	1	(2 2)
763-5	2	768 5	1	(4,3)
		804.8	1	(1,1)
834.5	3	840.1	3	(3,2)
		857.5	1	(5,3)
		874 8	1	(0,0)
		907.1	5	(2,1)
937-0	2	936.7	0	(4,2)
		954.0	1	(6,3)
		41979.6	1	(1,3)
42009 5	1	42017 1	1	(3,1)
112 0	1	113 3	1	(4,1)

TABLE VI

Vibrational analysis and Intensity distribution in CdI bands (E System)

v''/v'	0	1	2	3	4	5	6	7	8	9	10	11	12	83	14	15	$\Delta G'$
0	1				0	1	3	1	0		0			0	1	0	
1	1	1	0	0	1	3	?	4	4	3	4	1	1			1	103.7
2		3	1	3	4	3	4	3	1	1			1	1	1		107.1
3		1	3	3	3	3				1	1		0	0	0		102.6
4		1	0	1	0		0										18.5
5				1		0											89.0
6				1													96 5
$\Delta G''$	174.8	175.4	172.5	176.4	165.9	169 7	163.4	165.8	165.3	162.2	165.7	159 5	169 0	156.0			

On this basis, the (v', v'') numbering in the last column is suggested. The wave number intervals support the assignment. The electronic doublet width, 1300, is much less than the predicted value, 1140, although of the right order of magnitude.

SYSTEM E

28 heads were measured in this far ultraviolet system by Wieland from λ 2473 to λ 2364 and regularities were shown among them. These same regularities were presented in a Deslandre scheme by Howell, indicating ΔG (v'') values, in agreement with those of the lower state of the D system. Since the bands lie in the vicinity of $^1S - {}^1P$ line of cadmium, they are ascribed to the electronic transition $^2\Sigma - {}^2\Sigma$. In the present work, about 60 bands are altogether measured in this system as shown in Table V, in which Wieland's data are also given for the purpose of comparison. The vibrational analysis of these bands is presented in Table VI. The v'' values in this scheme are identical with those given by Howell but the v' values are increased by one, several band heads being thereby included in the analysis. The following vibrational formula is calculated:—

$$\lambda = 41912.4 + [108.5(v' + \tfrac{1}{2}) - 1.0(v' + \tfrac{1}{2})^2] - [179.1(v'' + \tfrac{1}{2}) - 0.8(v'' + \tfrac{1}{2})^2]$$

The final state values distinctly indicate a common ground level with the D system of bands.

PHYSICS DEPARTMENT
ANDHRA UNIVERSITY
WALTAIR

REFERENCES

Howell, (1943) *P.R.S.* (*Lond.*), **182**, 95.
Rao, K. R. and others, (1944a) *Curr. Sci.*, **13**, 279.
(1944b) *Ind. Jour. Phys.*, **18**, 323 and
(1946) *Ind. Jour. Phys.*, **20** (In Press).
Wieland, (1929) *Helv. Phys. Acta.* **2**, 46 and 77.

A STUDY OF SOME VEGETABLE FIBRES BY X-RAY DIFFRACTION METHOD

By C. R. BOSE, and N. AHMAD

(Plates VA and VB)

ABSTRACT. X-ray photographs of several kinds of clean, delignified and fat free cellulosic fibres were taken and their tensile strengths measured. The fibres showing extensions of the spots along the Debye Scherrer rings indicating dishevelling of the fibre molecules were found to have tensile strengths generally smaller compared with those of other fibres. The fibres of Agava Sisalana Perrine (Sisal hemp) and Sansevieria Roxburgiana gave ring shaped photographs showing that the distribution of micelles in them was chaotic and at random. Diffraction patterns of these two kinds of fibres in a stretched condition showed that stretching partially orients the micelles of these fibres in a direction parallel to the length of the fibre.

INTRODUCTION

The method of X-ray investigation for the study of the internal structure of cellulose fibres was first applied by Polanyi (1922) and more thoroughly by Mark and Meyer (1939) and Herzog (1928) and his collaborators. As revealed by X-ray diffraction photographs the fibres are crystalline in the sense that they contain countless thin, invisible, submicroscopic crystallites, the atoms and molecules inside which are distributed in regular order. The properties of the fibres depend, to a great extent, on the size and arrangement of these minute crystals and also on the disposition of atoms and molecules within each crystal.

It is with a view to having an idea about the relationship between the internal structure and the physical properties, particularly the tensile strengths of various fibres that the present investigation was undertaken. The tensile strengths of the fibres under investigation were carefully determined and also their structures were investigated by the X-ray diffraction method.

Mark and Meyer from accurate measurements of the positions of the spots in X-ray photographs of ramie fibres definitely decided that the elementary unit of cellulose structure is monoclinic with four glucose units contained in a cell. They came to the conclusion that the space group is $C_2^2P2_1$. Andress (1929) calculating from known carbon to carbon and carbon to oxygen distances and from consideration of the chemical properties of cellulose, arrived at a structure which gave theoretical intensities of X-ray reflections in agreement with the observed intensities. X-ray investigation of jute fibres was first undertaken in India by Banerjee and Ray (1940) and later by Sircar, Saha and Rudra (1044) and by Sircar and Saha (1945). They found that the unit cell of jute fibre is identical with that of cellulose from other sources. In the present investigations we have taken in addition to jute fibres, some other vegetable fibres whose botanical names and Indian names (where possible) are given later in Table II. These fibres were kindly supplied to us by the Government Agricultural farm, Manipur, Dacca.

The raw fibres are composite in nature. They contain lignin, gummy and fatty substances whose presence give the fibres their peculiar characteristic colours. When they are removed and the X-ray photographs are taken, we get fairly clear photographs without indicating any change in the fundamental diffraction patterns of the fibres.

EXPERIMENTAL

The X-ray tube used throughout the investigation was of the Hadding-Sieghbahn type. The tube current was adjusted between 8 to 12 milliamperes at a voltage between 50 to 62 K. V.

The raw fibres were cleaned in a sohxlet apparatus with a mixture of alcohol and benzene about (1:1) which is very efficient for removing fats, waxes and resins. Lignin present in the fibres was removed by treating the fibres in a moist condition with the vapour of chlorine peroxide (ClO_2) in an atmosphere of CO_2. After removing the lignin the fibres were preserved in a bottle containing CO_2. For the photographs very thin bunches of fibres were taken to keep them straight and parallel.

IDENTIFICATION OF SPOTS

The photographs were taken with fairly high exposures, while using extremely thin bundles of fibres. The voltage applied to the X-ray tube was high so that the characteristic radiations of copper were considerably intensified compared to the white radiations. For these reasons a much larger number of spots could be measured than have been recorded by Meyer and Mark (1929). This number was still further increased by using a cylindrical camera which allowed a much wider range of angles to be studied. Since many of these spots have not been recorded by earlier workers it was considered worth while to identify them. In order to identify spots, the unit cell was assumed in each case to be monoclinic with the following dimensions for the unit monoclinic cell:

$$a=8.35\text{A},\ b=10.3\text{A},\ c=7.9\text{A and } \beta=84^\circ.$$

These values were accurately determined by Mark and Meyer. The glancing angles for the various planes were calculated from the monoclinic formula given below :—

$$\sin\theta_B=\frac{\lambda}{2\sin\beta}\left(\frac{h^2}{a^2}+\frac{l^2}{c^2}-\frac{2hl}{ac}\cos\beta+\frac{k^2}{b^2}\sin^2\beta\right)^{\frac{1}{2}}$$

where θ_B is the glancing angle which was obtained from the geometry of the spot on the film ; β is the angle between the a and the c axes. h, k, l are the millerian indices of the plane giving rise to the spot in question. a, b, c are the axial lengths of the unit cell.

These measured glancing angles were then compared with those calculated from the formula for the various planes having the K index corresponding to the layer line in which the spot in question occurs and the other two indices could be thus found.

The results of identification of the spots in the X-ray diffraction photograph of delignified flax are given in Table I. Data for other fibres being quite similar are not reproduced.

TABLE I

Identification of the reflecting planes of lignin-free flax fibre.

Millerian indices.	Calculated θ_B for Cu K radiation.	Measured θ_B.	Estimated Intensity.
101	7° 18′	7° 13′	S
$10\bar{1}$	8° 6′	8° 12′	S
002	11° 18′	11° 24′	V S
201	11° 36′		
004	23° 6′	23° 12′	M W
$21\bar{2}$	17° 0′	17° 7′	M
311	17° 6′		
31	19° 24′	19° 16′	W
020	8° 36′	8° 40′	M W
120	10° 6′	10° 14′	M W
021	10° 18′		
221	14° 30′	14° 24′	M W
221	15° 24′	15° 28′	W
$12\bar{2}$	15° 42′		
321	18° 48′	18° 51′	V W
322	20° 51′	20° 55′	V W
421	23° 44′	23° 50′	V W
130	14° 0′	14° 5′	M
131	14° 54′	15° 14′	M W
$13\bar{1}$	15° 24′		
032	17° 18′	17° 15′	M S
232	21° 13′	21° 10′	M W
331	21° 16′		
040	17° 24′	17° 30′	M
141	19° 20′	19° 14′	W
042	20° 57′	20° 49′	M W

MEASUREMENT OF THE TENSILE STRENGTHS OF THE FIBRES

The tensile strengths of the fibres were determined with an apparatus shown in Fig. I. It consists of an ordinary balance in which the left pan has been replaced by two clips A and B. A is suspended from the left beam while B is attached to the balance pillar and can be moved up and down by rack and pinion arrangement. A and B lie in the same vertical line. A number of fibres of a particular sample were examined under a microscope and some two or three fairly uniform fibres were selected for determining the tensile strength. The diameter was measured with a travelling microscope at different parts of the fibre and the mean was taken. Readings were taken at some forty to fifty different points. Several readings were taken for the

diameter at each point after rolling the fibres sideways the mean giving the diameter at that point.

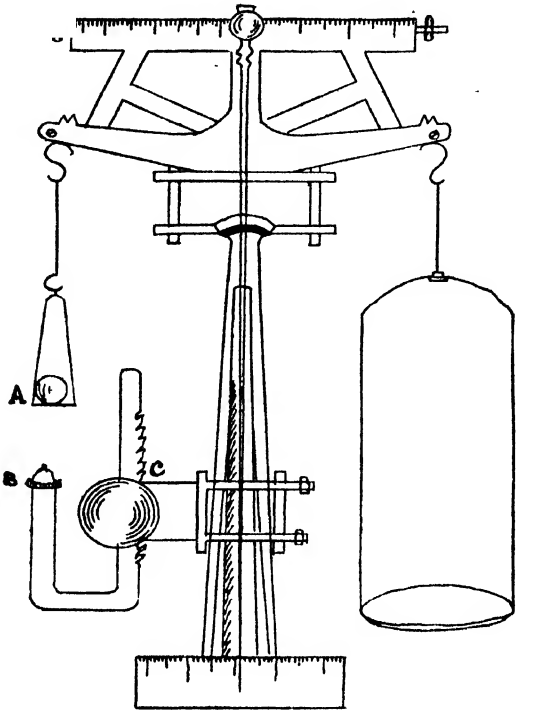

FIG. 1

Apparatus for measuring the tensile strength
A—upper clip B—lower clip
C—Rack-and-pinion arrangement

After carefully clamping a single fibre at both the ends A and B, C was very slowly turned to stress the fibre just properly so that on releasing the pan, the pointer remained at the zero position. The weights were slowly and gradually increased, for it had been found that a fibre broke with a smaller weight when the latter was placed at once. It was also noticed that at a certain weight the fibre did not break as soon as the beam was raised but only after a few seconds. Even with all possible precautions, it was very difficult to get consistent results. Reproducible results could, however, be obtained after a large number of experiments. The tensile strength T expressed in Kgm per mm^2 was calculated from the equation

$$T = \frac{w}{\pi r^2}$$

where w is the breaking weight expressed in Kgms and r is the mean radius of a single fibre in mm. The results are shown in Table II.

(1)

(2)

(3)

(4)

1. X-ray diffraction pattern of delignified Ramie
2. X-ray diffraction pattern of delignified Flax
3. X-ray diffraction pattern of delignified Hibiscus Esculantus
4. X-ray diffraction pattern of delignified Malachra Capitata

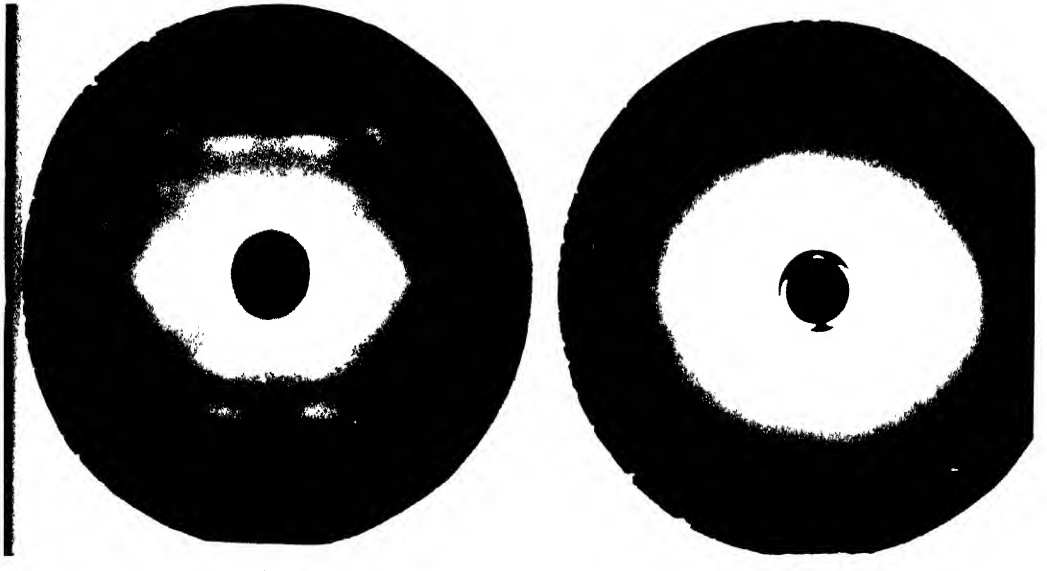

(1)

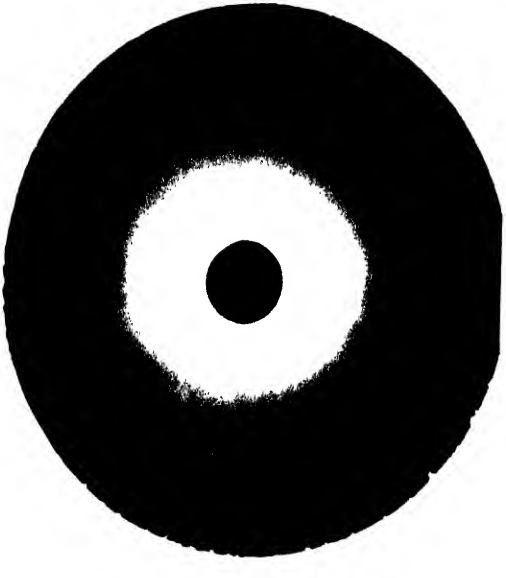

(3)

1. X-ray diffraction pattern of delignified Crotalania Juncea (Sunn hemp)
2. X-ray diffraction pattern of delignified Agave Sisalana (Tisol hemph) (unstretched)
3. X-ray diffraction pattern of stretched Agave Sisalana

Table II.

Tensile strengths of the different fibres

Botanical names	Indian Names	Mean radius of fibres	Mean tensile strength
Boehmeria Nivea Hook & Arn (Plate I) (Ramie)	Rhea	·01855	24. 24
Hibiscus Abelmosehns (Musk Mallow)	Kasturi	.02500	35. 10
Rinum Usitatissimum (Flax) (Plate II)	Tisi	.02953	38. 82
Hibiscus Esculantus (Plate III)	Dhenras	.02940	22. 66
Malachra Capitata (Plate IV)		.02753	21. 16
Hibiscus Sabdariffa Var-altissima	Chukoir	.04359	10. 71
C. Capsularis	Pat	.02476	22. 97
Sida Rhombifolia (Berella)	Berela	.02042	17. 02
Crotalaria Juncea (Sun hemp) (Plate V)	Sonn	03797	18. 68
Agava Sisalana Perrine (Sisal hemp) (Plate VI & VII)		.05779	9. 51
Sansevieria Roxburghiana Schult	Gorachakra Murba	.04083	14. 68

DISCUSSION

A large number of different types of vegetable fibres were examined. The diffraction patterns of the different fibres show that the fundamental constituent is in each case cellulose.

X-ray diffraction patterns of these fibres are not similar in the strictest sense of the term. Though many of the photographs resemble as regards their pattern and position of spot yet the character, shape and size etc. of these spots are quite different in different pictures. In some of the photographs the spots are more discreet and better resolutions are obtained. This shows that crystallities in the corresponding fibres are more regularly arranged in a direction parallel to the length of the fibres.

There are other pictures where the spots are remarkably long. These spots always take the form of an arc of a circle with the central spot on the film as their centre of curvature. This indicates that the micellels or the crystallites in the corresponding fibres are much more irregularly distributed in the fibre and they are not strictly parallel to each other or to the fibre axis.

Again there are two particular varieties of fibres namely, Agava Sisalana Perrine (Sisal hemp) and Sansevieria Roxburghiana which have almost got no discreet reflected spots except two intense spots in the central layer and these two are very much elongated and bent in the form of an arc of a circle making an angle of about 60° at the centre. These photographs also show

two or three complete circular rings of almost uniform blackness, corresponding to the rings obtained in a powder photograph.

A special X-ray diffraction pattern of one of these two fibres, (Sisal hemp) was taken with the fibre stretched to a great extent. The difference between the stretched and unstretched fibre photographs is that the rings in the stretched one show more pronounced intensity maxima along the rings. Thus it may be said that the distribution of the micelles in these two fibres are almost a chaos, even in the direction of the long axis of the fibres. The stretching of the fibres partially orients the micelles towards more or less parallelism to the length of the fibre.

The tensile strengths of fibres play an important part in their industrial application. Hence the tensile strengths of all the fibres were measured with care to see if any relation could be derived between the tensile strengths and the X-ray diffraction patterns of the fibres specially with regard to the character of the spots, their sizes and shapes and also the tendencies towards formation of rings. On examining the data it is found that the two fibres characterised by rings in the X-ray diffraction patterns have tensile strengths generally smaller compared with those of other fibres. On further examination of the data it is found that the mean radii of these two fibres (as measured for determining the tensile strength) are greater than those of the others. Thus it seems that the more random and chaotic are the micelles in them the less are their tensile strength.

ACKNOWLEDGMENT

The investigations were carried out at the Physics Laboratory of the Dacca University at the suggestion and under the guidance of Prof. S. N. Bose to whom our heartfelt thanks are due. Our sincere thanks are also due to Prof. K. Banerjee for his advice at the time of writing out the paper.

INDIAN ASSOCIATION FOR THE CULTIVATION OF SCIENCE
210, BOWBAZAR STREET, CALCUTTA.

REFERENCES

Andress, K. R., (1929), *Zs. f. Phys. Chem.* **2B**, 380.
Banerjee, K and Ray, A. K., (1941), *Proc Nat. Inst. Sci.* **7**, 377.
Herzog, R. O., (1928), *Zs. Phys. Chem* **139**, 235.
Mark, H and Meyer, K. H. (1929), *Zs. Phys. Chem.* **2** 115.
Meyer, K. H. and Mark, H., (1929), *Zs.f. Phys. Chem.* **4**, 431.
Polanyi, M., (1932), *Zs. Phys.* **10**, 44.
Sarkar, P. B., (1935), *Jour Ind. Chem. Soc.* **12**, 23.
Sirkar, S. C. and Saha, N. N., (1946), *Proc Nat Inst. Sci.* **12**, 151.
Sirkar, S. C., Saha, N. N. and Rudra, R. M., (1944), *Proc. Nat Inst. Sci.* **10**, 325.

ON THE RAMAN SPECTRA AT LOW TEMPERATURES. BENZENE DERIVATIVES

By S. C. SIRKAR* and B. M. BISHUI

ABSTRACT The Raman spectra of benzylamine, benzyl alcohol and benzoyl chloride have been investigated in the solid state at about −170°C and in the liquid state at the room temperature. The polarisation of the Raman lines of all these liquids has also been studied. From the observed depolarisation of some of the Raman lines it has been concluded that the molecules of these three compounds in the liquid state possess a plane of symmetry. In the case of benzyl amine in the solid state some of the Raman lines undergo changes in frequency and intensity and some new lines appear in the low frequency region, and it is concluded that in the liquid state the molecules are only loosely associated, but in the solid state they are strongly associated and form polymeric groups. In the case of benzyl alcohol and benzoyl chloride such Raman lines in the low frequency region appear even in the liquid state and no appreciable changes in the frequencies of the other prominent Raman lines take place with the solidification of the liquids at the low temperature. It is concluded from these facts that even in the liquid state the molecules of these two compounds exist as polymers

It was observed by Mizushima and Morino (1938) and by the present authors (1943, 1945, 1946) that the Raman spectra of some aliphatic compounds undergo some changes when these compounds are solidified at low temperatures. As pointed out previously by the present authors (1945), the explanation offered by the previous workers regarding such changes in the lines due to intramolecular vibrations is not quite satisfactory. As regards the origin of the new Raman lines, which appear in the low frequency region in the Raman spectra of many aliphatic and aromatic compounds, the view is held by many workers that these lines are due to lattice oscillations in which only intermolecular electrostatic field takes part. Sirkar (1937), however, pointed out some difficulty in such an interpretation, because in the case of centrosymmetrical molecules the intensity of the lines due to such intermolecular oscillations is expected to be negligible. He put forward the view that some secondary bonds may be formed between neighbouring molecules to form small polymeric groups, and the oscillations of constituent single molecules against each other in such groups may give rise to Raman lines in the low frequency region Experimental results regarding such new lines in the case of different types of molecules may be helpful in understanding the true origin of such lines and therefore, a programme has been undertaken to study the Raman spectra of a large number of aromatic and aliphatic compounds in the solid state at low temperatures. The present investigation deals with such spectra of three benzene derivatives, each having an aliphatic side chain.

The substances studied in the present investigation are benzylamine, benzyl alcohol and benzoyl chloride. Liquids from Kahlbaum's original packing were used after being redistilled in vacuum. The technique

* Fellow of the Indian Physical Society

Benzylamine. The Raman spectrum of benzylamine was studied formerly by Dadieu and Kohlrausch (1930) and by Reitz and Stockmair (1935). The results obtained by the latter authors are more recent and have been included in Table I. These results agree fairly well with those obtained by the present authors, which are given in column 2 of Table I, but there are some minor discrepancies. The weak lines 579 cm^{-1}, 895 cm^{-1}, 1176 cm^{-1}, 2973 cm^{-1} and 3385 cm^{-1} observed by them have not been observed by the present authors. Also the frequencies of some the of the lines reported by them are a little lower than those observed in the present investigation.

The lines 175 cm^{-1}, 628 cm^{-1}, 1458 cm^{-1}, 1590 cm^{-1} and 1605 cm^{-1} are found in the present investigation to be totally depolarised, This fact suggests that the molecule has a symmetry element which is most probably a plane of symmetry passing through the plane of the benzene ring. The carbon and nitrogen atoms in the CH_2 NH_2 group then also lie in this plane, and two of the four hydrogen atoms are above and the other two below this plane. No other alternative symmetry element of the single molecule is more probable than this plane of symmetry.

In the solid state at about -170^0 C the substance yields two new Raman lines at 92 cm^{-1} and 124 cm^{-1} respectively and some of the prominent Raman lines of the single molecule undergo changes in frequency and intensity at this low temperature. Thus the band at 175 cm^{-1} is split up into two lines at 160 cm^{-1} and 207 cm^{-1} and the lines 786 cm^{-1}, 1207 cm^{-1}, 1590 cm^{-1}, 1605 cm^{-1} and 2935 cm^{-1} shift to 774, 1138, 1584, 1596 and 2901 cm^{-1} respectively at the low temperature. Also the relative intensities of the lines 1590 cm^{-1} and 1605 cm^{-1} are reversed in the solid state. The line 3063 cm^{-1}, which has a diffuse wing in the lower frequency side in the liquid state, becomes sharper and is accompanied by a faint component at 3050 cm^{-1} in the solid state at the low temperature. As the Rayleigh line due to the liquid at the room temperature is accompanied by a wing extending upto about 125 cm^{-1} from its centre it is difficult to say whether the lines 92 cm^{-1} and 124 cm^{-1} observed in the solid state are also present in the spectrum due to the liquid. It is doubtful whether any intramolecular vibration of the single molecule can have such low frequencies. The diminution in the frequencies of the prominent Raman lines with the solidification of the liquid at the low temperature suggests that the molecules become strongly associated in the latter case and the new lines 92 cm^{-1} and 124 cm^{-1} may be due to vibrations of such groups of associated molecules. The fact that the C-H frequencies are lowered in the solid state shows that the association takes place through the hydrogen atoms of the molecules.

Benzyl alcohol. The Raman spectrum of this liquid was studied previously by Dadieu and Kohlrausch (1929), Howlett (1931) and Reitz and Stockmair (1935). The results reported by the last two authors being comparatively recent have been included in Table II. A comparison of the data given in the first two columns of Table II shows that the weak lines

585 cm^{-1}, 900 cm^{-1}, 1176 cm^{-1}, 1358 cm^{-1} and 3414 cm^{-1} have not been observed by the present authors. Also the frequencies of some of the hydrogen lines, *e.g.*, 2870 cm^{-1}, 2923 cm^{-1} and 2975 cm^{-1} reported by them are much lower than those observed in the present investigation.

The second and third columns of Table II show that with the solidification of the liquid at the low temperature the wing accompanying the Rayleigh line disappears and a line at 91 cm^{-1} is observed. It is not unlikely that this line may be present also in the Raman spectrum due to the liquid, but being masked by the intense wing, which extends upto 120 cm^{-1} from the centre of the Rayleigh line, it can not be detected. Fox and Martin (1940) concluded from the results of investigation of the absorption spectrum of benzyl alcohol in the near infra-red region at the room temperature that the molecules are present even in the dilute solution of the liquid as dimers and in the concentrated solution there is an equilibrium between dimers and tetramers. Although these conclusions were drawn from the observed structure of the band at 2,75μ, the Raman lines 91 cm^{-1} and 155 cm^{-1}, which correspond to bands in the extreme infra-red region, may also, be due oscillations in such dimers and polymers. In the solid state also probably the molecules exist as dimers and polymers, and therefore only the rotational wing is absent and the lines 91 $cm^{-1}$and 155 cm^{-1} due to vibrations in these polymers persist. It is significant that in the case of benzylamine the band at 175 cm^{-1} splits up into two lines at 160 cm^{-1} and 207 cm^{-1} in the solid state, while in the case of benzylalcohol even the liquid at the room temperature yields two lines at 165 cm^{-1} and 210 cm^{-1}. It is further observed that the prominent Raman lines of benzyl alcohol do not undergo any appreciable change with the solidification of the liquid, while in the case of benzylamine the lines undergo changes with the solidification. These facts clearly point out that in the case of benzyl alcohol the molecules are already strongly associated in the liquid state and the strength of the association does not further increase appreciably with the solidification of the substance at the low temperature, while in the case of benzyl amine such association is not so strong in the liquid state, but it becomes much stronger in the solid state.

Some of the Raman lines due to the liquid are observed in the present investigation to be totally depolarised, as can be seen from Table II. Hence the molecule possesses probably a plane of symmety, which is more probable than a two-fold axis of rotation.

Benzoyl chloride.—The data given in the first two columns of Table III show that some of the Raman lines due to this liquid at the room temperature observed by the present authors have not been observed by Thompson and Norris (1936). The Raman spectrum of the liquid had also been studied, previously by Dadieu and Kohlrausch (1929), Mastsuno and Han (1933), Thatte and Ganesan (1931) and Kohlrausch and Pongratz (1934), and the polarisation of the lines was studied by Simons (1932). The results obtained by Thompson and Norris being latest have been included in Table III. The

lines observed by Kohlrausch and Pongratz but not observed by Thompson and Norris are 1317 cm^{-1}, 2610 cm^{-1}, 2649 cm^{-1} and 3012 cm^{-1}. These lines have not been observed in the present investigation also. The line 846 cm^{+1} observed in the present investigation was not observed by Kohlrausch and Pongratz, but it was recorded as a line 840 cm^{-1} by Thompson and Norris, and the line 1164 cm^{-1} observed by the latter authors but not recorded by the former authors has not been observed in present invesigation. The line 201 cm^{-1} observed in the present investigation and also by Kohlrausch and Pongratz was not recorded by Thompson and Norris.

It can be seen from the third column of Table II that no remarkable change takes place in the frequencies of the prominent Raman lines when the liquid is solidified at about $-170°C$. The line 98 cm^{-1} observed at the low temperature is probably also present in the Raman spectrum of the liquid, and is masked by the strong wing accompanying the Rayleigh line and extending upto about 120 cm^{-1} from its centre. In this case also two lines at 161 cm^{-1} and 231 cm^{-1} are yielded by the liquid at the room temperature as in the case of benzyl alcohol. From these facts it may be concluded that just like the molecules of benzyl alcohol those of benzoyl chloride also are strongly associated to form polymeric groups in the liquid state. As in the previous cases some of the Raman lines due to the liquid are observed to be totally depolarised both by the present authors and by Simons (1932). Hence the single molecule has a plane of symmetry.

From the above discussions it can be concluded that the lines in low frequency region observed in the Raman spectra of these three benzene derivatives in the solid state at about $-170°C$ are not due to lattice oscillations in which only the intermolecular electrostatic field takes part, but they are due to vibrations in polymeric groups which are present even in the liquid state in two of the derivatives and are formed in the solid state in the case of benzylamine.

ACKNOWLEDGMENTS

The investigation was carried out in the Palit Laboratory of the Physics Department, University College of Science, Calcutta. The authors are indebted to Prof. M. N. Saha, F.R.S., for kindly providing all facilities for the investigation in the Palit Laboratory.

PHYSICS DEPARTMENT,
CALCUTTA UNIVERSITY.
92, UPPER CIRCULAR ROAD,
CALCUTTA.

REFERENCES

Dadieu A, and Kohlrausch, K. W. F. (1929) S. R. E. in benzene derivatives. *Monatsh*, **53, 54**, 282 (1930); S. R. E. in organic substances *Monatsh*, **55**, 379.

Fox, J. J. and Martin, A. E. (1940). Investigations on the Infra-red spectra. *Trans. Farad. Soc.*, **36**, 867

Howlett, L E. (1931). Raman effect in glycols and nitriles. *Canad. J. Res.*, **5**, 80.

Kohlrausch, K. W F. and Pongratz, A. (1934). S. R. E. in benzene derivatives, *Wien. Ber.*, **142**, 588

Matsuno, K and Han, K (1933). Raman effect in benzene derivatives *Bull. Chem. Soc. Japan*, **8**, 333.

Mizushima, S. and Morino, Y. (1938). Raman spectra and molecular configurations of ethylene dibromide *Proc. Ind Acad. Sc. A*, 8. 315.

Reitz. A. W. and Stock mair, W. (1935) Raman spectra of benzene derivatives, *Wien. Ber.* **144**, 666.

Simons, L. (1932). Polarisation of Raman lines of some organic substances. *Soc. Sc. Finnica. Comm. Phys. Math.* , 58 .

Sirkar, S C. (1937) On the intensities of Raman lines due to lattice oscillations. *Ind. J. Phys* , **11**, 343.

Sirkar, S. C. and Bishui, B M (1943). On the Raman spectra of a few alkyl sulphides in the solid state, *Proc. Nat Inst. Sc India*, **9**, 287.

Sirkar, S. C. and Bishui, B. M. (1945). On the Raman spectra of ethylene dibromide and dichlorethylene in the solid state *Ind. J Phys.*, **19**, 24.

Sirkar, S. C. and Bishui B. M. (1946). On the Raman spectra of a few aliphatic ketones in the solid state. *Ind. J. Phys.*, **20**, 35.

Thatte, V. N. and Ganesan, A. S. (2931). Raman spectra of organic substances. *Phil. Mag.*, **22**, 823.

Thompson, D. D. and Norris, J. F. (1936), Raman spectra of benzene derivatives. *Jour. Amer. Chem. Soc.*, **58**, 1953 ; **59**, 816.

The following special publications of the Indian Association for the Cultivation of Science, 210, Bowbazar Street, Calcutta, are available at the prices shown against each of them :—

No.	Subject	Author	Price Rs. A. P.
III	Methods in Scientific Research ...	Sir E. J. Russell	0 6 0
IV	The Origin of the Planets ...	Sir James H. Jeans	0 6 0
V	Separation of Isotopes ...	Prof. F. W. Aston	0 6 0
VI	Garnets and their Role in Nature. ...	Sir Lewis L. Fermor	2 8 0
VII (1)	The Royal Botanic Gardens, Kew. ...	Sir Arthur Hill	1 8 0
(2)	Studies in the Germination of Seeds. ...	,,	
VIII	Interatomic Forces ...	Prof. J. E. Lennard-Jones	1 8 0
IX	The Educational Aims and Practices of the California Institute of Technology ...	R. A. Millikan	0 6 0
X	Active Nitrogen A New Theory ...	Prof. S. K. Mitra	2 8 0

A discount of 25% is allowed to Booksellers and Agents.

RATES OF ADVERTISEMENTS

Third page of cover	...	...	...	...	Rs. 25,	full page
do.	do. ...	...	...	...	,, 15,	half page
do.	do. ...	...	...	...	,, 8,	quarter page
Other pages	...	...	...	...	,, 19,	full page
do.	...	...	...	...	,, 11,	half page
do.	...	...	...	...	,, 6/8,	quarter page

Journeys of the Future

To-day thousands of people traverse this vast land by rail, whether it be for private or business reasons

With growing national consciousness, the desire to see and know their own great country will impel many more to travel. Where thousands travel to-day, tens of thousands will travel to-morrow

In this essential service as in many other fields of industry and commerce, steel—the metal of strength—plays a conspicuous and vital part.

IMPROVED AMENITIES FOR LOWER CLASS PASSENGERS

Presenting the 1946-47 Railway Budget, Sir Edward Benthall said

Intensive study of new coach designs promises more comfortable travelling for inter and third class passengers with sleeping accommodation for both classes and better lighting and fans for inter-class compartments There will be increased space per passenger

An Artist's impression of a new type of coach.

TATA STEEL

Issued by The Tata Iron & Steel Co., Ltd. Head Sales office: 102A, Clive Street, Calcutta.

DIELECTRIC PROPERTIES OF INDIAN SOILS AT HIGH AND MEDIUM RADIO-FREQUENCIES

By S. R. KHASTGIR,* J. N. RAY AND A. BANERJEE

(Plate VI)

ABSTRACT. The dielectric properties of fifteen Indian soils on medium and high radio-frequencies have been determined under different controlled conditions. Measurements of the effective dielectric constant and the electrical conductivity have been made by the differential transformer method and the oscillographic method. From these data the true dielectric constants have been evaluated. Samples of soil are taken from Dacca, Calcutta, Lucknow, Delhi, Lahore, Peshawar, Bombay, Calicut, Trichinopoly, Ranchi, Cuttack, Bangalore, Madura, Vizagapatam and Trivandrum. The following studies have been made :

(1) The effect of packing.
(2) Variations of the soil constants with moisture-contents.
(3) Variations of the soil constants with frequency
(4) The effect of temperature.
(5) Comparison of the electrical properties of soils from different places.

A general interpretation of all the experimentantal results has been given in the paper.

INTRODUCTION

Apart from the chemical composition, the physical structure and the nature of the soil, there are *three* main factors on which the electrical constants are found to depend : (1) the amount of moisture present in the soil, (2) the degree of packing and (3) the frequency of the alternating field. The first is of great importance, since the variations of the soil constants with moisture-content are indeed, considerable. The experimental study of such variations engaged the attention of various workers for a long time. The dependence of the soil constants on the frequency of the measuring field was also studied by various workers on the subject. Little work has, however, been done on the effect of packing on the soil constants. Besides the three main factors which affect the dielectric properties of the soil considerably the effect of temperature, which is only slight, may also be mentioned.

PREVIOUS WORK ON THE DIRECT DETERMINATION OF THE SOIL-CONSTANTS

It was Bairsto (1912) who, for the first time, made some high frequency measurements of the effective dielectric constant and the electrical conductivity of the two principal constituents of the earth's crust, *viz.*, slate and marble. It had been known from the work of earlier investigators that for very low frequencies within the audio-frequency range, say, up to 5 Kc/s, the electrical

* Fellow of the Indian Physical Society.

conductivity of several dielectrics like ebonite, glass and sulphur, was, in general, *linear* function of the frequencies. The main results of Bairsto's investigations with slate and marble, as also with other dielectrics, *viz.*, dry blotting paper. glass, gutta-percha, vulcanised India rubber, over a wide range of frequencies are as follows :

(1) It was shown that in all cases there were present two independent sources of loss. The first, a hysteris loss, was usually the one that was important in the audio-frequency range. The second, a 'viscous' loss, had more influence at higher frequencies.

(2) The linear law found for audio-frequencies connecting the electrical conductivity with frequency was not obeyed at high frequencies. The electrical conductivity gradually rose to a maximum which remained constant for marble and slate over a considerable range of frequencies. With the other dielectrics, the conductivity was found to decrease steadily after attaining the maximum value, as the frequency was further increased. The dielectric constant, on the other hand, dropped rapidly at low frequencies and then decreased gradually with the increase of frequency.

The maximum range of frequencies employed in Bairsto's investigation was from 920 c/s to 2.65 Mc/s and the method of measurement was based on the resonance of a leaky condenser.

Long after Bairsto, Ratcliffe and White (1930) made some direct determinations of the electrical constants of some specimens of English soils by the method of resonance and the oscillographic method using medium radio frequency fields. Their study of the variation of the effective dielectric constant of the soil showed a rapid decrease followed by a gradual one, as the frequency was increased. The electrical conductivity, on the other hand, was found to increase and after attaining a peak value, was found to decrease gradually with the increase of frequency. White (1931) tried to interpret the results of Ratcliffe and White in the light of Debye's theory of di-polar molecules.

Smith-Rose (1938) studied in an elaborate manner the effect of moisture-content and of frequency variation for medium radio-frequency fields on the electrical constants of some specimens of English soils by a resonance method. With all the specimens, it was found that both the conductivity and the effective dielectric constant of the soil increased very rapidly as the moisture-content increased gradually. The effect of frequency variation showed that the electrical conductivity increased slowly with the increase of frequency, whereas the effective dielectric constant was found to decrease continuously with the increase of frequency. There was no peak in the conductivity-frequency curve as had been observed in some dielectrics by Bairsto and also by Ratcliffe and White in their soil measurements in the wide range of frequencies from 1000 c/s to 10 Mc/s employed by Smith-Rose.

In India, Khastgir and Sen Gupta (1936) directly determined the electrical constants of some specimens of Dacca soil by a resonance method for various

values of moisture-contents and for varying frequencies from 0·135 Mc/s to 2.7 Mc/s (*i.e.* from about 2000 metres to about 110 metres). The values of the soil constants were distinctly lower than those obtained by Smith-Rose with specimens of English soil, whereas they were of the same nature as those obtained by Ratcliffe and and White. The variation of the effective dielectric constant and the electrical conductivity with temperature was studied by Joshi (1938) in the medium radio-frequency range. Ansari, Toshniwal and Toshniwal (1940) also measured the electrical constants of the Allahabad soil for various values of the moisture-content at three different medium radio frequencies. Recently a study of the dielectric properties of soils from different parts of India was made by Rahman and Muhi (1944) in this laboratory. The soil-constants were measured by the differential transformer method for different medium radio frequencies and also with different moisture-contents.

In the ultra-high frequency range Smith-Rose and McPetrie (1932, 1933) determined the electrical conductivity of English soils. In India Khastgir and Chakravarty (1938) carried out similar observations with Dacca soil for a range of frequencies from 70 to 90 Mc/s. Banerjee and Joshi (1937) also did similar work with Benares soil for varying moisture-contents from 50 to 70 Mc/s. Prasad, Singh and Sinha (1940) also measured the electrical constants of the Patna soil using ultra-high frequencies.

SCOPE OF THE PRESENT INVESTIGATION

In most of the experiments, hitherto performed, on the direct determinations of the soil constants, no special attention was, however, paid to the degree packing. The soil specimen, under examination, was placed inside a container and the packing was made roughly the same, by eye-estimation, as what prevails in fields. It was only in the work of Smith-Rose, that the effect of packing was considered. He found that as the soil was packed more and more tightly the soil constants increased gradually attaining maximum values inside the cylindrical container in his experiment. Smith-Rose's determination of the electrical constants of the soils were claimed to have been obtained under the "desirable condition simulating soil in a well-rolled field or unploughed meadow." In view of the great importance of the effect of packing on the soil constants, it was thought desirable to undertake measurements of the maximum values of the electrical constants of the different Indian soils under optimum condition of packing. The measurements of the maximum values of dielectric constant and electrical conductivity of fifteen different soils taken from the various parts of India were accordingly made on high and medium radio frequencies under various controlled conditions.

From the electrical conductivity data, the *true* dielectric constants were evaluated. No attempt had so far been made of obtaining the true value

of the dielectric constant, except in the measurements with ultra-high frequencies. The correction due to the conductivity of the soil makes the value of the *true* dielectric constant substantially different from the effective value as obtained from the capacity-values of the experimental condenser with and without the soil in it. This is specially so, in the case of medium radio-frequency measuring fields and for the high-conductivity values of the soil.

The soil samples were taken from the following places: (1) Dacca, (2) Calcutta (Dum-Dum), (3) Delhi, (4) Lucknow, (5) Lahore, (6) Bombay, (7) Trichinopoly, (8) Peshawar, (9) Calicut (Madras Presidency), (10) Cuttack, (11) Ranchi, (12) Madura, (13) Vizagapatam, (14) Bangalore and (15) Trivandrum. There are transmitting stations of the All India Radio at the first eight places. In the cases of Calicut, Bombay, Madura, Vizagapatam, Bangalore, Trivandrum, Cuttack, Ranchi and Dacca, the specimens were taken from the soil profiles at a depth of $6'' - 3'6''$ from the ground surface. At the remaining places, the specimens used for investigation were surface soils within 6″ from the earth's surface.

Measurements were made of the dielectric constant and electrical conductivity of the different soils with special reference to the following :

(1) *The Effect of Packing :* For ordinary packing, a 'packometer' was devised to obtain a reliable measure of the degree of packing of the soil specimens. Alternatively, a load placed on a compressor pressing the soil contained in the intervening space between two co-axial metal cylinders was taken as a measure of the degree of packing. For high packing a hydraulic press with a pressure-gauge was employed. The variation of the soil constants with the degree of packing was thus studied for medium and high radio frequency fields, the temperature and moisture-content remaining the same.

(2) *The Effect of Moisture :* Variation of the soil constants with various values of moisture-contents was studied, keeping temperature and packing the same.

(3) *The Effect of Frequency of the Measuring Field :* Variation of the soil-constants with the variation of frequency in the high and medium radio-frequency ranges was studied, keeping packing, moisture-content and temperature the same.

(4) *The Effect of Temperature* : The variation of the soil constants with the variation of temperature was studied with dry soil having the same packing, for high and medium radio frequencies.

(5) *The Maximum values of Soil Constants :* The maximum values of the electrical constants of the soils from fifteen different places of India for 15% moisture content in all cases and for 20% moisture content in some cases, and for dry soils in a few cases, on high and medium radio-frequency fields were determined.

The soil measurements, for this comparative study were made in each case on 5 Mc/s and on the respective medium radio frequency of the A. I. R. transmitter located in each station from where the soil was taken. The medium frequency measurements with soils from (1) Cuttack, (2) Ranchi, (3) Bangalore, (4) Madras, (5) Vizagapatam and (6) Trivandrum, where there are no transmitting stations, were made at 1 Mc/s.

METHODS OF MEASUREMENT

Two methods of measurements were adopted in the present investigation : (1) the differential transformer method and (2) the oscillographic method. In most of the studies on medium radio frequencies the differential transformer method was followed. In the studies on high radio-frequencies, the oscillographic method was adopted.

DIFFERENTIAL TRANSFORMER METHOD

(a) *Experimental Arrangement*

The experimental arrangement is shown in Fig. 1. The differential

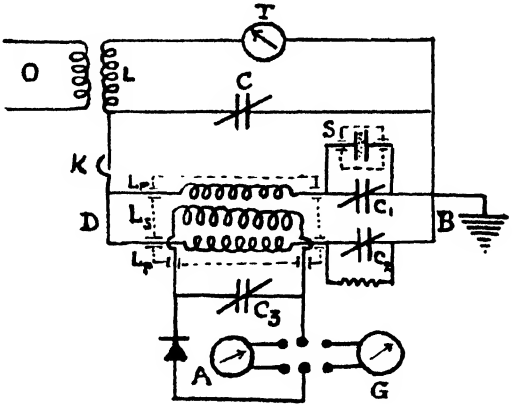

FIG. 1

transformer coils were wound on a wooden former. The number of turns in one primary branch was made exactly equal to that of the other primary branch and the directions of winding in the two cases were opposite, so that the voltage induced on the secondary by one would be neutralised by the voltage induced by the other. The soil condenser S was connected in parallel to a variable condenser C_1 which was in series with one primary branch of inductance L_p and a decade resistance box was connected in parallel (sometimes in series) with another variable condenser C_2 in series with the other primary branch of the same inductance L_p. The two ends of each branch were connected with one another as shown in the diagram and they were further connected by a key K to the main tuning circuit consisting of a

suitable coil L, a variable condenser C and a R. F. thermal milliammeter T. When the high frequency voltage from a Hartley oscillator was induced through L into the L−C circuit, the latter could be tuned to the required frequency with the key K closed. The tuning positions of the condenser C were not, however, the same when tuning was done with the key K open and closed. The secondary L_s was tuned to the frequency of the main primary circuit by a suitable variable condenser C_3 and the resonance current in the secondary was detected by means of a galvanometer G after having been rectified by a crystal detector. For larger currents, resonance was obtained with the help of a D. C. milliammeter A which was put into the secondary circuit by means of a throw-over switch.

THEORY OF THE METHOD

Let C_0 and C_s be the capacities of the soil condenser with air and soil in it respectively. When there is no current in the secondary, as is indicated by no-deflection in the galvanometer, the currents and also the impedances in both the primary branches are equal. With the empty soil condenser, let C_1 ond C_2 be the capacities of the two variable air condensers in the two branches under this balanced condition. The total capacity in one branch is equal to the total capacity in the other.

$$\therefore \quad C_2 = C_1 + C_0 \qquad \ldots \quad (1)$$

When soil is introduced in the soil condenser, the balance is lost and can be restored by changing C_2 to a new value C'_2 and by adjusting a suitable resistance R in series or in parallel with C_2. The capacity change compensates for the increase in capacity in the other branch due to the dielectric property of the soil, and the introduction of a resistance in the same branch due to the electrical conductivity of the soil is made up by the resistance R. We can thus write—

$$C'_2 = C_1 + C_s \qquad \ldots \quad (2)$$

From (1) and (2) we get

$$C_s = C'_2 - C_2 + C_0$$

Now if the effective dielectric constant of the soil is denoted by $e_{eff.}$, we have,

$$e_{eff.} = \frac{C_s}{C_0} = \frac{C'_2 - C_2 + C_0}{C_0} \qquad (3)$$

The parallel resistance R used to compensate for the conductivity effect of the soil is given by

$$R = \frac{1}{4\pi\sigma C_0} \qquad \ldots \quad (4)$$

where σ is the electrical conductivity of the soil.

Hence

$$\sigma = \frac{1}{4\pi R C_0} \qquad \ldots \quad (5)$$

When a resistance r is used in series with the soil condenser, then this resistance is equivalent to a parallel resistance R which is given by

$$R = \frac{1}{\omega^2 C'^2_2 r} \quad \ldots \quad (6)$$

where ω is the angular frequency of the measuring field.

In view of (5), we have then in the case of a series-resistance r

$$\sigma = \frac{\omega^2 C'^2_2 r}{4} = \pi f^2 C'^2_2 r \quad \ldots \quad (7)$$

where f is the frequency of the field.

Thus the electrical conductivity and the effective dielectric constant of the soil can be calculated from (3) and (5) or (7).

EXPERIMENTAL PROCEDURE

The procedure followed is explained here with reference to the diagram given in Fig. 1. The entire system LTBD consisting of the inductance L and the capacity C placed in parallel to the two primary branches was first tuned to the oscillator, keeping the capacity value of C_1 and C_2 almost equal. The tuning was observed by varying the condenser C in the main circuit by observing the maximum current in the thermal R. F. milliammeter T placed in the circuit. Next the empty soil condenser was placed in parallel to the condenser C_1. Now the tuning of the circuit was restored by varying the condenser C, if at all the tuning was disturbed on inserting the empty soil condenser. Then the current was observed in the secondary circuit which was already tuned to the oscillator. The condenser C_2 was then turned to bring the milliammeter current to the zero position. For more sensitive no-current adjusfment, the current was passed through a sensitive galvanometer by means of a double throw-over switch and the zero position of the galvanometer was restored as far as possible by varying the capacity C_2. The zero position was, however, not quite restored by the adjustment of C_2 only. Some resistance had to be included in the circuit to get the exact zero position of the galvanometer.

Next the experimental condenser was filled with the desired degree of packing. The tuning of the system was again made afresh. The no-deflection position of the galvanometer was again obtained by varying C_2 to some new value C'_2 and by inserting either a parallel resistance R or a series resistance r from the decade resistance box. All the requisite data were thus obtained for determining the effective dielectric constant and the electrical conductivity of the soil inside the condenser. The differential transformer was shielded properly, to eliminate stray fields. The oscillator was placed at some distance to avoid its direct effect on the arrangement. The connecting link between the coupling coil and the tuning condenser was also shielded.

THE OSCILLOGRAPHIC METHOD

(a) *Theory of the method*

When an alternating current I_0 passes through a soil condenser C_s placed in series with a perfect condenser C_p, the vector diagram can be represented

by the diagram in Fig. 2. The e.m.f. E_s across the soil condenser is in phase with resistance component of the current I_r but lags behind the total current

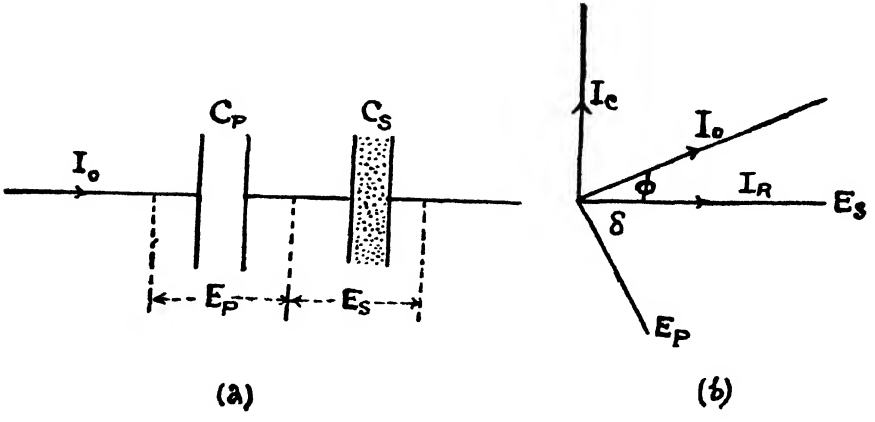

FIG. 2

I_0 by an angle ϕ. The e.m.f. E_p across the perfect condenser will be 90° behind I_0 and will lag behind E_s by an angle δ which is also the angle between the total current I_0 and the capacity component I_c of the latter. The angle δ can be found by measuring the phase-difference between the e.m.f. across the soil condenser and that across the perfect condenser.

Thus if ω is the angular frequency of the alternating current we have

$$\tan\phi = \frac{I_c}{I_r} = \frac{R}{1/\omega C_s} = R\omega C_s,$$

where R is the shunt resistance of the soil due to its conductivity. Assuming a parallel plate condenser, we have

$$R = \frac{1}{4\pi\sigma C_0},$$

where C_0 is the capacity of the empty soil condenser and since

$$\frac{C_s}{C_0} = \epsilon_{eff}.$$

by definition, we have

$$\tan\phi = \frac{\omega C_s}{4\pi\sigma C_0} = \frac{\epsilon_{eff}\omega}{4\pi\sigma}$$

Hence

$$\epsilon_{eff} = \frac{4\pi\sigma\tan\phi}{\omega} = \frac{2\sigma\cot\delta}{f} \qquad (8)$$

Here

Again

$$R = \frac{E_s}{I_r} = \frac{E_s}{I_0\sin\delta} = \frac{}{4\pi\sigma C_0},$$

whence we get

$$\sigma = \frac{I_0 \sin \delta}{4\pi C_0 E_s} \qquad \ldots (9)$$

Since $\frac{E_p}{I_0} = \frac{1}{\omega C_p}$ and $R = \frac{E_s}{I_0 \sin \delta}$, we get $\frac{E_s}{E_p} = \omega R C_p \sin \delta$

Therefore $$\sigma = \frac{1}{4\pi C_0 R} = \frac{\omega C_p \sin \delta}{4\pi C_0} \frac{E_p}{E_s} = \frac{f}{2} \frac{C_p}{C_0} \sin \delta \frac{E_p}{E_s} \qquad \ldots (10)$$

and $$\epsilon_{eff} = \frac{4\pi\sigma}{\omega} \cot \delta = \frac{C_p}{C_0} \cos \delta \frac{E_p}{E_s} \qquad \ldots (11)$$

In these expressions the values of C_p and C_0 are known, the values of E_s and E_p can be found in terms of the linear displacements in the x and y directions on the fluorescent screen due to the voltages E_s and E_p applied one after another to the x and y deflecting plates respectively, and the phase-difference δ between the voltages E_s and E_p can be easily obtained from the ellipse pattern on the oscillograph. Thus the electrical conductivity and the effective dielectric constant of the soil can be found from (10) and (11).

(*b*) *Measurement of* δ *from the elliptic oscillogram.*

The circuit arrangement in the oscillograph method is shown in Fig. 3.

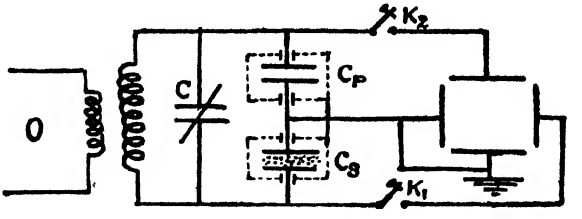

FIG. 3

The radio-frequency current from an oscillator was included into a circuit containing the variable air condenser C_p and the soil condenser C_s and a suitable coupling coil of inductance L. The voltages E_p and E_s across the condensers C_p and C_s were then applied to the y-and x-plates respectively of the oscillograph. Precautions were taken to eliminate stray effects by keeping the leads to the oscillograph as short as possible and by placing the coupling coils at a sufficient distance to prevent magnetic deflexion of the cathode ray beam. All connections were properly shielded by using insulated wires inside earthed metal tubes or inside glass sleeves covered by earthed tin foils. The soil condenser C_s and the air condenser C_p were both enclosed in an earthed tin box in two separate chambers. The key K_1 when switched on, gave the voltage E_s across the soil condenser to the x-plates and similarly with the key K_2 switched on and the key K_1 off, the voltage E_p across the pure condenser was applied to the y-plates. With both keys on, an ellipse

was observed on the fluorescent screen. The phase-difference δ between the two voltages E_s and E_p was given by

$$\text{Sin } \delta = \frac{lw}{A_x . A_y} \qquad \ldots \quad (14)$$

where l = major axis of the ellipse.
w = minor axis of the ellipse.
A_x = double the amplitude corresponding to E_s.
and A_y = double the amplitude corresponding to E_p.

THE TRUE VALUE OF THE DIELECTRIC CONSTANT OF A CONDUCTING MEDIUM

The relation between the effective dielectric constant $\epsilon_{eff.}$ and the true dielectric constant ϵ of a conducting medium can be found in the following manner. A 'leaky' condenser can be compared with a pure capacity C_s and a resistance r in series due to the conductivity of the soil. In such a system, a potential difference $Ve^{j\omega t}$ would cause a current given by

$$i = \frac{Ve^{j\omega t}}{r + \frac{1}{j\omega C_s}} = j\omega \left[\frac{C_s}{1 + \omega^2 C_s^2 r^2} - \frac{j\omega C_s^2 r}{1 + \omega^2 C_s^2 r^2} \right] . Ve^{j\omega t} \qquad \ldots \quad (12)$$

The complex dielectric constant of a conducting medium is given by

$$\epsilon' = \epsilon - j\frac{2\sigma}{f}$$

In view of this division into real and imaginary parts and remembering that the current through the soil condenser (containing soil) is given by

$$i = \frac{d}{dt}(\epsilon' C_0 V e^{j\omega t}) = j\omega \left((\epsilon - j\frac{2\sigma}{f}) C_0 V e^{j\omega t} \right) \qquad \ldots \quad (13)$$

we get from (12) and (13) the true value of the dielectric constant, *viz.*

$$\epsilon = \frac{C_s / C_0}{1 + \omega^2 r^2 C_s^2} \qquad \ldots \quad (14)$$

If ρ is the parallel resistance, corresponding to the series resistance r, we know

$$r = \frac{1}{\omega^2 C_s^2 \rho}$$

Again we know that $\rho = 1/4\pi\sigma C_0$, where σ = effective electrical conductivity of the soil. In view of the above two relations and putting $C_s/C_0 = \epsilon_{eff.}$ = effective dielectric constant, we get

$$\epsilon = \frac{\epsilon_{eff}}{1 + \frac{4\sigma^2}{f^2 . \epsilon_{eff.}^2}} \qquad \ldots \quad (15)$$

The true dielectric constant of soil can thus be obtained from (15), when the values of $\epsilon_{eff.}$ and σ are already known by direct measurements.

EXPERIMENTAL RESULTS

(i) Study of the variation of the electrical constants of some soils with the degree of packing, the temperature and moisture-content remaining the same, on high and medium radio frequencies

A 'packometer' was devised to have a reliable measure of the degree of packing in a soil specimen when the packing was not of a high order.

The instrument consisted of a spring balance which was held fixed in a vertical position by a clamp which could be raised or lowered. From the bottom of the spring balance was suspended a small scale pan as shown in Fig 4. A sharp blade, with a stout brass rod attached to the middle of the

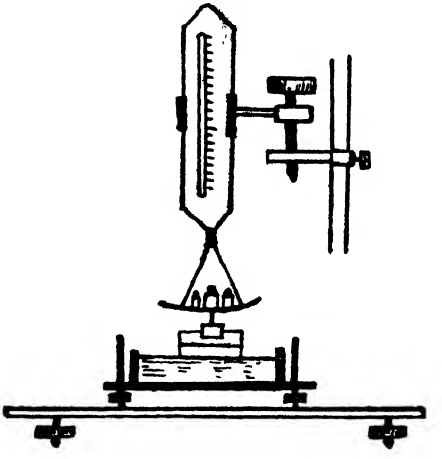

FIG. 4

blunt side in the plane of the blade, was held with its plane vertical by fixing the rod rigidly to the centre of the underside of the pan. The entire system had a free play in the vertical direction.

Usually for measurements of soil constants for low orders of packing this instrument was employed. The soil under examination was then taken inside a parallel plate condenser inside an ebonite container with an ebonite lid which could be tightly fixed by binding screws. After having taken the usual measurements, the lid of the container was carefully opened and the soil in the open container was placed on a glass slab provided with three levelling screws. The glass slab with the soil inside the container was brought under the blade of the packometer. By adjusting the top screw in the clamp, the spring balance was lowered gradually till the sharp edge of the blade just touched the soil surface. It was, however, necessary to level the glass slab during the above procedure. An index line, provided by a paper strip (parallel to the edge) pasted on the upper part of the blade, was arbitrarily

chosen. Weights on the pan were then carefully placed till the blade went down vertically up to the index line, cutting through the soil. If the weights totalled M gms., the degree of packing was given by M/A gms. per unit area, where A= surface area of the blade in contact with the soil.

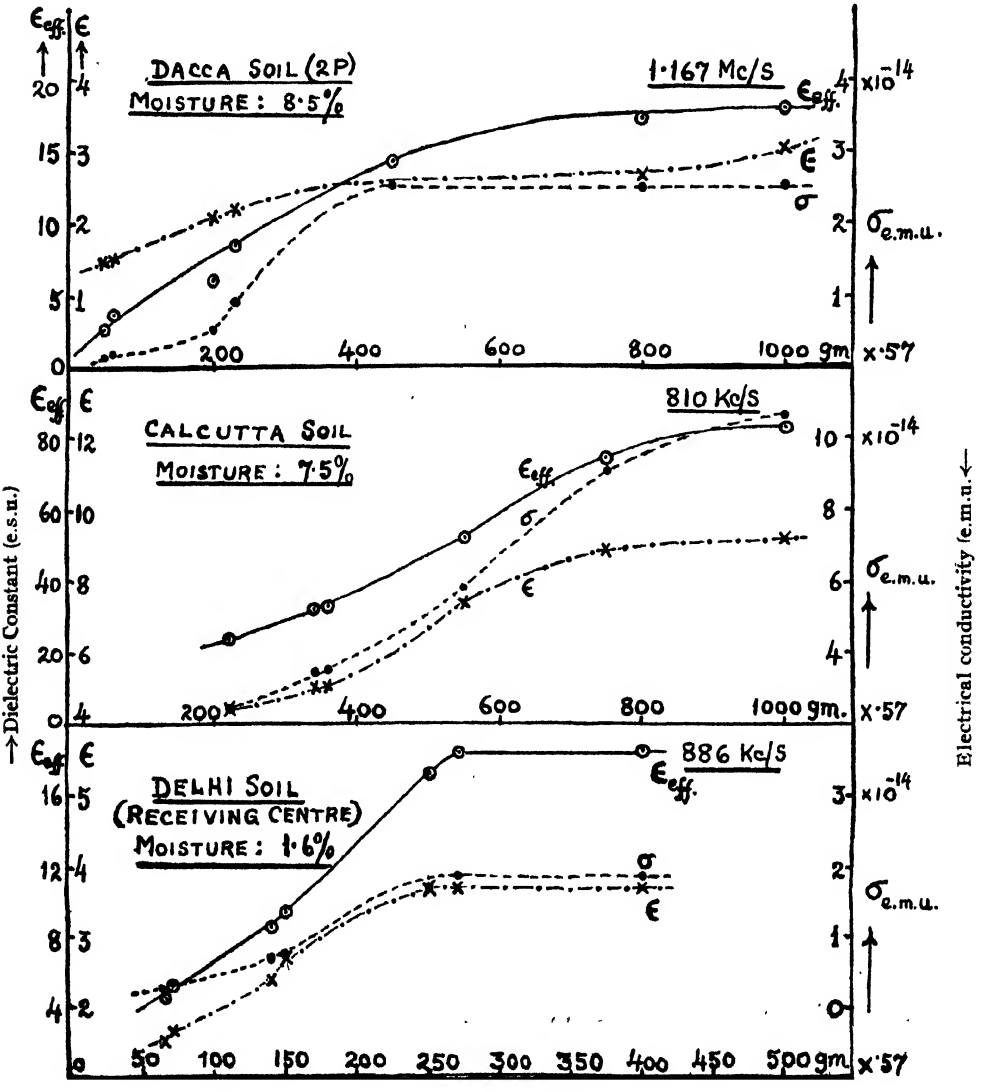

FIG. 5

For high degrees of packing a hydraulic press with a pressure-gauge was used. The soil condenser in this case consisted of two hollow concentric brass cylinders of the same length, one inside another with their ends fixed on a thick ebonite base. A hollow ebonite cylinder fitting tightly on to the outer surface of the outer brass cylinder was of sufficient length to project well beyond the brass cylinders. The soil specimen was rammed into the

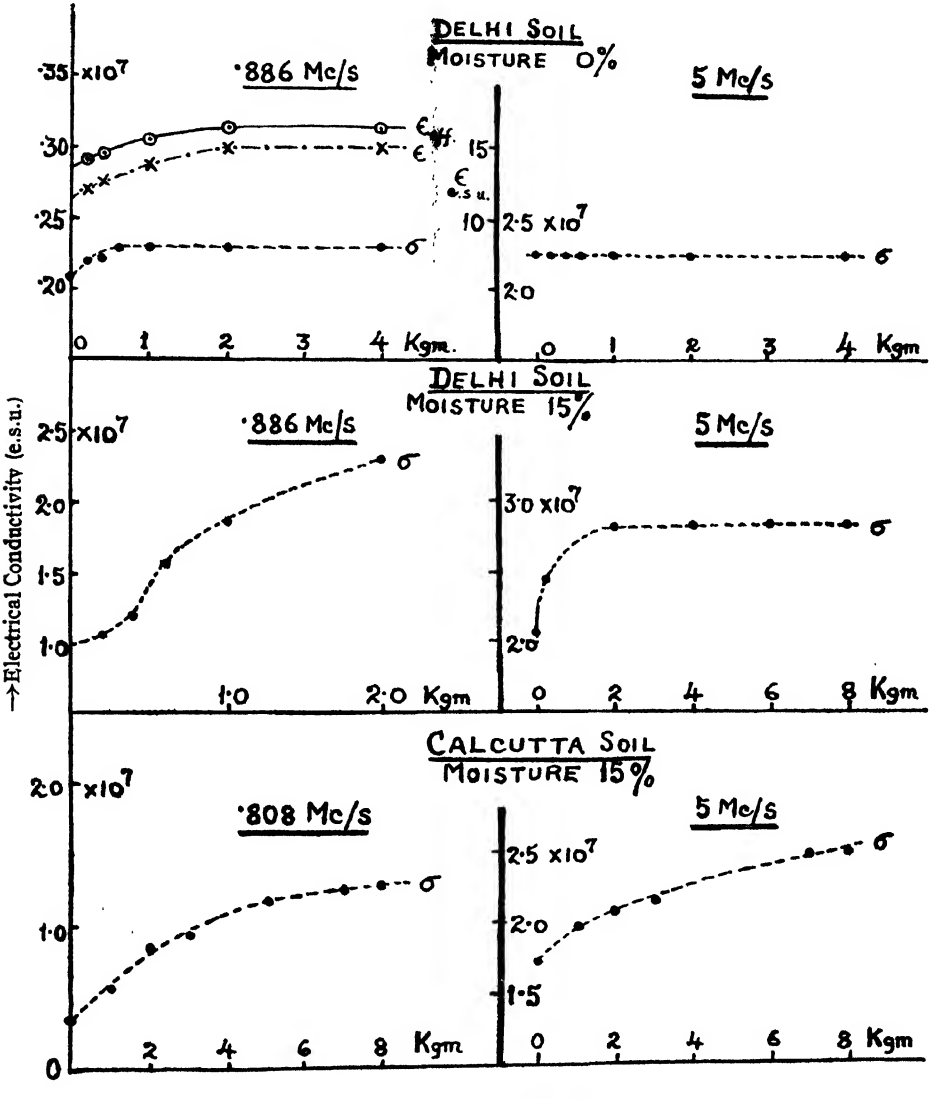

FIG. 6

space between the two concentric brass cylinders and was made to fill a portion of the outer ebonite cylinder above the top level of the brass cylinders. A solid wooden cylinder held vertically and loosely fitting into the ebonite cylinder was inserted in it above the soil. The ebonite base of the soil condenser was placed on the lower moving platform of the hydraulic press and the top surface of the wooden cylinder was made to press against the upper fixed platform of the press.

The same soil condenser was also used occasionally for measurements with soils of low orders of packing. In such cases, loads were placed on the top of the wooden cylinder pressing the soil in the cylinder system.

Typical experimental results by the differential transformer method with Dacca, Calcutta and Delhi soils on 1167Kc/s (257. m), 808 Kc/s (370.4 m.) and 886 Kc/s (338 m) respectively are shown in Fig. 5. The values of the electrical conductivity, effective and true dielectric constants are here plotted against various degrees of packing as indicated by the packometer. It is evident that all the values tended to approach saturation values.

Typical experimental results by the oscillographic method using cylindrical soil condensers with Calcutta and Delhi soils on high and medium radio frequencies are illustrated in Fig. 6.

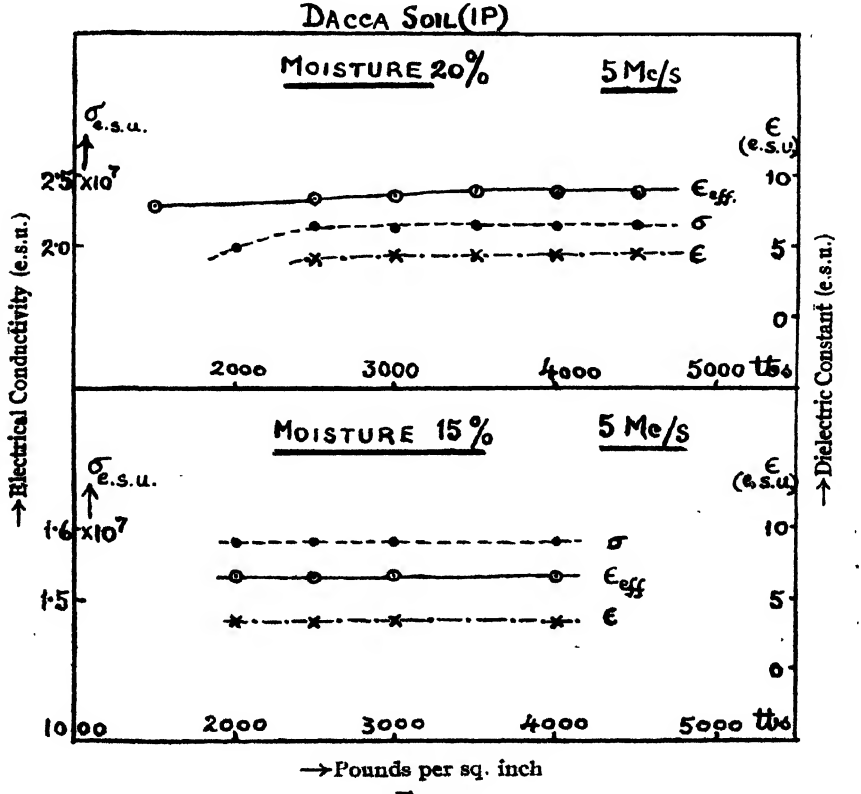

FIG. 7

For high degrees of packing obtained by using a hydraulic press the values of the soil constants were also measured by the oscillographic method and found practically constant from a pressure of 20000 lbs. per sq. in. to a maximum pressure of 45000 lbs. per sq. in. which the soil condenser was able to stand. These results for high packing with Dacca soil are shown in Fig. 7.

(ii) Study of the variation of the electrical constants of the Dacca soil with moisture content variation, for various degrees of packing (temperature remaining the same) on medium radio frequency

In preparing soil of a definite moisture content, the following procedure was adopted : the soil was heated in a double-walled air bath to a little over 100° C for about 12 hours and it was then considered as completely dry. Required quantity of this dry soil was then cooled inside a desiccator. Requisite quantity of distilled water was then added to the soil from a burette to make the moisture content percentage equal to some desired value.

The soil with a particular percentage of moisture was then packed inside the soil condenser to gradually increasing extent and the soil constants

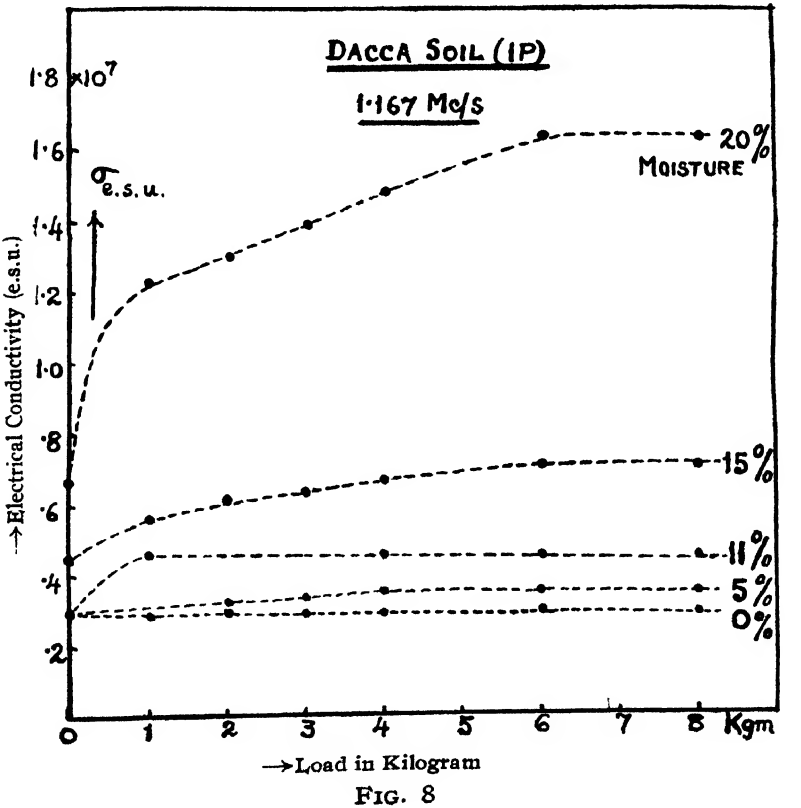

FIG. 8

measured on medium radio-frequencies by the differential transformer method. Different sets of similar measurements were made for moisture contents ranging from 0 to 20%.

The experimental results with the Dacca soil (1P) on 1167 Kc/s (the frequency of the Dacca A.I.R. transmitter) are shown in Fig. 8. It is to be noted that the soil constants increased with packing and were found to attain saturation values in most cases.

The variations of the soil constants of the Dacca soil (2P) with moisture content on 1167 Kc/s for three different degrees of packing are graphically shown in Fig. 9.

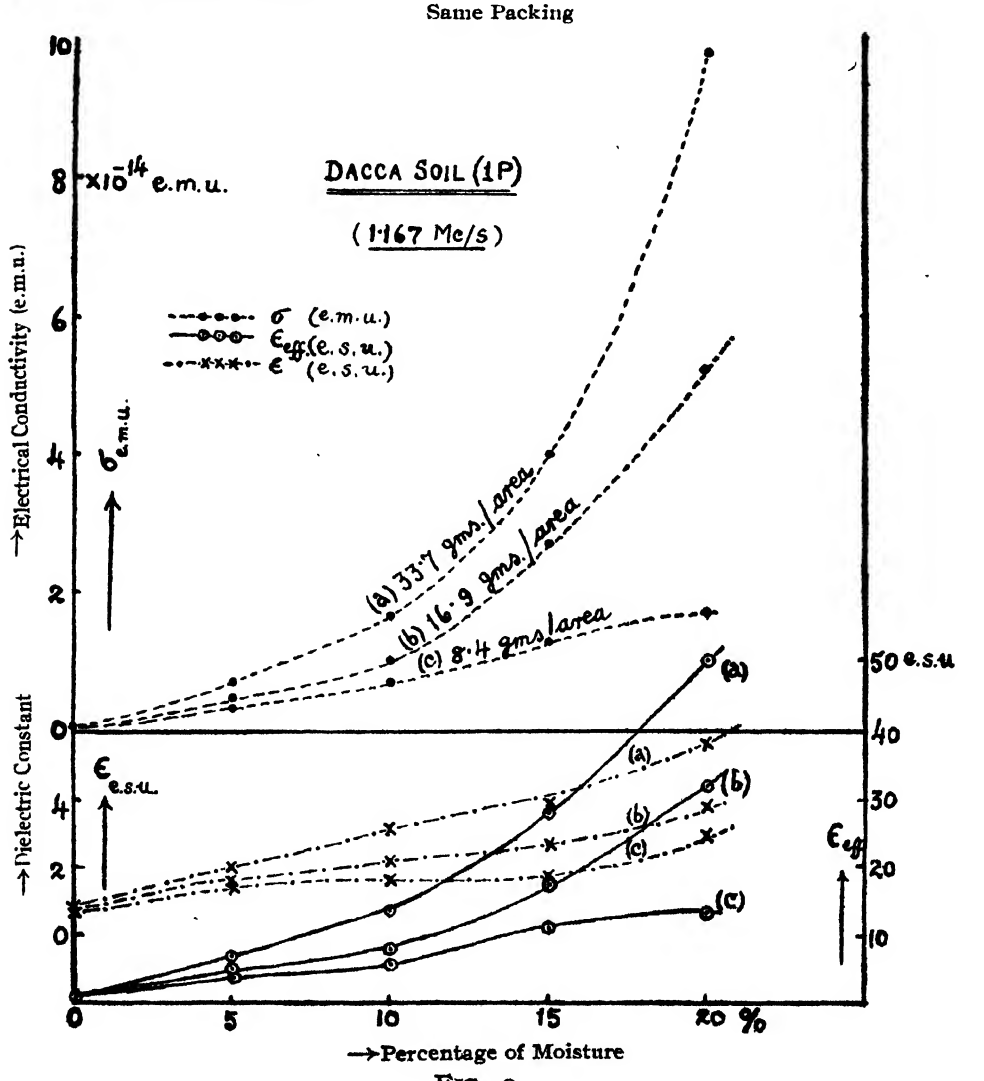

FIG. 9

(iii) Study of the variation of the electrical constants of different soils with frequency (the temperature, packing and moisture content remaining the same) on high and medium radio frequencies for low and high packing

In Fig. 10 are shown the values of electrical conductivity, effective and true dielectric constants of Calcutta, Dacca and Delhi soils obtained by the differential transfomer method for a range of frequencies from 600 Kc/s to 1200 Kc/s. The packing was kept at some fixed value and the moisture was 2-3%. It is to be noted that the electrical conductivity increased with frequency and that both effective and true dielectric constants decreased with the increase of frequency.

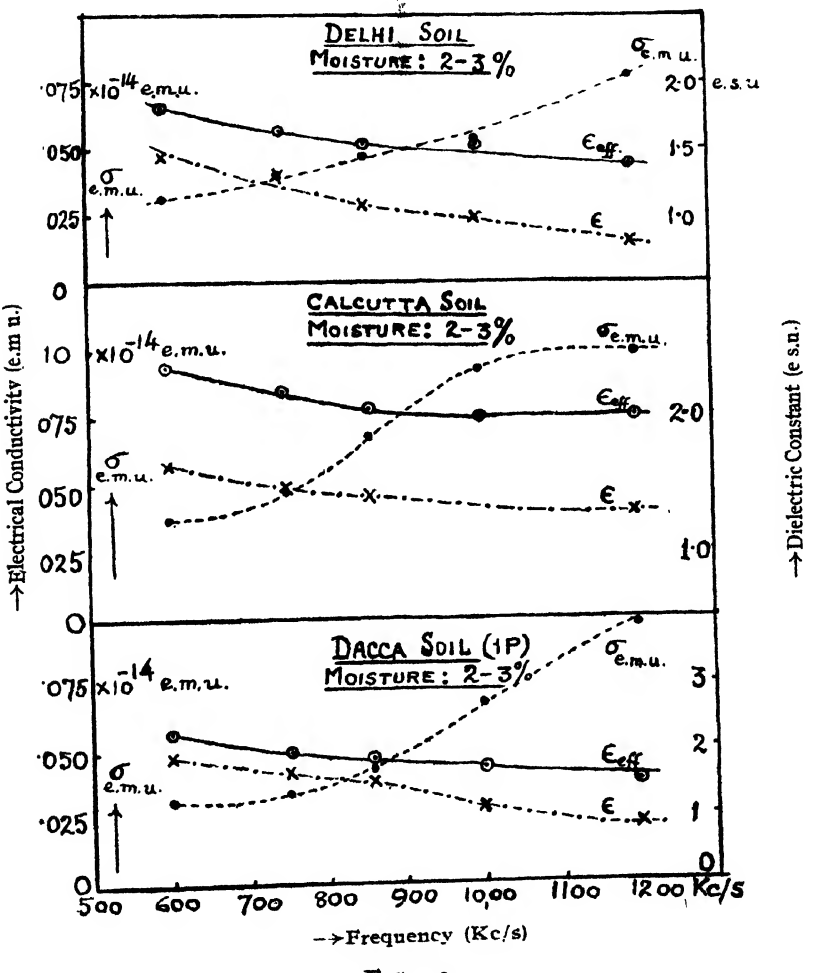

FIG. 10

The experimental results obtained by the oscillographic method working with various soils of a fixed degree of packing (400 gms/13·3) on high radio frequencies ranging from about 1 to about 8 Mc/s are shown in Fig. 11.

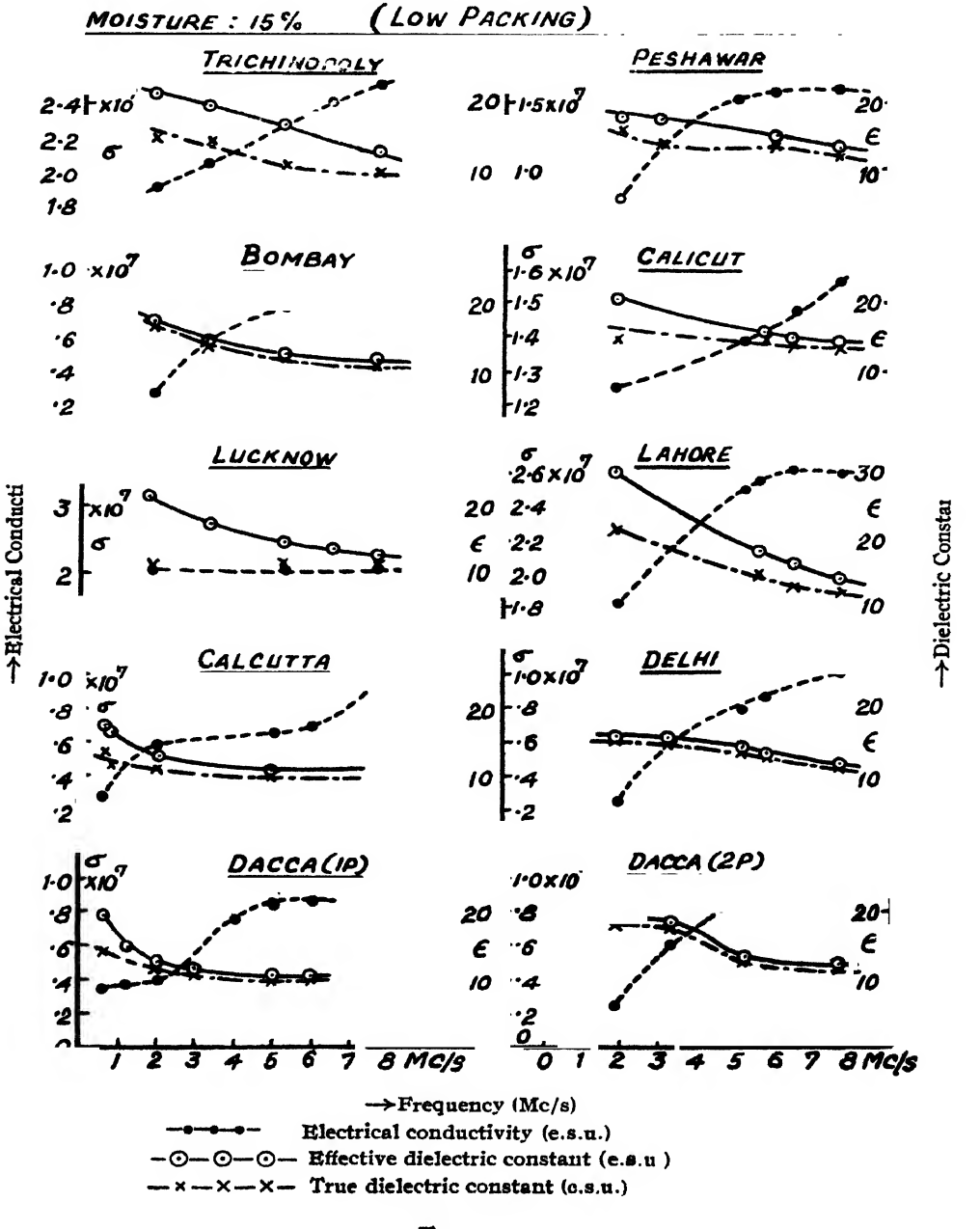

FIG 11

In all cases the dielectric constant decreased but the electrical conductivity increased with frequency tending in many cases to constant values. Measurements were also made with Calcutta, Dacca and Delhi soils for very high packing (4500 lbs. per sq. in.) on the same range of high radio frequencies. The results are shown in Fig. 12. As contrasted with the experimental results

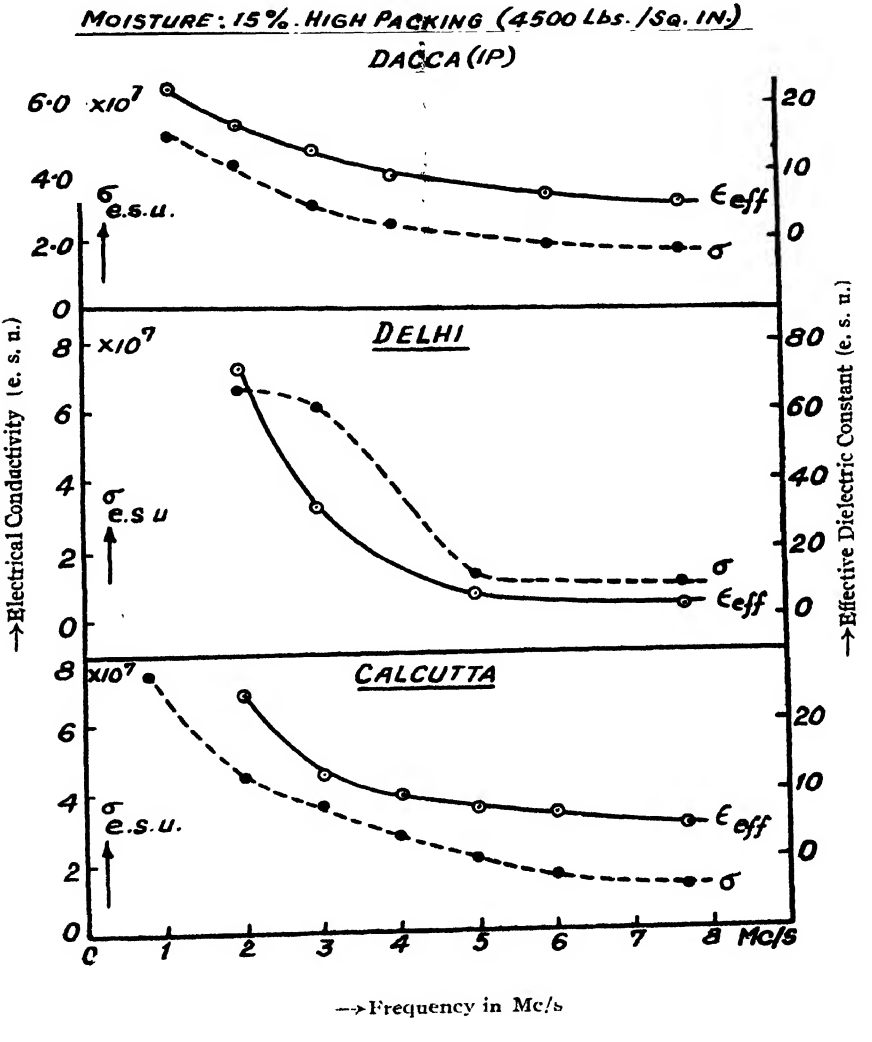

FIG. 12

with low packing, the electrical conductivity was found to diminish steadily with increasing frequency, whereas the effective dielectric constant decreased in the same way with the increase of frequency.

(iv) Study of the variation of the electrical constants of some dry soils with temperature for fixed values of packing (low and high)

(a) Experiments on medium radio frequency (1167 Kc/s.)

For this study by the differential transformer method on medium frequency, a special glass container with parallel platinum plates rigidly fixed by fusing platinum connections into the glass was constructed. The soil having been dried was introduced into the container and a thermometer was inserted inside the soil above the platinum plates through a stopper. The glass container with the soil inside and the thermometer, was then fixed inside a glass cylinder with a base so that the container rested on a piece of cork on the base of the outer cylinder. The open end of the outer cylinder at the top was closed with a cork through which the neck of the inner glass container was inserted. The short platinum wire connections from the plates were led out into the outer cylinder.

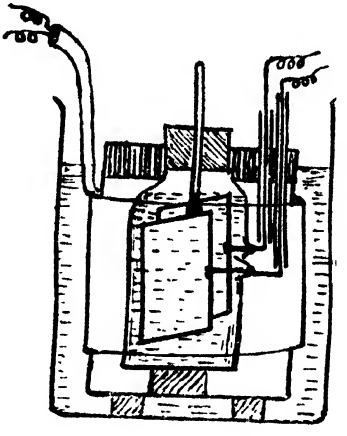

FIG. 13

Thin copper wire leads were then passed through narrow glass sleeves and were taken out as shown in the diagram in Fig. 13. The outer glass cylinder was then fitted inside a heater coil which was enclosed within a metal case in the form of a cylinder. The entire system was then placed inside a calorimeter containing water. On passing current through the heater coil the water in the calorimeter was heated. It was found convenient to increase the temperature of the soil to a high value and then to take measurements of the electrical constants when the temperature was falling. The temperature was noted carefully after stirring the water. With Dacca soil the effect of temperature variation for two frequencies from about 4°C to about 75°C was investigated.

The values of the soil constants for various temperatures are shown in Fig. 14 for each of the two medium frequencies of the Dacca and Calcutta transmitting stations. It is interesting that while the soil conductivity was found to increase with temperature, the effective dielectric constant remained practically constant. The true dielectric constant was found on calculation to decrease with the rise of temperature. It should be noted that the packing of the soil in this experiment was extremely low.

For high packing on the same medium radio frequency the oscillographic method was employed and the cylindrical condenser filled with dry soil and packed with the help of the hydraulic press was used for the purpose. The steel platform of the press could be electrically heated so that there was no difficulty in raising the temperature of the soil. For lower temperatures ice or iced water was used in a vessel surrounding the soil condenser. The lower limit of the temperature was 15°C, as below 15°C there was difficulty in taking

Dry Dacca Soil

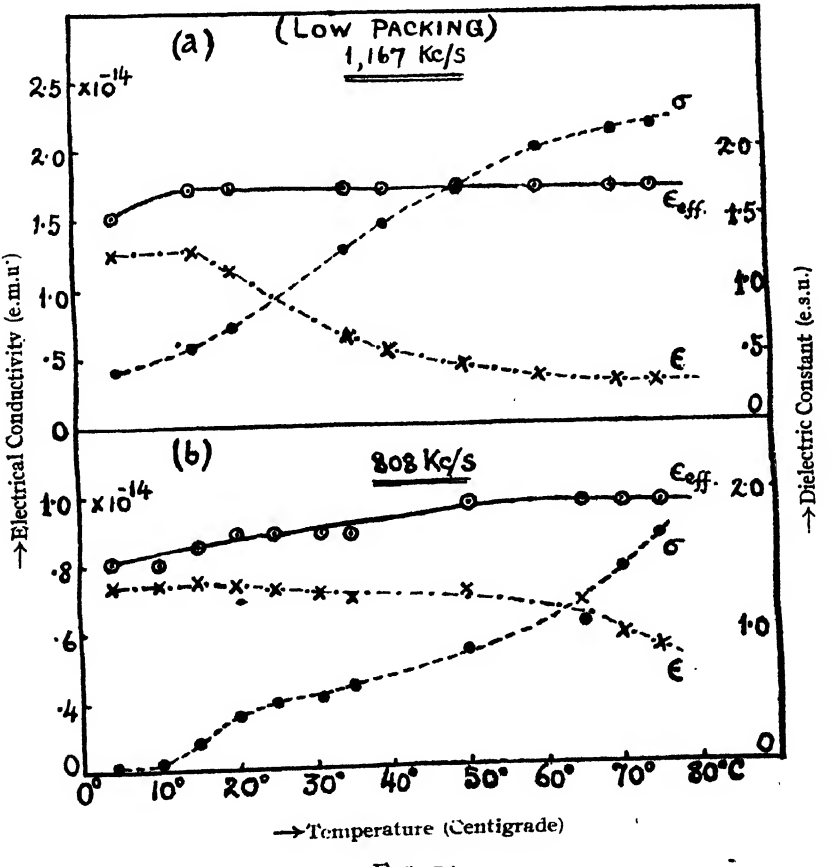

FIG. 14

reliable measurements owing to the wetting of the soil by the dew that was formed in appreciable quantity at such low temperature. The results with such high packing of Dacca soil are illustrated in a part of Fig. 15. The electrical conductivity increased with temperature but the effective dielectric constant was, in this case, found to decrease as the temperature was increased from 35° to 75°C.

(*b*) *Experiments on high radio-frequency* (5 *Mc/s*)

The experimental results on 5 Mc/s obtained by the oscillographic method employing Delhi and Dacca soils packed at a pressure of 4500 lbs per sq. in.

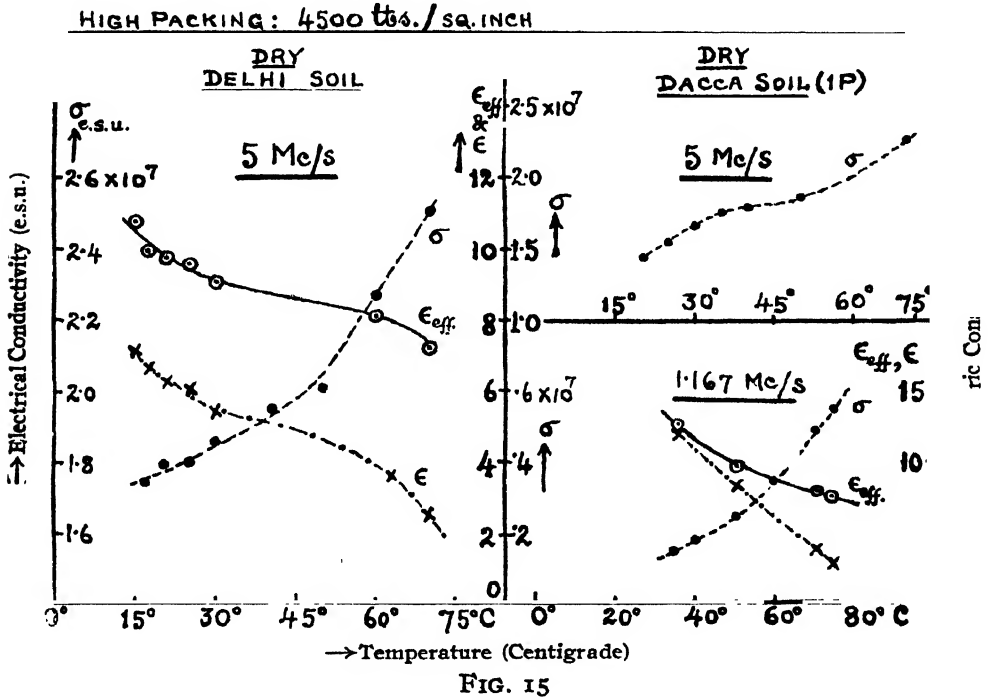

FIG. 15

are shown in Fig. 15. The electrical conductivity was found to increase and the dielectric constant to decrease as the temperature was raised from 15°C to 70°C.

In the study of the temperature effect, it was tested carefully that effect was not due to dimensional change of the soil condenser owing to temperature variations.

(*c*) *Comparative study of the maximum values of the electrical constants of the surface soils from fifteen different places on* 5 *Mc/s and on medium frequencies for a few soils for fixed moisture content values.*

A short description of the different soils employed, the depth from which they were obtained and the localities are entered in Table I. The p_H values

of the soils are also given there. In Table II are given the maximum values of the electrical conductivity, the effective and the true dielectric constants of the different soils. The frequency of the measuring field and the p_H values are also shown in the same table.

TABLE I

Place and Locality.	Depth.	Description.	Value.
*1. Dacca (1 P)	0"--6"	Grey loamy	5.7
,, (2 P) ... . (Agricultural Farm)	6"—2'-3"	Yellowish, heavy loam	5.8
2. Calcutta (Dum Dum Aerodrome) ...	0"—6"	Grey, Clayey	6.5
3. Delhi (A. I. R. Receiving Station) ...	0"—6"	Brownish	6.8
4. Luckuow (A. I. R. Transmitting station) ...	0"—6"	Light brown, clayey	6.6
5. Lahore (A. I. R. Transmitting station) ...	0"—6"	Grey, clayey	7.3
6. Peshawar (A. I. R. Transmitting station)...	0"—6"	Light brown	6.7
7. Trichinopoly (A. I. R. Transmitting station)	0"—6"	Grey, clayey	6.0
*8. Bombay (Kumata)	0"—6"	Red	5.1
*9. Calicut (Madras Presidency)	0"—6"	Red	4.8
*10. Ranchi (Ratu)	0"—1'	Red, clayey	4.5
*11. Cuttack (Tangi)	0"—1'	Grey, gravelly	6.2
*12. Bangalore	0"—3'-6"	Red, Loamy, granular	6.7
*13. Madura (Pasumalai)...	0"—1'-2"	Brownish, red sandy loam granular	6.2
*14. Vizagapatam (Muddilipalayam ..	0"—1'	Brownish, red sandy loam, granular	5.6
*15. Trivandrum (Khoddappanam Kunnu) . .	0"—1'-6"	Light red, gravelly	

* The description of the soil profiles is taken from the records of the Soil Science Section of the Chemistry department, Dacca University

It will be seen from Table II that there is no connection between the values of the soil constants and the p_H values of the soils. It is also significant that for such high packing the values of both the electrical conductivity and the dielectric constant at 5 Mc/s are decidedly lower than those at medium radio frequencies. This is consistent with the experimental results regarding the variation of the soil constant with frequency for such high degree of packing. (See Fig. 12).

Some typical oscillograms, on high and medium radio-frequencies, are shown in Plate (VI)

TABLE II

(Electrical constants in e. s. u.)

Soils	p_H values	Radio frequency f = 5 Mc/s (λ = 60m)						Medium radio-frequency							
		Moisture 15%			Moisture 20%			Moisture 15%			Moisture 20%			Frequency.	Wavelength
		$\sigma \times 10^{-7}$	ϵ eff.	ϵ	$\sigma \times 10^{-7}$	ϵ eff.	ϵ	$\sigma \times 10^{-7}$	ϵ eff.	ϵ	$\sigma \times 10^{-7}$	ϵ eff.	ϵ	Mc/s	metres
(1) Dacca (1P) ...	5.7	1.58	6.5	—	2.16	8.8	4.5	4.96	22.0	1.4	5.7	34.6	3.9	1.167	257.1
(2) Calcutta (Dum Dum)	5.8	1.52	5.7	2.67	1.69	6.4	3.1	7.5	—	—	14.8	—	—	.808	370.4
(3) Delhi ..	6.5	1.25	7 05	4.75	1 28	7 25	4.9	21.5	—	—	24.2	—	—	.886	338.6
(4) Lucknow ...	6.8	1.52	7.8	4.85	1.65	7.7?	4.4	1.01	46.2	39.0	—	—	—	1.022	293 5
(5) Lahore ...	6.6	1.33	5.7	3.05	1.50	5.6	2.6	7.04	70.1	15.85	10.3	—	—	1.086	276
(6) Bombay ...	6.0	1.45	6.7	3.83	2.01	6.4?	2.5	—	—	—	—	—	—	1.231	244
(7) Calicut (Madras)	5.1	1.42	6.1	3.27	1.71	4.9?	2.0	5.14	34.2	6.3	—	—	—	1.420	211
(8) Trichinopoly ...	6 7	2.68	15.5	10.50	—	—	—	—	—	—	—	—	—	.758	395.8
(9) Peshawar ...	7.3	1.75	9.3	5.94	—	—	—	1 46?	40.2	32.5	5.72	—	—	1.500	200
(10) Cuttack ...	4.5	1.71	9.2	5.93	—	—	—	—	—	—	—	—	—	—	—
(11) Ranchi ...	4 8	1 23	8.8	6.7	1.98	6.0	2.2	—	—	—	—	—	—	—	—
(12) Bangalore ...	6.2	1.72	6 7	3.26	1.91	6.2	2.5	—	—	—	—	—	—	—	—
(13) Madura ..	6.7	1.90	8.3	4.51	2.09	—	—	—	—	—	—	—	—	—	—
(14) Vizagapatam ...	6.2	1.76	8.5	5.04	1.93	6 7	2.9	—	—	—	—	—	—	—	—
(15) Trivandrum ...	5.6	1.63	8.1	4.92	1 94	7.35	3.5	—	—	—	—	—	—	—	—

INTERPRETATION OF EXPERIMENTAL RESULTS

(*a*) *The Effect of Packing*

As the soil is packed, some of the air gaps between soil particles are removed. As the degree of packing is increased, more and more air gaps are closed up resulting in a large values of the electrical conductivity and of the dielectric constant. As density also increases with the increase in the degree of packing, the dielectric constant would also increase with the degree of packing. We would also expect some limiting values of the soil constants for some high value of packing.

The experimental results with regard to the effect of packing are thus explained.

(*b*) *The Effect of Moisture*

The electrical conductivity and dielectric constant of water are both high. When water is added to dry soil, it gets into the innumerable air gaps among the soil particles. With more water, there is greater penetration and we should expect an increase of dielectric constant and electrical conductivity with the increase of moisture. For higher moisture contents it is also expected that the soil constants would tend to approach saturation values.

The experimental results showed that the soil constants increased considerably as the percentage moisture was increased from 0 to 20%.

(*c*) *The Variation of the Soil Constants with Frequency*

So far as the electrical conductivity is concerned, we have to consider the effect of (1) displacement currents in the soil medium, (2) the effect of orientation of dipolar molecules in the soil and (3) the skin-effect. The effect of an ionic space-charge formed in the soil condenser can be left out of consideration, as it is well established that the effect of such ionic charge has practically no effect except at very low audio-frequencies. In the range of audio-frequencies the variation of the electrical conductivity due to the orientation of molecules is of little importance and the major portion of the soil conductivity is due to displacement currents. In the region of high frequencies, however, the effect of orientation of the dipolar molecules, is predominant. The total electrical conductivity of soil at any frequency is, however, given by

$$\sigma = \sigma_0 + \sigma_d + \sigma_p \qquad \ldots \quad (16)$$

where, σ_0 = d.c. electrical conductivity ;

σ_d = electrical conductivity due to displacement currents in the dielectric ;

and σ_p = electrical conductivity due to orientation of polar molecules in the electrical field.

It can be shown that the electrical conductivity due to displacement currents is directly proportional to the frequency, so that in audio-frequency range, the variation of the electrical conductivity with frequency f would be of a linear form, *viz.*,

$$\sigma = \sigma_0 + k_1 f, \text{ where } k_1 \text{ is a constant.}$$

Considering, however, the conductivity of soil due to dipolar orientation, it can be shown that in range of radio-frequencies, where the product of angular frequency and relaxation time is very much less than unity, Debye's expression for the electrical conductivity would reduce to a simple square law, *viz.*,

$$\sigma_p = k_2 f^2, \text{ where } k_2 \text{ is a constant.}$$

Thus the expression for the total soil conductivity at any frequency would be given by

$$\sigma = \sigma_0 + {}_1kf + k_2 f^2$$

Bairsto's (*loc.cit.*) work substantiated this relation in the case of marble and slate. It is to be noted here that the d.c. conductivity term σ_0 is indeed a small quantity. When, however, it is high as in the case of tightly packed soil, the skin effect becomes appreciable and the expression for total electrical conductivity would be of the form :—

$$\sigma = \frac{k_0}{\sqrt{f}} + k_1 f + k_2 f^2 \qquad \ldots \quad (17)$$

where k_0 involves the d.c.conductivity.

This relation has been substantiated by our experimental results on the variation of soil conductivity with frequency. For low packing, the d.c. conductivity of soil is very small so that the conductivity terms due to displacement currents and the orientation of dipolar molecules in soil are only effective. For low packing, therefore, the soil conductivity should increase with frequency in accordance with (17). When the packing of soil is very high, the d.c. conductivity term becomes large in comparison with the other terms, and the skin-effect which is predominent determines the variation of the soil conductivity with frequency. Thus for such high packing, the soil conductivity is expected to decrease with frequency. Such results have actually been obtained experimentally.

The variation of the dielectric constant with freqnency, on the other hand, should be attributed solely to the orientation of the dipolar molecules in the soil medium. The experimental results on dielectric constant are in qualitative agreement with Debye's formula.

(*d*) *The Effect of Temperature*

As density decreases with the increase of temperature, it is expected that the true dielectric constant would decrease as the temperature is raised. Considering, however, Debye's expression for the dielectric constant, since it is known that the relaxation time decreases as temperature increases, the dielectric constant would gradually increase with the increase of temperature. This increase, however, is more than counter-balanced by the decrease of dielectric constant with temperature due to change in density. Usually, therefore, the true dielectric constant of soil would gradually decrease with the increase of temperature. This is what has been actually observed.

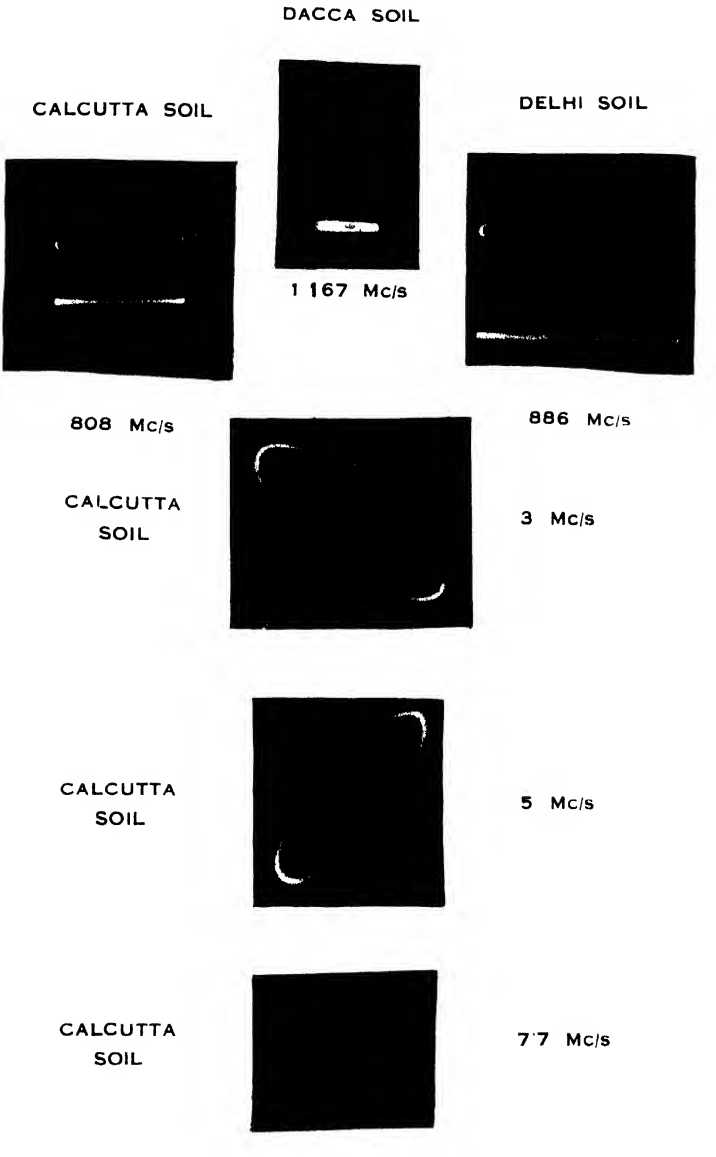
DACCA SOIL
CALCUTTA SOIL
DELHI SOIL
1 167 Mc/s
808 Mc/s
886 Mc/s
CALCUTTA SOIL
3 Mc/s
CALCUTTA SOIL
5 Mc/s
CALCUTTA SOIL
7·7 Mc/s

Regarding variation of electrical conductivity with temperature, it is evident that the d.c. conductivity part increases with temperature. The conductivity due to orientation of polar molecules would also gradually increase with temperature, since relaxation time decreases as the temperature is raised. The conductivity due to displacement current which is small in the region of radio-frequencies, is proportional to the dielectric constant and would decrease with the increase of temperature. On the whole, therefore, in the region of radio-frequencies, the soil conductivity would steadily increase as the temperature is raised. This is also what has been experimentally found.

Since the effective dielectric constant involves the true dielectric constant and the electrical conductivity, it is evident that its variation with temperature would be determined by the variations of both these quantities. We have seen that the true dielectric constant decreases and that the electrical conductivity increases as the temperature is raised. The latter variation is usually such that the effective dielectric constant of soil would slowly decrease with the increase of temperature. It may also remain constant over a range of temperature. Our experimental results on the effect of temperature on the soil constants are thus interpreted.

SUMMARY

The results of investigations on the dielectric properties of fifteen different soils from the different parts of India on medium and high radio frequencies are given in the paper. Measurements of the effective dielectric constant and the electrical conductivity were made by the differential transformer method or the oscillographic method. From these data, the true dielectric constants were evaluated. The following studies were made:

(*a*) *The Effect of Packing* : The packing effect on the electrical constants of some soils was studied on 5 Mc/s and also on the respective frequencies of the medium wave A. I. R. stations located at the places from where the soils were taken, for specified moisture contents. The packing effect was studied in two stages : (*i*) for low order of packing and (*ii*) for high order of packing as obtained by a hydraulic press. The soil constants were found to increase gradually till in many cases some constant values were attained.

(*b*) *The Effect of Moisture* : The increase of soil constants of the Dacca soil with the increase of moisture content from 0 to 20% was studied for various degrees of packing. Both electrical conductivity and dielectic constant were found to increase rapidly with the increase of moisture content. The degree of packing was kept at the same value for the soils with different moisture contents.

(*c*) *The Variation of the Soil Constants with Frequency* : The experiments were performed for low and high orders of packing. Some soils were studied for low packing in the range of medium radio frequencies, while all the fifteen soils were studied for low packing in the high frequency range from

about 1 or 2 to about 8 Mc/s. A slow *decrease* of dielectric constant and a rapid *increase* of electrical conductivity with the increase of frequency were noted for low packing.

Experiments with some soils with extremely high packing in the same high frequency range, on the other hand, showed a *decrease* of both the electrical conductivity and the effective dieletric constant of the soils with the increase of frequency.

(*d*) *The Effect of Temperature* : The experiments on the temperature effect with some soils both on medium and high radio frequencies showed an increase of electrical conductivity and a slow decrease of the effective dielectric constant with the rise of temperature for very high packing. For low packing on medium radio frequency the effective dielectric constant of the Dacca soil was found to be constant over a wide range of temperature. The true dielectric constant was found, however, on calculation, to decrease in all cases as the temperature was raised both for low and high packing.

(*e*) *Comparative study of the maximum values of the soil constants of soils from fifteen different places on 5 Mc/s and on medium radio frequencies for some soils* : The maximum values of the electrical constants of the soils from Dacca, Calcutta (Dum Dum), Delhi, Lucknow, Lahore, Peshawar, Bombay, Trichinopoly, Calicut, Ranchi, Vizagapatam, Cuttack, Bangalore, Madura and Trivandram were measured on 5 Mc/s for 15% and 20% moisture contents.

The maximum values of these constant were also obtained for the soils from Dacca, Calcutta, Delhi, Lahore, Peshawar and Calicut (Madras) on the respective frequencies of the medium wave stations located at these places.

The values of the soil constant do not appear to have any correlation with the p_H-values of the soils.

A general interpretation of all experimental results is given.

ACKNOWLEDGEMENTS

We are indebted to the Soil Science Section of the Chemistry Department of the Dacca University for supplying us with all the soil profiles used in the present investigation. Our sincere thanks are also due to the A. I. R. Station Engineers of some of the stations for kindly sending us the surface soil from the neighbourhood of their transmitters and to Prof. S. K. Mitra, D.Sc., M.B.E., for supplying us with Calcutta soil specimens. We also thank the Head of the Chemistry Department for the use of the Carver Laboratory Hydraulic Press.

Finally we offer our warm thanks to Prof. S. N. Bose for his help and interest in this investigation.

PHYSICS DEPARTMENT,
DACCA UNIVERSITY.

REFERENCES

Ansari, Toshniwal and Toshniwal, 1940 *Proc. Nat. Inst. Sciences* (India), **6**, 627
Bairsto, 1912, *Proc. Roy. Soc. A.*, **96**, 363.
Banerjee and Jo hi, 1937, *Science and Culture*, **2**, 587
Joshi, 1938, *Science and Culture*, **4**, 196
Joshi, 1938, *Ind. Jour. Phys.*, **12**, 1
Prasad, Singh and Sinha, 1940, *Science and Culture*, **6**, 243
Khastgir and Chakravarty, 1938, *Phil Mag*, **25**, 793
Khastgir and Sen Gupta, 1936, *Phil. Mag*, **22**, 265
Rahman and Muhi, 1944, *Ind. Jour Phys.*, **18**
Ratcliffe and White, 1930, *Phil Mag.*, **10**, 667
Smith-Rose, 1938, *Proc. Roy. Soc A.*, **111**, 359
Smith-Rose and McPetrie, 1932, *Proc. Phys Soc.*, **44**, 1933, *Proc. Phys. Soc*, **45**
White, 1931, *Proc Camb. Phil. Soc.*, **27**, 268

ULTRA VIOLET BAND SYSTEMS OF THE MERCURY IODIDE MOLECULE—PART II

By V. RAMAKRISHNA RAO and K. R. RAO*

(Plate VI)

ABSTRACT. Continuing the study of the bands of the mercury iodide molecule three new systems are obtained between λ 2530 and λ 2320 which are designated as F_1, F_2 and F_3 systems. Vibrational analysis is given for the F_1 and F_3 systems and regularities are presented among the bands of the F_2 system. F_1, F_3, C and D systems are found to have a common final state which is presumably the ground state of the HgI molecule.

INTRODUCTION

In Part I of these investigations, Rao, Sastry and Krishnamurty (1944) showed that the band spectrum of the mercury iodide molecule consists of seven different systems (designated by them as B, C, D, E, F, G and H). Of these, analysis is known definitely only for the two systems C and D. These were shown to have a common ground state with vibrational constants $\omega''=125.8$ and $\chi''\omega''=1.09$ cms^{-1}, which are in keeping with the corresponding values for the other halides of mercury, as seen from Table I below.

TABLE I

	ω''	$\chi''\omega''$
HgF	490.8	4.05
HgCl	293.4	1.82
HgBr	186.3	0.98
HgI	125.8	1.09

It was also suggested that the two systems form the components of an electronic transition $^2\Pi-{}^2\Sigma$ with the $^2\Pi$ interval 3538 cms^{-1}, being approximately equal to the atomic coupling constant for the 6p electron giving the 6s 6p ^{3}P state of the mercury atom. Further work on these band systems has been undertaken by the authors in order to interpret the remaining band systems. In the course of this attempt, new band systems have been observed which are considered as due the mercury iodide molecule. The purpose of this paper is to report the data and the analysis, as far as is obtained, of the new bands.† A consideration of the entire band systems will be taken up in another communication.

* Fellow of the Indian Physical Society.

† A brief report appeared in Curr. Sc. 1 1945, 14, 319).

EXPERIMENTAL

The bands are excited, in an ordinary H-form pyrex discharge tube, by a transformer, as described previously in Part I. In addition to this source, the emission bands are obtained also by the use of a specially constructed valve oscillator of low power designed to give a frequency of one to five megacyles. The substance is heated in a quartz tube with an end-on sealed quartz window for observation and evacuated continuously by a Cenco Hyvac pump. The electrodes are external and the distance between them is varied. When the discharge is bright bluish violet, the mercury iodide bands are emitted intensely. Exposures of half an hour to six hours are given depending on the dispersion of the instrument used.

RESULTS

Besides the seven previously known systems, three systems are newly obtained on our plates. They occur in the spectral region between the F and G systems and therefore designated as F_1, F_2, and F_3. They are shown in Plate VI.

The F_1 system consists of about twenty red-degraded bands, some of which have intense and sharp edges. The system extends over the short region λ 2532 – 2455 just at the violet end of the F system, with which there may be a slight overlapping. The wave lengths of the bands and the wave numbers are shown in Table II. The large intensity of two of the bands λ 2521 and λ 2513 is probably due to the partial superposition by the strong and diffuse bands of the Hg_2^+ molecule at λ 2525 and λ 2518 which might also have obscured some of the weaker bands of the F_1 system.

The F_2 system consists of a succession of closely spaced bands degraded to the red with the interval between successive bands diminishing towards the longer wave lengths. About thirty bands of this system have been measured; several other fainter bands could be seen but not measured.

The F_3 system is small, comprising of about fifteen bands, diffuse in appearance but mostly headless. It resembles the brief system of mercury bromide reported by Rao and Ramachandra Rao (1944). As in the F_1 system there seems to be a partial overlapping of the bands at λ 2341 and λ 2337 by those of Hg_2 at λ2342 and λ2337. Tables III and IV present the band head data of systems F_2 and F_3 respectively.

As the bands constituting these three systems have not been recorded by any of the previous investigators, particular care was taken to establish by systematic experiments that they are not due to any possible impurity in the source or to other molecules containing mercury or iodine. Various spectra are taken and by comparison, the assignment of the systems to HgI is considered to have been confirmed from the experimental standpoint.

The vibrational scheme obtained for the F_1 system is shown in Table V in the usual diagonal array. A dozen bands have been included in the scheme, comprising nearly all the intense heads. Classification is not suggested

TABLE II—F_1 System

Wave length.	Wave Number.	Intensity.	Classification.
2532.83	39470.7	6	1,6
2530.08	39512 5	3	2,7
2528 50	39537.3	3	0,4
2526.21	39573.1	3	1,5
2523.37	39617.6	(00)	—
2521.13	39652 8	7	0,3
2519 01	39686 9	3	1,4
2517.52	39709.7	3	2,5
2513.61	39771.4	8	0,2
2510 22	39825.3	4	2,4
2508 56	39851.5	2	3,5
2 c6 28	39886.2	5	4,6
2500.87	39974.1	2	5,7
2487 97	40181.3	1	—
2485 94	40214 1	0	—
2476 76	40363.1	(00)	—
2475.23	40387.1	0	-
2470.47	40465.9	0	—
2460.03	40638 6	0	—
2454.97	40721.5	(00)	—

TABLE III F_2 System.

Wave Length	Wave Number	Intensity	Classification
2380.99	41986.3	0	
2381.15	41983.7	0	
2382.30	41963.4	1	
2385.13	41913.6	1	
2387.57	41870.3	1	
2388.77	41849 8	1	
2390.95	41816.2	1	(5,v″)
2393.94	41759.4	1	(4,v″)
2396.37	41717.1	1	(3,v″)
2397.40	41699.1	1	(5,v″+1)
2393.68	41677.9	0	(2,v″)
2400.51	41645.0	0	(4,v″+1)
2401.91	41620.9	2	
2403.42	41594.7	3	(3,v″+1)
2404.40	4 577.8	3	(5,v″+2)
2405.76	41554.3	3	(2,v″+1)
2406.71	41538.0	2	
2407 31	41527.3	3	(4,v″+2)
2408.29	41510.6	2	
2410.22	41477.4	4	(3,v″+2)
2412.63	41436.0	3	(2,v″+2)
2414.78	41399.1	4	(1,v″+2)
2416.74	41365.5	3	(3.v″+3)
2419.09	41325.3	4	(2,v″+3)
2421 12	41290.7	5	(1,v″+3)
2423.37	41252.3	3	(0,v″+3)
2424.81	41227.8	4	(2,v″+4)
2426 84	41193.3	2	(1,v″+4)
2428.83	41159.7	2	(0.v″+4)
2430 50	41131.3	2	(2,v″+5)
2432.50	41097 5	2	(1,v″+5)
2433 96	41072.8	2	(0,v″+5)
2435.85	41041.0	2	(2,v″+6)
2437.08	41020.2	2	

TABLE IV. F_3 SYSTEM

Wave Length	Wave Number	Intensity	Classification
2347.36	42587.3	00	
2346.35	42605.4	00	2,11
2345.49	42621.8	0	0,8
2344.51	42639.9	2	3,12
2342.56	42674.5	2	1,9
2340.92†	42705.5	7bd	2,10
2339.53	42731.1	1	0,7
2336.92†	42778.6	5bd	1,8
2335 64	42802,4	2	2,9
2334.68	42818.9	3	3,10
2333.60	42839.1	2	0,6
2332.23*	42864.8	0	
2331.13	42885.0	2	1,7
2329.95	42905 3	4	2,8
2326 76±	42964.3	6	
2321.97±	43053.1	5	

*Probaly due to Hg_2 bands
†Superposed by Hg_2 bands
± Broad and complex

for eight weak bands towards the violet end ; they possibly represent heads involving higher (v', v'') values. The analysis shows no bands with $v''=0$ or 1 ; the values of $\Delta G''(v)=118{\cdot}6$, 115,5, 114.7 etc., have suggested this particular vibrational numbering, beginning with $v''=2$. Such a feature might be expected in band systems characteristic of a molecule of the type of mercury iodide. A justification of the assignment is seen from the following formula calculated for the bands on the basis of this numbering :—

$$\nu=4000.5+[153.8(v'+\tfrac{1}{2})-2.0(v'+\tfrac{1}{2})^2]$$
$$-[124\ 5(v''+\tfrac{1}{2})-0.98(v''+\tfrac{1}{2})^2]$$

The constants for the final state $\omega''=124{\cdot}5$ and $\chi''\omega''=0.98$ agree closely with corresponding values for the C and D systems.

The structure of the F_3 system is shown in Table VI. Of the sixteen bands comprising this system all the strong ones with the exception of two have entered into the scheme. The overlapping by Hg_2 bands accounts probably for the abnormal intensity of the bands at λ2341 and λ 2337 and for the divergencies in the $\Delta G''(v)$ involving these two bands, chiefly λ 2341. The strong unclassified bands at λ 2327 and λ 2322 may be complexes of several close bands, which could not be resolved. λ 2332 (o) may be due to Hg_2. As in the F_1 system, here too the v'' values assigned to the bands begin with higher values ; it is as high as $v''=6$. The following formula,

$$\nu=43521.5+[172.4(v'+\tfrac{1}{2})-10.5(v'+\tfrac{1}{2})^2]$$
$$-[124.6(v''+\tfrac{1}{2})-1.1(v''+\tfrac{1}{2})^2]$$

giving $\omega''=124.6$ and $\chi''\omega''=1.1$ is considered to be in support of the

TABLE V

Vibrational analysis of the F_1 system.

v''/v'	2	3	4	5	6	7	$\Delta G'(v)$
0	39771.4 (6)	39652.8 (5)	39437.3(1)				149.6
1			39686.9(1)	39573.1(1)	39470,7(4)		137.5
2			39825.3(2)	39709.7(1)		39512.5(1)	141.8
3				39851.5(0)			
4					39886.2(3)		
5						39974.1(0)	
$\Delta G''(v)$	118.6		115.5	114.7	102.4		

TABLE VI

Vibrational analysis of the F_2 system.

v''/v'	6	7	8	9	10	11	12	$\Delta G'(v)$
0	42839.1(2)	42731.1(1)	42621.8(0)					155.8
1		42885.0(2)	42778.6(5)	4274.5(2)				127.3
2			42905.3(4)	42802.4(0)	42705.5(7)	42605.5(00)		113.4
3					42818.9(3)		42639.9(2)	
$\Delta G(v'')$		108.0	107 8	103.5	96.9	100.1		

Table VII—Regularities in the band heads of the F_2 system

v''/v'	v''	$v''+1$	$v''+2$	$v''+3$	$v''+4$	$v''+5$	$v''+6$	$\Delta G'(v)$
0				41252 3(3)	41159.7(2)	41072.8(2)		32 2
2			41399.1(4)	41200 7(5)	41193.3(2)	41097.5(2)		33,9
2	41677 9(0)	41554,3(3)	41436.0(3)	41225.3(4)	41227 8(4)	41131,3(2)	41041 0(2)	40.3
3	41717.1(1)	41594.7(3)	41477.4(4)	41365.5(3)				47 5
4	41759.4(1)	41645.0(0)	41527 3(3)					53.8
5	31816.2(1)	41699.1(1)	41577.8(0)					
$\Delta G''(v)$		121.9	118.7	110.3	95.8	93.1	90.3	

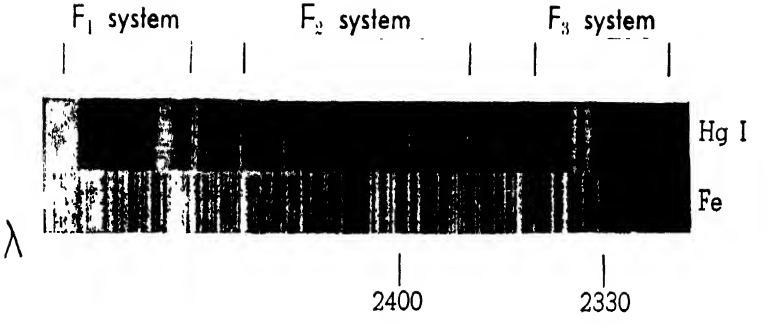

Fig. A. New Bands of the HgI molecule.

assignment. On the basis of this analysis the system F_1 and F_3 as well as C and D have a common final electronic state, which is presumably the ground $^2\Sigma$ state of the HgI molecule.

The F_2 system presents a different appearance altogether from the remaining bands, as can be seen from the reproduction of the bands in Plate VII. The authors have not succeeded in confidently arriving at a vibrational analysis of this system. Out of several attempts, the arrangement shown in Table (VII) may be pointed out. The order of the $\Delta G''(v)$ values agrees with the corresponding values for the classified system. But the second differences leading to χ'' ω'' are not consistent. The $\Delta G''(v)$ values are found to be increasing. The bands themselves have fairly sharp edges compared to the other system and large errors in measurement are not expected. The suggested v',v'' numbering must be treated as only tentative. No formula is therefore calculated for this system. Further work on this and the remaining systems is in progress and a discussion of all these will be presented in succeeding parts of the investigations.

ACKNOWLEDGMENT

The authors are indebted to Mr. C. Rama Sastry for the high frequency oscillator set and much help in the experimental work.

PHYSICS DEPT.
ANDHRA UNIVERSITY
WALTAIR

REFERENCES

(1) Rao, Sastry and Krishnamurthy, (1944) *Ind. Jour. Phys.*, **18**, 323.
(2) Rao and Ramachandra Rao, (1944) *Ind. Jour. Phys.* **18**, 281.

X-RAY INVESTIGATION OF THE PARA-DIHALOGEN DERIVATIVES OF DIPHENYL

By JAGATTARAN DHAR

ABSTRACT. The isomorphous crystals of 4-4′-difluoro-diphenyl, 4-4′-dichloro-diphenyl and 4-4′-dibromo-diphenyl have been studied by X-ray methods. The dimensions of the unit cell have been found in each case. They point to the presence of 8 molecules per unit cell. The crystal of 4-4′-dichloro-diphenyl has been further studied by the moving film camera. The absence of reflections (oko) in odd orders suggests that this crystal belongs to the space group C_{2h}^5 ($p\ 2_1/m$) of the monoclinic holohedral class.

INTRODUCTION

In diphenyl (Dhar, 1932) as well as in terphenyl (Picket, 1933) and quaterphenyl (Picket, 1926) the two benzene rings lie in a plane and are linearly extended. In dibenzyl (Dhar, 1934; Robertson, 1934 and 1935) due to the introduction of the two aliphatic carbon atoms the rings deviate appreciably from the mean plane on opposite sides. In striking contrast with the structure of dibenzyl, the benzene rings have been found by Robertson to be almost coplanar in stilbene (Robertson and Woodward, 1937).

It would be of interest to find if the simple substitution of some of the hydrogen atoms in diphenyl would affect its planar and linearly extended structure. For this purpose 4-4′ disubstituted compounds of diphenyl would naturally be the simplest and among them the difluoro, dichloro- and dibromo-derivatives form a good series of isomorphous monoclinic crystals. They have, therefore, been chosen for the X-ray study. It is proposed to give in this paper an account of the preliminary investigation made with the crystals of these substances.

UNIT CELL AND DIMENSIONS

As reported in Groth's Chemische Krystallographie (1905) all the crystals belong to the monoclinic prismatic class. Crystals of 4-4′ dichloro-diphenyl and 4-4′ dibromo-diphenyl have been grown out of the solution of alcohol and benzene by slow evaporation. They have been obtained as prisms elongated along the *c*-axis with a (100) face bounded by q (011) and seldom r (101) faces. Sufficiently good single crystals of 4-4′ difluoro-diphenyl could not be obtained after several trials. Consequently for this crystal only Debye-Sherrer powder diagram was taken. The other two crystals were studied by the rotating crystal method. The copper K-radiation was used. It was filtered through a nickel foil whenever necessary.

The dimensions of the unit cells of three crystals are given in the following table :—

TABLE I

Crystal	Sp. gr.	'a'	'b'	'c'	β	Number of Molecules per unit-cell
4-4′ Difluoro-diphenyl	1.361	14.83 Å	13.30 Å	9.45 Å	96°8′	8
4-4′ Dichloro-diphenyl	1.439	15.94 Å	13.61 Å	9.79 Å	96°48′	8
4-4′ Dibromo-diphenyl	1.897	15.80 Å	14.09 Å	9.82 Å	94°30′	8

The data for the dichloro- and the dibromo- derivatives were obtained from the rotation pictures, assuming the values of β as given in Groth's Kristallographie. The values of β were later on confirmed from the measured spacings of some axial planes identified in the rotation photographs. Specific gravity values in column 2 have been taken from the Groth's book.

For the difluoro-derivative for which only the powder photopraph was taken the dimensions of the unit cell cannot, of course, be uniquely determined. Since it is isomorphous with the other two crystals, the different spacings observed could be identified by comparing them with the latter crystals, The observed spacings for the difluoro derivative and those calculated on the basis of the cell dimensions given in Table I are given below :

TABLE II

Powder photograph of 4-4′-difluoro-diphenyl (with nickel filter)

Serial No.	Observed (Bragg angle)	Spacing observed	Spacing calculated	Planes assigned	Remarks on intensity
1	9°26′	4.695 Å	(4.695 Å)	002	v. s.
2	10°31′	4.216 Å	4.17 Å	202	s.
3	12°03′	3.686 Å	(3.686 Å)	4[illegible]	v.s.
4	14°25′	3.090 Å	3.13 Å	003	m.
5	16°11′	2.777 Å	2.76 Å	340	w.
6	17°49′	2 515 Å	2.46 Å	600	w.
7	20°19′	2.217 Å	(2.217 Å)	060	m.
	23°28′	1.932 Å	...	...	v.w.

For a detailed study of the crystal structure, 4-4′-difluoro-diphenyl would have been the most suitable among the three isomorphous derivatives of diphenyl because of its least absorption of X-rays. But unfortunately sufficiently good single crystals of difluoro-derivatives were not available. So 4-4′-dichloro-diphenyl, being next in order of absorption was chosen and studied in detail.

WEISSENBERG PHOTOGRAPHS AND THE INDEXING OF THE REFLECTED SPOTS

Weissenberg photographs of the zero layerline of 4-4′-dichlorodiphenyl were taken adout the '*b*' and '*c*' axes. In these photographs reflexions from the axial and prism planes only are present. In order to study the general planes another Weissenberg photograph of the first layerline of the crystal about the '*b*' axis was taken.

To identify the reflecting planes to which the spots are due in the zero layerline of the Weissenberg photograph the most straightforward method which is indeed an adaptation of the method described by Bernal (1927) is used. The perpendicular distance ξ_ω from the central line in the diagram for each spot is read and then converted into the ξ value with the help of the relation

$$\frac{\xi_\omega}{2\pi r_F} = \frac{\theta}{180} \qquad \ldots \quad (1)$$

$$\xi = 2 \sin\theta \qquad \ldots \quad (2)$$

The ξ value of each plane can also be calculated from the reciprocal lattice canstants of the crystal as for example for rotation about the '*c*' axis of the crystal.

$$\xi = \{k^2 b^{*2} + (ha^* + lc^* cos\beta^*)^2\}^{\frac{1}{2}}$$

The comparision between the observed and calculated ξ values makes the assignment of the indices to the planes of the respective spots possible.

For the first layerline weissenberg diagram about the '*b*' axis, the experimental values of Bragg angle θ were deduced by measurement of ξ_ω values for the various spots from (1). They were then compared with the calculated values of the Bragg angle from the relation

$$\mathrm{Sin}^2\theta_{hll} = \frac{\lambda^2}{4\sin^2\beta}\left[\frac{h^2}{a^2} + \frac{l^2}{c^2} - \frac{2hl}{ac}\cos\beta + \frac{\sin^2\beta}{b^2}\right]$$

Where the terms have the usual significance.

A chart has also been prepared on the basis of Wooster and Wooster's (1933) method, corelating the Bragg angle of reflexion θ instead of ξ_ω against the angle of rotation of the crystal and the two series of curves are drawn.

The photographic film is laid over the graphical chart so drawn and the correct assignment of the indices is confirmed as the spots all lie on the intersections of the two series of curves. For the zero layerline Weissenberg diagram about the '*b*' axis, one series of curves runs with (n o l) and another with (h o n) where n is a constant along any one curve while h or l changes by steps of unity.

The Weissenberg diagrams are in this way deciphered and the reflecting planes so obtained are entered in the following Tables III, IV and V.

TABLE III

Weissenberg photograph of the zero layerline of 4-4'-dichloro-diphenyl crystal about '*c*' axis.

Axial Planes	Prism Planes	Prism Planes	Prism Planes
400 (v. s.)	140 (v. s.)	340 (s)	530 (w.m.)
600 (w)	180 (m)	380 (w)	540 (w.m.)
800 (m)	250 (m)	410 (m)	610 (w.m.)
040 (m)	270 (s)	430 (w.m.)	760 (w)
080 (w m.)	310 (m)	440 (m)	810 (w)
0(10)0 (v.w)	330 (w)	510 (w.m.)	
0(12)0 (w m.)			

TABLE IV

Weissenberg photograph of the zero layerline of 4-4'-dichloro-diphenyl about '*b*' axis.

Axial Planes	Prism Planes	Prism Planes
400 (s)	102 (v.s.)	$40\bar{1}$ (v.w.)
600 (v.w.)	$10\bar{3}$ (s)	402 (s)
800 (m)	106 (w.m.)	$60\bar{2}$ (m)
(12)00 (w)	201 (m)	$60\bar{4}$ (w)
(16)00 (w)	204 (m)	$80\bar{2}$ (w)
002 (v w.)	$20\bar{4}$ (w)	$(10)0\bar{3}$(v.w.)
004 (w)	302 (s)	$(10)0\bar{5}$(v.w)
	306 (w)	

TABLE V

Weissenberg photograph of the 1st layer-line of 4-4′-dichloro-diphenyl about '*b*' axis.

Prism Planes	General Planes	General Planes	General Planes
$01\bar{6}$ (w)	$11\bar{2}$ (w.m.)	314 (w.m.)	$71\bar{2}$ (v.w)
$01\bar{7}$ (w)	$11\bar{3}$ (w.m.)	$31\bar{5}$ (w.m.)	713 (w)
310 (w)	$11\bar{4}$ (w)	$\bar{3}1\bar{5}$ (v.w.)	714 (v w)
510 (s)	$11\bar{5}$ (v.w.)	511 (w)	$71\bar{4}$ (w)
710 (v.w.)	$\bar{1}1\bar{8}$ (v,w.)	$51\bar{1}$ (v w.)	811 (v.w.)
810 (w)	$\bar{2}1\bar{4}$ (w)	$51\bar{2}$ (s)	$81\bar{1}$ (w)
(14)10 (v.w.)	$\bar{2}1\bar{9}$ (w)	$51\bar{3}$ (w)	812 (w)
	$21\bar{6}$ (v.w.)	514 (w m.)	$81\bar{2}$ (w m.)
	311 (w)	$51\bar{4}$ (w)	$81\bar{3}$ (w)
	212 (w m.)	$51\bar{6}$ (v.w.)	(10)11 (w)
	$31\bar{2}$ (v.w.)	$51\bar{8}$ (v.w.)	(10)14 (w)
	313 (s)	711 (v w.)	(12)12 v w.)
	$31\bar{3}$ (s)	$71\bar{1}$ (v.w.)	(14)11 (v.w)

It is evident from the above tables that all planes of the type (oko) are absent when k is odd. In addition, planes of the type (hoo) as well as (ool) have also been found to be absent when h or l is odd. But because the latter planes are not symmetry planes their absence is not significant and is regarded as accidental. The crystal of 4-4′-dichlorodiphenyl is consequently assigned to the spacegroup C_{2h}^{2} ($P2_1/m$) of the monoclinic holohedral class.

The study of the 4-4′-dibromo-diphenyl crystal by the moving-film camera is in progress.

ACKNOWLEDGEMENT

The author wishes to express his best thanks to Dr C. Forster, Ph.D, Principal, Indian School of Mines, and to Prof. K. Banerjee, D.Sc. of the Indian Association for the Cultivation of Science, Calcutta for their keen interest in this work.

INDIAN SCHOOL OF MINES,
DHANBAD

REFERENCES

Bernal, J. D., (1927), *Proc. Roy. Soc.* A, **113**, 117.
Dhar, J., (1932), *Ind. J. Phys.*, **7**, 43.
Dhar, J , (1934), *Ind. J. Phys.*, **9**, 1.
Groth, (1905), *Chem. Kryst.*, **5**, 8.
Pickett, L. W., (1933), *Nature*, **131**, 513, and (1933), *Proc. Roy. Soc.* A, **142** 332.
Pickett, L. W , (1936), *Jour. Amer. Chem., Soc.* **58**, 2299.
Robertson, J M., (1934), *Proc. Roy. Soc.* A, **146**, 473.
(1935), *Proc Roy. Soc.* A, **150**, 348.
Robertson, J. M. and Woodward, I., (1937), *Proc. Roy. Soc.* A, **162**, 568.
Wooster, W. A and Wooster, N. (1933), *Zeit. f. Kryst.* A, **84**, 327.

The following special publications of the Indian Association for the Cultivation of Science, 210, Bowbazar Street, Calcutta, are available at the prices shown against each of them :—

No.	Subject	Author	Price Rs. A. P.
III	Methods in Scientific Research	Sir E. J. Russell	0 6 0
IV	The Origin of the Planets	Sir James H. Jeans	0 6 0
V	Separation of Isotopes	Prof. F. W. Aston	0 6 0
VI	Garnets and their Role in Nature.	Sir Lewis L. Fermor	2 8 0
VII (1)	The Royal Botanic Gardens, Kew.	Sir Arthur Hill	1 8 0
(2)	Studies in the Germination of Seeds.	,,	
VIII	Interatomic Forces	Prof. J. E. Lennard-Jones	1 8 0
IX	The Educational Aims and Practices of the California Institute of Technology	R. A. Millikan	0 6 0
X	Active Nitrogen A New Theory	Prof. S. K. Mitra	2 8 0

A discount of 25% is allowed to Booksellers and Agents.

RATES OF ADVERTISEMENTS

Third page of cover	...	Rs. 25, full page
do. do.	...	,, 15, half page
do. do.	...	,, 8, quarter page
Other pages	...	,, 19, full page
do.	...	,, 11, half page
do.	...	,, 6/8, quarter page

EMISSION BANDS OF THE PO MOLECULE*

By R. RAMANADHAM, G. V. S. RAMACHANDRA RAO AND C. RAMASASTRY

(*Received for publication, October 12, 1946*)

(Plate VIII)

ABSTRACT. In the course of an investigation on the bands of the P_2 molecule, excited under different conditions, the characteristic bands, ascribed by previous investigators to the PO molecule, in the region λ 2600 and λ 3300, are found to be strongly emitted in a wide open heavy current arc between graphite poles containing phosphorus pentoxide. The bands at λ 3300, which are not yet analysed, are partly red and violet degraded. Several attempts to include all the heads into one system having failed, the red-degraded bands are analysed into one vibrational system and the violet-degraded bands into another system, suggested to be due respectively to the electronic transitions $^2\Sigma - ^2\Pi$ and $^2\Pi - ^2\Pi$ with a common lower $^2\Pi$ state, same as the ground $^2\Pi$ state of λ 2600 system, established by Ghosh and Ball and by Sen Gupta.

INTRODUCTION

Band spectra of the diatomic oxide molecules of Group V-b elements have been extensively studied and our knowledge of these has been much extended in recent years (Connelly, 1934 ; Sen Gupta, 1939, 1944, 1945). Four systems (γ, β, δ and ε) are analysed in NO, one in PO, two systems (A and B) in AsO, three (A, B and C) in SbO, and one in BiO molecule. In all these homologous molecules it has been suggested that the lower ground state is a $^2\Pi$ and the upper is either a $^2\Sigma$ or a $^2\Pi$, giving rise to doublet systems of bands with the $^2\Pi$ interval, increasing from 121 cm^{-1} for NO to 2272 cm^{-1} for SbO. Although the main features of these spectra are known, it is obvious that for a complete correlation there is need for further investigation, particularly of the bands of the oxides of phosphorus and of bismuth.

The early work on the PO bands was summarised by Petrikaln (1928) who investigated these bands in emission and in absorption and reported the existence of two characteristic systems for this molecule, one at λ 2600 and another in the region λ 3300. Ghosh and Ball (1931), however, were the first to report a complete vibrational analysis of the more refrangible of these two systems. It was shown to consist of double double-headed bands analogous to the γ bands of nitric oxide, with well-marked sequences and represented by the vibrational constants,

$\nu_e = 40264.7$ cm^{-1}	$\omega' = 1391.0$	$x'\omega' = 7.65$
40488.5 cm^{-1}	$\omega'' = 1230.6$	$x''\omega'' = 6.52$

The rotational structure was investigated by Sen Gupta (1935) who established the electronic transition of this system as $^2\Sigma - ^2\Pi_i$ with the $^2\Pi$ interval

* Communicated by Prof K. R. Rao

equal to 224 cm^{-1}. But the less refrangible system at λ 3300 remained as yet unanalysed. Curry, Herzberg and Herzberg (1933) recorded the following molecular constants,

$$\nu_0 = 30584, \qquad \omega_0' = 1151, \qquad \omega_0'' = 1228,$$

but no detailed analysis has, as far as the authors are aware, been published till now. Even the published wave-length data of the bands does not appear to be definite; the measurements made by Petrikaln do not correspond well with those by Geuter. In view of this and the peculiar appearance of the bands a study of this system was undertaken.

EXPERIMENTAL

The experimental work on the bands formed part of an earlier investigation on the P_2 bands (N. Rao, 1943) in the course of which several different sources of exciting the bands were utilised. The PO bands were found to be strongly emitted in a wide-open heavy current arc between carbon electrodes fed by phosphorus pentoxide and absent altogether in the ordinary transformer discharge through P_2O_5, which only gave bands due to oxygen, phosphorus and CO or NO. The arc consisted of a lower positive graphite electrode about 1.5 cm. in diameter in which a cylindrical hole 10 mm. × 7 mm. was drilled, and the phosphorus pentoxide powder transferred directly into it. The upper graphite electrode was about 6 mm. in diameter. The arc fed by a current of 7 to 8 amperes was drawn out into a long flame, the central portion of which was focussed on the slit of the spectrograph. Preliminary photographs before introducing P_2O_5, taken with the graphite rods alone under identical conditions, served as comparision spectra. A well-developed band system was obtained in the region from λ 3580 to λ 3150, the most peculiar feature of which is that some of the bands were degraded to the red and others to the violet. This feature was recorded also by Petrikaln who photographed the bands in absorption using specially prepared phosphorus trioxide.

Plate VIII is a reproduction of the spectra obtained with a Hilger quartz Littrow spectrograph type E_1, with and without phosphorus pentoxide in the electrodes and iron arc comparison. The exposure was for about half-an-hour.

The wavelengths of all the band heads in order are recorded in Table I; they closely agree with the published measurements due to Geuter. The letter V or R in the last column indicates the direction of degradation (violet or red) of the band.

ANALYSIS

As mentioned earlier, each of the diatomic oxide molecules, homologous with PO, gives band systems due to transitions into a $^2\Pi$ state from one or more upper states which may be either a $^2\Sigma$ or a $^2\Pi$. The PO bands under

TABLE I

Bands of PO molecule

Wave length	Intensity	Wave number	Classification	
			Violet-degraded system	Red-degraded system
3579.4	1	27930	V (3, 5)	
3578.6	1	27936	V	
3567 9	1	28019	V (2. 4)	
3563 2	1	28057	V	
3562 6	1	28061	V	
3550.2	0	28159	V (0, 2)	
3542 6	1	28220	V	
3541.9	1	28225	V	
3539 0	1	28249	V (2, 4)	
3530.1	0	28320	V (1, 3)	
3521.2	1	28391	V (0, 2)	
3478.6	1	28739		R
3470 8	1	28804		R (3, 4)
3460 1	2	28893		R (1, 2) ?
3450 9	1	28969		R (0, 1)
3442.4	1	29041		R
3431.7	1	29132		R (1, 2)?
3424.4	3	29194	V (2, 3)	
3413.9	3	29284	V (1, 2)	
3409.7	3	29320	V (3, 4)	
3405 7	3	29354	V (0, 1)	
3397.8	3	29422	V (2, 3)	
3396 4	2	29435	V	
3387.8	3	29509	V (1, 2)	
3386.3	2	29522	V	
3379.8	3	29579	V (0, 1)	
3366.1	3	19647		R
3362.5	2	29731		R (4, 4)
3360.8	2	29746		R (4, 4)
3346.3	3	29875		R (2, 2)
3340 7	2	29925		R (3, 3)
3339.7	2	29934		R (3, 3)
3328.4	3	30036		R (1, 1)
3321.0	3	30103		R (2,2)
3319.8	2	30114		R (2, 2)
3312.0	3	30185		R (0, 0)
3303.2	2	30265		R (1, 1)
3301.1	2	30284		R (1, 1)
3296.5	3	30327		R (10, 8)
3286.0	3	30423		R (0, 0)
3280.4	1	30475		R (5, 4)
3270.4	2	30569	V (0, 0)	
3269.3	2	30579		R (10, 8)
3266.8	1	30602	V (2, 2)	
3255.2	2	30711	V (1, 1)	
3253.6	2	30726		R (4, 3)
3246.2	3	30796	V (0, 0)	
3238.6	1	30869		R (3, 2)
3217.4	1	31027		R (2, 1)
3204.3	1	31199		R (7, 5)
3198.9	1	31252		R (1, 0)
3198.2	1	31259		
3188.2	2	31357		R (6, 4)
3180.7	2	31431		R (7, 5)
3173.4	2	31503		R (1, 0)
3164.9	1	31587		R (6, 4)
3149.8	2	31739		R (9, 6)

investigation may be expected to be due to a similar electronic transition. If they all belong to one system, say $^2\Sigma - {}^2\Pi$, they must consist of double double-headed bands with the doublet width equal to 224 cms^{-1}. Examination of the bands has, no doubt, revealed several heads with the wave-number intervals either equal to or not far from the value of 224 cms^{-1}. But not all the component heads show the doublet structure: some of these are close doublets and others are not. This has led to the suspicion that the bands under investigation may comprise of two overlapping systems. Another peculiar feature leading to the same view is that some of the bands are red-degraded (mostly those which show close doublet structure) and others are violet-degraded, although instances are known of band systems where, in one and the same system, there is a change in the direction of degradation of the bands. The previous investigators, *e.g.* Petrikaln, as also Curry, Herzberg and Herzberg seem to have attempted the analysis of the PO bands on the supposition that there is only one system and the latter authors have suggested a possible $^2\Pi - {}^2\Pi$ transition. The first attempts of the authors were to examine the possibility of including all the band heads into one and the same system either a $^2\Sigma - {}^2\Pi$ or a $^2\Pi - {}^2\Pi$ (the latter transition possibly giving rise to single-headed bands). The constants recorded by Curry, Herzberg and Herzberg were also considered and on the basis of these values the possibility of fitting all the bands into one system was studied. All these attempts having failed, recourse was taken to the alternative possibility of regarding the bands as belonging to two overlapping systems. The analysis thus arrived at is shown in Tables II and III.

TABLE II

Vibrational Analysis of the PO Bands. (Red-degraded system.) (System A.)

		0	1	2	3	4	5
0	Q	30423(3)					
	Q	30185(3)	28969(1)				
1	R	...	30284(2)				
	Q	31503(2)	30265(3)				
	Q	31252(1)	30036(3)				
2	R		...	30114(1)			
	Q		...	30103(3)			
	Q		31072(1)	29875(3)			
3	R			...	29934(2)		
	Q			...	29925(2)	28804(1)	
	Q			30869(1)	...	...	
4	R				...	29746(2)	
	Q				...	29731(2)	
	Q				30726(2)	...	
5	Q					...	
	Q					30475(1)	
6	Q					31587(1)	
	Q					31557(2)	
7	Q						31431(2)
	Q						31199(1)

(a) Iron Arc (b) P_2O_5 in Carbon Arc showing PO bands (c) Carbon Arc

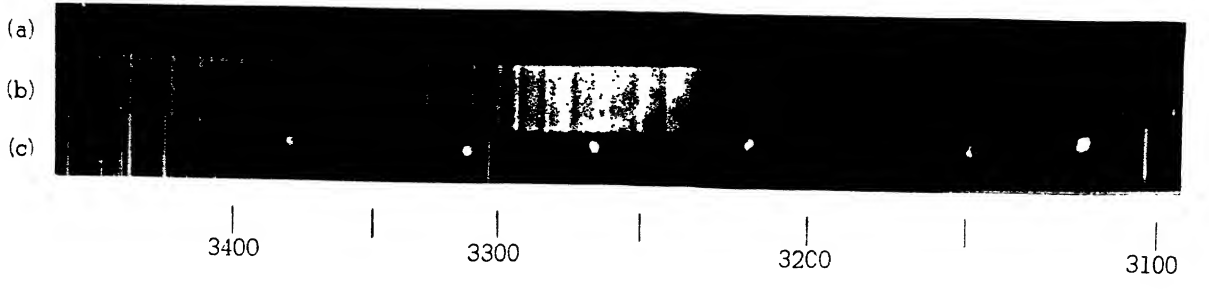

PO Bands

TABLE III

Vibrational Analysis of the PO Bands. (Violet-degraded system.) (System B.)

	0	1	2	3	4	5
0	30569(2) 30796(3)	29354(3) 29579(3)	28159(0) 28391(1)			
1		... 30711(2)	29284(3) 29509(3)	28320(0)		
2			... 30602(1)	29194(3) 29422(3)	28019(1) 28249(1)	
2					... 29320(3)	27930(1) ...

All the red-degraded bands form one system. The Q head interval is nearly 224 cms^{-1} and in most cases the component R heads are also detected. The electronic transition is probably $^2\Sigma - {}^2\Pi$. The bands are approximately represented by the formula

$$\nu = 30260.8 + [1094(v' + \tfrac{1}{2}) - 14.5(v'' + \tfrac{1}{2})^2] - [1234(v'' + \tfrac{1}{2}) - 9.5(v'' + \tfrac{1}{2})^2]$$

The violet-degraded bands are all arranged into a second system. The bands are single-headed. They are perhaps due to the transition $^2\Pi - {}^2\Pi$ and may be represented approximately by the formula

$$\nu = 30606.5 + [1151.9(v' + \tfrac{1}{2}) - 14.2(v' + \tfrac{1}{2})^2] - [1224.(v'' + \tfrac{1}{2}) - 6.5(v'' + \tfrac{1}{2})^2]$$

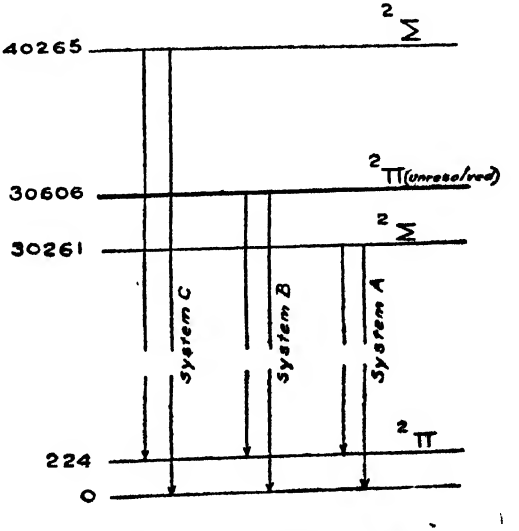

Electronic transitions in PO bands.

FIG. 1

If the analysis proves correct, an interesting feature of this system, which deserves mention, is that while the bands themselves are degraded to the violet, the sequence degradation is towards the red.

The lower state for these two band systems is considered to be identical with the lower state of the most refrangible system which was analysed by Ghosh and Ball. There are thus three identified systems among the PO bands which may be designated as A, B, and C, in the order of diminishing wavelength and the electronic transitions concerned, may be represented diagramatically as in the Fig. 1.

PHYSICS DEPARTMENT,
ANDHRA UNIVERSITY,
WALTAIR

REFERENCES

Connelly, 1934, *Proc. Phy. Soc. (Lond.)*, **46**, 790.
Curry, Herzberg and Herzberg, 1933, *Zeits. f. Phys.*, **86**, 364.
Ghosh and Ball, 1931, *Zeits. f. Phys.*, **71**, 362.
Pearse and Gaydon, "Identification of Molecular Spectra," p. 162.
Petrikaln, 1928, *Zeits. f. Phys.*, **51**, 395.
Rao, Narahari, 1943, *Ind. Jour. Phys.*, **17**, 135 and 149.
Sen Gupta, 1935, *Proc. Phy. Soc. (Lond.)*, **47**, 247.
Sen Gupta, *Ind. Jour Phys.*, 1939, **13**, 145; 1944, **17**, 216; 1945, **18**, 183.

SENSIVITY TESTS OF SOME RADIO RECEIVERS FROM 1 Mc/s TO 20 Mc/s

By I. L. CHAKRAVARTY and S. R. KHASTGIR*

(*Received for publication, September 12, 1946*)

ABSTRACT. Sensitivity tests were made for five different radio receivers (Philips 313 H, Philips 595 HN, Philips 335 HN, G.E. 6 U 5 and H.M.V. 17 Q 7) from about 1 to 20 Mc/s. The Philips 595 HN showed the highest sensitivity and the H.M.V. 17 Q 7 the poorest over the range of frequencies tested. The two old receivers (Philips 313 H and G.E. 6 U 5) showed insensitive points, one at 7 Mc/s and the other at 4 Mc/s.

Sensitivity tests were made for five different radio receivers over a range of frequencies from about 1 to 20 Mc/s. The receivers under test were :—(1) Philips 313 H, (2) Philips 595 HN, (3) Philips 335 HN, (4) G.E. 6 U5 and (5) H.M.V. 17 Q 7. Each of the receivers examined was of the superheterodyne A.C./D.C. Type.

DEFINITION OF SENSITIVITY

The sensitivity of a receiver is that characteristic which determines the minimum R.F. input signal voltage capable of giving a desired value of audio output. Thus the R.F. input voltage in millivolts or microvolts required to give an audio output of 50 milliwatts to the loudspeaker, when the receiver is connected to a standard dummy antenna, measures the sensitivity required, the output being measured across a non-reactive resistance equal to the impedance of the voice coil.

METHOD OF MEASUREMENT

From a standard signal generator a definite frequency was generated at which the receiver under test was expected to operate. The carrier was then modulated by the 400 cycles modulation of the signal generator. The radio receiver was tuned to this frequency. The volume-control setting was kept at the maximum position and the tone-control setting at the minimum position. By means of Weston's analyser the voltage across the output terminals was measured. By adjusting the attenuator of the signal generator the output voltage level of the carrier was varied until the voltage indicated by the output analyser indicated a voltage that corresponded to 50 milliwatts output.

If R be the value of a non-reactive resistance equal to the impedance of the voice coil and V the required voltage corresponding to 50 milliwatts output across the resistance R,

Then $$\frac{V^2}{R} = .05 \text{ watts} \quad \text{or} \quad V = \sqrt{R \times .05} \text{ volts.} \quad \ldots \quad (1)$$

* Fellow of the Indian Physical Society.

The impedance of the voice coil of the loudspeaker for each receiver was measured in the usual way and the voltage V was then found by calculation according to (1). The input voltage (in μV) into the receiver could then be adjusted to give the requisite output voltage across R. Actually, however, the voltage across the voice coil was made to have the requisite value by adjusting the attenuator in the signal generator. This procedure gave substantially the same result.

SENSITIVITY MEASUREMENTS

In Table I are given all the measured values of sensitivity for the radio receivers over a range of frequencies from about 1 Mc/s to 20 Mc/s. The sensitivity curves for the three comparatively new receivers (Philips 595 HN., Philips 335 HN. and H.M.V. 17 Q 7) are shown in Fig. 1. The curves for the two old receivers (Philips 313 H and G.E. 6 U 5) are shows in Fig. 2. The two old receivers showed insensitive points, one at 7 Mc/s and the other at 4 Mc/s.

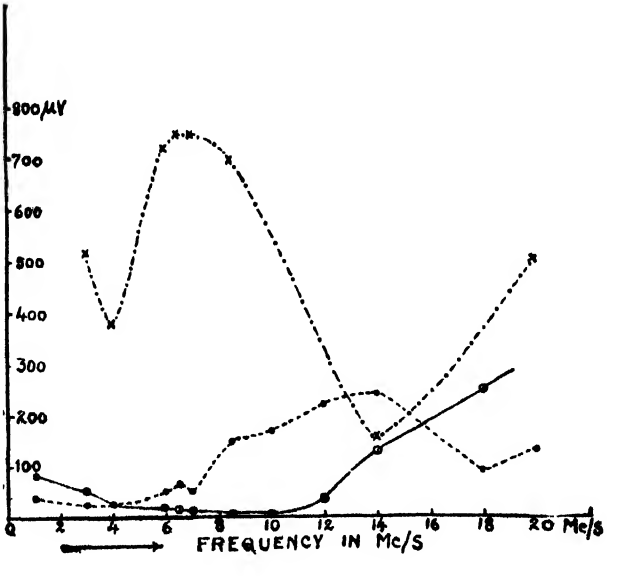

—⊙—⊙—⊙— Philips 595 HN.
—•—•—•— ,, 335 HN.
—×—×—×— H.M.V. 17 Q 7.

FIG. 1

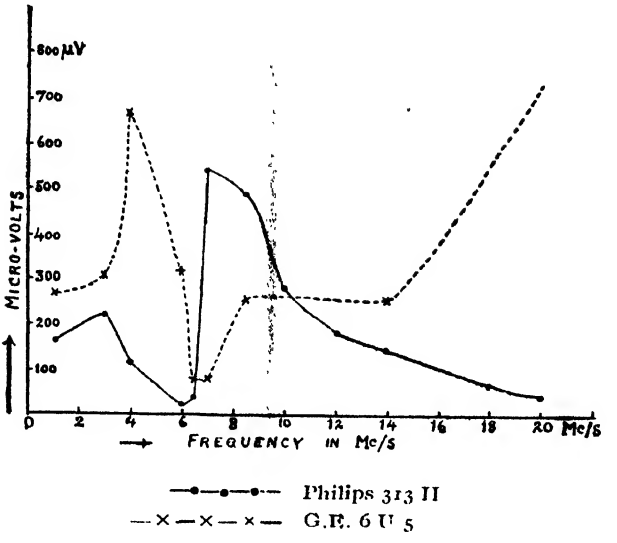

FIG 2

TABLE I

Freq. Mc/s	Sensitivity in μV				
	P 313 H.	P. 595 HN.	P. 335 HN.	G.E. 6 U 5	H.M.V. 17 Q 7
1 1	165	86	40	270	—
3.0	220	56	25	310	520
4.0	115	23.6	26	670	380
6.0	26	22	51	320	720
6.5	42	14.0	65	80	750
7.0	545	13.5	50	80	750
8.5	490	8.5	150	260	700
10.0	285	6.0	170	—	—
12.0	185	38	220	—	—
14.0	150	128	240	255	160
18.0	70	250	90	—	—
20.0	50	—	130	820	500

GENERAL CONCLUSIONS

I. *Philips 313 H.*—The maximum sensitivity was observed at 6 Mc/s, the value being 26 μV. There was a point of very low sensitivity at 7 Mc/s, the value being as high as 545 μV from 7 to 20 Mc/s, the sensitivity was found to increase steadily.

II. *Philips 325 HN.*—The maximum sensitivity was observed at 10 Mc/s, the value being 6 μV. There was a very gradual increase in sensitivity from 1 Mc/s to 10 Mc/s after which the sensitivity decreased steadily.

III. *Philips 335 HN.*—The maximum sensitivity was observed at 3 Mc/s, the value being 25 μV. The sensitivity was found to decrease steadily up to 14 Mc/s where the minimum sensitivity observed was 240 μV.

IV. *G.E. 6 U 5.*—The maximum sensitivity was observed at 7 Mc/s, the value being 80 μV. The sensitivity showed an abrupt fall at 4 Mc/s, its value being as high as 670 μV. From 7 Mc/s the sensitivity was found to decrease steadily.

V. *H.M.V. 17 Q 7.*—The sensitivity was found to be small at about 6.5 Mc/s, the value being as high as 750 μV. From 6.5 Mc/s the sensitivity increased till a maximum value of 150 μV was attained at 14 Mc/s, beyond which the sensitivity decreased.

The maximum sensitivity values of the five receiving sets under test are given in Table II.

TABLE II

Name of Receiver	Max. sensitivity in μV	Years in use
Philips 313 H.	26 μV at 6 Mc/s	6
Philips 595 HN.	6 ,, at 10 Mc/s	2
Philips 335 HN.	25 ,, at 3 Mc/s	½
G.E. 6 U 3	80 ,, at 7 Mc/s	7
H.M.V. 17 Q 7	160 ,, at 14 Mc/s	1

The comparison shows that the Philips 595 HN. receiver has the highest sensitivity over a range of frequencies from 1 to 20 Mc/s (15 metres to 300 metres). Over the same range the H.M.V. 17 Q 7 showed the poorest sensitivity. The receivers under test were not, however, brand-new Some of them were six or seven years old. The years, the different receivers are known to be in use, are also noted in Table II.

ACKNOWLEDGEMENT

In conclusion we place on record our sincere thanks to the owners of the receiving sets for their kind loan which made these measurements possible.

PHYSICS DEPARTMENT
DACCA UNIVERSITY.

THREE-PHASE R-C OSCILLATOR FOR RADIO AND AUDIO FREQUENCIES

By H. RAKSHIT* and K. K. BHATTACHARYYA

(*Received for publication, Oct. 30, 1946*)

(Plate IX)

ABSTRACT. The R-C tuned type of oscillator has received close attention in recent years because of its stability and purity of wave form The usual procedure is to provide regenerative feedback from the output to the input of an R-C coupled amplifier which may consist of one or more stages. The oscillations are generally limited to the audio frequency range because the choic of components required for producing radio frequencies presents practical difficulties. These have been overcome in the present three-phase oscillator consisting of three identical stages. This oscillator has been used to produce three-phase audio as well as radio frequency oscillations Mathematical formulae have been deduced which are corroborated by actual experiments.

INTRODUCTION

It is well known that an amplifier having a feedback path between the output and the input is liable to produce self-oscillations when the feedback is positive and the overall gain of the amplifier and feedback path is not less than unity. The frequency of the maintained oscillations is that at which the overall phase shift round the loop path is zero. The oscillator may consist of one or more stages of amplification. If a single valve is used and the desired feedback obtained by means of phase-shifting ladder networks, then the unavoidable attenuation in such networks necessitates high amplification and greater excursion of anode voltage with consequent distortion. This can be avoided by using more than one stage of amplification. A three-phase system, due originally to M. Van der and B. Van der Pol(1934), which has been in vogue during recent years, is seen to behave like a selective tuned circuit as the overall phase difference is extremely sensitive to frequency. This is why the waveform of oscillation is nearly sinusoidal. The oscillations are generally limited to the audio frequency range because the choice of components required for producing radio frequencies presents practical difficulties.

In a recent communication by the authors (Rakshit aud Bhattacharyya, 1946) it was shown that the conventional circuit of the three-phase oscillator with components selected for producing audio frequency oscillations invariably generates high radio frequencies by virtue of the unavoidable stray and inter-electrode capacities. Audio frequency can be generated by such a system only after making some modifications of the simple circuit. The present paper gives the details of the arrangement.

* Fellow of the Indian Physical Society.

THEORETICAL CONSIDERATIONS

The principle of the maintenance of oscillation is to provide the usual regenerative feedback from the output to the input of a three stage R-C coupled amplifier. Fig. 1 shows the diagram of any of the three symmetrical stages

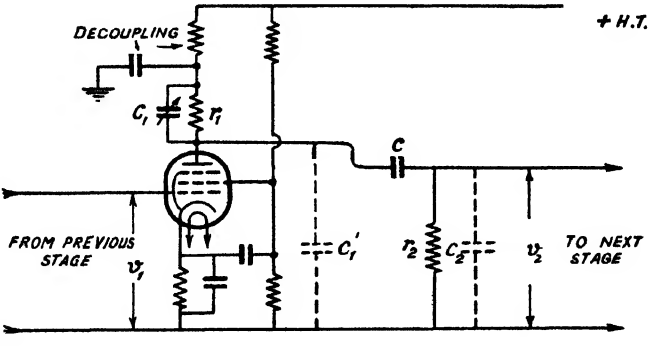

FIG. 1

constituting the feedback chain where pentodes are used to minimise inter-electrode capacities and special care is taken to ensure minimum change of electrode voltages due to mains voltage fluctuations.

Assuming a perfect three-fold symmetry let us denote

r_1 = plate load,

r_p = a.c. plate resistance of the valve,

C_1 = shunting condenser across the load,

C = coupling condenser,

r_2 = grid-leak resistance,

C_1' = plate to cathode capacity together with stray wiring capacity to the left of the coupling condenser C,

C_2 = input grid to cathode capacity together with stray wiring capacity to the right of the coupling condenser C, and

g = mutual conductance of the valve.

The exact equivalent circuit of the above is given in Fig. 2(*a*) which reduces to Fig. 2(*b*), assuming $r_1 << r_p$ which is very high for pentodes.

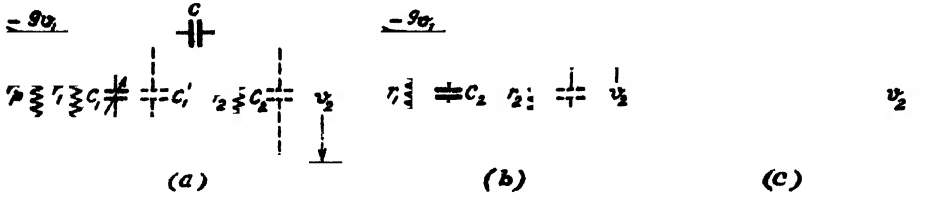

FIG. 2

Fig. 2(*b*) is again equivalent to Fig. 2(*c*) by putting Z_1 for $\frac{r_1}{1+j\omega C_1 r_1}$ and

Z_2 for $\frac{r_2}{1+j\omega C_2 r_2}$ where ω = angular frequency of the oscillations maintained and $C_t = C_1 + C_1'$.

The alternating current along the branch Z_2 is given by

$$i_{z_2} = gv_1 \frac{Z_1}{Z_1 + Z_2 + 1/j\omega C}$$

Therefore the output voltage which is equal to the input voltage at the next valve is given by

$$v_2 = Z_2 . i_{z_2} = -gv_1 \frac{Z_1 Z_2}{Z_1 + Z_2 + 1/j\omega C}$$

On substituting the values of Z_1 and Z_2,

$$v_2 = -\frac{gv_1 r_1 r_2 . j\omega C}{j\omega C r_1(1+j\omega C_2 r_2) + j\omega C r_2(1+j\omega C_t r_1) + (1+j\omega C_2 r_2)(1+j\omega C_t r_1)}$$

$$= \frac{-gv_1 r_1 r_2 C}{\Sigma C r - \frac{j}{\omega}(1-\omega^2 r_1 r_2 \Sigma CC)}$$

where $\Sigma Cr = Cr_1 + Cr_2 + C_t r_1 + C_2 r_2$ and $\Sigma CC = CC_2 + CC_t + C_2 C_t$

Or,
$$v_2 = \frac{gv_1 r_1 r_2 C}{\left[(\Sigma Cr)^2 + \left(\frac{1-\omega^2 r_1 r_2 \Sigma CC}{\omega}\right)^2\right]^{\frac{1}{2}}} . e^{\pi+\theta} \quad \ldots \quad (1a)$$

$$= |Av_1| . /\pi + \theta \quad \ldots \quad (1b)$$

where
$$\theta = \tan^{-1} \frac{1-\omega^2 r_1 r_2 \Sigma CC}{\omega \Sigma Cr} \quad \ldots \quad (1c)$$

Hence we see that each stage considered as a separate amplifier produces an amplification given by

$$A = gr_1 r_2 C \Big/ \left[(\Sigma Cr)^2 + \left(\frac{1-\omega^2 r_1 r_2 \Sigma CC}{\omega}\right)^2\right]^{\frac{1}{2}} \quad \ldots \quad (2a)$$

and a phase shift with respect to its input voltage given by

$$\phi = \pi + \theta \quad \ldots \quad (2b)$$

Now considering the system as a whole it is clear that for the maintenance of oscillation we must have

$$\left.\begin{array}{l} (i)\ A \not< 1 \\ \text{and } (ii)\ 3\phi = 2n\pi \end{array}\right\} \quad \ldots \quad (3)$$

where n is any integer.

According to condition (*ii*) the possible values of ϕ between 0 and 2π are $\frac{2\pi}{3}$, $\frac{4\pi}{3}$ and 2π. Of these three values the third one, *viz.*, $\phi = 2\pi$, though mathematically correct, is, however, physically impossible in our system and hence we are left with two alternative cases— $\phi = \frac{2\pi}{3}$ and $\phi = \frac{4\pi}{3}$.

Case I.—High Frequency Oscillations.

For the first case, $\phi=\frac{2\pi}{3}$, *i.e.*, $\theta=-\frac{\pi}{3}$. Writing ω_1 for ω we have from equation (1*c*)

$$\frac{1-\omega_1^2 r_1 r_2 \Sigma CC}{\omega_1 \Sigma Cr}=\tan\theta=-\sqrt{3} \qquad \ldots \quad (4a)$$

Or, $$\omega_1^2 r_1 r_2 \Sigma CC-\sqrt{3}\,\omega_1 \Sigma Cr-1=0 \qquad \ldots \quad (4b)$$

i.e., $$\omega_1=\frac{\sqrt{3}\Sigma Cr \pm \sqrt{3(\Sigma Cr)^2+4r_1 r_2 \Sigma CC}}{2r_1 r_2 \Sigma CC}$$

Neglecting the negative value of ω_1 and assuming $r_2 \gg r_1$ and $C_2 \ll C$, so that $4r_1 r_2 \Sigma CC$ is neglected in comparison with $3(\Sigma Cr)^2$, we have,

$$\omega_1=\frac{2\sqrt{3}\Sigma Cr}{2r_1 r_2 \Sigma CC}=\frac{\sqrt{3}(Cr_1+Cr_2+C_t r_1+C_2 r_2}{r_1 r_2(CC_2+CC_t+C_2 C_t)}$$

$$\doteq \frac{\sqrt{3}(C+C_2)}{r_1 C(C_2+C_t)} \qquad \ldots \quad (4c)$$

Or with more approximation

$$\omega_1=\frac{\sqrt{3}}{r_1(C_2+C_t)}=\frac{\sqrt{3}}{r_1(C_1+C_1'+C_2)}=\frac{\sqrt{3}}{r_1(C_1+C_s)}$$

where $C_s=C_1'+C_2$, *i.e.*, C_s denotes the total stray capacity on either side of the coupling condenser C.

$$\therefore \qquad f_1=\frac{\sqrt{3}}{2\pi r_1(C_1+C_s)} \qquad \ldots \quad (5a)$$

Applying eqn. (4a) to determine the value of the amplification "A" in eqn. (2a) we get

$$A=\frac{g r_1 r_2 C}{2\Sigma Cr}=\frac{g r_1}{2}\cdot\frac{1}{\left[\frac{r_1}{r_2}+1+\frac{C_t}{C}\cdot\frac{r_1}{r_2}+\frac{C_2}{C}\right]}$$

Hence condition (ii) for the maintenance of oscillation as given by eqn. (3) becomes

$$g r_1 \not< 2\left[\frac{r_1}{r_2}+\frac{C_t}{C}\cdot\frac{r_1}{r_2}+\frac{C_2}{C}\right] \qquad \ldots \quad (5b)$$

Case II.—Low Frequency Oscillations.

For the second case, $\phi=\frac{4\pi}{3}$, *i.e.*, $\theta=\frac{\pi}{3}$. Writing ω_2 for ω we get from equation (1*c*)

$$\frac{1-\omega_2^2 r_1 r_2 \Sigma CC}{\omega_2 \Sigma Cr}=\tan\theta=\sqrt{3} \qquad \ldots \quad (6a)$$

Or,
$$\omega_2^2 r_1 r_2 \Sigma CC + \sqrt{3}\omega_2 \Sigma C r - 1 = 0 \qquad \ldots \quad (6b)$$

i.e.,
$$\omega_2 = \frac{-\sqrt{3}\Sigma C r \pm \sqrt{3}\Sigma C r \left[1 + \frac{4 r_1 r_2 \Sigma CC}{3(\Sigma C r)^2}\right]^{\frac{1}{2}}}{2 r_1 r_2 \Sigma CC}$$

Neglecting, as before, the negative value of ω_2 and taking $r_2 \gg r_1$ so that $\frac{4 r_1 r_2 \Sigma CC}{3(\Sigma C r)^2} \ll 1$, we have by expanding the square root by the Binomial Theorem and retaining the first two terms

$$\omega_2 = \frac{-\sqrt{3}\Sigma C r + \sqrt{3}\Sigma C r \left[1 + \frac{2 r_1 r_2 \Sigma CC}{3(\Sigma C r)^2}\right]}{2 r_1 r_2 \Sigma CC}$$

$$= \frac{1}{\sqrt{3}\Sigma C r} \doteq \frac{1}{\sqrt{3} r_2 (C + C_2)} \qquad \ldots \quad (6c)$$

Or with further approximation, when $c \gg c_2$,

$$\omega_2 = \frac{1}{\sqrt{3} C r_2}, \quad i.e., \quad f_2 = \frac{1}{2\pi\sqrt{3} C r_2} \qquad \ldots \quad (7a)$$

Here also condition 3(*ii*) for the maintenance of oscillation becomes

$$g r_1 \ll 2\left[1 + \frac{r_1}{r_2} + \frac{C_1}{C} \cdot \frac{r_1}{r_2} + \frac{C_2}{C}\right] \qquad \ldots \quad (7b)$$

Vector Relations

The relations between the currents and voltages in the different branches of the circuit are depicted vectorially in Figs. 3 and 4 where the suffixes in i and v refer to the currents and voltages for the respective branches. Figs.

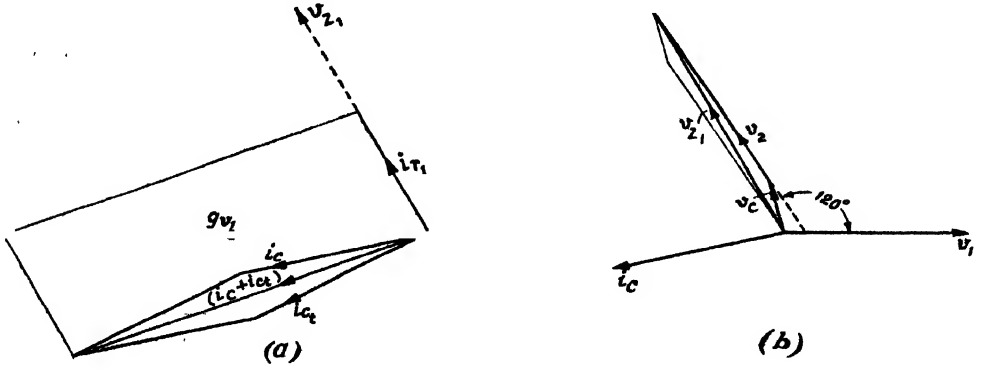

FIG. 3

3(*a*) and (*b*) represent the relations for Case I and Figs. 4(*a*) and (*b*) for Case II. From Figs. 3(*b*) and 4(*b*) it can easily be seen that the phase advance

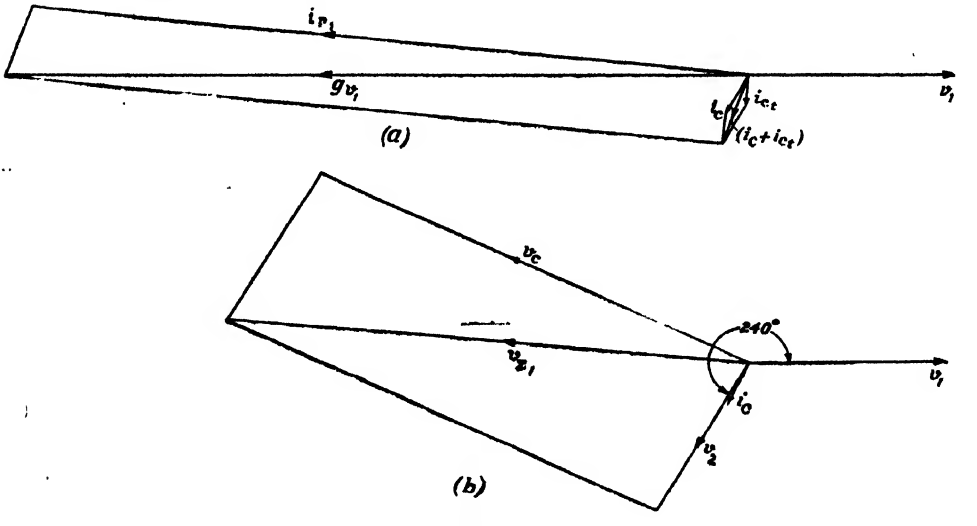

FIG. 4

per stage at f_1 and f_2, corresponding to Cases I and II, are 120° and 240° respectively, so that the feedback in both the cases is positive.

Simultaneous R.F. and L.F. Oscillations

From the above analyses we see that as the gain is the same for the two cases there is probability of the two frequencies f_1 and f_2 being maintained simultaneously. Now eqns. (5*a*) and (7*a*) show that under average working conditions f_1 can be easily made to lie in the radio frequency range and f_2 generally limited to the audio frequency range. It may, however, be mentioned in this connection that this probability of more than one oscillation being simultaneously maintained is a general feature of multiphase oscillators. For example, in a 7-phase oscillator two sets of oscillations are possible, each having two frequencies—one in the radio and the other in the audio frequency range. Thus for one set the phase advances per stage are $154\frac{2}{7}°$ and $205\frac{5}{7}°$, while the corresponding values for the other set are $102\frac{6}{7}°$ and $257\frac{1}{7}°$. It can be shown that this latter set of oscillations requires greater gain and can thus be easily suppressed. In the present three-phase oscillator, although the two modes of oscillation are equally probable, since the required gain is the same in either case, experiments have shown that under the above arrangement the radio frequency f_1 only is maintained to the exclusion of the audio frequency f_2. This is due to the fact that in a system where oscillation grows up from an initial impulse, having frequency components from zero to infinity, the highest probable frequency will build up quickly and so in the present case, as the building up of oscillation at f_1 is much quicker than

that at f_2, f_1 grows up first and once f_1 is built up it is not generally possible for f_2 to grow thereafter. Under certain favourable conditions, however, it is possible to have both radio and audio frequency oscillations simultaneously maintained. This is discussed later.

Production of audio frequency oscillations

From the above considerations it is obvious that to obtain f_2 we must somehow suppress f_1 without of course adversely affecting f_2. This can be done by connecting a capacitance from the anode to cathode of only one stage. The magnitude of this capacity should be such that it will effectively reduce the overall gain of the system below unity at the radio frequency but its reactance at the audio frequency should be large compared with the load resistance r_1.

It will be seen from the discussion of harmonic distortion that oscillations are purest when the three stages are identically the same and the overall gain is just greater than unity. Any asymmetry in the stages requires greater load resistances for the production of oscillations. In actual practice it is more difficult to maintain symmetry for f_2 than for f_1. An attempt to suppress f_1 by connecting a suitable capacitance as explained above with a view to build up the audio frequency introduces further asymmetry, specially for the highest audio frequencies. Hence if initially the radio frequency oscillation be going on at critical maintenance condition, the use of such a capacitance will no doubt suppress f_1, but f_2 may not actually be maintained in that condition. In such a case it will be necessary to increase the load resistance and then only f_2 will build up.

The double function of suppressing f_1 and increasing the gain without at the same time introducing any asymmetry, can be effected simultaneously by incorporating in each stage a small resistance r in series with r_1 and forming part of the total load, but left unshunted by C_1, as shown in Fig. 5(*a*). Fig. 5(*b*) shows the simplified equivalent circuit at radio frequency. Now if C_1

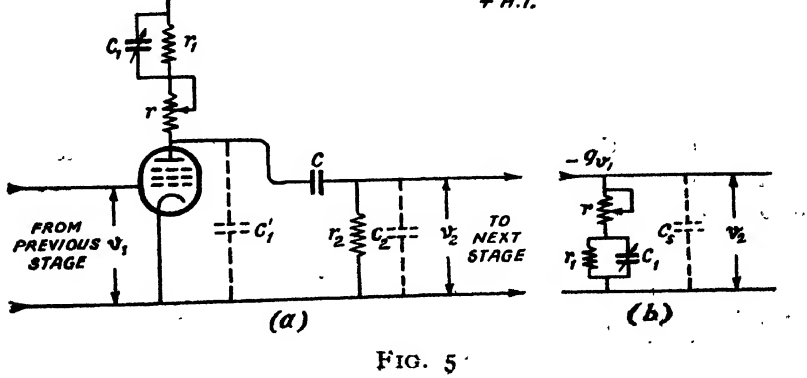

FIG. 5

be large compared with C_s but not large enough to have any appreciable shunting influence at the highest audio frequency we can, as a first approximation, neglect C_s in our equivalent circuit. This will not vitiate our inference of the effect of r at radio frequency but will on the other hand simplify the analysis.

The output voltage is then given by

$$v_2 = -gv_1\left[r + \frac{r_1}{1+j\omega C_1 r_1}\right] = \frac{gv_1}{1+\omega^2 C_1^2 r_1^2}[(R+\omega^2 C_1^2 r_1^2 r)^2 + (\omega C_1 r_1^2)^2]^{\frac{1}{2}} \cdot e^{\pi+\theta} \quad \ldots (8)$$

where $\tan\theta = -\frac{\omega C_1 r_1^2}{R+\omega^2 C_1^2 r_1^2 r}$ and $R = r_1 + r$.

Or, $$v_2 = |Av_1| \angle \pi+\theta \quad \ldots (9a)$$

where the amplification A is given by

$$A = \frac{g}{1+\omega^2 C_1^2 r_1^2}\left[(R+\omega^2 C_1^2 r_1^2 r)^2 + (\omega C_1 r_1^2)^2\right]^{\frac{1}{2}} \quad \ldots (9b)$$

As before the conditions for maintenance of oscillation are (i) $A \nless 1$ and (ii) $3(\pi+\theta) = 2n\pi$. For the radio frequency mode under consideration, $\theta = -\frac{\pi}{3}$ and hence condition (ii) is satisfied if

$$-\frac{\omega C_1 r_1^2}{R+\omega^2 C_1^2 r_1^2 r} = \tan\theta = -\sqrt{3} \quad \ldots (9c)$$

This gives

$$\omega = \frac{C_1 r_1^2 \pm \sqrt{C_1^2 r_1^4 - 12 C_1^2 r_1^2 r R}}{2\sqrt{3} C_1^2 r_1^2 r}$$

Or, neglecting the positive sign before the radical which is obviously inadmissible, if we consider the limit when $r = 0$,

$$\omega = \frac{C_1 r_1^2 - C_1 r_1 \sqrt{r_1^2 - 12 r R}}{2\sqrt{3} C_1^2 r_1^2 r}$$

$$= \frac{r_1 - \sqrt{r_1^2 - 12 r R}}{2\sqrt{3} C_1 r_1 r} \quad \ldots (9d)$$

Now in order that ω may be real, the expression under the radical sign must be positive. Remembering that $R = r_1 + r$, it is easy to see that the necessary condition is

$$r \not> \frac{r_1}{6+4\sqrt{3}} \not> 0.077 r_1 \quad \ldots (10)$$

In other words, if we make $r > 0.077 r_1$, no radio frequency oscillation can be maintained. In practice the effect of C_s is to make the limiting value of r slightly greater than that given by equation (10).

Comparing equations (9b) and (9c) we have

$$A = \frac{2g(R+\omega^2 C_1^2 r_1^2 r)}{1+\omega^2 C_1^2 r_1^2}$$

$$= 2g\left(r + \frac{r_1}{1+\omega^2 C_1^2 r_1^2}\right) \qquad \ldots \text{(11a)}$$

On substitution from (9d), this further reduces to

$$A = \frac{2gr}{1 - \frac{6r}{r_1 - \sqrt{r_1^2 - 12rR}}} \qquad \ldots \text{(11b)}$$

Since the value of r required to just suppress the r.f. oscillations is a small fraction of r_1, as given by equation (10).

$$\sqrt{r_1^2 - 12rR} = r_1 - 6r\left[1 + 4\frac{r}{r_1} + 24\left(\frac{r}{r_1}\right)^2 + \text{higher powers of } \frac{r}{r_1}\right]$$

Hence, as a first approximation, for small values of r,

$$A = \frac{2gr}{4\frac{r}{r_1} + 8\left(\frac{r}{r_1}\right)^2} = \frac{gr_1}{2+4\frac{r}{r_1}} \qquad \ldots \text{(11c)}$$

Similarly the expression (9d) for frequency becomes

$$\omega = \frac{\sqrt{3}}{C_1 r_1}\left(1 + 4\frac{r}{r_1}\right) \qquad \ldots \text{(11d)}$$

Equations (11c) and (11d) show that as r is gradually increased from zero the frequency of the generated r. f. oscillations continuously increases whereas the gain of the system continuously decreases. The variations of $f = \frac{\omega}{2\pi}$ and A with r, for two different values of r_1, are shown in Table I.

These variations are shown plotted in Fig. 6. Fig. 6(*a*) refers to $r_1 = 3000\Omega$ and Fig. 6(*b*) to $r_1 = 1850\Omega$. The two sets of curves at once show that if r_1 is near the critical value required for maintenance then gain is reduced below unity for values of r less than that given by equation (10). If, therefore, the value of r_1 be such that the r.f. oscillations are just maintained and r is gradually increased, the limitation of gain is primarily responsible for the stoppage of r.f. oscillations. Fig. 6 further shows that when r_1 is sufficiently greater than the critical value, the limitation of phase shift is attained first and the r.f. oscillations stop even though the gain is greater than unity. The value of r required for suppression of the r.f. oscillations for such values of r_1 is given by equation (10).

TABLE I

$C_1 = 150\mu\mu f$; $g = 1{\cdot}2 \times 10^{-3}$ mho

$r_1 = 3{,}000\ \Omega$; $gr_1 = 3.6$; $0.077r_1 = 231\Omega$			$r_1 = 1{,}850\Omega$; $gr_1 = 2\ 22$; $0.077r_1 = 142.5\Omega$		
r	$f \times 10^{-5}$	A	r	$f \times 10^{-5}$	A
0	6.13	1.80	0	9.93	1.11
10	6.21	1.79	18.5	10 33	1.09
40	6.45	1.75	37	10.72	1.07
60	6.62	1.73	55.5	11.12	1.05
100	6.94	1.69	74	11.52	1.03
150	7.35	1.64	92 5	11.92	1 01
200	7.76	1.59	111	12.31	0.99
230	8.00	1.56	140	12.93	0.96

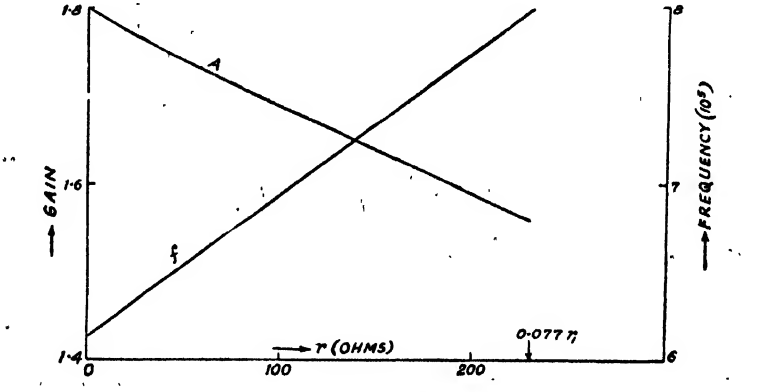

FIG. 6(a)

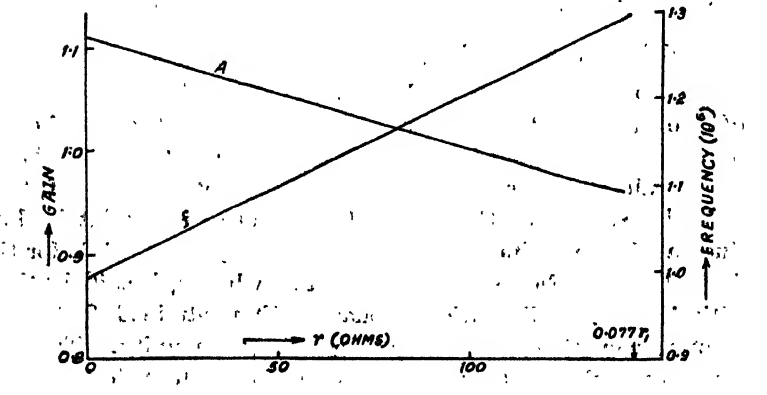

FIG. 6(b)

Thus with r_1 near the critical value, if r is gradually increased, the amplitude of the r.f. oscillations would gradually decrease to zero and then die out. On the other hand if the value of r_1 is much greater than the critical value the amplitude will no doubt decrease with increase of r, but instead of dying out on reaching zero amplitude the oscillations suddenly stop when the amplitude is still sufficiently large. These features are clearly observed when the experiments are performed with a cathode ray oscillograph as a visual indicator of the oscillations.

EXPERIMENTAL RESULTS

A series of experimental tests were performed to verify the validity of the theoretical relations discussed above. The complete oscillator was fitted up according to Fig. 1, modified by the introduction of r as shown in Fig. 5. The three resistances r_1 were wound with manganin wire on thin mica cards.

A. *Radio Frequency Oscillations—r Short-circuited*

In this condition it is immaterial whether C_1 is directly connected across r_1 as shown in Fig. 1. or connected between the anode and the H. T. negative line. In practice, for studying the effect of the variations of C_1, a three-gang condenser was used for the C_1's, the common shaft being connected to the H. T. negative line.

According to eqn. (5a) we have

$$f_1 = \frac{\sqrt{3}}{2\pi r_1 (C_1 + C_s)}$$

Or

$$C_1 = \frac{\sqrt{3}}{2\pi r_1} \cdot \frac{1}{f_1} - C_s \qquad \ldots (12)$$

TABLE II

Case	C_1 ($\mu\mu$f)	f_1 (kc/s)	$1/f_1 \times 10^6$	Cs ($\mu\mu$f) from graph
I	65	1490	0.67	44
	106	1085	0.92	
	185	695	1.44	
	270	516	1.93	
	350	440	2.27	
II	80	1538	0.65	28
	150	922	1.08	
	200	735	1.36	
	250	610	1.64	
	300	512	1.95	
	350	440	2.27	

This shows that if f_1 be changed by varying C_1 and $\frac{1}{f_1}$ is plotted along y-axis

and C_1 along x-axis, the graph will be a straight line cutting the x-axis on the negative side, the intercept giving the value of C_s. This gives us a ready method of estimating experimentally the total stray and inter-electrode capacity on the two sides of the coupling condenser. Table II gives the record of observations on two typical oscillators. The values for Case I refer to the oscillator using 6K7G type valves and those for Case II to the second oscillator using 6SK7 type valves in which the connections were short and made with special care to minimise stray wiring capacities. The load resistance r_1 was in each case 2,000 ohms.

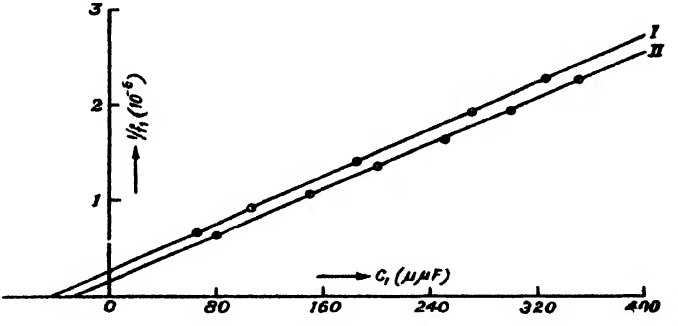

FIG. 7

The results are shown graphically in Fig. 7 from which we see that the stray capacity in Case II has been considerably diminished. It will be noted that there is a slight difference in the inclinations of the two straight lines to the x-axis, although according to eqn. (12) such a discrepancy should not have existed since r_1 was the same in each case. If, however, we remember that eqn. (12) is derived from (5a) which in itself is an approximation from (4c) it will be clear that the slope of the straight line is more correctly,

$$\tan^{-1} \frac{2\pi r_1}{\sqrt{3}\left(1+\frac{C_2}{C}\right)}$$

Now the values of C in the two cases concerned were different and C_2 automatically changed due to altered wiring. This explains the difference in the two slopes.

Fig. 8(*a*), Plate IX, shows a typical oscillographic record of the r.f. oscillations generated by the oscillator, frequency 500 Kc/s.

It is evident that to make f_1 very high, valves with high mutual conductance and low input and output capacitance must be used. Using 6SK7 valves with 1500 ohm load and having no external C_1 a frequency of 9 Mc/s has been obtained.

Quartz Control —The r.f. oscillations can be established by using a single quartz crystal in place of the coupling condenser C in any one stage. The crystal is selected to have resonant frequency within the range of the oscilla-

tion. The three-gang condenser for the C_1's in the three stages is adjusted till the crystal frequency is obtained. In this condition the coupling condenser C of any one stage is replaced by the mounted quartz crystal. It is found that the frequency of the maintained oscillations remains constant even though the ganged condenser C_1 is varied within wide limits.

Three-phase symmetry.—In the r.f. mode the phase shift produced by any one stage is primarily dependent upon $(C_1 + C_s)$ and r_1 when the grid leak and coupling condenser are, as usual, comparatively very large. By using three similar valves, identical wire-wound resistances for r_1, ganged condenser for C_1 and making symmetrical connections it is easy to maintain the phase shift produced by each stage at 120°.

The equality of output voltage at each plate is checked by thermionic voltmeters. To test the 3-phase symmetry, the grids of the three oscillator valves are connected to the grids of three other triodes of which the anodes are tied together. The H.T. of the triodes is applied through a common load resistance. If the triodes are identical, it is obvious that the combined output will be zero when 3-phase symmetry exists. This has been verified experimentally.

B. *Audio Frequency Oscillations*

The short-circuits across the r's are removed for this mode of oscillation. The 3-gang condenser used for the r.f. mode is disconnected and three equal mica condensers are connected across the three resistances r_1. For generating oscillations of varying audio frequency the three coupling condensers C are this time replaced by a 3-gang condenser having each section completely insulated from the other two.

For a given setting of C the value of r is gradually increased till a stage is reached when the *r.f.* oscillation (f_1) stops and the audio frequency (f_2) builds up immediately. Fig. 8(*b*), Plate IX, shows a typical record of the a.f. oscillations, frequency 600 *c/s*. In a typical case using 6K7G valves with $r_1 = 3{,}000$ ohms and $C_1 = 150\mu\mu f$, the minimum value of r required to suppress f_1 was found to be 230 ohms. This agrees with eqn. (10). As explained in connection with Fig. 6, it has been found that when r_1 is very near the critical value, f_1 stops for r much less than that given by eqn. (10). In a typical case with $r_1 = 1850$ ohms., f_1 stopped at $r = 100$ ohms. In such critical cases, however, it has been observed that f_2 does not build up as soon as f_1 dies down but that it is necessary to increase r still further for the start and maintenance of f_2. This would seem rather puzzling as with increase of r the audio gain increases, although the *r.f.* gain decreases.

It can be shown, however, that if the three stages are not identically the same and the grid leaks of two stages are equal while that of the third stage

is either greater or smaller than the other two, the overall gain of the system for audio frequencies, is less than $gr_1/2$. The r.f. gain is not affected by variations in r_2. Under these conditions, therefore, when r_1 is very near the critical value, the r.f. oscillations are normally maintained when $r=0$. As r is gradually increased the r.f. gain decreases and finally f_1 dies down. The a.f. gain no doubt increases with increase of r but due to this asymmetry may still be less than unity for the value of r which just suppresses the r.f. oscillations. This explains why in such cases r has to be further increased in order to maintain the a.f. oscillations.

C. *Simultaneous R.F. and A.F. Oscillations*

When r_1 is neither very nearly equal to nor much greater than the critical value, it is found that if r is slowly increased from a small value with a view to build up the a.f. oscillations, a transition stage is reached when both the a.f. and r.f. oscillations may be simultaneously present. The oscillographic record, Fig. 8(*c*), Plate IX, depicts this condition with the time base synchronised to the generated a.f. oscillations, as may be noted from the trace of the fly-back path.

It may be noted in this connection that in a system capable of maintaining simultaneously two oscillations at frequencies widely different from each other, the higher one is generally believed to be modulated by the lower one. But no such modulation is present in the oscillographic record as is evident from the constancy of the amplitude of the r.f. oscillations. A radio receiver used to receive these oscillations also failed to indicate the presence of modulation under these conditions. When, however, r_1 is further increased and the valves no more operate within the linear regions of their characteristics, the audio oscillations cease to be sinusoidal and the trace on the cathode ray oscillograph indicates variations of the amplitude of the r.f. oscillations, indicating modulation. The radio receiver in that case gives the audio frequency output.

HARMONIC DISTORTION

The phase-shift oscillator system behaves as a selective tuned circuit in so far as the overall phase shift is a function of the frequency, *i.e.*, at frequencies other than those given by equations (5a) and (7a) the feed back is not positive. Once oscillation has started from an initial minute impulse it will build up to such an amplitude that due to overloading the transconductance of a valve is reduced below the initial value and the overall gain of the amplifier is reduced just to unity. This will necessarily produce harmonics as in other conventional self-maintained oscillators. To reduce harmonic distortion it is therefore essential to make the load resistance r_1 just enough

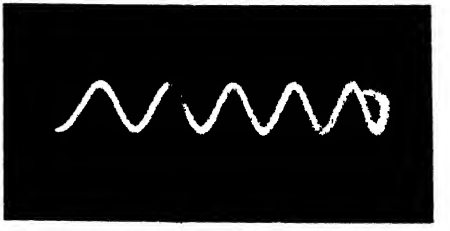

(a)

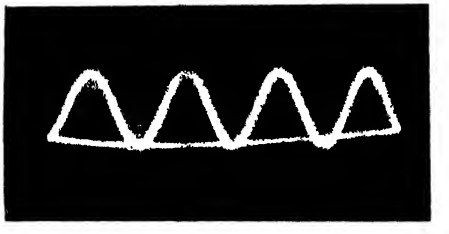

(b)

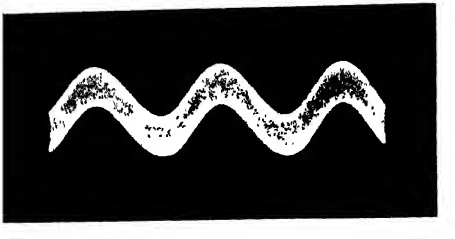

(c)

to satisfy equation (5b). With further increase in r_1, the distortion will go on increasing.

It should be noted in this connection that, on a comparative basis, the radio frequency oscillation is purer than the audio frequency one. This will be appreciated if we remember that the limitation of the amplitude of oscillations is due to the variation of g with variations of grid voltage during an oscillation cycle. The allowable change in g being the same for either mode of oscillation, since the expression for effective gain is the same for either case, it is obvious that the particular mode for which the excursion of anode voltage is smaller will necessarily be purer. Now the effective anode load for the r.f. mode is half that for the a.f. mode with a given value of r_1 because of the shunting influence of C_1. The harmonic distortion is therefore comparatively less for the r.f. oscillations.

Further, as already mentioned, when the three stages are not identical, the grid leak of one stage being different from those of the other two, the overall a.f. gain of the system is less, for any given value of the load r_1, than if three-fold symmetry existed. In other words for a given overall gain a larger value of r_1 is required if three-fold symmetry is not maintained. In a system consisting of three identical stages oscillations are therefore maintained at a relatively lower value of r_1 and hence it is essential to maintain symmetry of the stages in order to keep the harmonics at a low level. For the r.f. mode the gain and phase shift depend primarily upon the resistances r_1, a ganged condenser being used for C_1. In practice, by using wire-wound resistances for r_1, it is fairly easy to maintain symmetry for this mode. For the a.f. oscillations when a ganged condenser is used for C, it is necessary to match the three grid leaks r_2 to equality if harmonic distortion is to be reduced. If this precaution is not adopted the oscillator will give greater distortion for the a.f. mode than for the r.f. mode. Again, when the grid excursion of any stage is sufficiently high to drive it positive and causes grid current to flow, the effective value of r_2 and hence the a.f. oscillations are thereby affected. From this point of view also the r.f. oscillations are purer than the a.f. ones.

CONCLUSION

In the present paper some of the essential features of the symmetrical type 3-phase R-C tuned oscillator have been discussed. The properties of the asymmetrical type will form the subject matter of a subsequent communication. It may however, be mentioned in this connection that the symmetrical r.f. oscillator can easily be made to generate frequency-modulated oscillations. A very simple method would be to shunt any of the three valves by, say, a triode and apply the modulating audio voltage to the grid of this triode. The effective anode load resistance of the corresponding stage will then vary and consequently produce wide-band frequency modulation.

ACKNOWLEDGMENTS

The work was carried out at the Kanodia Electrical Communication Engineering Laboratory, Department of Applied Physics, University of Calcutta. The authors are thankful to Prof. P. N. Ghosh, Ph.D., Sc.D., for providing all facilities for the work.

REFERENCES

Rakshit, H. and Bhattacharyya, K. K., 1946, *Science and Culture*, **9**, 509.
Van der M. and Van der B, Pol., 1934, *Physics*, **1**, 437.

COMPARATIVE STUDIES OF THE *JOSHI-EFFECT* WITH A VACUO-JUNCTION AND DIODE DETECTION

By B. N. PRASAD

(*Received for publication, Aug. 15, 1946*)

ABSTRACT. Production of the *Joshi-Effect*, an instantaneous and reversible photo-diminution Δi of the discharge current i is studied in chlorine excited by 2-6 kV at 50 cycles frequency. A vacuo-junction and double diode (the latter being coupled inductively and resistively with the L.T. of the ozoniser) served as detectors. As established by Joshi, Δi does not occur below the 'threshold potential' and that $\%\Delta i$ is maximum near it. Based on Joshi's result that Δi predominates in the high frequency part of i, an explanation is developed for Joshi's general finding that $\%\Delta i$ decreases by increasing the circuital resistance, on an analysis of the behaviour of the H.F., L.F. and supply frequency parts of i in terms of the corresponding damping and skin effects.

INTRODUCTION

The marked dependence, on the nature of the operative conditions and of the current detector employed, of the magnitude of the above phenomenon was emphasised by Joshi (1943, 1945a). Metal oxide and similar type rectifiers and subsequently low resistance Cambridge vacuo-junctions were used in these Laboratories during earlier work on this effect. Their use limited appreciably the range of the working conditions such as, for example, the magnitude of the applied potential (kV), etc. In the present work, the *Joshi-Effect* Δi was studied using a double diode as a current detector, which comparatively is less subject to the above limitations. This arrangement has revealed that the magnitude of this phenomenon can be as high as 81% current decrease with but ordinary light.

EXPERIMENTAL ARRANGEMENT

The general apparatus and the circuit used are shown in Fig. 1. Chlorine gas, purified carefully over liquid air, was contained in the annular space of a Siemens' type ozoniser at about 200 mm. pressure and excited at potentials varied in the range 2-6 kV (r.m.s.) at 50 cycles frequency. The discharge current i was measured (*i*) in dark and (*ii*) under irradiation from one 220 volt, 200 watt incandescent (glass) bulb by manipulation of the shutter shown in Fig. 1.

Three series of observations of i were made. In the first, the low tension electrode of the chlorine tube, L.T., was earthed directly through a vacuo-junction connected to a reflection galvanometer with an appropriate shunt. This part of the circuit is shown by α in Fig. 1.

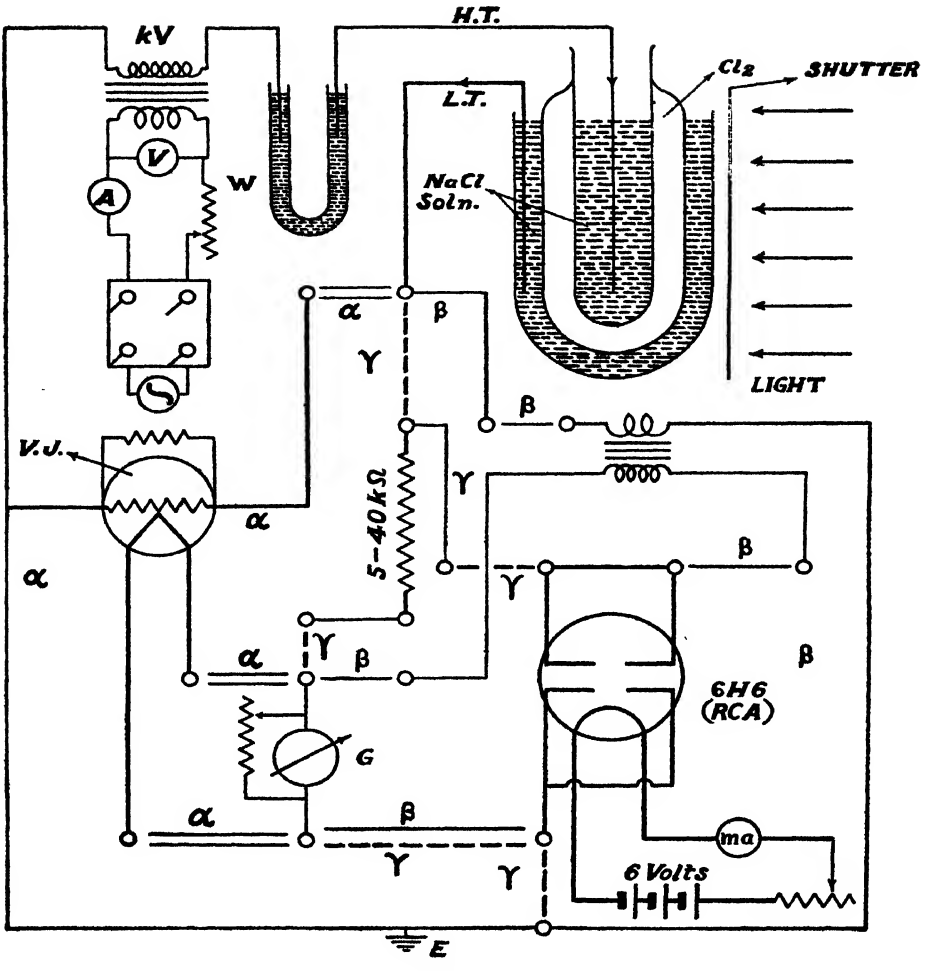

FIG. 1

Production of *Joshi-Effect* in chlorine

In the next series, a double diode, 6H6 (RCA), was used as a half-wave rectifier by short circuiting the two plates : the cathodes were heated indirectly with 270 mA. D.C. from a storage cell. The discharge current i was allowed to flow through the primary of a Bell type iron core, step up transformer (1 : 3) ; its secondaries were connected to the plates and the cathodes through the galvanometer as shown by β in Fig. 1. Finally in γ in Fig. 1, the input to the diode was tapped from a non-inductive and practically non-capacitative Dubilier resistance R, varied in the range 5-40 kΩ.

Fig. 2 shows the characteristic current potential curves observed in dark and in light using a vacuo-junction, in the range 2-6 kV applied to the ozoniser. In experiments to which Figs. 3 and 4 refer the vacuo-junction

was substituted by a double diode, coupled inductively and resistively with L.T. respectively. From these curves the net *Joshi-Effect* Δi, using a given detector, can be obtained at a given kV ; the relative *Joshi-Effect* $\%\Delta i$ is $\Delta i \times 100/i_{dark}$.

DISCUSSION

During these observations the fundamental importance of the ' Threshold-potential ' V_m (Joshi, 1929, 1945b), for reactions under electrical discharge in general and the *Joshi-Effect* in particular, were noticed (Joshi, 1945b, 1944). Below V_m, which depends upon a number of operative conditions such as temperature, gas pressure and especially frequency, the *Joshi-Effect* is not noticed. It is interesting to observe that the curves in Figs. 2, 3 and 4 show that despite the widely divergent modes of i measurement, V_m for the above chlorine tube was about 2.4 kV. The maximum $\%\Delta i$ indicated by the vacuo-junction was about 64 at 2.93 kV ; and that with the diode fed inductively, from the L.T. circuit of the excited ozoniser, was about 81 at 2.67 kV near V_m (Joshi, 1945c). It is also seen that an increase of kV increases i and also Δi, the corresponding $\%\Delta i$, however, decreases (Joshi, 1943). In agreement with previous results (Joshi, 1945c), it is found that $\%\Delta i$ is reduced greatly in the resistive coupling of the detector diode. At $R = 5{,}000$ ohms, the maximum $\%\Delta i$ is only about 10, the operative conditions being the same as those with the other detectors. Furthermore, as compared with results with inductive coupling, this maximum $\%\Delta i$ occurs fairly above V_m. Results at greater R than the above value showed large i (input being larger) but a reduced Δi and $\%\Delta i$. It is significant that this influence of R in suppressing Δi and $\%\Delta i$ was markedly uniform under all conditions of excitation employed in this work.

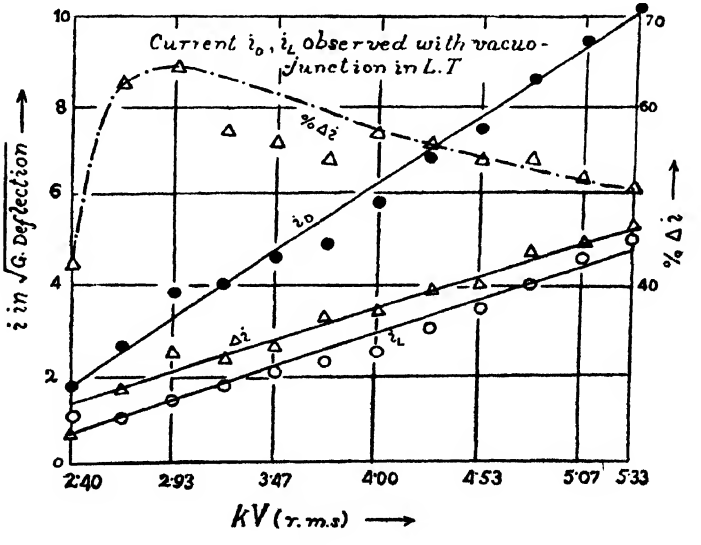

FIG. 2

Joshi-Effect with vacuo-junction detection

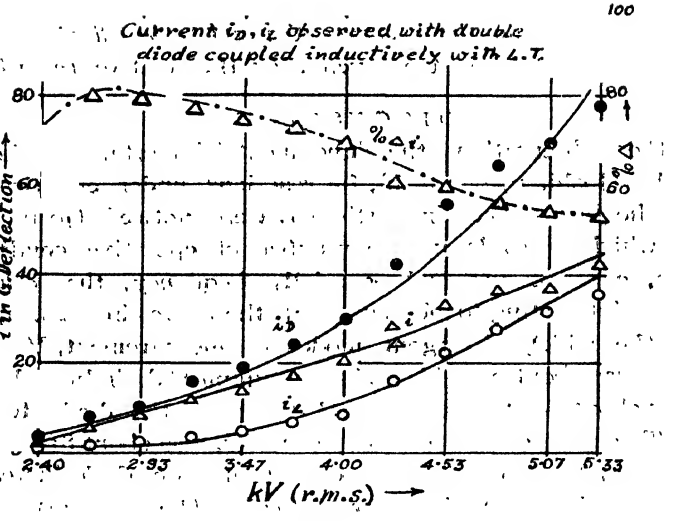

FIG. 3

Joshi-Effect with diode detection

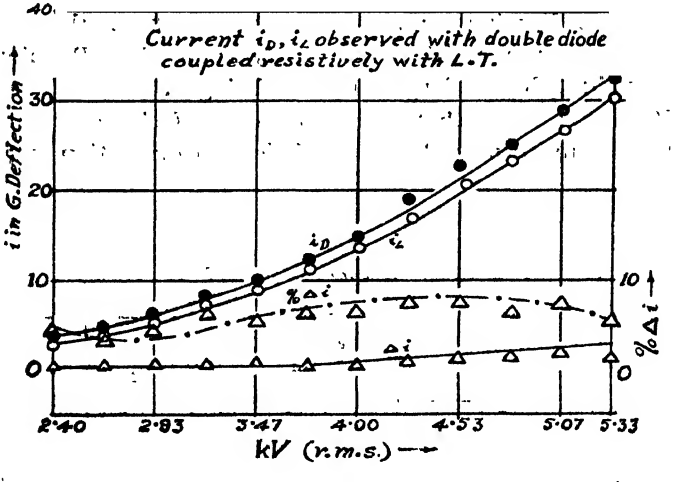

FIG. 4

Joshi-Effect with diode detection

From Figs. 2, 3 and 4, it is seen that the values for $\%\Delta i$ differ markedly with the mode of the current measurement employed. An explanation of this apparent variability is now suggested. From the oscillographic studies of the ozoniser, discharges under conditions appropriate to the production of large Δi (Joshi 1945a, 1945b, 1943), has established that (*a*) the discharge current i contains high frequency i_{HF}, low frequency i_{LF}, and the supply frequency component i_s and that i_{HF} represents the chief seat of this phenomenon Δi;

(*b*) the damping constants $R/2L$ of an oscillatory circuit consisting of R, the inductance L and the capacity C ; (*c*) the ' skin-effect.' From (*a*)

$$i_{diode} = i_{HF} + i_{LF} + i_s \qquad \ldots \quad (1)$$

These quantities are added vectorially.

In order to realise the significance of (*b*), the state of an oscillatory circuit in which C stands for a compound (gas-solid) dielectric, should be taken into account. In a *forced* oscillatory discharge, the current flowing through the circuit is given by

$$I = I_0' \sin(\omega' t + \phi') + I_0 e^{-R/2L} \sin(\omega t - \phi) \qquad \ldots \quad (2)$$

The symbols have their familiar significance. From (2) it may be deduced that the initial wave-form of the current would result from the superposition of an undamped wave of frequency f' and a damped one of frequency f. The former persists while the latter is damped at a rate that depends upon $R/2L$; finally I becomes equal to $I_0' \sin(\omega' t + \phi')$. It should be emphasised that equation (2) has been derived by considering the dielectric C to be in an unionised state. The *Joshi-Effect* is, however, observed only when the gas is ionised under the discharge. Besides, therefore, the two components in equation (2), an ionisation current consisting also of i_{HF} and i_{LF} is present. This non-sinusoidol ionisation current i_e (Joshi, 1945a, 1945b, 1943) may be expressed to a sufficient approximation by

$$i_e = e^{-R/2L} \{I_{m1} \sin(\omega t + \theta_1) + I_{m2} \sin(2\omega t + \theta_2) + I_{m3} \sin(3\omega t + \theta_3) + \ldots\} \ldots \quad (3)$$

where I_m represents maximum value of the current.

The ' skin-effect ' arises from the uneven radial distribution of current in a conductor ; the effective resistance R of a straight circular wire is given by

$$R' = R \sqrt{\pi^2 f \mu a^2 / \rho} \qquad \ldots \quad (4)$$

where R is the D.C. resistance and the other symbols have their usual significance.

It is easily shown that in the inductive coupling $\%\Delta i$ would be largest due to the low (ohmic) resistance in the oscillatory circuit. On the other hand, with a resistive coupling and also in the vacuo-junction detection an appreciable resistance is introduced. This last increases the ' damping constant ' and also the ' skin-effect ' ; as a consequence a reduction of the HF oscillations occurs prior to irradiation, and therefore, in the corresponding $\%\Delta i$, as is actually observed. A like reduction in $\%\Delta i$ is not appreciable in a thermal device like a vacuo-junction, since the corresponding loss by resistive damping of i_{HF} is represented by conversion into heat. It is to be anticipated, therefore, that $\%\Delta i$ would decrease as R is increased. This is in agreement with the results. These considerations also account for the decrease in $\%\Delta i$ with increase in the exciting potential, since it has been found experimentally that as kV increases i_{LF} preponderates.

ACKNOWLEDGMENT

In conclusion, I express my grateful thanks to Prof. Joshi, D.Sc. (London), F.N.I., for suggesting the problem and kind interest during the work.

PHYSICAL CHEMICAL LABORATORIES,
BENARES HINDU UNIVERSITY.

REFERENCES

1 Joshi, 1929, *Trans. Faraday Soc.*, **25**, 120.

2 ,, 1943, Presi. Address, Chem. Sec., Indian Sci. Cong.

3 ,, 1943, *B. H. U. Journ.*, **8**, 99.

4 ,, 1944, *Curr. Sci.*, **13**, 253.

5 ,, 1945a, *Curr. Sci*, **14**, 67.

6 ,, 1945b, *Nature*, **154**, 147.

7 ,, 1945c, *Proc. Ind. Acad. Sci*, **22**, 4.

MEASUREMENTS OF TEMPERATURE OF THE DIFFERENT PARTS OF A RADIO RECEIVER AND OF THE OSCILLATOR DRIFT DURING WARMING-UP PERIOD

By I. L. CHAKRAVARTY

(*Received for publication, Sept. 12, 1946*)

ABSTRACT. Temperature variations of the different parts of a radio receiver (Philips 595 IIN) were measured. The temperature rise was the highest above the ballast tube, the maximum temperature rising to about 84°C. Near the I.F. transformer the temperature rose to little over 42°C. Of the five positions the region just above the gang condenser showed the minimum rise in temperature. The steady temperature was attained at least after 2½ hours' operation.

The frequency of the oscillator was found to decrease gradually from 2515 Kc/s to 2492 Kc/s, corresponding to the change of temperature from 31° to 35°C near the oscillator coil.

INTRODUCTION

To the designer of a radio receiver, the study of temperature variations of the different parts is indeed an important problem, so far as the selection, treatment and proper placing of the component parts are concerned. The different parts of the receiver rise to widely different temperatures during the warming-up period. This rise of temperature has sometimes a marked effect on the working of a receiver and its longevity. Temperature variations cause minute mechanical movements and distortion of components and they also change the electrical properties, such as the dielectric constant and insulation resistance of materials. Owing to high order of sensitivity in modern receivers, these small changes may effect a serious change in efficiency and alignment of a receiver. In many cases these changes are not fully restored when a corresponding decrease in temperature takes place. This leads to a gradual deterioration in efficiency and performance of a receiver. The rise of temperature may often vary the tuning position, this being due to variation in capacity of the tuning condenser. This drift that occurs during the warming-up period may persist for some time and necessitates alteration of the tuning control to keep the desired station in exact tune. This trouble is often to be found in the short wave bands of a receiver. It is due to gradual changes in the I.F. alignment of a superheterodyne receiver or more frequently to changes in frequency of the oscillator of the receiving system. A study of temperature variation of the different parts of a receiver and its effect is thus of practical importance to a design engineer.

In the present paper results of some experiments on temperature variation of the different parts of a superhet receiver and on the frequency drift of the

oscillator system in the receiver during the warming-up period are given. The receiver under test was a Philips set, Model No. 595 HN. Similar work on the effect of temperature was reported by Scott (1938).

ARRANGEMENT AND PROCEDURE

The Philips 595 HN. receiver was placed in the middle of a room such that the walls were at least at a distance of 10′ feet on all sides. This was done to ensure that there was no appreciable reflected radiation from the walls affecting the receiver parts. Sensitive thermometers were placed one at each of the following positions.

1. Above the ballast tube.
2. Beneath the chassis centre.
3. Near I.F. transformer.
4. Beneath the chassis near coils.
5. Just above gang condenser.

Before the commencement of observations the receiver was not worked at all for about 4 to 5 hours in order to ensure that all parts of the receiver were at the room temperature at the time of the commencement of observation. Observations were started as soon as the receiver was switched on. For an hour, readings of the thermometers were noted down at an interval of 10 mins. and then at an interval of half an hour for three hours more.

EXPERIMENTAL RESULTS ON TEMPERATURE VARIATION

The experimental results of the temperature variations for the five

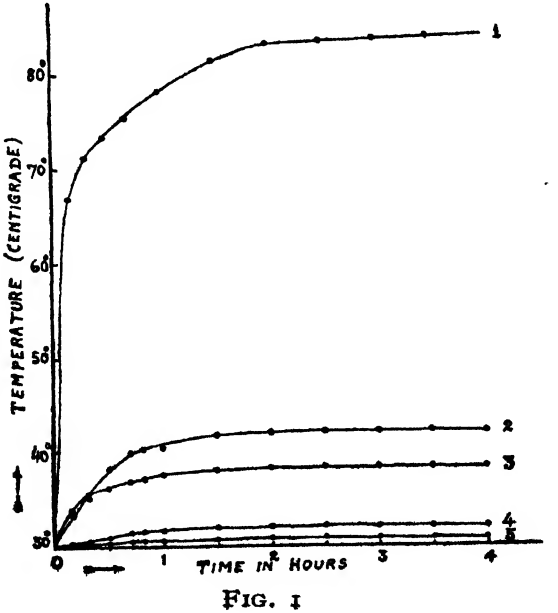

FIG. 1

different parts of the receiver are shown in Fig. 1. The temperature rise was the highest above the ballast tube—the maximum temperature rising to about 84°C. Near the I.F. transformer the temperature rose to a little above 42°C. Of the five positions the region just above the gang condenser showed the minimum rise in temperature. It will be noted that the steady temperatures were not attained until after at least 2½ hours' operation.

DETERMINATION OF OSCILLATOR FREQUENCY DRIFT WITH TEMPERATURE

The change in the frequency of the oscillation of the receiver was noted on a small calibrated vernier-condenser placed in parallel with the main tuning condenser of a heterodyne wave-meter. There was a definite fre-

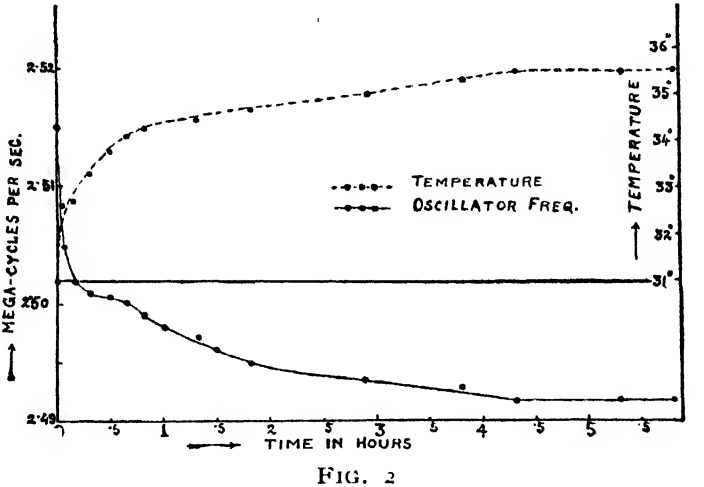

FIG. 2

quency drift which is graphically shown in Fig. 2. Initial oscillator frequency was 2515 Kc/s. The temperature change during this experiment is also shown in the same diagram.

The temperature near the oscillator coil changed from 31°C to 35°C. The frequency of the oscillator was found to decrease gradually from 2515 Kc/s to 2492 Kc/s. In this experiment the temperature attained a constant value after about 4 hrs. The total reduction of oscillator frequency during this time was 22.2 Kc/s.

ACKNOWLEDGEMENT

My sincere thanks are to Dr. S. R. Khastgir, D.Sc., for suggesting the problem and for his help in this work.

PHYSICS DEPARTMENT
DACCA UNIVERSITY.

REFERENCE

Scott, A. H., 1938, Proc. World Radio Convention, April (Sydney).

The following special publications of the Indian Association for the Cultivation of Science, 210, Bowbazar Street, Calcutta, are available at the prices shown against each of them :—

No.	Subject	Author	Price Rs. A. P.
III	Methods in Scientific Research ...	Sir E. J. Russell	0 6 0
IV	The Origin of the Planets ...	Sir James H. Jeans	0 6 0
V	Separation of Isotopes ...	Prof. F. W. Aston	0 6 0
VI	Garnets and their Role in Nature. ...	Sir Lewis L. Fermor	2 8 0
VII (1)	The Royal Botanic Gardens, Kew. ...	Sir Arthur Hill	1 8 0
(2)	Studies in the Germination of Seeds. ...	,,	
VIII	Interatomic Forces ...	Prof. J. E. Lennard-Jones	1 8 0
IX	The Educational Aims and Practices of the California Institute of Technology ...	R. A. Millikan	0 6 0
X	Active Nitrogen A New Theory ...	Prof. S. K. Mitra	2 8 0

A discount of 25% is allowed to Booksellers and Agents.

Born Feb 11, 1884

Died Dec 23, 1946

Prof. P. N. Ghosh

M.A., Ph.D., Sc.D. (Hon.), F.Inst.P, F.N.I.

Honorary Secretary, Board of Editors, Indian Journal of Physics
(1936 1946)

President, Indian Physical Society (1943 1945)

Sir R. B. Ghosh Professor and Head of the Department of Applied Physics, Calcutta University, since the foundation of the Department.

Member of the Managing Commitee and Fellow of the Indian Association for the Cultivation of Science, Calcutta.

President, Physics Section, Indian Science Congress, (1941)

Foundation Fellow of the National Institute of Science, India.

Chairman of the Industrial Survey Committee, Government of Bengal.

Member of the Senate, Calcutta University.

Member of the Faculties of Arts and Science, Calcutta University.

Fellow of the Royal Asiatic Society of Bengal.

THE EFFECT OF THE SOLVENT ON DIPOLE MOMENT

By G. R. PARANJPE* AND M. B. VAJIFDAR

(Received for publication, Oct. 15, 1946)

ABSTRACT. The dielectric constant of dilute solutions of propyl bromide, propyl iodide, butyl chloride, butyl bromide and butyl iodide is measured in each of the solvents hexane, heptane, carbon tetrachloride, benzene and toluene by the method of resonance. The results are used to calculate the apparent electric moment in solution using the Debye equation and volume fractions.

The various empirical and theoretical relations are found suitable for representing the results. The customary extrapolation to $\epsilon=1$ for calculating μ_{gas} has failed to give consistent results. Extrapolating to $\epsilon=1.7$ the values obtained from the various relations are not only self-consistent but also agree with the experimentally determined value in the vapour state.

The formula of Goss is found to give a better agreement than the rest.

The effect of the solvent in the measurements on dipole moment was brought into prominence by the results of Müller (1933) on the polarization of chlorobenzene in a number of solvents. It was then realised that electric moments estimated from measurements on dilute solutions needed reconsideration and the problem was studied from both theoretical and practical points of view in an effort to discover a relationship between the apparent moment in solution and the real moment in the gaseous state. It is usual to extrapolate to $\epsilon=1$ to obtain the moment in the gaseous state. Davar and Paranjpe (1941) observed that extrapolation to $\epsilon=1.7$ gave a better agreement between the values derived from the various empirical equations. The present work was undertaken to re-examine the validity of the various solvent effect equations and of the suggestion of Davar and Paranjpe to extrapolate to $\epsilon=1.7$ instead of to $\epsilon=1$.

The apparent electric moment of propyl bromide, propyl iodide, butyl chloride, butyl bromide and butyl iodide was measured in each of the solvents hexane, heptane, carbon tetrachloride, benzene and toluene. Sugden (1937) has determined the electric moment in the vapour state of the solutes and his values are useful for comparison with our experimental results.

The apparatus and the procedure are the same as in the previous work on this subject carried out in this laboratory, except that in the present work a tri-tet crystal-controlled oscillator was used.

Tables I*a* and I*b* give the experimental results.

* Fellow of the Indian Physical Society.

TABLE Ia

	Propyl Bromide			Propyl Iodide		
	$_\infty P_2$	$_\infty P_{E_2}$	μ_{sol}	$_\infty P_2$	$_\infty P_{E_2}$	μ_{sol}
Hexane ...	111.2	24.0	2.07	102.2	25.1	1.94
Heptane	109.5	24.0	2.06	100.4	25.2	1.92
Carbon Tetrachloride ...	104.9	24.0	1.99	98 7	27.9	1.86
Benzene ...	102.3	23.4	1.97	98.6	29.3	1.84
Toluene ...	98.9	23.2	1.93	95.8	27.7	1.83

TABLE Ib

	Butyl Chloride			Butyl Bromide			Butyl Iodide		
	$_\infty P_2$	$_\infty P_{E_2}$	μ_{sol}	$_\infty P_2$	$_\infty P_{E_2}$	μ_{sol}	$_\infty P_2$	$_\infty P_{E_2}$	μ_{sol}
Hexane ...	109.3	24.8	2.03	114.6	25.6	2.09	111.1	29.2	2.00
Heptane ...	108.9	25.3	2.02	114.2	30.4	2.03	110.8	30.4	1.98
Carbon Tetrachloride ...	103.3	25.3	1 95	108.6	28.4	1.98	109 6	33.0	1 94
Benzene ...	102.3	25.6	1.94	107.4	27 5	1.98	106.2	32 3	1.93
Toluene	100.4	25.5	1.92	105.8	27.5	1.96	105.8	32.4	1.90

$_\infty P_2$ stands for molar polarization of the solute at infinite dilution.

$_\infty P_{E_2}$ stands for electronic polarization (molar refraction) of the solute at infinite dilution.

μ_{sol} stands for the electric moment in solution.

In calculating the molecular polarization we used Van Arkel and Snoek's (1934) modification based on volume fractions. In this method it is not necessary to determine the density of the solution at different concentrations and the observations and calculations are considerably simplified. Polarization at infinite dilution was calculated on the assumption of Sugden's relation. The electronic polarization, P_{E_2}, was calculated from the measurement of refractive index using a Pulfrich refractometer (Na-D lines). The electric moment of the solute was calculated from

$$\mu = 0.01273 \sqrt{(_\infty P_2 - _\infty P_{E_2})T} \text{ Debye units,}$$

T being the absolute temperature of the solution.

The discussion of our experimental results will be considerably facilitated by dividing the discussion under three headings, *viz.* (1) empirical relations for correcting the solvent effect, (2) theoretical considerations of factors not included in the Debye equation and (3) the empirical relations of Goss.

1. EMPIRICAL RELATIONS FOR CORRECTING THE SOLVENT EFFECT

The following empirical relations have been tried :—

$$\frac{P_0^{sol}}{P_0^{gas}} = 1 - 0.075\,(\epsilon - 1)^2 \qquad \text{(Müller, 1933, 1934)}$$

$$P_2 = A \pm B\,\frac{\epsilon - 1}{\epsilon + 2} \qquad \text{(Sugden, 1934)}$$

$$P_2 = K_1 + \frac{K_2}{\epsilon} \qquad \text{(Jenkins, 1934)}$$

$$P_2 = \frac{a}{\sqrt{\epsilon}} \qquad \text{(Davar and Paranjpe, } \textit{loc. cit.}\text{)}$$

Tables II and III give the values of P_0^{gas} and μ_{gas} calculated from our observations on the assumption of Müller's relation.

TABLE II

P_0^{gas} calculated from Müller's relation

	Propyl Bromide	Propyl Iodide	Butyl Chloride	Butyl Bromide	Butyl Iodide
Hexane	92.57	81.80	89.66	94.55	87.07
Heptane	92.	80 60	89.51	89.69	86.06
Carbon Tetrachloride	91.05	9 68	87.70	90 17	86.20
Benzene	89 60	78 78	87.11	90.75	86.17
Toluene	87.89	79.08	86.98	90.96	85.21
Mean	90.75	79.98	88.19	91.24	86.14
Observed values in vapours (Sugden)	94.45	82.55	90.97	94.45	88.40

TABLE III

μ_{gas} calculated from Müller's relation

	Propyl Bromide	Propyl Iodide	Butyl Chloride	Butyl Bromide	Butyl Iodide
Hexane	2.13	2.00	2.10	2.15	2.06
Heptane	2.13	1.99	2.09	2.10	2.05
Carbon Tetrachloride	2.11	1 98	2.07	2.10	2.05
Benzene	2.09	1.96	2.07	2.11	2.05
Toluene	2.07	1.97	2.06	2.11	2.04
Mean	2.11	1 98	2.08	2.11	2.05
Observed values in vapours (Sugden)	2.15	2.01	2.11	2.15	2.08

Tables IV and V give similar values calculated on the assumption of other relations. In each table we give Sugden's values as determined in the vapour state for ready reference.

TABLE IV

P_2^{gas} calculated from empirical relations
(extrapolation $\epsilon = 1$)

	Propyl Bromide	Propyl Iodide	Butyl Chloride	Butyl Bromide	Butyl Iodide
Sugden's relation	146 4	115.5	134.6	140 4	127.0
Davar & Paranjpe's relation	157.2	119.8	142.2	148:1	131.9
Jenkins' relation	169 3	124.7	150.5	156.6	148.6
Observed values in vapours (Sugden)	118.2	111.5	116.4	122.8	121 9

TABLE V

P_2^{gas} calculated from empirical relations
(extrapolation $\epsilon = 1.7$)

	Propyl Bromide	Propyl Iodide	Butyl Chloride	Butyl Bromide	Butyl Iodide
Sugden's relation	117 8	104.1	113 8	119 3	114.5
Davar & Paranjpe's relation	118.6	104.4	114.4	119 8	114.9
Jenkins' relation	119.4	104.7	114.9	120 3	117 4
Observed values in vapours (Sugden)	118 2	111.5	116.4	122 8	121.9

It will be seen from these tables that none of the relations when extrapolated to $\epsilon = 1$ give consistent results. When the extrapolation is carried out only to $\epsilon = 1.7$, the values obtained from the various relations are not only self-consistent but they also agree with the experimentally determined value in the vapour state. It should be pointed out that the extrapolation to $\epsilon = 1.7$ does not appear to improve the agreement in the case of propyl iodide.

II. THEORETICAL CONSIDERATION OF FACTORS NOT INCLUDED IN THE DEBYE EQUATION

All the theories of the solvent effect agree in stating that

$$\mu_s = \mu_{gas} + \mu_{induced}.$$

They, however, differ from one another in considering the various factors responsible for the induced moment, $\mu_{induced}$. Still all agree in assuming that

$\mu_{induced}$ depends on the shape of the molecule and the position of the dipole in it. The parameters in the following relations depend on these two factors, *viz.*, the shape of the molecule and the position of the dipole:—

$$\frac{\mu_{sol}}{\mu_{gas}} = 1 + \frac{\epsilon - 1}{\epsilon + 2} C \qquad \text{(Weigle, 1933)}$$

$$\mu_{sol} = a + \frac{b}{\epsilon} \qquad \text{(Frank, 1935)}$$

where $a = (1 + A_1 + A_2).\mu_{gas}$ and $b = -(A_1 + A_2).\mu_{gas}$.

Here also μ_{gas} can be calculated for $\epsilon = 1$ and for $\epsilon = 1.7$ and again as before $\epsilon = 1.7$ gives a much better agreement (Tables VI and VII). Further, we find that an equation of the type

$$\mu_{sol} = \frac{a}{\sqrt{\epsilon}}$$

can also be applied to the experimental results.

TABLE VI

μ_{gas} calculated from the equations of Weigle, Frank, and the authors (extrapolation $\epsilon = 1$)

	Propyl Bromide	Propyl Iodide	Butyl Chloride	Butyl Bromide	Butyl Iodide
Weigle's equation	2.48	2.26	2.37	2.33	2.28
Frank's equation	2.68	2.46	2 58	2.50	2 45
Authors' equation	2.55	2 35	2.47	2.41	2.36
Observed values in vapours (Sugden)	2.15	2.01	2.11	2 15	2.08

TABLE VII

μ_{gas} calculated from the equations of Weigle, Frank, and the authors (extrapolation $\epsilon = 1.7$)

	Propyl Bromide	Propyl Iodide	Butyl Chloride	Butyl Bromide	Butyl Iodide
Weigle's equation	2.15	1.99	2.09	2.11	2.05
Frank's equation	2.14	2.01	2.11	2.11	2.06
Authors' equation	2.14	2.00	2.10	2.11	2.06
Observed values in vapours (Sugden)	2.15	2.01	2.11	2.15	2.08

Hobbs (1939) has modified Onsager's theory of reaction field and calculated the value of ${}_{\infty}P_0^{sol}$ from the known values of P_0^{gas}. In the present work we determine P_0^{sol} experimentally and we desire to calculate P_0^{gas}. We, therefore rewrite Hobbs's equation as

$$\frac{P_0^{gas}}{P_0^{sol}} = 1 + \frac{C'\mu R}{3KT}$$

The results obtained on the assumption of this equation are given in Table VIII.

TABLE VIII

P_0^{gas} and μ_{gas} calculated from Hobbs's equation

		Propyl Bromide	Propyl Iodide	Butyl Chloride	Butyl romide	Butyl Iodide
P_0 gas	Calculated from Hobbs's equation	115.3	92·8	102.1	100.2	95.3
	Observed values in vapours (Sugden)	94·5	82.6	91 0	94.5	88.4
μ_{gas}	Calculated from Hobbs's equation	2 38	2.13	2 24	2.22	2.16
	Observed values in vapours (Sugden)	2.15	2.01	2.11	2.15	2.08

It will be seen that the values of P_0^{gas} and μ_{gas} thus calculated are much higher than those experimentally observed by Sugden for vapours. This probably means that in this calculation, following Hobbs, we have over-emphasised the effect of the reaction field.

We also tried to calculate the values of μ_{gas} by using the following equation of Higasi (1936) :

$$\frac{\mu_{sol}}{\mu_{gas}} = 1 + 3\frac{\epsilon - 1}{\epsilon + 2}A.$$

As direct determination of the ratio of the axes of molecular ellipsoid as required by Higasi is not available for the solutes, an attempt was made to estimate it by three methods, *viz.* (1) from optical polarizabilities, (2) from molecular model and X-ray data, and (3) from the empirical relations of Goss. Values of μ_{gas} calculated with the values of this ratio obtained by these three methods showed differences among themselves and the agreement with the value of μ_{gas} observed is not satisfactory, the variations being from 5% to 10%.

III. THE EMPIRICAL RELATIONS OF GOSS

The assumptions made by Goss (1937, 1940) in his empirical relations for the solvent effect are the same as those of Raman and Krishnan, and Onsager. Goss's equation is

$$P_\infty = P_{R+A} + \left(\frac{\epsilon-1}{\epsilon+2}\right)^4 . Z + \frac{Y}{\epsilon}$$

where $P_{R+A} = 1.05\,[R_L]_D$, 5% of the molar refraction being added to account for the atomic polarization. Y and Z are constants.

Goss uses a graphical method to determine the value of these parameters Y and Z. He, however, uses a curvilinear extrapolation of the graph which cannot be justified. His formula and the index 4 attributed to $e^{\frac{\epsilon-1}{\epsilon+2}}$ seems to be reasonable. We have seen by trial and error method that index 4 gives the best agreement between the experimental values from solution and vapour data. Thus we prefer to retain Goss's equation but not his method of curvilinear extrapolation. Even here extrapolations to higher values than $\epsilon = 1$ seems to give better agreement. We observed that the values calculated from the formula of Goss without the curvilinear extrapolation give a better agreement with Sugden's data for vapours. This agreement is much better than the agreement obtained by the use of any other empirical formula.

TABLE IX

μ_{gas} calculated from different equations
$\epsilon = 1.7$ for all solvents (together)
$\epsilon = 1.81$ for carbon tetrachloride (singly)

Equations	Propyl Bromide	Propyl Iodide	Butyl Chloride	Butyl Bromide	Butyl Iodide
Müller	2.10	1.98	2.08	2.11	2.05
Jenkins	2.17	1.95	2.09	2.13	2.05
Sugden	2.15	1 94	2.08	2.12	2.02
Davar and Paranjpe	2.16	1.95	2 09	2 12	2.02
Weigle	2.15	1 99	2.09	2.11	2.05
Frank	2.14	2.01	2 11	2 11	2.06
Authors	2.14	2.00	2.10	2.11	2.06
Goss	2.14	2.00	2.10	2.13	2.08
Mean of 2 to 8	2.15	1.98	2 09	2.12	2.05
Observed values in vapours (Sugden)	2.15	2.01	2.11	2.15	2.08

ACKNOWLEDGMENTS

Our thanks are due to Dr. D. J. Davar for assisting at various stages of the work and to Dr. S. M. Sethna for preparing pure samples of the solutes used in the work.

DEPARTMENT OF PHYSICS,
ROYAL INSTITUTE OF SCIENCE,
BOMBAY.

REFERENCES

Davar and Paranjpe, 1941, *Ind. Jour. Phys*, **15**, 178.
Frank, 1935, *Proc. Roy. Soc.*, **152A**, 171.
Goss, 1915, *J C. S.* 1937, *ibid.*, 1940, 752
Goss, 1937, *J. C. S*, 1915
Goss, 1940, *J C. S.*, 752.
Higasi, 1936, Sci. Papers, *Inst. Phys. Chem Res. (Tokyo)*, **28**, 284.
Hobbs, 1939, *J. Chem Phys.*, **7**, 849.
Jenkins, 1934, *Trans. Farad. Soc.*, **30**, 739
Müller, 1933, *Physik. Zts.*, **34**, 689,
Müller, 1934, *Physik. Zts.*, **35**, 346.
Sugden, 1934, *Nature*, **133**, 802.
Sugden, 1937, *J. C. S.*, **161**.
Van Arkel and Snoek, 1934, *Trans Farad Soc*. **30**, 721.
Weigle, 1933, *Helv. Phys. Acta.*, **6**, 68.

MEASUREMENTS OF THE INTENSITY OF THE NIGHT SKY LIGHT AT CALCUTTA

By S. N. GHOSH

(*Received for publication, Nov. 29, 1946*)

ABSTRACT. The paper describes the results of measurements of the night sky intensity variation made at Calcutta on selected nights in 1943-45, taking advantage of the black-out condition of the city. It was found that on undisturbed nights, the night sky intensity decreased with advance of night, attained a minimum near about local midnight and then again increased. This trend of variation is the same as that observed by Karandikar (1934) at Poona and Elvey (1943) at Texas.

Of the total 50 nights observed, 30 per cent were found to be disturbed *i.e.*, the intensity variations were erratic. Not all such nights were associated with magnetic activity. On disturbed nights which were accompanied by magnetic disturbance, the trend of variation was approximately the same as the variation of maximum ionisation of Region-F. (The data for the latter were available from the regular ionospheric observations made at the University College of Science, Calcutta, under the auspices of the Radio Research Committee of the Council of Scientific and Industrial Research.) The significance of this correlation is discussed and it is shown that it supports the hypothesis of Mitra (1943) in which the luminescent layer is identified with Region-F.

There were also nights in which the night sky intensity varied abnormally but the electron density of Region-F did not follow the same trend. These nights were found to be *free* from magnetic disturbance.

INTRODUCTION

Measurements of the intensity of the night sky light (both the total intensity and the intensities of the different spectral components) carried out in different parts of the world show that the intensity is variable. The variations, as measured by different observers, may conveniently be classified as follows:

1. Long period (eleven-year solar cycle) variation.—This shows strong positive correlation with the mean yearly sunspot area (Rayleigh and Jones, 1935; Smith, Gilliland and Kirby, 1938).

2 Seasonal variation.—This has maxima at equinoxes and minima at solstices (Martyn and Pulley, 1936).

3. Nightly variation.—This has a regular and an irregular part. The irregular variation shows strong correlation with magnetic activity (Barber, 1941) and, as such, its origin may be the same as that of aurora and magnetic storm, namely, bombardment of the upper atmosphere by charged particles emanated from the sun. In regard to the regular part, opinions of observers are unfortunately not the same as to its variation. In the Table given below, the available data on this point are summarised.

It will be noticed from the Table that there is considerable divergence regarding the nature of the variation as observed in different parts of the world. It was therefore thought that additional data might throw more light on the point and observations were made at Calcutta (lat. 22°33 N., long. 88° 21 E.) on selected nights during the years 1943-45 taking advantage of the black-out condition of the city. It should be mentioned that owing to unfavourable weather condition, observations could be carried out only for seven months in a year—October to April.

Another object of the investigation was to test Mitra's hypothesis of the night sky emission (Mitra, 1943 ; Ghosh, 1943). In this hypothesis, Region-F of the ionosphere has been identified with the luminescent layer of the night sky. The reaction which excites the night sky spectrum is one of electron transfer from negative ions of atomic oxygen to positive ions of nitrogen molecules, both of which are abundantly present in the Region-F at night. According to the theory, therefore, one would expect some sort of a correlation between nocturnal variation of electron density of Region F and that of night sky intensity. In order to test if such correlation existed, simultaneous observa-

Observer	Place of observation	Observed region of spectrum	Nature of variation
Rayleigh (1929)	Terling, England	Wavelengths shorter than λ5577	The intensity increases as night progresses ; attains a maximum near about local midnight and then begins to decrease again.
Cerniajev, Kvostikov and Panschin (1937)	Caucasus mountains	λλ4550 to 5900	,, ,,
Barber (1941)	Mt. Hamilton, Central California	Yellow green region	In addition to a maximum near about local midnight, there is some indication of a secondary maximum at about 3 A M.
Bradbury and Sumerlin (1940)	,, ,,	Red and blue regions	For the blue radiation, the variation is same as that found by Rayleigh. For the red , there is a steady decrease throughout the night.
Karandikar (1934)	Poona, India	Red, green, blue and violet regions	The intensity decreases as night progresses, attains a minimum near about local midnight and then begins to rise again.
Elvey (1943)	McDonald Observatory, Texas, U. S. A.	Total intensity	The variations can be classified into two groups: (i) Same as that found by Karandikar. (ii) There is a slow and steady decrease in intensity throughout the night.

tions of night sky intensity and of the electron density were made on dark clear nights as were available, four days before and four days after the new moon of every month. Unfortunately, the electron density measurements

could only be started from October, 1944. This was because the transmitting licence of the ionosphere apparatus with which the observations were being carried out under the auspices of the Radio Research Committee of the C. S. I. R. had been withdrawn due to war. This was restored from about that date.

With the cessation of the black-out condition in the city in May, 1945, the investigation had to be suspended due to interference of stray light.

EXPERIMENTAL ARRANGEMENT

The experimental equipment for the measurement of the night sky light is essentially that used by Fabry (1910) and is shown in Fig. 1. A telescope with

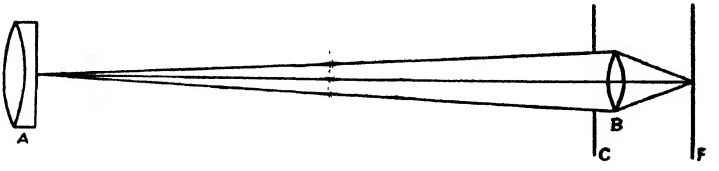

FIG. 1

Telescopic arrangement for intensity measurement of night sky light by photographic blackening. A—object glass, C—a circular opening in the focal plane of A. B forms an image of the exit pupil of the objective on the photographic film F.

objective A and eyepiece B is pointed towards the region of the sky to be studied. The objective is achromatic, 4″ in diameter and 57 cm. in focal length. In its focal plane a circular opening C is placed. The eyepiece placed behind the opening is a double convex lens of focal length 3 cm. A single lens is used as the eyepiece in order to reduce the absorption of light. The eyepiece throws on the photographic film F an image of the exit pupil of the objective. The telescope receives light from a solid angle of about 1.5×10^{-3} radian of the sky. It is clear that C being in the focal plane of the objective, the image on the photographic film will have uniform illumination. The film-holder could be moved up and down by a rack and pinion arrangement so that different parts of the film could be exposed when necessary.

Observations were made on dark clear nights at every hour, starting in majority of cases at 9 P.M. and ending before the morning twilight. The telescope was focussed 6° above the Pole Star. This region was chosen because of the absence of bright stars therein throughout the night. Photographic impressions were taken on H.P. 3 (Ilford) cut-film which gives sufficient blackening for an exposure of 3 minutes only. All the impressions of a single night were taken on one and the same film and were measured by a Moll microphotometer next day.

RESULTS OF OBSERVATIONS

Out of the total 50 nights observed, the variation on 35 nights followed a typical course. On such nights the intensity decreased with the advance of night, attained a minimum near about local midnight then again increased (Fig. 2). From data obtained from Alibag Observatory, it was found that

these nights were free from magnetic activity. The trend of variation of

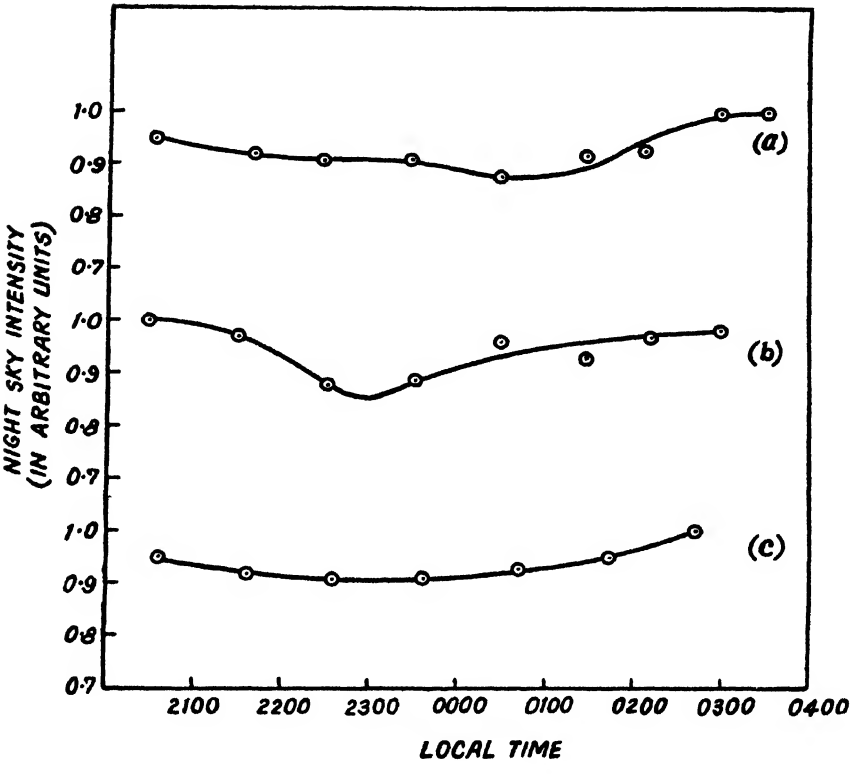

FIG. 2

Typical variation of the night sky intensity. (a) Feb. 23-24, 1944; (b) Feb. 26-27, 1944; (c) Oct. 17-18, 1944. The intensity decreases with the advance of the night, attains a minimum near about local midnight and then again increases. (The maximum intensity is taken as unity.)

night sky light at Calcutta is, therefore, same as that observed by Karandikar (1934) at Poona and Elvey (1943) at Texas. Elvey, however, found in addition nights in which there is a slow and steady decrease in intensity throughout the night. No such nights were found in our observations.

30 per cent of the observed nights were found to be disturbed, *i.e.*, the intensity variation was erratic. Not all of such nights were, however, associated with magnetic activity.

Simultaneous observations of Region-F electron density and of the night sky light showed that on undisturbed nights, on which, the night sky intensity showed a typical variation, f_F^2 (which is proportional to electron density) also did the same. The two variations, however, did not follow similar trend. While the typical variation of the night sky intensity was as described above,

that of the Region-F electron density was as follows: there was a decrease of electron density immediately after nightfall, the decrease continued up to the midnight when there was a tendency to rise. Afterwards the density fell gradually to about one-fourth of the evening value before sunrise. Fig. 3 shows typical variations of night sky intensity and the corres-

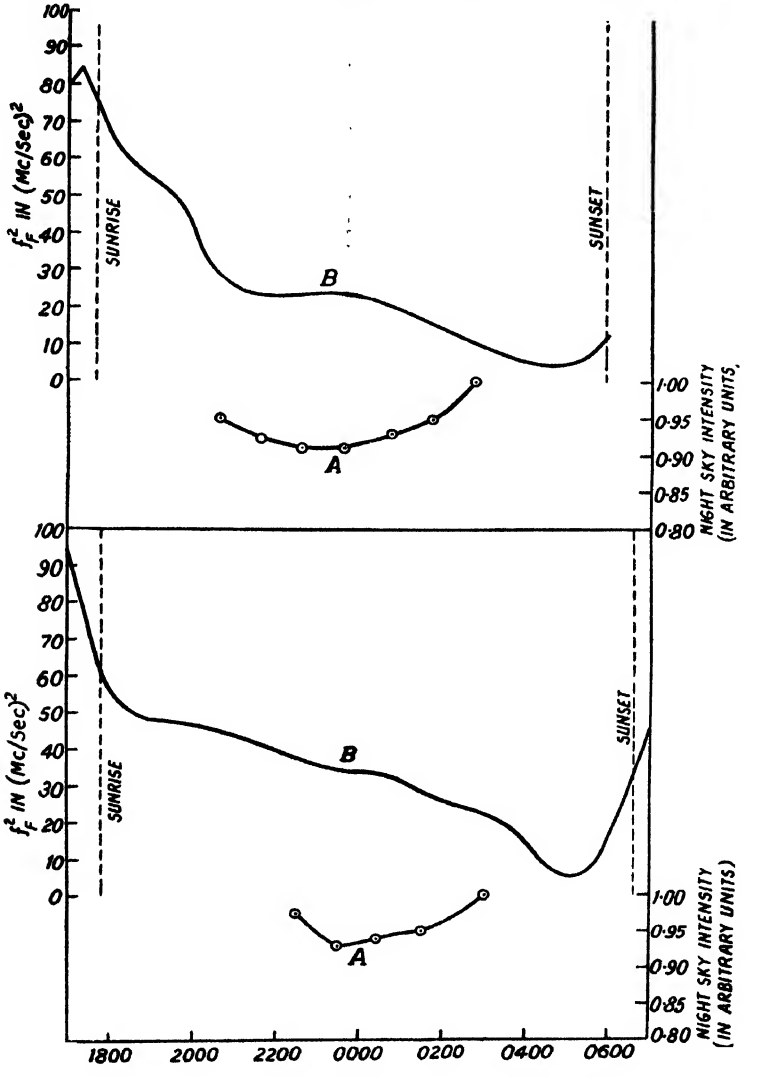

FIG. 3

Comparison of the variations of the night sky intensity (A) with the corresponding variation of $f_F{}^2$ (B) for two *normal* nights. Upper curves are for Oct. 5-6, 1944 and the lower for Oct. 17-18, 1944. Note that the variation of the night sky light intensity does not follow that of $f_F{}^2$.

ponding variation of f_F^2 for two normal nights. It is at once noticed that the two variations do not follow each other. That there may not be any correspondence between the two variations is also expected from Mitra's hypothesis.

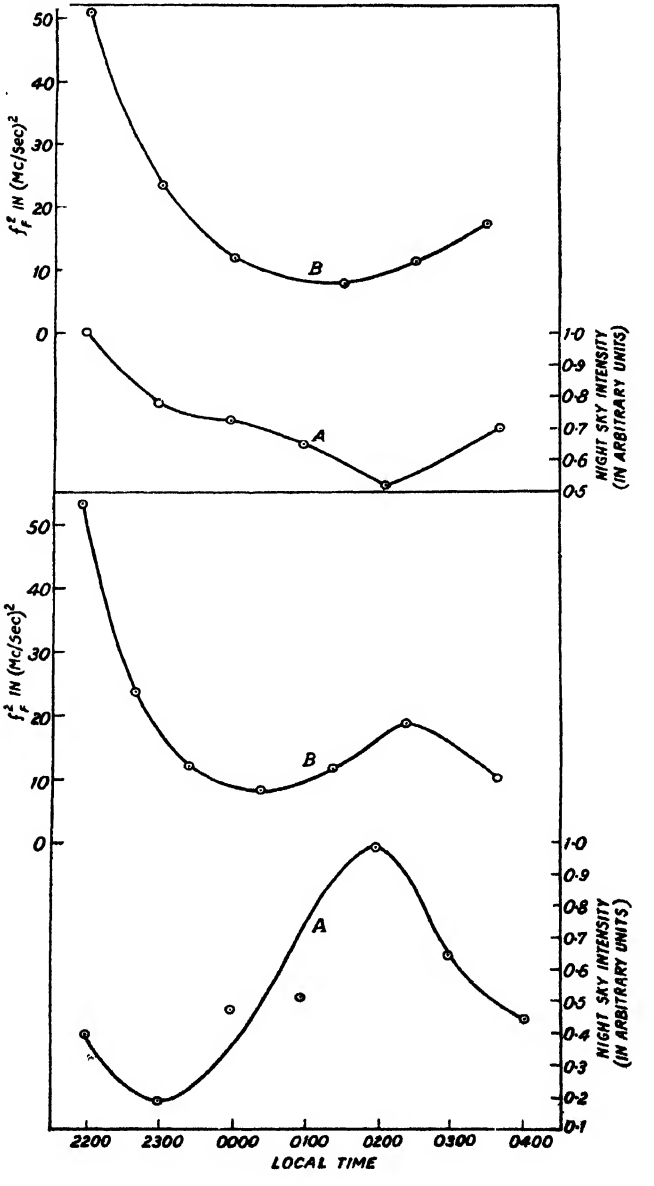

FIG. 4

Comparison of the variations of the night sky intensity (A) with that of f_F^2 (B) for two *abnormal* nights *with* magnetic disturbances. The upper curves are for Feb 14-15, 1945 and the lower curves for Feb. 15-16, 1945. It is to be noticed that the variation of the night sky intensity follows the same trend as that of f_F^2.

During the period of the investigation, there were two abnormal nights, namely, Feb. 14-15 and 15-16, 1945 on which there were magnetic disturbances. On these nights it was found that the variation of the intensity of the night sky light followed the same trend as that of f_F^2. In Fig. 4 the two variations are compared. It will be noticed that the two curves run approximately parallel to each other. A proof in support of Mitra's hypothesis is thus furnished.

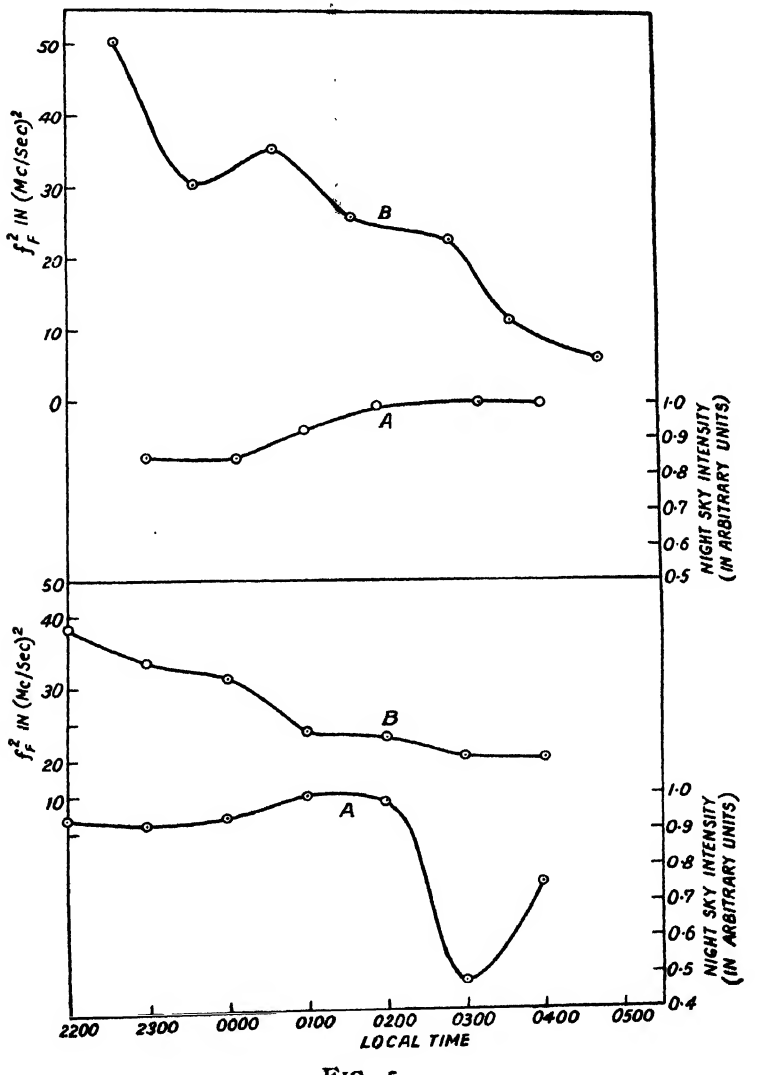

FIG. 5

Comparison of the variations of the night sky intensity (A) with that of f_F^2 (B) for two *abnormal* nights *free* from magnetic disturbances. Upper curves are for April, 16-17, 1945 and the lower curves for January 18-19, 1945. Note that the variation of f_F^2 does not follow that of the night sky intensity.

There are also nights in which, though the night sky light varied abnormally, the variation of f_F^2 did not follow that of the night sky intensity. These nights were found to be *free* from magnetic activity. In Fig. 5 the variations of night sky intensity for two such nights are compared with those of f_F^2. It will be seen that there is hardly any similarity between the two.

DISCUSSION

It appears that on undisturbed nights, the variation of the night sky intensity in sub-tropical latitudes like those of India follows a trend similar to that at Texas (lat. 31°30 N).

On disturbed nights which are accompanied by magnetic disturbance, the trend of variation is approximately the same as the variation of maximum ionisation of Region-F. This correlation is discussed below and supports the hypothesis of Mitra that the luminescent layer is to be identified with Region-F.

The variations of electron density, as obtained from ionospheric measurements, are those occurring in the region of maximum ionisation. These variations do not tell anything about the nature of variation of the total number of electrons present in a column of unit cross-section of Region-F. But the intensity of the night sky emission depends precisely on this latter quantity. The electron density, for instance, may increase due to contraction by cooling of the ionised region as a whole, but the total number of electrons in a column of unit cross-section may remain more or less constant.

A positive correlation between the variation of the night sky intensity and the variation of the Region-F maximum density would, therefore, be expected only when the latter variation follows a trend similar to the variation of the electron content of the region as a whole. This is the case with abnormal nights associated with the magnetic activity when the electron content of the region as a whole (not merely the maximum electron density) may be expected to be affected.

Correlation between the variation of the night sky intensity and of the maximum electron density of Region-F may not, therefore, always be expected. It occurs only on nights of abnormal activity with magnetic disturbance.

For similar reason, the long-period variations of night sky intensity and maximum electron density of Region-F should vary concurrently. Several workers (Rayleigh and Jones, 1935, Smith, Gilliland and Kirby, 1938 and Martyn and Pulley, 1936) have, in fact, found unmistakable correlation between the seasonal and eleven-year solar cycle variations of night sky intensity with those of the maximum electron density of Region-F.

It is very significant that no correlation whatsoever has been observed between the Region-E electron density variation and the night sky intensity variation (Bradbury and Sumerlin, 1940). This is what is expected if the night sky luminescence is to originate from Region-F.

ACKNOWLEDGMENTS

The work described in the paper was carried out when I was enjoying an Adair, Dutt Research Scholarship. It is my pleasant duty to record my thanks to the Adair, Dutt Research Fund of the Indian Science News Association for having granted me the scholarship.

I also express my sincere and grateful thanks to Prof. S. K. Mitra for suggesting the work to me and for many helpful discussions in course of the preparation of the paper.

WIRELESS LABORATORY,
UNIVERSITY COLLEGE OF SCIENCE,
92, UPPER CIRCULAR ROAD,
CALCUTTA.

REFERENCES

Barber, D. R., 1941, *Lick. Obs. Bull*, **19**, 105.

Bradbury, N. E. and Sumerlin, W. T., 1940, *Terr. Mag. and Atmos. Elec.*, **45**, 19.

Cerniajev, Kvostikov and Panschin, 1937, *J. de Phys.*, **7**, 149.

Elvey, C. T., 1943, *Astrophys. J.*, **97**, 65.

Fabry, C., 1910, *Comptes Rendus*, **150**, 272.

Ghosh, S. N., 1943, *Proc Nat. Inst. Sci. (India)*, **9**, 301.

Karandikar, J. V., 1934, *Ind. J. Phys.*, **8**, 547.

Martyn, D. F. and Pulley, O. O., 1936, *Proc. Roy. Soc. A*, **154**, 455.

Mitra, S. K., 1943, *Science and Culture*, **9**, 46

Rayleigh, Lord, 1929, *Proc. Roy. Soc A*, **124**, 395.

Rayleigh, Lord, and Jones, H. S., 1935, *Proc. Roy. Soc. A*, **151**, 22.

Smith, N., Gilliland, T. R. and Kirby, S. S., 1938, *J. Nat. Bur. Stand.*, **21**, 835.

THEORY, CONSTRUCTION AND WORKING OF MAHAJAN'S HUMIMETER

By L. D. MAHAJAN*

(*Received for publication, October 15, 1946*)

ABSTRACT. A new type of hygrometer (Mahajan's Humimeter) has been devised. It has simple costruction and works on the principle of balance. The readings of percentage humidity are indicated by its pointer directly on the scale marked on its dial.

It is a portable instrument of the size of a small table clock, and is useful for factories, offices, workshops and observatories where and when approximate value of the relative humidity of the surrounding atmosphere is required in a short time.

It is not as accurate as the Mahajan's Optical hygrometer but is, however, much more accurate than many other types of hygrometers, such as, hair hygrometer, paper hygrometer, etc, Its aproximate percentagge of error is ± 2.

The details of its construction, working and theory are given below.

INTRODUCTION

In 1941, the author devised an Optical hygrometer (later on called the Mahajan's optical hygrometer, (Mahajan, 1941*a*), Government of India patent No. 30221), which works on the principle of balance, and the observations of which are recorded by means of lamp and scale arrangement ; This instrument proved a most sensitive and accurate hygrometer, it is used in observatories and laboratories where and when very accurate observations are required, or when very minute changes of humidity are to be detected. But this has its own difficulties, such as, long time in setting; extra care to look after it, and not easily portable due to lamp and scale arrangement. It is why it cannot be used in factories and offices where rough values of the relative humidity or percentage humidity of the surrounding air is required. In view of all these difficulties, the author has now devised another type of hygrometer (called Mahajan's Humidity meter, in brief, Humimeter) which will serve the above mentioned purposes.

It is a portable instrument of the size of a small table clock. It indicates directly on its dial, the approximate value of the percentage of humidity of its surrounding atmosphere in a short time. Its construction and theory are simple and are given below in detail:

CONSTRUCTION

Its complete construction is given in figure 1, where E G and F H are two thin circular discs of any light metal, and diameter about 10 cms. They

* Fellow of the Indian Physical Society.

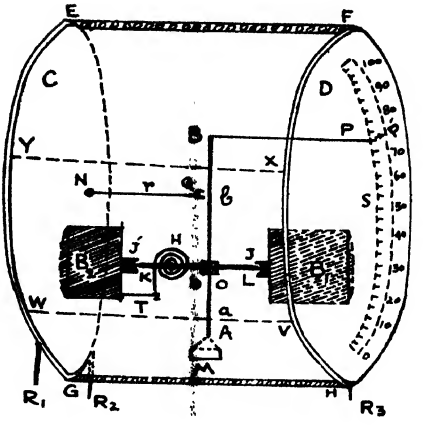

FIG: 1.

are joined together by means of four rods E F, Y X, W V, and G H, each about 2 mm. thick and about 5 cms. long. Each disc has a small cylindrical block of iron, B_1 or B_2, rigidly attached to it. In the centre of each block, there is a small groove J or J'. These grooves are fitted with jewels as shown in the figure. The hard ends K and L of a strong steel rod about 3 cms. long rest in those grooves. To this revolving rod KL is attached rigidly a balancing rod AB, by means of two small screws O and O'.

The balancing rod AB is made of a light metal and is about 6 cms. long, 2 mm. broad and 0. 5 mm. thick. It rests edgewise on the revolving rod, and has two unequal arms *a* and *b*. The arm *a* is about 1. 5 cms. long, and supports a pan M, while the other arm which is about 3 times longer, has no such pan, but is bent twice at right angles at B and P. The end P' of this arm forms the pointer which moves on the scale S.

On its front, there is a circular dial. On one side of it, there is a half circular slit S, about 3 mm. wide, cut into it. It runs from its bottom to top and is shown in the figure by dotted lines. The arm BP of the pointer after passing through the slit moves on the scale S which is marked on one side of this slit. The slit is graduated in terms of percentage of humidity from 0 to 100%. This scale is coverd with a transparent glass plate, about 2 mm. above it.

The free movement of the revolving rod KL is controlled by means of a fine hair spring H, one end of which is fixed to it, and the other to the support T, The pan M hangs freely from the end A of the balancing rod. It contains some substance which absorbs moisture from the atmosphere surrounding it, and gives out moisture accordingly when the moisture content of the atmosphere decreases. In this case, the same substances were used which had been tested and utilized in the Mahajan's optical hygrometer (Mahajan, 1944*a*).

The whole of its cylindrical side is perforted with small holes for free circulation of air inside it. The whole instrument is supported by the levelling screws R_1, R_2 and R_3, and is always kept in horizontal position. On its back, there is a disc C having a screw N connected to a thin rod *r*. It has a fine jaw Q at its other end. On screwing it in, the jaw holds the balancing rod in position and does not allow it to move. On screwing it out, it loosens the balancing rod, and allows it to move freely. Thus it controls its movements, and makes it convenient for protable purposes.

The quantity of the substance put into the pan M is just sufficient to bring the pointer P′ at zero % humidity when the air is absolutely dry and it points 100% when the surrounding air is fully saturated. This scale is then calibrated by comparison with a standard wet and dry bulb hygrometer.

The figure 1 is not according to any scale, but has been made such that it depicts all the parts of the instrument.

THEORY

The main principle of working is the same as that of Mahajan's optical hygrometer. But it differs in construction from it in some respects, namely:—

(*i*) Instead of two pans in the optical hygrometer, there is only one in the Humimeter.

(*ii*) In place of the second pan, there is a long pointer which moves on the scale S marked on the dial,

(*iii*) The two arms of the balancing rod are not equal. The pointer arm is about three times longer than the pan arm.

(*iv*) There is a hair spring attached to the revolving rod to control its movements.

(*v*) The external shape is cylindrical.

When the humidity of the air increases, the substance in the pan absorbs more moisture, and when the humidity decreases, it gives out some of its moisture to the surrounding air. This increase or decrease in weight is directly proportional to the increase or decrease of % humidity of the air. This variation in the weight of moisture content affects the balancing beam. By increase of weight, the pan M goes down, and the pointer P′ goes up, and the reverse takes place, when there is decrease of weight. This movement of the pointer P′ has been calibrated with a standard wet and dry bulb hygrometer. Thus the scale on the dial gives the direct reading of the % humidity of the surrounding air or vapours.

SENSITIVENESS

It is not so sensitive as the optical hygrometer (Mahajan, 1944*b*). But it indicates approximate % humidity in a much shorter time than the optical hygrometer.

It is, however, much more sensitive than many other types of hygrometers which are commonly used for approximate value of relative humidity, such as, hair hygrometers, paper hygrometers, chemical hygrometers, etc. The average percentage of error of these hygrometers is ± 5 while that of the Humimeter is ± 2 only.

USES

It is a useful instrument for the factories, workshops and offices, where high accuracy is not needed. It can be used for all other general purposes as well.

PRECAUTIONS

The author has already published some precautions (Mahajan, 1941*b*) for the working of the optical hygrometer. The same precautions should also be observed in its working.

CONCLUSIONS

It is hoped that this instrument will prove useful to the scientific world as well as to the public in general.

ACKNOWLEDGMENT

The author takes this opportunity to thank His Highness's Government, Patiala for providing facilities to carry out this work in the Physics Research Laboratory, Mahindra College, Patiala.

PHYSICS RESEARCH LABORATORY,
MAHINDRA COLLEGE,
PATTIALA.

REFRENCES

Mahajan, L. D., 1941a, *Current science*, **9**, 10.
Mahajan, L. D., 1944a, *Ind. Jour. Phys.*, **18**, 216-220.
Mahajan, L. D., 1944b, *Ind. Jour. Phys.*, **18**, 293-302.
Mahajan, L. D., 1941b, *Ind. Jour Phys.*, **18**, 425-432.
Mahajan, L. D., 1945, *Science and Culture*, **20**, 448.

STUDIES IN GLASS SYSTEMS—MAGNETIC SUSCEPTIBILITY OF POLAR CRYSTALS DISSOLVED IN BORAX GLASS

By SUBODH KUMAR MAJUMDAR and RAMA PRASAD BANERJEE

(*Received for publication, Nov. 8, 1946*)

ABSTRACT. The present paper is an extension of the work done on magnetic properties of polar salts dissolved in glass (Majumdar and Saha, 1945) using a magnetic torsion balance instead of the Guoy balance Alkali salts like NaCl, Li_2SO_4, Na_2SO_4 and K_2SO_4 were dissolved in fused borax and the diamagnetic susceptibilities of the dissolved salts determined. The values thus obtained are remarkably large, indicating an expansion of the lattice. This conclusion runs counter to that drawn from previous measurements of mole-refraction and Xray diffraction.

INTRODUCTION

The problem, in what form polar crystals exist when dissolved in a glass medium, has been engaging the attention of some workers during the last few years. Measurement of mole-refraction of various salts dissolved in fused boric oxide and borax glasses have brought out the fact that these salts are very strongly deformed in solid solution in glass, as shown by their remarkably small values of mole-refraction and the results in the main support the Deformation Rule proposed by Fajans (Majumdar and Sarma, 1942 ; Majumdar and Banerjee, 1946). In a previous paper (Majumdar and Saha 1945), the results of magnetic susceptibility of alkali chlorides dissolved in borax glass, as measured in a Guoy balance, were recorded. As is wellknown the sources of error in a Guoy balance are far too many and it is for this reason a more accurate method has been employed in this investigation. The magnetic torsion balance, first used by Krishnan and Banerjee, (1933) and later modified by Datta (1944), has been used to measure the diamagnetic susceptibility of the following glass systems :

$NaCl-Na_2B_4O_7$; $Li_2SO_4-Na_2B_4O_7$; $Na_2SO_4-Na_2B_4O_7$ and $K_2SO_4-Na_2B_4O_7$.

The salt-content of the glasses was determined analytically and their diamagnetic susceptibilities were determined from the additivity formula :

$$100\chi_g = p.\,\chi_1 + (100-p)\chi_2,$$

where χ_g represents the mass susceptibility of the glass (experimental value), χ_1, the mass susceptibility of the dissolved salt, χ_2, the mass susceptibility of borax, p, the percentage of the dissolved salt and (100-p) that of borax in the glass.

Preparation of the samples.—Lithium sulphate was prepared by dissolving lithium carbonate in dilute sulphuric acid and twice recrystallising in vacuum. Merck's *Pro Analyse* quality of NaCl, Na_2SO_4 and K_2SO_4 were recrystallised once from conductivity water and dried. Pure borax (Merck) was similarly recrystallised from its solution in conductivity water and the salts carefully dehydrated first in an air oven and then in a vacuum desiccator. The samples were prepared by fusion in a platinum crucible as described in the previous papers.

Analysis of the samples.—For the $NaCl-Na_2B_4O_7$ system, the chlorine content was determined by the following method. Weighed amounts of the glass were dissolved in hot water, acidified with nitric acid and excess of a standard solution of silver nitrate added. The whole solution was diluted to a definite volume (250 c.c.); 50 c.c. was dry-filtered and titrated against standard NH_4CNS solution, using ferric alum as indicator.

The total sodium was determined by taking a known weight of the glass in a weighed platinum crucible, treating it repeatedly with a mixture of HF and H_2SO_4 and evaporating to dryness until a constant weight was obtained. The sodium, corresponding to NaCl, was subtracted from this and the remainder agreed fairly well with the $Na_2B_4O_7$ of the glass.

For the sulphate glasses, the following procedure was adopted. Weighed amounts were dissolved in hot water, excess of HCl was added and the sulphate precipitated as $BaSO_4$ from the boiling solutions. The precipitation was carried out by taking the necessery precautions and the precipitated $BaSO_4$ weighed.

Determination of the Magnetic Susceptibility of the glass.—The magnetic susceptibility of the glass pieces was determined in a magnetic torsion balance after suspending them in two suitable liquids of known susceptibilities between the flat pole pieces of a powerful electro-magnet. The experimental piece was rigidly attached to one end of a vertical Pyrex glass rod about 15 cm. long, by slightly melting the borax glass at one point, the other end of the glass rod being attached to the middle of a fine silver wire stretched horizontally between a torsion head and a metal chuck. A small lateral displacement could thus be given by turning the torsion head. The whole thing was so adjusted that the glass piece was roughly at a distance of 3-4 cm. away from the edges of the flat pole pieces of the electro-magnet and was, therefore, in a non-homogeneous field with the gradient in the horizontal direction.

The glass piece was first suspended in a liquid of known susceptibility and the current switched on. The glass being dia-magnetic was displaced laterally along the gradient in a direction away from the field. The reflected light from a mirror on the glass rod very near the experimental piece was viewed through a tele-microscope and the torsion head turned until it came back to the original position.

If K_c be the volume susceptibility of the glass piece and K_1 that of the liquid, the force turning the piece from the field is given by

$$\tfrac{1}{2}A.\, H_x.\, \frac{dH_x}{dx}\,(K_c - K_1),$$

where A is the cross-section of the piece, H, the field strength, the x-direction being the horizontal one. If θ_1 is the angle through which the torsion head is turned, then this force is $R\theta_1$, where R is the torsional constant of the wire. Hence

$$\tfrac{1}{2}A.H_x.\, \frac{dH_x}{dx}\,(K_c - K_1) = R.\, \theta_1 \qquad \ldots \quad (1)$$

If θ_2 be the angle through which the torsion head is turned while immersed in the second liquid of volume susceptibility K_2, then

$$\tfrac{1}{2}.\, A.\, H_x,\, \frac{dH_x}{dx}\,(K_c - K_2) = R,\, \theta_2 \qquad \ldots \quad (2)$$

Dividing (1) by (2)

$$\frac{K_c - K_1}{K_c - K_2} = \frac{\theta_1}{\theta_2} \qquad \ldots \quad (3)$$

K_1, K_2, θ_1, θ_2 being known, K_c can be calculated from (3). The mass susceptibility was determined by multiplying K_c by the density of the sample.

The liquids selected for immersion were Kahlbaum's pure pyridine and Merck's diethylaniline freshly redistilled. The values of mass susceptibilities of these are respectively -0.623×10^{-6} and -0.78×10^{-6} and their respective densities are 0.982 and 0.934 at 25°c (the average temperature of the experiments). These values are taken from the International Critical Tables. Thus K_1 and K_2 work out respectively -0.612×10^{-6} and -0.78×10^{-6}. Wider apart the values of K_1 and K_2, the greater will be the divergence between θ_1 and θ_2 and therefore smaller the experimental error.

In order to test the accuracy of the method and the purity of the liquids, a check experiment was performed by taking a crystal of known magnetic susceptibility and suspending it successively in distilled water and the same two liquids as before.

The calculated values compare favourably with the values given in the International Critical Table.

Although both borax and alkali sulphate crystals are optically anisotropic (bi-axial), yet the glass was perfectly isotropic as proved under crossed Nicols in a polarisation microscope. This may be due to the random distribution of the molecules in the glass neutralising the mutual anisotropic effects. They, however, showed slight *magnetic anisotropy*.

The densities of the glass pieces were determined at the room temperature in a hydrostatic balance using nitro-benzene as the suspending liquid, and unspun silk fibre for suspending the glass. The density of the sample of nitro-benzene was determined at the room temperature by a specific gravity bottle.

EXPERIMENTAL RESULTS

In the following table, the readings of the torsion head are recorded in columns 3 and 4 ; column 5 gives the value of volume susceptibility K_v and the last column gives the values of mass susceptibility.

TABLE I

Magnetic susceptibility data.

Sample No	% salt in glass	θ_1 (mean)	θ_2 (mean)	$K_v \times 10^6$	Density	Mass susceptibility $\times 10^6$
NaCl—$Na_2B_4O_7$ system						
1.	8.97	84°	69°	—1 55	2.325	—0.6667
2.*	14 85	74°	60°	—1.50	2.282	—0.6573
3.	15.22	98°	81°	—1.58	2.269	—0.6965
4.	16.84	55°	46°	—1.636	2.249	—0.7276
5.	17.22	54°	46°	—1.746	2.303	—0.7580
Li_2SO_4—$Na_2B_4O_7$ system						
1.	7.02	65°	51°	—1.392	2 381	— 0.5846
2.	9.55	95°	79°	—1 610	2.383	—0 6759
3.	11.50	71°	60°	— 1.70	2 379	—0.7145
4.	12 98	79°	68°	—1.819	2.379	—0 7643
Na_2SO_4—$Na_2B_4O_7$ system						
1.	8 68	41°	33°	—1 473	2.377	—0.6195
2.	10.67	57°	47°	—1 570	2 382	—0.6591
3.	13.43	40°	34°	—1.732	2.374	— 0.7292
4.	15.62	38°	33°	— 1.888	2.436	—0 7752
5.	17.36	50°	44°	—2.012	2 377	—0 8455
6.	17.71	170°	150°	—2 040	2.382	—0.8563
K_2SO_4—Na_2B_4O7 system						
1.	5.46	88°	67°	—1 320	2 366	—0.558
2.	8.64	77°	60°	— 1.370	2.357	—0 581
3.	11.14	107°	85°	— 1 430	2 356	—0 607
4.	15.38	123°	102°	—1 540	2.356	—0.654
5.	18.42	92°	79°	—1 800	2.374	—0.758
$Na_2B_4O_7$—glass						
1.	0	73 5°	63.3°	—1.264	2.333	—0.5418
2.	0	100°	75°	—1.284	2 372	—0.5414

The following table records the values of mass susceptibility and gm.-molecular susceptibilities of the dissolved salts calculated from the additivity

formula, taking the observed values of the susceptibilities of the glass pieces ; the value for borax glass which is supposed to remain unaltered is taken as -0.5416×10^{-6}, the mean of the two observed values. These values are compared with those of the pure salts.

TABLE II

Mass and gm.-molecular susceptibilities of the dissolved salts.

% salt in the glass	χ obs $\times 10^6$ of the glass	χ calc (of dissolved salt from additivity formula) $\chi^M \times 10^6$		χ(of pure salt) $\times 10^6$	$\chi_M \times 10^6$
NaCl—$Na_2B_4O_7$ system					
8.97	—0.6667	—1.937	—113.2*	—0.499	—29.17
14.85	—0.6573	—1.320	— 77.18		
15.22	—0 6965	—1.559	— 91.16		
16.84	—0,7276	—1.646	— 96.25		
17.22	—0 7580	—1 799	—105.2		
Li_2SO_4—$Na_2B_4O_7$ system					
7.02	—0.5846	—1.1541	—126.89	—0.38	—41.77
9.55	—0.6759	—1.9479	—214.15		
11.50	—0.7145	—2.0452	—224.84		
12.98	—0.7643	— 2.2574	—248.18		
Na_2SO_4—$Na_2B_4O_7$ system					
8.68	—0 6195	—1 4389	—204.40	—0.337	—47.87
10.67	—0.6591	—1.6428	—233.37		
13.43	—0 7292	—1.9384	—275.35		
15.62	—0.7752	—2.0372	—289 38		
17.36	—0.8455	—2.2922	—325.60		
17.71	—0 8563	—2.3186	—329.35		
K_2SO_4—$Na_2B_4O_7$ system					
5.46	—0.558	—0.8417	—146.68	—0.403	—70.22
8 64	—0.581	—0.9976	—173.83		
11.14	—0.6c7	—1.1286	—196,67		
15.38	—0.654	—1.2724	—221.72		
18.42	—0.758	—1.7165	—299.1		

DISCUSSION

It appears from the results that the values of the susceptibility of the dissolved salts in glass as calculated from the addivitity formula are very much greater than those of the pure crystals. The variation is much greater than is usually found with aqueous solutions. In a subsequent communication this point will be elucidated.

The gm.-atomic susceptibility of a dia-magnetic mono-nuclear system is given according to the simple Langevin theory by

$$\chi = -\frac{e^2}{6mc^2} \cdot \sum n\bar{r}^2 \qquad \ldots \quad (4)$$

where n is the number of electrons in the system,

$\sum \bar{r}^2$ is the summation of the squares of the radii of the projected orbits in a plane perpendicular to the magnetic field, e is the electronic charge, m, the mass and c, the velocity of the electron.

It is apparent, therefore, that an increase in the dia-magnetic susceptibility points to increased electronic orbits or what comes to the same thing, in the case under investigation, an enlargement of the lattice of the dissolved crystals. That the lattice exists in such systems has been proved by workers in this laboratory (Majumdar and Palit,1942, 1945, and Majumdar, Banerjee and Banerjee, 1945.)

With NaCl the molecular susceptibility is found to vary between -77 to -105×10^{-6} corresponding to a concentration range between 14.85 – 17.22%, the value for the pure salt being only -28.63×10^{-6}. The former values are abnormally large and cannot be accounted for by any compound formation as the cations in the dissolved salt and the solvent medium are the same. Mole-refraction measurements of these salts dissolved in the same glass (Majumdar and Banerjee, *loc. cit.*) throws an interesting light. The values of R_{NaCl} in such systems are remarkably small indicating a strong deformation of the dissolved salt. The slope of the mole-refraction—concentration curve, however is not so steep as that of the susceptibility—concentration curve for this salt. And this is true for the other salts investigated in this paper. A strong deformation would naturally mean a closer packing of the lattice with consequent *decrease* of the spacing, the susceptibility measurements on the other hand point clearly to an *increase* of the spacing. This point was sought to be cleared by X-ray diffraction experiments. The preliminary measurements of Majumdar and Palit (*loc. cit.*) seemed to support such a conclusion and this is also supported by theoretical considerations regarding the forces operating within an electro-static lattice. The purely electro-static (Coulomb) forces between the charges as well as the short-distance repulsive forces will be decreased by the introduction of a medium of higher dielectric constant as borax glass and a new equilibrium will be set up in which the spacing will be higher than in vacuum or in air. But subsequent work (*cf* Majumdar, Banerjee and Banerjee, *loc. cit.*) did not reveal any appreciable change in the spacings of the dissolved salts.

In the case of the sulphates a very large increase of the susceptibilities is noticeable in every case. For Li_2SO_4, the molecular susceptibility increases

from—126.9 to—248.2 $\times 10^{-6}$ for concentration range between 7.02—12.98%, whereas the value for the pure crystal is only -41.7×10^{-6}. For Na_2SO_4 the increase is from -204.4 to -329.35 $\times 10^{-6}$ within the concentration range 8.68—17.17%, the value for the pure crystal being only -47.8×10^{-6}, and for K_2SO_4, the values lie between -146.68 and -299.1 $\times 10^{-6}$ for the concentration range 5.46 —18.42%, the corresponding value for the pure salt being only -70.22×10^{-6}. Such abnormal increase in the values cannot be explained merely by cationic exchange, which, however, is not possible in the two of the four cases, namely NaCl-$Na_2B_4O_7$ and Na_2SO_4-$Na_2B_4O_7$ systems.

It is wellknown, however, that a small difference does exist between the values of susceptibilities of salts in dilute aqueous solution and in the solid state, as would be seen from the following table,

TABLE III

Gm.-molecular susceptibilities of salts

$-\chi_M \times 10^6$.

		Solid	Aqueous solution
NaCl	...	30.1	30.8
KCl	...	39.1	39.6
$CaCl_2$	...	54.45	55.6

The increase, which in no case is more than a few percent, can be easily explained as due to the removal of the mutual polarisation of the outer electron shells of the ions in aqueous solution, which would naturally increase the average value of $\bar{r}^2$ within the meaning of equation (4). One would, therefore, expect to find a still smaller value of χ_M, as the deformation of the crystal in the glass is still greater. The results of magnetic susceptibility determination of salts dissolved in glass therefore run counter to those of mole-refraction and X-ray diffraction experiments.

ACKNOWLEDGMENTS

Our thanks are due to the authorities of the Indian Association for the Cultivation of Science, Bowbazar, Calcutta for permission to use the magnetic torsion balance, to the M. L. Sirkar Professor of the Association, Dr. K. Banerjee for suggestions and help and to Professor P. B. Sarkar of the University College of Science, Calcutta, for kindly preparing a sample of pure lithium sulphate. Our thanks are also due to the Board of Scientific and Industrial Research of the Government of India for award of a monetary grant.

PHYSICAL CHEMISTRY LABORATORY,
PRESIDENCY COLLEGE, CALCUTTA.

REFERENCES

Datta, A K., 1944, *Ind. Jour. Phys.*, **18**, 249

Krishnan and Banerjee, 1933, *Phil Mag.* A, **231**, 235

Majumdar and Banerjee, 1946, *Jour. Ind. Chem. Soc.*, **23**, 171

Majumdar, Banerjee and Banerjee, 1945, *Nature*, 6th Oct.

Majumdar and Palit, 1942, *Jour. Ind. Chem. Soc.*, **19**, 461

,, ,, 1945, ,, ,, ,, ,, **22**, 317

Majumdar and Saha, 1945, ,, ,, ,, ,, **22**, 147

Majumdar and Sarma, 1942, ,, ,, ,, ,, **19**, 241

SOFT X-RAY K-ABSORPTION AND EMISSION SPECTRA OF Mg, Al, Si AND THEIR OXIDES

By K. DAS GUPTA

(*Received for publication, December 12, 1946*)

ABSTRACT. The K-absorption spectra of Mg, Al, and Si in pure state and in oxides and also their K-emission bands have been taken with a concave crystal (gypsum) spectrograph designed and constructed in Prof. Siegbahn's laboratory. Coincidence of the absorption and emission edges in Al and Mg have been studied accurately in the same film by half shadow device. The absorption edges for oxides are shifted towards short wavelength side with respect to the metal emission bands for the oxides. For the oxides the gap between the beginning of the absorption edge and the short wavelength limit of the emission band is, according to the Zone theory, the forbidden energy gap which has to be correlated with the order of insulation.

INTRODUCTION

The group of papers, of which the present is the first, describes the results of examination of the soft X-ray K-absorption and emission spectra of Mg, Al, Si and their oxides. To interpret the distinctive properties of solid matter in general, *e.g.*, copper (metallic), rocksalt (ionic), carborandum (homo-polar), copper-oxide (semi-conductor) etc. a unified theory based on modern quantum and wavemechanical conceptions have been developed by Brillouin, Bloch, Peirles and others. On the experimental side the soft X-ray spectroscopy of the solid state, investigated by, Siegbahn and Karlson, Skinner and O'Bryan, Magnusson and Johnson, Farineau and others, throws much light on the proposed theory of the solid state.

Soft X-ray absorption spectra give information relating to those states of the solid which in the normal state of the lattice are unoccupied, while the emission bands give information relating to those states of the solid which are normally occupied. A complete study of the zone structure necessitate the investigation both by absorption and emission process. The discrepancies of the experimental data of the soft X-ray spectra for different investigators will at once suggest a thorough study of a particular substance by the same experimenter in the same spectrograph. If possible, the absorption as well as the emission spectra for a particular substance is to be taken on the same photographic film by some half-shadow device.

Considerable work has already been done on the soft X-ray absorption and emission bands. The K-absorption of Mg and Al and L_{23} absorption of Mg were investigated by Sandstrom (1935) Skinner and Johnston (1937). Skinner and O'Bryan (1940) have studied the L and M emission bands lying in the range from about 17 to 300A with ruled grating. Although the resolution in the region between 40 to 500A is better compared to the region between 5 to 15A, there is an advantage of studying the K-absorption or

emission bands between 5 to 15A compared to the study of L_{23} bands for the same substances between 40 to 500A. The K-emission bands produced by the transition of valence electrons to the vacant K level will obviously be simpler compared to the L_{23} bands produced by the transition of the same valence electrons to the vacant L_{23} levels which are themselves splitted and for the compounds of low atomic numbers are profoundly modified due to the lattice formation.

EXPERIMENTAL TECHNIQUE

The range of wavelengths for the present investigation stretches from about 5A to 12A; this region of spectra being highly absorbable in air the whole spectrograph with crystal, plateholder etc. had to be kept in the same vacuum as the X-ray tube itself The bent crystal method enables us to obtain good photographs of emission bands as well as absorption edges with natural crystals gypsum, mica as grating without a slit the latter being for a long time considered as a necessary implement in the apparatus. The principle of focussing of the spectra is the same as in Rowland's grating. X-ray from anti-cathode passing through a 4 mm aperture forming a divergent beam strike the bent crystal and are focussed to a point on the Rowland's circle. The bent crystal with a portion of the Rowland's circle known as the 'cassette' moves as a whole about an axis passing through the centre of the crystal. The cassette with the crystal holder can be rotated by a pointer from outside without disturbing the vacuum of the spectrograph for suitable angles for different wavelengths. Sandstrom (1935) has calculated the broadening of the spectral line for various causes and has shown that apart from other factors, it increases with the square of the effective reflecting surface of the bent crystal. This defect is generally met with a spectrograph of large radius and small crystal width. In the spectrograph used the Rowland's circle has got a radius of 250 mm and the crystal is bent to an arc of radius 600 mm. Between the two curved steel pieces (500mm radius) is placed a thin slice of a single crystal of gypsum of about 0.5 mm thickness and the bending is effected by screws attached to the steel piece. The reflecting surface of the crystal has been limited by controlling the width of the diverging X-ray beam by an wedge moving at right angles to the crystal surface. In the present investigation the spectrograph was used between glancing angles 20°-50°. The maximum possible broadening as calculated by Sandstrom was found to be ·05 X.U within this range of angles which is of little importance to us as the experimental errors for measuring broad bands are larger than this value. The lattice constant and the refractive index of bent crystal could not be determined directly and the value of the same for the unbent crystal has been used. The change in the spacing value due to bending has been discussed by Sandstrom and the ratio $\Delta d_n / d_n$ where d_n is the spacing of the nth order was found to be practically constant for all orders of reflections. The error due to broadening is in the

fourth place of the '*d*' value and decreases rapidly with the higher orders. In the same paper other possible errors of secondary importance, *e.g.* due to any flaw in the bending of the crystal, due to difference of penetration of the higher order reference lines into the photographic film and the like, have been discussed. These probable errors are always less than the experimental limit. The anti-cathode which is water cooled and the cathode which is a 'dull emitter' consisting of oxide coated platinum wire face each other inside a light-tight enclosure fitted with a slightly tapering cone of about 2 cm. in length and 4 mm aperture to allow X-rays to be admitted to the spectrograph. A thin piece of Al of thickness about 0.5μ is generally used for covering the aperture to protect the film from the glow of the filament. A good oxide coating has been prepared with BaO and SrO taken at a definite proportion and the coating on the filament lasts for about 30 hours.

The dispersion in this region varies from 0.2 to 0.7 volt/mm. It was calculated in every case for the particular region under investigation by taking suitable reference lines. In some cases reference lines of higher orders have to be taken and this generally increased the background radiation to such an extent that finer details of soft X-ray absorption and emission bands were completely lost. In order to avoid this difficulty the film was carefully half covered when the line in question was photographed in the other half. To calculate the wavelength for the higher order spectra the corresponding '*d*' values for the gypsum and wavelengths for reference lines were taken from Siegbahn's 'Spectroscopy der Rontgenstrahlen.'

Preparation of absorption screens: In taking absorption spectra it has been noticed that the suitable thickness and the quality of the absorbing screens are essential for having a good photograph. Based on absorption laws of Jonsson, Sandstrom (1935) derived a formula for calculating the optimum thickness of screens so as to have the maximum difference between the intensity on each side of an edge, but this can be taken as the lower limit of the screen thickness. From experience it has been found that fine structure details come out better if the thickness of the absorbing screen is too small while a greater thickness is necessary to have a prominent primary edge. Films of different samples were made by different suitable processes and therefore it was difficult to determine the actual thickness of the film. Metal films of Mg and Al were prepared by rolling process whereas oxides were coated on a thin film of celluloid.

Aluminium.—Six pieces of Al, each of thickness of about 0.5 μ, gave only a prominent absorption edge, while with three pieces three secondary absorption edges are clearly visible on the film.

Magnesium.—A rod of pure metallic Mg was rolled and the film thickness was found to be too great. This was then scrapped with a fine blade and a fairly uniform film could be made which have a prominent primary edge.

Silicon and Al_2O_3.—Very fine powders of metallic Si preserved in sealed tubes was thoroughly mixed with a large quantity of a solution of celluloid

in acetone and spread over a ground glass. Acetone soon evaporates and the thin film of silicon in celluloid sticking to the glass is removed by adding water and dried in vacuum. The film for Al_2O_3 was also prepared in a similar way.

MgO.—For MgO pure Mg was burnt in air and MgO smoke was allowed to deposit on an Al foil of thickness 0.5 μ.

Photographic film.—Single coated Agfa Laue film used by workers in this region was not available in the market due to war censor. Fine grain cinema films used for sound track photography was found suitable for the purpose. The grains are remarkably fine for good microphotometer work though the speed is much less than that of the sensitised Laue films.

GENERAL INTERPRETATION OF RESULTS

According to the theory of solids, all the energy levels of an atom, particularly the valency ones, are greatly modified by the interaction of neighbouring atoms in the lattice and as a result these levels become broad. The broad valency levels may sometime overlap with the next possible higher one. The combined level thus formed is now filled up with electrons according to Pauli-principle up to a certain limit and the rest is empty. This limit which demarcates the two portions of the combined level is known as Fermi-surface which is very sharp at ordinary temperature and is usually denoted by energy maximum E_{max}. The beginning of the band is, however, represented by E_o. It is evident that the intensity of any emission line, corresponding to transition of electrons from the valency shell to a deeper vacant level, will suddenly vanish at E_{max} where the absorption edge of the atom in the crystal will just begin. The theory of solid metal correctly interprets the general experimental observations on both the emission and absorption spectra in the soft X-ray region. Further, it is found that the emission edges of the elemement of the second group of metals in the L series are very sharp and are of the order of 1/10 e.v. suggesting the sharpness of the Fermi-surface, whereas the same surface as measured from K-emission spectra for those elements varies from 2 to 4 volts. It has been pointed out by Ray and Bhowmik (1941) that the K-emission edge is partly modified by the absorption of general radiation by the inner surface of the anticathode and has been verified by the author in the case of Mg and Al by taking emission band at high and low voltage of excitation.

K-valence emission band of Mg, Al and Si and the absorption edges of these elements were studied under similar conditions that is the effective surface of the reflecting crystal, the aperture of the incident radiation, the slit system of the micro-photometer were kept constant. In the curves Fig. 2(*a*), (*b*), (*c*) maximum blackness on the plate, *i.e.*, peak of the emission band I_{max} of all the spectra was taken as a standard at a definite length and corresponding points on the emission lines were necessarily altered in the

same ratio. In the absorption spectra the maximum difference in blackness before and after the absorption was similarly taken at the same length as in emission curve. The other points were then plotted as before. The abscissa is drawn on the voltage scale. It will not be out of place to mention here that I_{max} in the intensity curve is necessarily different from E_{max}, the latter depends on the energy value of the Fermi-surface of the combined level whereas the former is related by the following equation : $I=N(E).f(E)$, where $N(E)$ denotes the density of states and $f(E)$ the transition probability. Thus intensity will be maximum when $N(E).f(E)$ is maximum and it will be zero just after E_{max} where there are no electrons.

In the emission process an electron is knocked out from inner shell into the vacancy, transition of an electron from the continuous band of filled valence levels may occur. This gives accurately the characteristics of the $N(E)$ curve over the region of filled levels. Before the emission process the lattice has all its normally occupied states filled except that there is a vacancy in the inner shell. The energy of the initial state is therefore sharply defined within the limits of the breadth of the inner level. After the emission an electron may be missing from any of the levels of the filled valence electron band. While in the case of absorption we are simply concerned with the probability of transition from the inner level into one of the vacant levels. The characteristics of the $N(E)$ curve for the vacant levels will obviously be reflected in this absorption curve.

The photometer records of absorption spectra for Mg, Al, Si and their oxides are given in Fig 1. The point of interest in the experiment was to

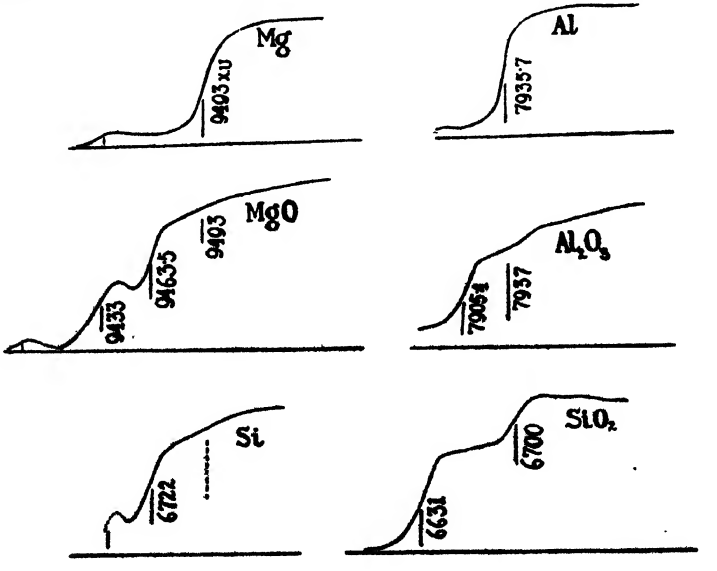

FIG. 1

Photometer records of K-absorption spectra of Mg, Al, Si and their oxides, wavelengths in X.v.

investigate the exact position in the wavelength scale of the beginning of K—absorption edge of Mg, Al, and Si and to compare this with the short wavelength limit of the emission edge E_{max}. In the first set of experiments the emission and absorption photographs were taken in different photographic films and it was really two different settings of the spectrograph. In order to have a more decisive result, the crystal angle was kept same in both emission and absorption experiments, and the lower-half of the photographic film bent round the Rowland's circle (cassette) was first covered by a rectangular strip of metal and emission band was taken on the upper part of the film. In the next set of absorption experiment, the upper portion was covered similarly and the absorption edge was recorded in the lower portion of the *same film*. This was necessary because a slight variation of pressure over the film could alter the position of the film relative to the Rowland's circle. In this way we got on the same film both K-absorption edge and K-β emission band of Mg, Al, and Si under the same condition.

The film was then etched by a fine blade so that the scratch is parallel to the sharp emission lines which are also present along with emission bands. The scratch, the emission lines and the absorption edges were all made parallel to the vertical slit of the micro-photometer.

First the photometer record of the emission band was taken along with the scratch which was recorded as a sharp peak, then the absorption edge was taken by lowering or raising the film by a simple mechanism without disturbing the film and this time also the fine scratch of blade on the film gives a peak. Now it was seen that the position of the peaks, *i.e.*, fine scratch does not alter in the two cases showing thereby that there is no lateral movement of the film when it is simply raised or lowered.

From several such experiments it was found that decidedly there is no lateral shift in the two sets of photometer records, *i.e.*, on the bromide paper on which record is taken the peaks for the fine scratch come on the same position. The micro-photometer record thus consists of superposed emission and apsorption spectra, the dispersion and magnification for the two being the same. From the superposed spectra it is evident that absorption begins definitely at a longer wavelength than the wavelength corresponding to the most intense (I_{max}) part, *i.e.*, peak of the emission band and at a still more longer wavelength than the wavelength corresponding to E_{max} of the emission band. The experiment was repeated several times.

Beginning from the long wavelength side we have marked three important positions of the emission band. First 'E_0' Fig. 2(*a*) which corresponds to the beginning of the band on the longest wavelength side, *i.e.*, X-ray produced by the transition of electrons from the bottom of the filled conduction band to the inner shell. The second point marked, is named as I_{max} corresponding to intense peak of emission band, *i.e.*, when $N(E) \times f(E)$ is maximum. The third point marked in the emission band is E_{max} corresponding to the shortest wavelength of the emission band, *i.e.*, according to the theory

corresponding to the transitions of electrons from the Fermi-surface to the inner shell.

In the absorption spectra we have also marked the three points *viz.*, the beginning B and end L of the absorption curve and middle portion K where usually primary edge K is measured. Absorption begins at the longest wavelength corresponding to the energy required to transfer a K-electron to the bottom of the empty zone or just after the Fermi-surface where there is no electron. The K-absorption edge and K-valence emission band taken carefully on the same film clearly show that absorption begins at a much longer wavelength than I_{max} of the emission band in the case of Mg, Al, and Si.

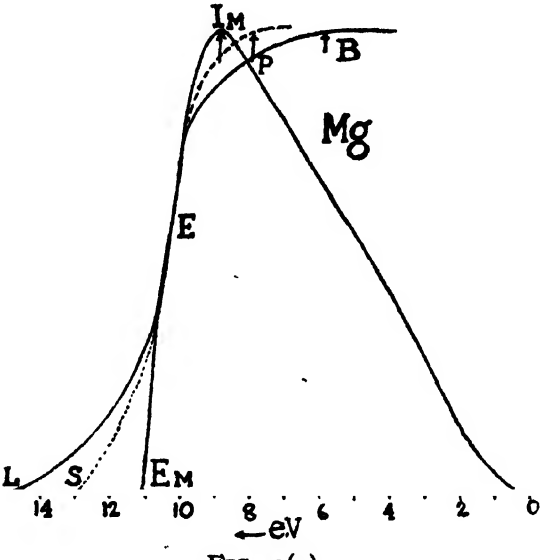

FIG. 2(*a*)

I_M is the peak of the K-emission band of Mg and B is the beginning of K-absorption for short period exposure and P is the same for long exposure. L is the end of absorption curve for long exposure and S the same for short exposure. E_M is the short wavelength limit of the emission band. The point P is one volt from I_M on the low energy side. E is emission edge coincident with absorption edge.

Magnesium and Aluminium.—The absorption curves for magnesium and aluminium are given in Fig. 1, in magnesium one secondary edge and in aluminium three prominent secondary edges have been obtained. The breadth $I_M - E_M$ in Mg emission band is 2 volts and in Al it is 4.5 volts Fig. 2(*a*) and 2(*b*). The position of E_{max} that is, E_M in the figure is, however, uncertain as it depends on the time of exposure and this has been shown to be due to the absorption of general radiation by the inner surface of the anti-cathode and can be sometimes avoided by taking emission band at a low exciting voltage of the tube. The dotted and continuous lines near the end of the absorption curve are found to occur under short and long exposures

respectively. The difference between them for Mg is 1.8 volt. Altogether five absorption photographs were taken both for Mg and Al, having different time of exposures and it has been found that the beginning of the absorption B, *i.e.*, the bending of the absorption curve also shifts towards the short

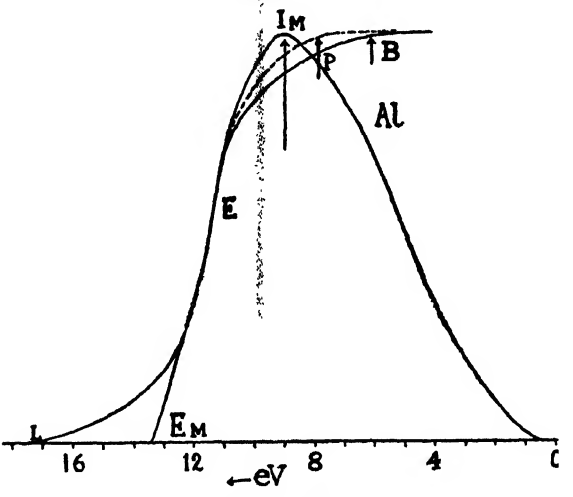

FIG. 2(*b*)

I_M is the peak of the K-emission band of Al and B is the beginning of K-absorption for short period exposure and P the same for long exposure. E_M is the short wavelength limit of the emission band. L is the end of the absorption curve. The point P is about 1 volt from I_M on the low energy side. E is emission edge coincident with absorption edge.

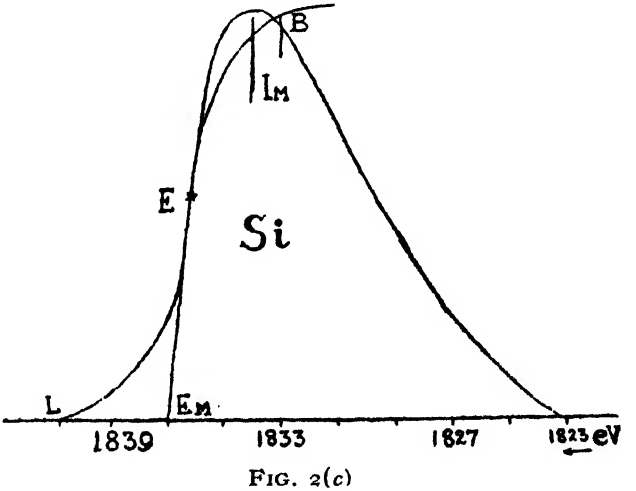

FIG. 2(*c*)

I_M is the peak of K-emission band of Si and B the beginning of K-absorption. E_M is the short wave limit of the emission band and L the end of the absorption curve. The point B is about one volt from I_M on the low energy side. E is the emission edge coincident with the absorption edge.

wavelength side with prolonged exposure. This is shown in Fig. 2(*a*), 2(*b*). The photometer record of Mg emission band superimposed on Mg absorption curve taken on the same film by half-shadow device and the same for Al is given in Fig. 3. From repeated experiments it is seen that absorption begins at least one volt before I_M, the peak of the emission band, on the long wavelength side, both in the case of Mg and Al.

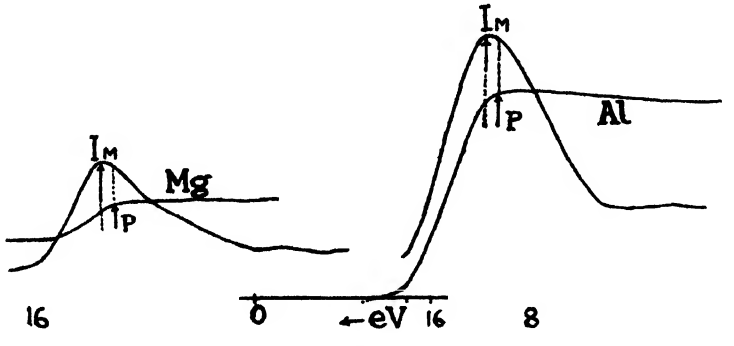

FIG. 3

Micro-photometer record of absorption and emission curves taken in the same film by half-shadow device. I_M is the peak of the emission band and P is the beginning of absorption.

According to the solid theory of the metals the combined level is filled up with necessary electrons according to Pauli-principle, an electron from the K shell cannot find any place within the limit E_0 to E_M. The experiment shows that absorption surely begins before E_M, in other words the total number of *p*-electrons allowed by Pauli-principle which are responsible for K-emission band is not actually present in the combined portion of s, p zones of Mg in the solid, at least under the experimental condition The absorption experiment shows that '*p*'-electrons can be accomodated in the '*p*'-band even within the overlapping portion of 's,' 'p' zones, but the number of such *p*-electrons is found to be small (as estimated from absorption intensity) inside the deepest *p*-level and it gradually increases till E_M is reached, just after which the absorption becomes maximum. It is interesting to note that Skinner (1940), from observations of the kinks in L_{23} bands, suggests that an overlapping between 's', 'p' zones in Mg solid is of the order of 2 volts. According to us it is of the order of 3 volts or more.

The total width of the *p* level in the crystal where K electrons can be accomodated, as measured from the K-absorption edge (including the overlapping position) in Mg solid, is 9 volts and 7 volts for long and short exposures respectively. It is found that the middle portion of the absorption edge coincides with that of the emission edge. The suggestion which has been made in Mg spectra may also be applied in the case of Al. Skinner finds that the overlapping of 's', 'p' zones from L_{23} band spectra is of

the order of 3 to 4 volts in the case of Al and according to our absorption result in Al the overlapping is of the same order, *i.e.*, 3 to 4 volts. The total breadth of the 'p' band from absorption edge is 9 volts and 11 volts for short and long exposures.

Silicon —In the case of Si metal K-emission band is always associated with a weak K band of Si in SiO_2. The peak of K band of metal is at 6731 X.U. and of SiO_2 is 6746 X.U. The empirical band width of Si metal is 14 volts. Uncertainty for the position of E_M is introduced, as in the case of Mg and Al, due to anti-cathode absorption and on the long wavelength side due to superposition with K band of Si in SiO_2, the long wave limit is difficult to be determined.

In the absorption spectra of Si metal there seems to be on the longer wavelength side a faint edge and it is difficult to find out the position of the edge (see Fig 1). In Fig. 2(*c*) the K-emission band of Si metal is drawn on the same scale, as stated previously along with the prominent primary K-absorption edge. As in the case of Mg and Al the middle portion of both emission and absorption edge do coincide, marked E in the Fig. 2(*c*). The absorption, however, begins one volt before I_M, the peak of the emission band.

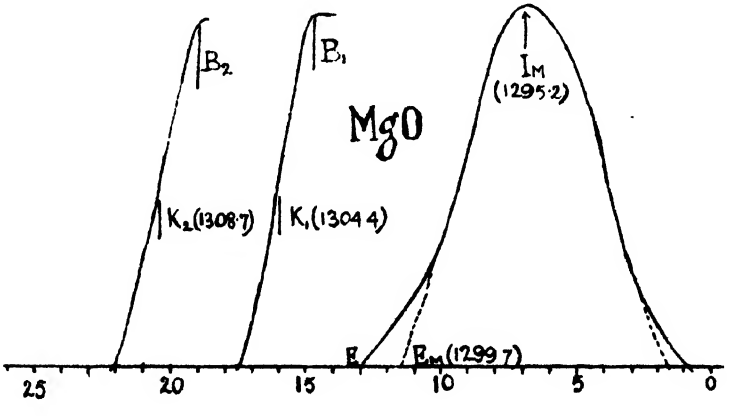

FIG. 4(*a*)

I_M is the peak of K-emission band of MgO and E_M is the empirical short wave limit of emission band, neglecting the weak band at short wavelength end. B_1 and B_2 are the beginning of primary and secondary edges respectively.

Magnesium Oxide.—The absorption curve photometer record is shown in Fig. 1. The edge Mg in MgO shifts towards the short wavelength side with respect to K edge of metallic Mg and absorption begins at a shorter wavelength than emission end E_M. The difference between the K-absorption edge and I_M the peak of the emission band is 9 volts Fig. 4(*a*). An ultra-violet absorption band of this order is to be expected for MgO. The difference

between the beginning of K-absorption and E_M is the width of the forbidden zone, and is equal to 3.4 volts. This value is unreliable due to uncertainty in the position of E_M caused by the presence of a weak band at the short wave end of the main band. A faint edge due to metal is present in MgO absorption spectra.

Aluminium Oxide.—In Al_2O_3 Fig. 4(*b*) the gap K edge I_M is 12.4 volts, an ultra-violet absorption band of this order is expected. The forbidden energy gap B-E_M is 4.2 volts. A faint edge due to metal is present in the spectra of Al_2O_3 as in the case of MgO. A weak secondary edge has been obtained which is too weak to be accurately determined.

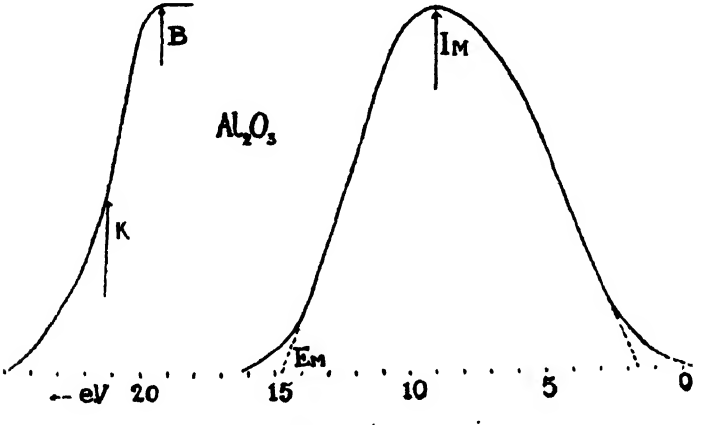

FIG. 4(*b*)

I_M is the peak of the K-emission band Al in Al_2O_3 and B is the beginning of K-absorption. Reduced emission band width is equal to the total K band width of oxygen in Al_2O_3 (Skinner) Fig. 5. The width of the forbidden zone measured from E_M is about 4.7 volts.

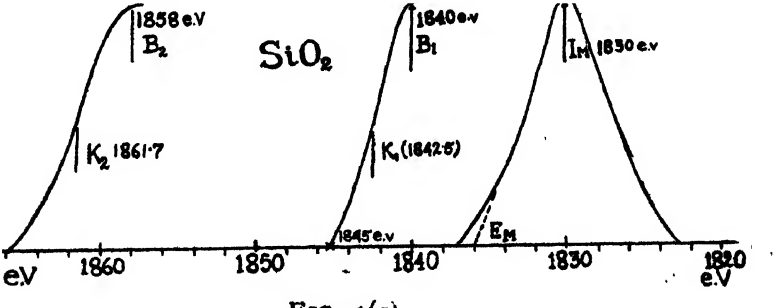

FIG. 4(*c*)

K_1 and K_2 are two absorption edges of Si in SiO_2. Edge K_2 is more prominent. I_M the peak of K-emission band of Si in SiO_2. B_1 and B_2 are the starting point of the two edges. E_M dotted signifying uncertainty of position

Silicon Dioxide.—Two prominent absorption edges have been obtained in the case of SiO_2. Both edges are shifted towards the shorter wavelength

side compared to the edge of metallic silicon. In Fig. 4(*c*) the oxide edges along with the emission band of Si in SiO_2 are drawn on the same scale. The first absorption edge K_1 is less prominent than the second edge K_2. The energy difference between the peak I_M of the emission band of Si in SiO_2 with edges K_1 and K_2 of SiO_2 are 12.5 and 31.7 volts respectively. The forbidden energy gaps B_1-E_M and B_2-E_M are 4 volts and 28 volts respectively.

For various polar and semi-polar compounds the difference K-I_M has been found to agree well with the ultra-violet absorption bands and will be discussed in another paper. The difference B-E_M is a measure of the order of insulation of the material. The total breadth of the absorption edge in oxide is always lower than the corresponding value in metal while in emission spectra they are found to be of the same order of magnitude. Secondary edges are more prominent in oxide compared to those obtained in the case of metals.

(In electron volts)	Mg.	MgO	Al	Al_2O_3	Si	SiO_2
Total breadth of absorption edges:	7.0	3.0	9.0	5.5	8.0	5(Edge K_1) 8(Edge K_2)
Total breadth of emission bands:	11.0	12.0 *10 0	12.8	16.0 *13.0	14.0	14.0 *13.0
Absorption edge-Emission peak:	1.2	9.2(K_1-I_M) 13.5(K_2-I_M)	2.4	12.8 ...	2.0	12.5(K_1-I_M) 31.7(K_2-I_M)
Beginning of absorption—short wave limit of emission band. B-E_M		3.4(B_1-E_M) 7.7(B_2-E_M)		4.2		4,0(B_1-E_M) 28 0(B_2-E_M)

* Reduced empirical width after Skinner.

The K band width of oxygen in various oxides taken by O'Bryan and Skinner (*loc. cit.*) is greater for semi-polar compounds MgO, Al_2O_3, SiO_2, B_2O_5 etc. and less in the case of more polar crystals *e.g.* Li_2O.

The width of valence emission band depends on the amount of overlapping of zones. In a compound of R^+, X^- type there may be three types of overlapping; between R^+ and R^+, X^- and X^- and between R^+ and X^-. Overlapping between R^+ and R^+ and X^- and X^- depends on the ratio of the ionic diameters R^+/X^-. If the size of the negative ion is large compared to that of the positive ion then X^-, X^- overlapping will be predominant and *vice versa*. The amount of broadening due to overlapping of R^+ and X^- will of course be prominent according to the degree of polarity of the crystal. In oxides if a K electron of oxygen is knocked out the vacancy may be filled up by the transition of electron from the valency band, whether it is attached to the positive centre or negative centre. Thus an electron attached to positive ion can fill up the vacancy of the K shell of negative ion and similarly a vacancy of K shell of positive ion may be filled up by the transition of electrones round the negative ion. The above suggestion implies that the K band width of oxygen

in an oxide should be equal to the K band width of metal ion in the same oxide.

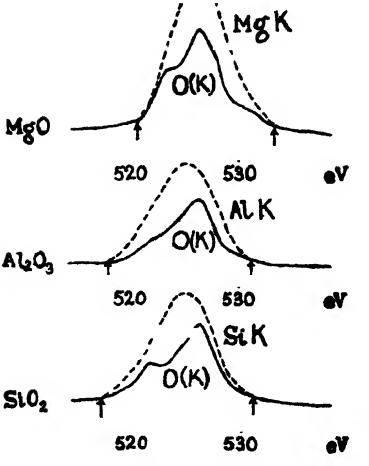

FIG. 5

Photometer records of K bands of oxygen from MgO, Al_2O_3 and SiO_2 O'Bryad and Skinner (1940). Dotted line curves are K metal emission bands of oxides drawn on the same scale.

Our experimental data on the total K band width of Mg, Al and Si in their oxides agree with the K band width of oxygen obtained by Skinner. In Fig. 5, oxygen K band for MgO, Al_2O_3, SiO_2 are drawn on the same scale along with the metal K band. Of course much uncertainty is introduced due to the presence of weak bands at both ends, as well as, due to the tailing effect. In a separate paper the total band width of constituent elements of compounds which are polar, semi-polar and homo-polar will be discussed in detail.

ACKNOWLEDGMENT

I take this opportunity of expressing my gratefulness to the Late Prof. B. B. Ray, University College of Science, Calcutta, under whom the work was done. I am greatful to Prof. S. N. Bose, University College of Science, Calcutta, under whose guidance I am continuing my work on problems of alloys by soft X-ray spectroscopy.

KHAIRA LABORATORY OF PHYSICS
UNIVERSITY COLLEGE OF SCIENCE, CALCUTTA.

REFERENCES

Ray and Bhowmik (1941), *Proc. Nat. Inst. Sci. India*, **7**, 3.
Sandstrom (1935), *Nova Acta Soc. Sc, Upasala*, **9**.
Skinner and Johnston (1937), *Proc. Roy Soc.*, **161A**.
Skinner and O'Bryan (1940), *Phil. Trans. Roy. Soc., Lond.*, **239**, 801.
,, ,, *Proc. Roy. Soc.*, 1. 176.

The following special publications of the Indian Association for the Cultivation of Science, 210, Bowbazar Street, Calcutta, are available at the prices shown against each of them :—

No.	Subject	Author	Price Rs. A. P.
III	Methods in Scientific Research	Sir E. J. Russell	0 6 0
IV	The Origin of the Planets	Sir James H. Jeans	0 6 0
V	Separation of Isotopes	Prof. F. W. Aston	0 6 0
VI	Garnets and their Role in Nature.	Sir Lewis L. Fermor	2 8 0
VII (1)	The Royal Botanic Gardens, Kew.	Sir Arthur Hill	1 8 0
(2)	Studies in the Germination of Seeds.	,,	
VIII	Interatomic Forces	Prof. J. E. Lennard-Jones	1 8 0
IX	The Educational Aims and Practices of the California Institute of Technology	R. A. Millikan	0 6 0
X	Active Nitrogen A New Theory	Prof. S. K. Mitra	2 8 0

A discount of 25% is allowed to Booksellers and Agents.

THE SCIENTIFIC APPARATUS & CHEMICAL WORKS, LIMITED.

CIVIL LINES, AGRA,

(Originally founded in 1918)

GOLDEN OPPORTUNITY

The Company's Managing Director Mr. S. P. Khandelwal has brought with him from America and Europe a number of Schemes for the Scientific development in India. Hence the Company invites,

TEMPORARY DEPOSITS

on interest as detailed below :

For one year Rs. 5/4/- p.c. per annum.

For two years Rs. 6/- p.c. per annum.

For long periods please write or see personally the Managing Director.